UNIVERSITY OF MICHIGAN
JUL 5 1960
ENGINEERING

JOURNAL OF FLUID MECHANICS

VOLUME 8 PART 2

JUNE 1960

PUBLISHED BY

CAMBRIDGE UNIVERSITY PRESS

BENTLEY HOUSE, 200 EUSTON ROAD, LONDON, N.W.1

AMERICAN BRANCH: 32 EAST 57TH STREET, NEW YORK 22, N.Y.

Price 30*s.* (*U.S.A.* $5.00)

The JOURNAL OF FLUID MECHANICS exists for the publication of theoretical and experimental investigations of all aspects of the mechanics of fluids, and is issued in four parts per volume.

EDITOR

DR G. K. BATCHELOR

Department of Applied Mathematics and Theoretical Physics, University of Cambridge, Free School Lane, Cambridge, England

ASSISTANT EDITORS

DR T. B. BENJAMIN, DR I. PROUDMAN, DR P. G. SAFFMAN

Department of Applied Mathematics and Theoretical Physics, University of Cambridge, Free School Lane, Cambridge, England

ASSOCIATE EDITORS

PROF. G. F. CARRIER

Pierce Hall, Harvard University, Cambridge 38, *Massachusetts, U.S.A.*

DR W. C. GRIFFITH

Research and Development Laboratory, Missile Systems Division, Lockheed Aircraft Corporation, Palo Alto, California, U.S.A.

M. J. LIGHTHILL

Royal Aircraft Establishment, Farnborough, Hampshire, England

PROF. R. R. LONG

School of Engineering, The Johns Hopkins University, Baltimore 18, *Maryland, U.S.A.*

Authors wishing to have papers published in the JOURNAL should communicate them to any one of the persons named above, choosing one in their own country where possible.

Authors are urged to ensure that their papers are written clearly and attractively, in order that their work will be readily accessible to readers.

Manuscripts should be typed in double spacing on one side of the paper only, with references listed at the end in alphabetical order of authors. Drawings should be done on a large scale in Indian ink on tracing cloth or drawing paper, the lettering being shown clearly in pencil for reproduction by the printer; the list of captions should be typed at the end of the manuscript. Proofs of papers from overseas will usually be despatched to authors by airmail. There is no charge for publication. Authors are entitled to receive 50 offprints of a paper in the JOURNAL free of charge, and additional offprints can be purchased if ordered in advance.

SUBSCRIPTIONS

The subscription price for a volume of four parts is £5. 10*s*. net, post free, payable in advance; separate parts 30*s*. net, plus postage. Subscriptions may be sent to any bookseller, or to the Cambridge University Press, Bentley House, 200 Euston Road, London, N.W.1.

Subscribers in the United States should send their orders to the Cambridge University Press, American Branch, 32 East 57th Street, New York 22. The subscription price per volume is $18.50, post free, payable in advance; separate parts $5.00, plus postage.

Quotations for available back volumes and parts may be obtained on application to the Cambridge University Press.

Dynamics of a dissociating gas

Part 2. Quasi-equilibrium transfer theory

By M. J. LIGHTHILL

Department of Mathematics, University of Manchester*

(Received 26 October 1959)

1. Introduction

The introduction to Part 1 (Lighthill 1957) proposed a paper in three parts, in the nature of a broad introductory discussion of the dynamics of a pure dissociating gas, which might act as a source of ideas for later, more comprehensive investigations. Part 1 treated 'equilibrium flow', Part 2 was to treat transport properties under 'quasi-equilibrium' conditions, and Part 3 flows in which large departures from equilibrium occur. When Part 1 was submitted for publication, much of Part 2 had already been written. At this moment, however, the author suddenly became obliged to abandon the project for two years, in order that his contributions to two collective works, *Laminar Boundary Layers* and *Incompressible Aerodynamics*, could be produced in time to avoid serious delay in the appearance of the contributions of other authors.

In the meantime, the publication of many valuable papers has reduced the need for a study of the kind described above. In particular, material closely along the lines intended by the author for Part 3 has been expounded in papers by Freeman and Clarke (as well as in some parts of other papers, referred to in the next paragraph). Freeman (1958) treats the flow outside the boundary layer and Clarke (1958) that inside a boundary layer, in the case of large departures from equilibrium, both using the 'ideal dissociating gas' introduced by Lighthill (1957), together with assumptions on rates of dissociation and recombination compatible with the 'ideal dissociating gas' approximation. As a result, the author considers that a separate Part 3 is no longer necessary, and concludes the series with the present Part 2 on the quasi-equilibrium theory of the transport properties—including, however, some occasional remarks on flows with larger departures from equilibrium.

It might well be argued that the existence of many recent and older papers on boundary layers in dissociating gases (such as Moore 1952; Beckwith 1953; Lees 1956; Kuo 1957; Fay & Riddell 1958) makes equally unnecessary the appearance of much of Part 2. However, on comparing those papers with the material already written, the author felt that Part 2 would be worth completing and publishing, as including a more elementary account of this material, or, at least, one which might help certain classes of reader to greater understanding of the physical mechanisms involved. An additional feature of Part 2, which has been less widely treated in the literature, is the theory of radiative heat transfer to the surface of a projectile travelling at very high speeds. This subject also is discussed with the emphasis entirely on fundamentals.

* Now Director, Royal Aircraft Establishment, Farnborough, Hampshire.

The author has elsewhere published a more 'popular' account of the subject of this paper (Lighthill 1959), with some additional material.

2. Requirements for quasi-equilibrium

The quasi-equilibrium theory of the gaseous transport properties, both diffusive (like viscosity, heat conduction and the interdiffusion of constituents) and radiative, assumes that, although the distribution of molecular velocities and other phase-space co-ordinates has departed from the isotropic, Maxwell–Boltzmann form, sufficiently to produce net transport, the deviations are small enough for their squares to be neglected. Thus, restriction (ii) of Part 1, § 3.1 is removed, but restriction (i) is not.

The diffusive transport properties in a pure dissociating gas, that is, a binary mixture of molecules and free atoms, will be considered first. The theory of transport in a binary mixture of monatomic gases is well developed (see, for example, Chapman & Cowling 1952). The extension to a system where non-translational energy is present requires more care than is sometimes realized. The treatment in §§ 3–7 follows the general lines of the author's treatment (Lighthill 1956) of the analogous problem in a pure gas. A feature special to the present problem is that, since the internal energy includes an important contribution ($\frac{1}{2}Dn_A$ in Part 1, equation (19)) due to the energy difference between two free atoms and a molecule, the interdiffusion of molecules and free atoms is one of the most important mechanisms of heat transfer.

The condition for departures of all quantities from their equilibrium values to remain small is most likely to be violated by α, the proportion by mass of free atoms in the mixture. Thus, diffusion of free atoms from a region of higher temperature (and therefore higher α) to one of lower temperature must soon force α far above its local equilibrium value in the latter region, unless recombination can occur fast enough to keep the difference small. Note that it is only if such recombination (with the resulting release of energy) occurs that the mechanism of heat transfer by interdiffusion described in the last paragraph can affect the translational temperature.

In the quasi-equilibrium theory of radiative transfer, emission and absorption of radiation by the gas are estimated on the assumption that its molecules have their equilibrium energy distribution. We do not, however, assume that emission and absorption balance one another. This more complete equilibrium ('radiative equilibrium') occurs in enormous masses of homogeneous gas, or in gas enclosed in an isothermal oven, but is not reached even approximately in the small layer of incandescent gas around a projectile. Therefore, the radiative transfer to its surface is far less than 'black-body radiation' at the temperature of the surrounding gas. It can be estimated only from details of how molecules absorb or emit radiation; here, this is exhibited simply for the case of a pure dissociating gas, with O_2 as an illustrative example.

3. The basic equations of quasi-equilibrium flow

In quasi-equilibrium hydrodynamics, as in equilibrium hydrodynamics, we have basically only five equations, expressing conservation of mass, three

momentum components, and energy. In suffix notation (where the suffixes i and j may take any of the values 1, 2 and 3, and each term in which a suffix occurs twice stands for the sum of the realizations of that term obtained by giving the suffix all three of its possible values), these equations are

$$\frac{\partial \rho}{\partial t} + \frac{\partial}{\partial x_i}(\rho v_i) = 0, \tag{1}$$

$$\frac{\partial (\rho v_i)}{\partial t} + \frac{\partial}{\partial x_j}(\rho v_i v_j + p_{ij}) = 0, \tag{2}$$

$$\frac{\partial \{\rho(u + \frac{1}{2}v_i^2)\}}{\partial t} + \frac{\partial}{\partial x_j}\{\rho v_j(u + \tfrac{1}{2}v_i^2) + p_{ij}v_i + q_j\} = Q, \tag{3}$$

where ρ is the density, v_i the velocity component in the x_i direction, p_{ij} the compressive-stress tensor, u the specific internal energy, q_j the heat-flow vector, and Q the heat input rate per unit volume, due to the difference between the rates of absorption and emission of radiation. Certain linear combinations of these equations are also useful, notably

$$\rho\left(\frac{\partial v_i}{\partial t} + v_j \frac{\partial v_i}{\partial x_j}\right) + \frac{\partial p_{ij}}{\partial x_j} = 0, \tag{4}$$

$$\rho\left(\frac{\partial u}{\partial t} + v_j \frac{\partial u}{\partial x_j}\right) + p_{ij}\frac{\partial v_i}{\partial x_j} + \frac{\partial q_j}{\partial x_j} = Q. \tag{5}$$

In a mixture it must be emphasized that the fluid velocity v_i is *defined* so that ρv_i is the momentum per unit volume (else (1) would not hold); thus, v_i is the mean velocity of all the molecules and free atoms weighted according to their respective masses; for this reason Chapman & Cowling (1952) call it the 'mass velocity'. Also, p_{ij} is the flow of the x_i-component of momentum in the x_j-direction per unit area, u is the energy per unit mass, and q_j is the flow of energy in the x_j-direction per unit area, provided that in each case 'momentum' and 'energy' signify their values in a frame of reference in which the local momentum density is zero—that is, in a frame moving with fluid velocity v_i. In the *original* frame of reference the momentum flow is $\rho v_i v_j + p_{ij}$, the energy per unit mass $u + \frac{1}{2}v_i^2$, and the energy flow $\rho v_j(u + \frac{1}{2}v_i^2) + p_{ij}v_i + q_j$, as was already implied in equations (2) and (3).

Since there are only five independent equations, and ρ, u and v_i are five unknowns, the equations are soluble only if one has expressions for the compressive-stress or momentum-transport tensor p_{ij}, and the heat-flow or energy-transport vector q_j, in terms of ρ, u and v_i and their derivatives. These expressions have to be inferred from the kinetic theory of gases. The manner of their inference (see Chapman & Cowling 1952; Hirschfelder, Curtiss & Bird 1954) is sufficiently well known in general, except perhaps for one point: there has been confusion about the mean $p_m = \frac{1}{3}p_{ii}$ of the diagonal elements of the stress tensor, and whether this should bear the same relation to ρ and u as it does in exact equilibrium (when p_m is simply the pressure). The true situation (discussed at length, for example, in Lighthill 1956; see also Appendix B and p. 503 of the books just cited) is that this is so for monatomic gases, but that for others changes in the specific internal energy u lag behind changes in the translational part of it (which can be written

$3p_m/2\rho$). Fortunately this effect, although crucial in the theory of acoustic attenuation, is of little importance in the theories of frictional drag and heat transfer, in which transport takes place through a 'boundary layer' where diagonal terms in p_{ij} make a much smaller contribution to the equations of motion than off-diagonal terms.

4. Momentum transport in a dissociating gas

The momentum flow p_{ij} depends only on the translational motion of the molecules and atoms, and may therefore be expected to be the same as for a mixture of monatomic gases with the same molecular weights. For this, the kinetic theory gives

$$p_{ij} = p_m \delta_{ij} - \mu \left(\frac{\partial v_i}{\partial x_j} + \frac{\partial v_j}{\partial x_i} \right) + \tfrac{2}{3} \mu \frac{\partial v_k}{\partial x_k} \delta_{ij}, \tag{6}$$

where δ_{ij} is 1 when $i = j$ and 0 otherwise.

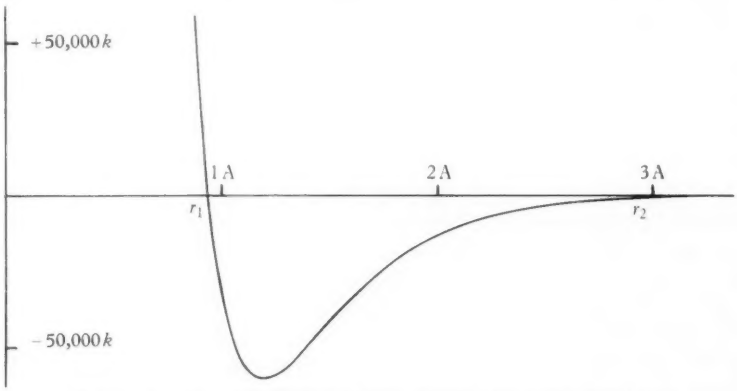

FIGURE 1. Potential energy of two oxygen atoms as a function of the distance between their nuclei.

Here, μ is the viscosity of the mixture, which is a function of the translational temperature and of α, the concentration of free atoms. Formulas exist, for example, equation (12.5.1) of Chapman & Cowling 1952, relating μ to the viscosities of the pure constituents. If the latter differ only slightly, the formula cited shows that the viscosity of the mixture must be close to those of the separate consituents.

Now, although no actual measurements of the viscosity of both A and A_2 for any element A are known to the author, it is unlikely that they differ much. While the higher molecular weight of A_2 tends to make its viscosity greater by a factor $\sqrt{2}$, its larger collision cross-section works the other way, reducing the viscosity by the cross-section ratio, a factor probably not greatly different from $\sqrt{2}$. Note that the cross-section for collision of two A atoms is not rendered large by their strong chemical attraction for one another. The potential energy of attraction as a function of the internuclear distance r takes a form like that illustrated in figure 1 for oxygen. For $r_1 < r < r_2$ the potential energy is negative, and very

large compared with the typical molecular translational energy kT. Most collisions therefore take the form illustrated in figure 2 and do not differ much from collisions of hard spheres of diameter r_2. Any increase of cross-section above the resulting value πr_2^2, due to the longer-range van der Waals forces, could be represented by a Sutherland-type factor $1+S/T$ and would be small at high temperatures (when, indeed, the cross-section will fall somewhat below πr_2^2 as the 'effective' sphere becomes softer). Since r_2 is about 2·8 Å and the collision diameter of O_2 is 3·4 Å this points to a ratio of the order of $\sqrt{2}$ in the cross-sections.*

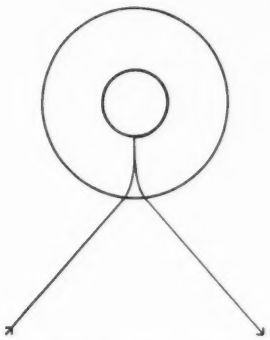

FIGURE 2. Typical collision between two oxygen atoms. Only the motion of one nucleus relative to the other is shown, the position of the latter being taken at the centre of the circles, which have the radii r_1 and r_2 defined in figure 1.

Hence, in the absence of better information, it is reasonable to obtain μ by simply extrapolating the measured viscosity of A_2 to the high temperatures with which we are concerned. By their theoretical work and comparisons with experiment for the '(13, 7)' molecular model, Hirschfelder, Bird & Spotz (1948, 1949) have established that it is reasonable to assume $\mu \propto T^{\frac{3}{4}}$ at high temperatures in making this extrapolation.

The difference between p_m and the equilibrium pressure p associated with the local values of ρ and u will be touched on in § 7 but not elaborately treated, as the difference is unimportant in boundary-layer theory.

5. Energy transport in a dissociating gas

The heat-flow vector q_j takes a complicated form, because, in addition to the direct transfer of translational energy of molecules and atoms, and rotational and vibrational energy of molecules, down the temperature gradient (that is, the heat-conduction term), there are also terms due to the interdiffusion of molecules and atoms, as follows:

(i) Each free atom may be regarded as carrying internal energy $\frac{1}{2}D$, in addition to its translational energy (Part 1, § 2.3).

(ii) Each molecule, on the other hand, carries some rotational and vibrational energy, on the average $\frac{3}{2}kT$ for the 'ideal dissociating gas' of Part 1.

* Similarly, arguments for the cross-section for collision of A and A_2 to be about 80% of that for A_2 and A_2 are given by Lees (1956).

(iii) There is also what may be called the 'diffusion thermo-effect', although this expression is normally used (Chapman & Cowling 1952, p. 404) to include only a small part of the effect. Most of it is due to the fact that the average translational energy is the same for both molecules and atoms. Hence, at uniform temperature (or more generally, if the heat-conduction term, proportional to temperature gradient, is removed), one would expect no translational-energy transfer in a frame of reference in which the *unweighted* average velocity of all particles is zero. The fact that we are, instead, interested in energy transfer in a frame of reference in which the average *momentum* is zero leads to a term in q_j equal to $\frac{5}{2}kT$ times the number of particles per unit volume, times the relative velocity of these two frames. An additional term (the diffusion thermo-effect in the sense of Chapman, which depends closely on the law of force between the molecules) is present (see (8) below) but is only about 10 % of the former term.

Conversely, the *rate* of interdiffusion depends (i) on the concentration gradient, (ii) on the pressure gradient, (iii) on the temperature gradient, although the last effect (thermal diffusion) is small. Hence ten terms in all are present in the heat-flow vector q_j—the conduction term, and all combinations of the three kinds of diffusion with the three kinds of heat flow which result from diffusion. They are calculated as follows.

Let the momentum per unit volume of the molecules and atoms, respectively, in the frame of reference (moving with velocity v_i) in which the total momentum density is zero, be M_i and $-M_i$. Then equation (8.4.7) of Chapman & Cowling 1952, rewritten in our notation, becomes

$$M_i = \rho D_{12}\left\{\frac{\partial \alpha}{\partial x_i} + \tfrac{1}{2}\alpha(1-\alpha^2)\frac{\partial \log p_m}{\partial x_i} + \alpha(1-\alpha)\,\alpha_T\frac{\partial \log T}{\partial x_i}\right\}, \tag{7}$$

where D_{12} is the mutual diffusion coefficient for the atoms and molecules, T is the translational temperature, and α_T the 'thermal diffusion factor' (called α in Chapman & Cowling, 1952, p. 399). The heat-flow vector includes the terms described in the first paragraph of this section, namely,

$$q_i = -\lambda\frac{\partial T}{\partial x_i} + M_i\left\{-\frac{D}{2m} + \frac{\frac{3}{2}kT}{2m} - \frac{\frac{5}{2}kT + 2\alpha_T kT/(1+\alpha)}{2m}\right\}, \tag{8}$$

where λ is the thermal conductivity of the binary mixture. The last term in curly brackets represents the diffusion thermo-effect, and has the form given because the unweighted sum of the velocities of the molecules and free atoms (all measured relative to v_i) is $M_i/2m - M_i/m = -M_i/2m$ per unit volume. Substitution of (7) in (8) yields the stated ten terms, whose further simplification is postponed to § 7.

6. Values of diffusivity ratios

Relations between the viscosity μ, the conductivity λ and the diffusivity D_{12} for a binary mixture have been much discussed, usually in terms of the ratios between the 'diffusivity of momentum' $\nu = \mu/\rho$, the 'diffusivity of heat' $\kappa = \lambda/\rho c_p^f$ (where c_p^f is the specific heat at constant pressure of the mixture, when

supposed of fixed composition—in other words, without any change of α with T), and D_{12}. Their ratios are called Prandtl number, Schmidt number and Lewis number, which respectively are

$$\sigma = \frac{\nu}{\kappa} = \frac{\mu c_p^f}{\lambda}, \quad S = \frac{\nu}{D_{12}} = \frac{\mu}{\rho D_{12}}, \quad L = \frac{D_{12}}{\kappa} = \frac{\sigma}{S} = \frac{\rho c_p^f D_{12}}{\lambda}. \tag{9}$$

The variation of Prandtl number is small, from about 0·71 when $\alpha = 0$ (diatomic gas) to about 0·67 when $\alpha = 1$ (monatomic gas). Intermediate values occur for intermediate α, as the following 'Eucken-type' argument indicates for the ideal dissociating gas. Kinetic theory shows that the diffusivity of translational energy is about $2{\cdot}5\,\nu$ (such energy being much better correlated with speed of diffusion in a given direction than is a momentum component in a direction at right angles). One expects the diffusivity of rotational and vibrational energy, on the other hand, to be intermediate between ν and $D_{22} \doteqdot 1{\cdot}4\nu$, the coefficient of self-diffusion of molecules through one another; this is because (Lighthill 1956, p. 259) such energies 'persist' for more collisions than does a momentum component, but for less than does the identity of a molecule. With the value of $1{\cdot}25\nu$ for this diffusivity, we get

$$\lambda = (2{\cdot}5\nu)\frac{\rho(1+\alpha)}{2m}(\tfrac{3}{2}k) + (1{\cdot}25\nu)\frac{\rho(1-\alpha)}{2m}(\tfrac{3}{2}k), \tag{10}$$

where $\frac{3}{2}k$ is the addition, per unit temperature rise, either to the translational energy per particle, or to the combined rotational and vibrational energy per molecule, while $\rho(1-\alpha)/2m$ is the number-density of molecules and $\rho(1+\alpha)/2m$ that of all particles. Since, by Part 1, equations (14) and (20),

$$c_p^f = \left[\frac{\partial}{\partial T}\left(u + \frac{p}{\rho}\right)\right]_{\alpha\ \text{constant}} = \frac{k}{2m}(4+\alpha), \tag{11}$$

we deduce that

$$\kappa = \frac{\lambda}{\rho c_p^f} = \tfrac{3}{2}\nu\,\frac{2{\cdot}5(1+\alpha) + 1{\cdot}25(1-\alpha)}{4+\alpha}, \tag{12}$$

whence $\sigma = \nu/\kappa$ varies monotonically from 0·71 when $\alpha = 0$ to 0·67 when $\alpha = 1$.

It is sometimes suggested that Schmidt number and Lewis number also remain closely constant, and a value $S \doteqdot 0{\cdot}5$ (corresponding to $L \doteqdot 1{\cdot}4$), as proposed by Lees (1956) from arguments for *small* α only, and supported for small α by the detailed expressions of Chapman & Cowling (1952), and by experimental results, has been used. Fay & Riddell (1958), for example, adopt the hypothesis of constant L in their boundary-layer calculations; admittedly, they had to assume something, and chose three values (1, 1·4 and 2) for the constant to see how dependent on L the results were; the experimental observations of Rose & Stark (1958) show best agreement with the calculations for $L = 1{\cdot}4$, although the others too lie within the experimental scatter.

On the other hand, theory indicates that S can vary almost by a factor of 2. This is because in a binary mixture the product pD_{12} is closely a function of temperature alone, independent of composition. (This result is exact to the 'first approximation' of Chapman & Cowling 1952, from which the higher approxima-

tions differ only slightly.) Hence, if μ also is almost independent of composition, then

$$\frac{S}{1+\alpha} = \frac{\mu}{\rho(1+\alpha)\,D_{12}} = \frac{\mu kT}{2m(pD_{12})} \tag{13}$$

also is, indicating that S is closely proportional to $(1+\alpha)$ at a given temperature, and therefore rises from its value around 0·5 for $\alpha = 0$ to a value around 1·0 for $\alpha = 1$. (Compare the observed value $S = 0{\cdot}9$ for a mixture of N_2 and CO_2 when the concentration of the lighter gas approaches 1.) In this case, $L = \sigma/S$ varies closely like $(1+\alpha)^{-1}$, from around 1·4 for $\alpha = 0$ to around 0·7 for $\alpha = 1$.

To sum up, L and S do not remain nearly so constant as σ, although, from a qualitative point of view, the important conclusion is that all the diffusivity ratios remain of order 1.

7. Quasi-equilibrium theory of convective heat transfer

In the quasi-equilibrium theory, equations (7) and (8) are simplified by replacing α, p_m and T by their equilibrium values. In the light of the discussion of diffusivity ratios, we can estimate the accuracy of this approximation as follows.

It is α which is most likely to lag behind its equilibrium value α_{eq} for given density ρ and translational temperature T, so causing u and p_m also to lag. (By contrast, the translational and rotational energies adjust in a few collisions, and we have excluded consideration of variable excitation of vibrational energy.) Now, the equation describing small departures of α from α_{eq} is

$$\rho\left(\frac{\partial\alpha}{\partial t} + v_i\frac{\partial\alpha}{\partial x_i} + \frac{\alpha-\alpha_{eq}}{\tau}\right) = \frac{\partial M_i}{\partial x_i}, \tag{14}$$

where τ is a 'relaxation time' (see, for example, Lighthill 1956) for dissociation and recombination, and the right-hand side represents the effect of diffusion. Writing (14) as

$$\alpha = \alpha_{eq} - \tau\left(\frac{\partial\alpha}{\partial t} + v_i\frac{\partial\alpha}{\partial x_i}\right) + \frac{\tau}{\rho}\frac{\partial}{\partial x_i}\left\{\rho D_{12}\left(\frac{\partial\alpha}{\partial x} + \text{p.a.t.t.}\right)\right\}, \tag{15}$$

where p.a.t.t. means 'pressure and temperature terms', we see that for α to remain close to α_{eq} the relaxation time τ must satisfy two conditions:

(i) For the second term on the right of (15) to be small compared with α_{eq}, τ must be small compared with the time in which α_{eq} changes by a substantial fraction of itself *along the path of a fluid particle*.

(ii) If δ is the least distance in *any* direction in which α changes by a substantial fraction of itself, then, for the third term on the right of (15) to be small, τ must be small compared with δ^2/D_{12}.

In a boundary layer, for example, δ would be the thickness and δ^2/D_{12} a typical time of diffusion across the layer. Since all diffusivities are of the same order of magnitude (§ 6), the thickness δ must adjust itself so that this time is of the same order as a typical convection time, so that conditions (i) and (ii) are in this case substantially identical, and equivalent to that already imposed in Part 1, § 3·1, that τ be small compared with the typical time-scale for flow past the body. We continue to make this assumption throughout Part 2.

In particular, the equilibrium relationships between ρ, u, α, p_m and T are freely used to simplify (7) and (8). Because those equations describe already 'small' effects of deviations from equilibrium, this procedure involves an error of the order of the squares of those deviations. One could not similarly replace p_m by its equilibrium value in (6), where it appears as the zero-order term. However, as has already been pointed out, the term in (6) due to the departure of p_m from equilibrium *is* negligibly small in a boundary layer, and so the difficulty of estimating it need not worry us here.

Now it follows from Part 1, equations (13) and (14), that in any change between states of equilibrium

$$d\alpha + \tfrac{1}{2}\alpha(1-\alpha^2)\,d\log p - \tfrac{1}{2}\alpha(1-\alpha^2)\left(\frac{D}{kT}+1\right)d\log T = 0. \tag{16}$$

Accordingly, the concentration-gradient and pressure-gradient terms can both be eliminated from (7), giving

$$M_i = \rho D_{12}\,\tfrac{1}{2}\alpha(1-\alpha^2)\left(\frac{D}{kT}+1+\frac{2\alpha_T}{1+\alpha}\right)\frac{\partial \log T}{\partial x_i}, \tag{17}$$

whence by (8)

$$q_i = -\left\{\lambda + \frac{D_{12}\rho k\alpha(1-\alpha^2)}{4m}\left(\frac{D}{kT}+1+\frac{2\alpha_T}{1+\alpha}\right)^2\right\}\frac{\partial T}{\partial x_i}. \tag{18}$$

Equation (18) gives a check that, as required by the second law of thermodynamics, no heat flow occurs on the quasi-equilibrium theory when the temperature is uniform. It allows us to describe the heat transfer by means of a 'total thermal conductivity' λ_{tot}, equal to the contents of the curly brackets. The result of § 6, that the Lewis number $L = \rho k(4+\alpha)\,D_{12}/2m\lambda$ is of order 1, indicates that, when D/kT is large and α is not very close to 0 or 1, λ_{tot} is much greater than λ; in other words, interdiffusion is responsible for the bulk of the heat transfer. Note also that the term involving Chapman's 'thermal diffusion factor' α_T, which (Grew & Ibbs 1952) is less than 0·2 for constituents with mass-ratio 2, is quite negligible compared with the large term D/kT.

It is important that the great increase which dissociation produces in the effective thermal conductivity, that is, in the rate of heat transfer down a given temperature gradient, is accompanied by a similar increase in specific heat, in such a way that the rate of heat transfer down a given *enthalpy* gradient (which is what matters in boundary-layer theory) is little altered. The 'total' specific heat at constant pressure includes a term additional to (11), due to the variation of α with T as specified in (16), and is

$$c_p = c_p^f + \frac{k\alpha(1-\alpha^2)}{4m}\left(\frac{D}{kT}+1\right)^2. \tag{19}$$

The effective Prandtl number

$$\sigma_{\text{tot}} = \frac{\mu c_p}{\lambda_{\text{tot}}}, \tag{20}$$

which compares λ_{tot}/c_p (the rate of heat transfer down a given enthalpy gradient) with μ, is therefore

$$\sigma_{\text{tot}} = \frac{\mu c_p^f + \mu(k/4m)\,\alpha(1-\alpha^2)\,(D/kT+1)^2}{\lambda + D_{12}\rho(k/4m)\,\alpha(1-\alpha^2)\,(D/kT+1)^2} \tag{21}$$

if the negligibly small thermal-diffusion term in (18) be neglected. Clearly, (21) lies always between $\mu c_p^f/\lambda = \sigma = 0{\cdot}7$ and $\mu/D_{12}\rho = S$, which in turn varies between 0·5 and 1. Accordingly, the effective Prandtl number σ_{tot} lies always between these latter limits, and hence is not greatly changed by dissociation; whence, the structure of the quasi-equilibrium boundary layer, which depends on the relation of heat transfer to enthalpy gradient, not temperature gradient, is also not much changed.

8. Radiative equilibrium

We pass now to transport by radiation in a dissociating gas. It is likely that most aerodynamic readers will be helped by a brief summary of the general theory of radiative transfer, beginning with the concept of radiative equilibrium.

Photons of frequency between ν and $\nu+d\nu$ can be in equilibrium in volume V with matter at temperature T if their total energy is

$$\frac{8\pi V\nu^2 d\nu}{c^3}\,\frac{1}{e^{h\nu/kT}-1}\,h\nu = Ve_\nu d\nu, \tag{22}$$

where the first factor on the left is the total number of states of such photons in volume V, the second is the Maxwell–Boltzmann factor as modified (Bose–Einstein) to allow for the indistinguishability of the particles,* and the third is the energy per photon. The total energy integrated over all frequencies is aVT^4, where

$$a = \frac{8\pi^5 k^4}{15c^3h^3} = 7{\cdot}67\times10^{-15}\,\text{ergs/cm}^3/(^\circ\text{K})^4 \tag{23}$$

is the Stefan–Boltzmann constant. When the matter with which the radiation is in equilibrium is a perfect gas filling the volume V, the term aVT^4 must be regarded thermodynamically as a contribution to the internal energy U of the gas; but even for gas at 10,000 °K and as low a density as 10^{-6} g/cm^3, it is less than 2 cal/g (while $u > 5000$ cal/g for O_2 or N_2 under these conditions), and so it could reasonably be neglected in the discussion of equilibrium thermodynamics in Part 1, § 2. On the other hand, the high velocity c of photons means that the associated rate of heat transfer across unit area, namely

$$\tfrac{1}{4}acT^4 = 5{\cdot}7\times10^{-5}T^4\,\text{ergs/cm}^2/\text{sec}, \tag{24}$$

can be extremely large (for example, 57 kW/cm^2 when $T = 10{,}000$ °K).

The equilibrium just described, if it exists, is maintained by a balance between the absorption of photons by molecules (which are raised by such absorption to states of higher rotational, vibrational or electronic energy,† or to dissociated or ionized states), and the emission of photons in the processes inverse to these (including processes which involve recombination). The balance between absorp-

* This modification makes little difference below, where we are concerned principally with values of $h\nu/kT$ for which $e^{h\nu/kT} \gg 1$. Then practically no two photons are in the same state, and so their indistinguishability is irrelevant, like that of the molecules in the statistical mechanics of a perfect gas.

† Not of translational, because of the very high energy-momentum ratio ($= c$) of photons.

tion and emission when the equilibrium number of photons is present can be expressed by the equation

$$(c\alpha_\nu)\, V e_\nu d\nu = V E_\nu d\nu, \tag{25}$$

where $c\alpha_\nu$ is the proportion of photons with frequency between ν and $\nu + d\nu$ which are absorbed by the gas per unit time (so that α_ν is the proportion of the energy in a light beam of this frequency which is absorbed per unit *distance*) and $VE_\nu d\nu$ is the energy emitted in volume V per unit time in the form of such photons.

Clearly, equilibrium of the kind described is achieved (even approximately) only if the gas is in an approximately uniform state throughout a region with linear dimensions $\gg 1/\alpha_\nu$, so that almost all the energy reaching a point has been emitted at points where the gas is in nearly the same state. Now, for every gas there are important frequency ranges in which $1/\alpha_\nu$ is comparable with 1 km (though in other ranges it may be a small fraction of 1 mm). Hence, there can be no question of assuming radiative equilibrium in projectile problems.

9. Quasi-equilibrium radiation theory

We may, however, adopt a quasi-equilibrium theory, as in the earlier sections, in which the atoms and molecules of the gas are assumed to be very nearly in equilibrium among themselves. Then the absorption coefficient α_ν (which depends only on the state of the atoms and molecules) must be the same as when equilibrium with radiation is also present, and so must the emission rate E_ν. In particular, the relation between them,

$$E_\nu = c\alpha_\nu e_\nu = \frac{8\pi h\nu^3}{c^2(e^{h\nu/kT} - 1)}\alpha_\nu \tag{26}$$

(see (22) and (25)), must still be satisfied.

On the other hand, the local density of radiation energy, say f_ν, may be totally different from e_ν because much of the radiation reaching a point comes from where the gas is in a quite different state. In consequence, the absorption rate, $A_\nu = c\alpha_\nu f_\nu$ per unit volume per unit time, will differ from the emission rate E_ν; their difference, integrated over all frequencies, is

$$Q = \int_0^\infty Q_\nu d\nu = \int_0^\infty (A_\nu - E_\nu)\, d\nu, \tag{27}$$

the 'heat input rate' (per unit volume) of equation (3).

This local energy density f_ν may be calculated by geometrical optics if the spatial distribution of gas density and temperature (and hence of E_ν) be known, provided that photons move almost in a straight line between emission and absorption, that is, provided that scattering can be neglected. Rayleigh scattering is in fact quite negligible over distances of the order of 1 m, and Raman scattering (in which a photon is scattered as a photon of different frequency) by any atomic process occurs at a much lower rate than does absorption by the same process (because absorption is a first-order perturbation of the steady state, and Raman scattering is a second-order perturbation), so that it can be neglected over lengths in which only moderate absorption occurs. Refraction by inequalities of

density, again, leaves the light rays with a radius of curvature of at least 3000 times the distance in which the density changes by 1 mg/cm^3 (for all common gases except H_2, for which the factor is about 600), and deflexions due to this are negligible in the gas flow about a projectile; as an extreme case of high density gradient, a shock wave can reflect glancing rays as in a mirage, but it reflects only those few which make an angle less than $1{\cdot}5\,(\Delta\rho)^{\frac{1}{2}}$ degrees with it, where $\Delta\rho$ is the density change across the shock in mg/cm^3. Accordingly, simple geometrical optics will be used in what follows.

Then $f_{\nu P}$, the energy density at a point P, may be written as

$$f_{\nu P} = \frac{1}{c}\int_0^\infty \int_0^{4\pi} E_\nu(r, \Omega)\,\frac{1}{4\pi r^2}\,e^{-\tau_\nu(r,\Omega)}\,r^2\,dr\,d\Omega, \tag{28}$$

where $E(r, \Omega)$ signifies the emission rate at a distance r from P along a thin cone (identified by the symbol Ω) which subtends solid angle $d\Omega$ at its apex P, and the integral represents the intensity (or energy flux) $cf_{\nu P}$ by summing the effect of emission from all points of space,* after attenuation by the spherical factor $1/4\pi r^2$ and by an exponential factor $e^{-\tau_\nu}$ due to absorption all along the said cone. Here,

$$\tau_\nu(r, \Omega) = \int_0^r \alpha_\nu(r, \Omega)\,dr, \tag{29}$$

which is usually described as the 'optical depth' (for frequency ν) of the light path.

By (26) and (28) we may write the heat input rate Q_ν per unit frequency band (see (27)) at P as

$$\begin{aligned} Q_{\nu P} &= c\alpha_{\nu P}(f_{\nu P} - e_{\nu P}) \\ &= c\alpha_{\nu P}\left\{\frac{1}{4\pi}\int_0^{4\pi} d\Omega \int_0^\infty e_\nu(r, \Omega)\,\alpha_\nu(r, \Omega)\,e^{-\tau_\nu(r,\Omega)}\,dr - e_{\nu P}\right\}, \end{aligned} \tag{30}$$

or, changing one of the variables of integration from r to τ_ν, as

$$Q_{\nu P} = c\alpha_{\nu P}\left(\frac{1}{4\pi}\int_0^{4\pi} d\Omega \int_0^\infty e_\nu e^{-\tau_\nu}\,d\tau_\nu - e_{\nu P}\right), \tag{31}$$

a simple expression which in particular makes it obvious that $Q_{\nu P}$ vanishes (as thermodynamics requires) when the temperature (and therefore also e_ν, which is a function of temperature and frequency alone) is uniform.

From (31), the heat input rate Q (see (3) and (27)), which represents the sole effect of radiation on the hydrodynamical equations, can be estimated. The solution of those equations would then give the heat-flow vector q_i, and particularly its component normal to the surface of the body. This represents heat transfer to the surface (which from a practical point of view is perhaps the most important thing to predict) by direct collision of gas molecules with the surface. The total heat transfer to the surface, however, will include another term, the direct radiative transfer, which therefore is considered next.

* On how to treat the parts of space not occupied by the gas, see § 10.

10. Radiative properties of the body surface

If P is a point on the body surface, then the integral in (28) (the undirected intensity at P) can be made to represent the flow of radiation into the surface if the integrand is multiplied by $\cos\theta$. Here, θ is the angle that the ray-cone specified by Ω makes with the outward normal to the surface, and indeed one could write $\Omega = (\theta, \lambda)$, where $d\Omega = \sin\theta\, d\theta\, d\lambda$ and (r, θ, λ) are spherical polar co-ordinates centred on P.

Hence, the rate of radiative transfer into the surface, say q_ν per unit area of surface per unit frequency band, is

$$q_\nu = \frac{1}{4\pi}\int_0^{4\pi} \cos\theta\, d\Omega \int_0^\infty E_\nu\, e^{-\tau_\nu}\, dr = \frac{c}{4\pi}\int_0^{4\pi} \cos\theta\, d\Omega \int_0^\infty e_\nu\, e^{-\tau_\nu} d\tau_\nu, \tag{32}$$

where we have again applied the transformation leading to (31). This q_ν represents heat transferred to the surface when the latter is perfectly absorbent, that is, when it scatters or reflects radiation of frequency ν to a negligible extent. Since in the integral one may take $e_\nu = e_{\nu P}$ for $\theta > \frac{1}{2}\pi$, because on each ray pointing into the surface the optical depth τ_ν becomes effectively infinite before the temperature has changed significantly, we may write

$$q_\nu = \frac{c}{4\pi}\int_0^{2\pi} d\lambda \int_0^{\frac{1}{2}\pi} \cos\theta \sin\theta\, d\theta \int_0^\infty (e_\nu - e_{\nu P})\, e^{-\tau_\nu}\, d\tau_\nu, \tag{33}$$

or else

$$q_\nu = \frac{c}{4\pi}\int_0^{2\pi} d\lambda \int_0^{\frac{1}{2}\pi} \cos\theta \sin\theta\, d\theta \int_0^\infty e_\nu\, e^{-\tau_\nu}\, d\tau_\nu - \tfrac{1}{4} c e_{\nu P}, \tag{34}$$

forms which are both useful.

If, however, a surface scatters, or specularly reflects, a fraction $1 - \epsilon_\nu$ of the energy of frequency ν which is incident upon it, then the first term in (34) must be reduced by the factor ϵ_ν to give the rate of energy absorption. The second term, representing energy emitted from the surface, which is subtracted to give the net rate of heat transfer, must also be multiplied by ϵ_ν, on the thermodynamic argument that q_ν must still vanish in the particular case when the gas outside the surface is all at the same temperature as the surface (so that $e_\nu = e_{\nu P}$). Accordingly, the factor ϵ_ν, by which expressions (33) and (34) for q_ν must both be multiplied if they are to apply for a general surface, is usually called the 'emissivity' of the surface (for frequency ν).

We note also the modifications to (31) due to the presence of a solid surface. For a perfectly absorbent surface, which the ray-cone Ω meets at a point S, one may take $e_\nu = e_{\nu S}$ for all $\tau_\nu \geqslant \tau_{\nu S}$, as in the arguments leading to (33). For a surface of reduced emissivity, however, this part $\tau_\nu \geqslant \tau_{\nu S}$ of the integral, representing emission from the surface, must be multiplied by ϵ_ν. In this case, there remains the problem of including the effect at P of the fraction $(1 - \epsilon_\nu)$ of energy, incident on each point of the surface, which is scattered or specularly reflected.

If all the incident energy were specularly reflected, the problem could be treated by including virtual images inside the body as in geometrical optics. Then in (31), along each ray which enters the body, one would have to take the

distribution of e_ν with τ_ν which corresponds actually to the reflected ray. One would multiply the contribution so obtained by $(1-\epsilon_\nu)$, because at most the unabsorbed energy can be reflected, and add it to that discussed in the last paragraph, namely, ϵ_ν times the contribution obtained by putting $e_\nu = e_{\nu S}$ for $\tau_\nu \geqslant \tau_{\nu S}$.

This is probably a sufficiently good approximation also for the more realistic case when a proportion of the unabsorbed energy is scattered, since, with a diffuse source like the hot gas around a projectile, the effects of scattering and reflexion do not differ greatly. Accordingly, the complications of a more accurate scattering theory (which include variability of the proportions of scattered and reflected radiation with angle of incidence) are not worth introducing.

11. Absorption spectra of pure diatomic gases

We must now discuss the factors governing the dependence of the absorption coefficient α_ν on ν, ρ and T for any particular diatomic gas. We work with α_ν instead of E_ν (which by (26) is simply related to α_ν) largely because experimental evidence is more reliable for α_ν, especially at the higher frequencies, for which e_ν (and hence also E_ν) is extremely small at experimentally convenient temperatures.

Normally, for fixed ν and T, α_ν is directly proportional to the density ρ (Beer's law), implying that the absorption results solely from interactions between photons and isolated molecules or atoms. Interactions with such pairs of molecules as happen to be in collision at a particular instant causes slight frequency shifts ('pressure broadening'), but the value of α_ν, if taken smoothed over suitable frequency intervals to allow for this, is usually unaffected. Occasionally interactions of this sort make possible absorptions which are quite absent in a unimolecular process; in such a case α_ν becomes a quadratic function of ρ.

When Beer's law applies, a good approximation to α_ν (neglecting second-order perturbations of the steady state) is

$$\alpha_\nu \Delta\nu = \frac{8\pi^3\nu}{3ch} \sum_{\nu<(E_1-E_2)/h<\nu+\Delta\nu} M_{12}^2, \tag{35}$$

where the sum is over all the molecules in unit volume, and also, for each molecule (which we suppose to have energy E_2), over all those alternative *states* of the molecule whose energy E_1 satisfies the inequality noted. Here, M_{12} is the electric dipole moment of the *transition* from state 2 to state 1. This is defined in wave mechanics as the product of the wave functions of the two states, multiplied by the electric moment of the configuration of the electrons and the nuclei, and integrated with respect to all the co-ordinates of those particles.

Now, for most pairs of states 1 and 2, M_{12} is zero. Transitions between two such states are described as 'forbidden'. It should be emphasized that 'forbidden transitions' are not completely absent; they can be observed spectroscopically, but because they involve at least second-order perturbations of the steady state (or quadrupole instead of dipole radiation) they are too infrequent to be energetically important.

States 1 and 2 may differ as regards both the rotational and vibrational state of the molecule and its electronic configuration. For homonuclear molecules, A_2, transitions between states differing only with respect to rotation and vibration are all forbidden. This is because the product of the electronic wave functions for the two states is even with respect to reflexion in the centre of symmetry.

Absorption therefore depends on a transition from a low electronic state (usually the lowest) to a higher one, although again the majority of such transitions are forbidden, owing to considerations regarding oddness or evenness of wave functions, or more complicated considerations concerned with changes in the dependence of the electronic wave functions on the angular variables. These latter considerations affect also what changes in the rotational state of the molecule as a whole are possible at a permitted transition, and the analysis of the rotational structure of the absorption bands is correspondingly complicated. If, however, one is willing to ignore this detailed line structure, one has the simple rule that in any permitted transition to a higher electronic state each of the rotational states of the unexcited molecule leads on the average to exactly one possible rotational state of the excited molecule (all other transitions being forbidden). This follows, for example, from Weizel (1931), equation (199).

Transitions between particular vibrational states of the unexcited and excited molecules are never forbidden, but the values of M_{12}^2 vary greatly for the different transitions. On the crude but valuable Born–Oppenheimer approximation, in which the wave function of a complete state of the molecules is expressed as a vibrational wave function, say $\psi_v(r)$, multiplied by a function independent of the internuclear distance r, we can write

$$M_{12} = M \int_0^\infty \psi_{v1}(r)\, \psi_{v2}(r)\, dr = M P_{12}, \tag{36}$$

where M is the electric dipole moment of the electronic transition (obtained by carrying out the integration in M_{12} with respect to all the variables except r) and the 'overlap integral' P_{12} lies between -1 and $+1$ because both ψ_{v1} and ψ_{v2} satisfy the normalization condition

$$\int_0^\infty \psi_v^2(r)\, dr = 1. \tag{37}$$

Clearly, P_{12} must be very small if the regions where $\psi_{v1}(r)$ and $\psi_{v2}(r)$ are non-small (corresponding in classical mechanics to the intervals of oscillation) do not overlap. On the contrary, P_{12} is fairly large when peaks of $\psi_{v1}(r)$ and $\psi_{v2}(r)$ coincide. The largest peaks are near the extreme positions of the vibration (in the classical sense) and so transitions between states which have one of their extreme positions in common are particularly frequent (the Franck–Condon principle).*

Often, it is useful to know that, for a fixed vibrational state E_1, the sum $\sum_{E_2} P_{12}^2$, over all possible vibrational states E_2 of the molecule in its electronic state 2, is

* Originally interpreted by saying that a vibrating system spends most of its time near its extreme positions, so that a transition at such a time (when the kinetic energy of the nuclei is small) is the most probable.

equal to unity. Similarly, for fixed E_2, the sum $\sum_{E_1} P_{12}^2$ over all possible E_1 is unity. Mathematically, this follows from a theorem on orthogonal functions; and, physically, from the interpretation of P_{12}^2 as a 'transition probability'.

12. Absorption by oxygen

Oxygen illustrates well the principles set out in § 11, and has been particularly closely studied. The lowest stable electronic state is $^3\Sigma_g^-$ (in the usual notation; see, for example, Gaydon 1953), and transitions to the next three stable states ($^1\Delta_g$, $^1\Sigma_g^+$, and $^3\Sigma_u^+$) are forbidden. Absorption due to these transitions is very weak (although the extremely thick layer of oxygen separating us from the sun enables two of them to be observed, and Herzberg has observed the third by special means). The first permitted transition (Schumann–Runge) is to a state $^3\Sigma_u^-$.

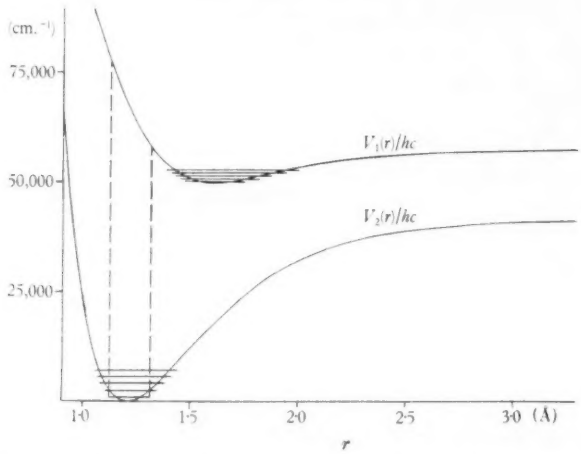

FIGURE 3. Graphs of the potential energies $V_2(r)$ and $V_1(r)$, of (respectively) the lowest electronic state of O_2, and the next excited state such that transitions to it are not 'forbidden'. Horizontal segments show the first five vibrational energy levels of each state.

Figure 3 shows 'potential energy curves', that is, graphs of the energy V of the electronic and nuclear arrangement as a function of the internuclear distance r, for the lowest electronic state $^3\Sigma_g^-$ of O_2 and for this higher state $^3\Sigma_u^-$. (The lower curve was already given in figure 1, but the zero of V was there taken as the value for $r \to \infty$, not as the minimum of the curve.) In each case the relative vibration of the nuclei is exactly equivalent to the vibration of a single particle of mass $\frac{1}{2}m$ (the 'reduced mass') on such a potential curve. The five lowest vibrational states, both of the unexcited and of the excited molecule, are shown in the figure as horizontal segments each at the appropriate energy level, whose lengths indicate the intervals of r in which the corresponding wave function is non-small.

Figure 3 shows that absorption from the lowest vibrational state (which is all the absorption that is significant at room temperature) leads to a state with

energy above the dissociation energy even of the excited molecule. Thus, it produces dissociation (such dissociation by a photon being called 'photo-dissociation'), and the excess energy becomes translational energy of the products of dissociation, which consist of one atom in its lowest electronic state (that is, in one of the states of the triplet ^3P) and one atom in the next highest electronic state $^1D_2$.

Since translational energy states are very thickly spaced indeed, a continuum spectrum is found, over a frequency region corresponding to the variation in the vertical distance between the two potential curves above the 'horizontal segment' corresponding to the lowest vibrational state. In other words, $h\nu$ lies between the values given by the lengths of the two vertical broken lines in figure 3. On a wavelength scale, this region lies between 1300 and 1750 Å, and the absorption coefficient therein is very great. Ladenburg, Voorhis & Boyce (1932) found that it reached (at N.T.P.) a maximum of 480 cm^{-1} at 1450 Å, and in these experiments the theory that dissociation results from the absorption was confirmed by the fact that the O_2 gradually disappeared, probably by direct combination of the free O atoms with the material of the tube walls.

Stueckelberg (1932) obtained very satisfactory agreement with these experiments in a calculation using (35) and (36). To use (35), he gets a precisely defined spacing of the energy states in the 'continuum' region above the dissociation energy level by applying a boundary condition, say $d\psi_v/dr = 0$, at $r = R$, where R is large. The number R does not, however, appear in the answer, because the larger it is the smaller ψ_{v1} must be in the integral (36) if equation (37), with upper limit replaced by R, is to be satisfied. This cancels out the increased number of states 1 in the sum (35).

The wave function $\psi_{v1}(r)$ is approximated as an Airy function, involving two constants which initially are unknown, namely, the values of $V_1(r)$ and $V_1'(r)$ at $r = r_{e2}$, the minimum of $V_2(r)$. The integral (36) is then easily evaluated for the lowest vibrational state, being to good approximation a Gaussian curve. Stueckelberg next selects $V_1(r_{e2})$ and $V_1'(r_{e2})$ to make the frequency for maximum absorption and the spread of the curve of α_ν against ν agree with experiment, in which case the detailed shapes of the theoretical and experimental curves are also found to be in good agreement.

The values of $V_1(r_{e2})$ and $V_1'(r_{e2})$ so obtained were used to draw the upper part of the graph $V_1(r)$ in figure 3. The part below the dissociation energy level was taken as a 'Morse function', with parameters determined from the moment of inertia of the molecule and the spectroscopically derived vibrational levels. The fact that a smooth interpolation between the two is possible is valuable support for Stueckelberg's theory, as he points out. Finally, from the observed value, 480 cm^{-1}, of the maximum of α_ν, he infers the value of M for use in (36). After corrections in the Errata, this is

$$M^2 = 6 \times 10^{-36}\,\mathrm{g\,cm^5\,sec^{-2}}, \quad M = 0{\cdot}5\,\text{Å} \times (\text{electronic charge}), \tag{38}$$

which Stueckelberg suggests is reasonable in view of the physical interpretation of M and the dimensions of the molecule, whose equilibrium internuclear distance r_e is 1·2 Å in the unexcited state and 1·6 Å in the excited state.

13. Emission from a layer of oxygen

The data of § 12, with the formulas of §§ 10 and 11, can be used to predict the radiative heat transfer to the surface of a high-speed projectile flying through oxygen, which has been chosen as our illustrative example. For air, similar considerations would need to be applied to the other main constituents of the layer of hot gas around the projectile, notably nitrogen, NO and, at the highest speeds, ions.

For any frequency ν we may calculate first $\tilde{q}_\nu$, which we use to signify expression (34) for q_ν, with the last term (representing radiation from the surface) omitted, and with $e^{-\tau_\nu}$ replaced by 1. This $\tilde{q}_\nu$ is an upper bound for the rate of radiation absorption by the surface, being close to it if (i) the layer of hot gas is optically thin, so that τ_ν is negligibly small throughout it; (ii) the emissivity of the surface, by which (34) must be multiplied, is near 1; (iii) the surface is not so hot that it is radiating away much of the energy absorbed by it. Corrections to allow for (ii) or (iii) are of course straightforward, while we shall see that condition (i) is usually satisfied for the frequencies responsible for most of the radiation.

We can write

$$\tilde{q}_\nu = \frac{c}{4\pi}\int_0^{2\pi} d\lambda \int_0^{\frac{1}{2}\pi} \cos\theta \sin\theta \, d\theta \int_0^{\infty} e_\nu \alpha_\nu \, dr, \tag{39}$$

and if we approximate by taking the temperature T to be a function only of the distance z from the solid surface, we have $z = r\cos\theta$ and $e_\nu \alpha_\nu$ a function only of z and ν. Hence

$$\tilde{q}_\nu = \tfrac{1}{2} c \int_0^{\delta} e_\nu \alpha_\nu \, dz, \tag{40}$$

where δ is the thickness of the layer, and so the total radiative transfer to the surface has the upper bound

$$\tilde{q} = \int_0^{\infty} \tilde{q}_\nu \, d\nu = \int_0^{\delta} \hat{q}(z)\, dz, \tag{41}$$

where

$$\hat{q} = \tfrac{1}{2} c \int_0^{\infty} e_\nu \alpha_\nu \, d\nu \tag{42}$$

is the contribution in all frequencies per unit volume of gas.*

Substituting for e_ν from (22) (where the 1 in the denominator may be ignored compared with $e^{h\nu/kT}$), and for α_ν from (35) and (36), we obtain

$$\hat{q} = \Sigma \frac{32\pi^4 M^2}{3c^3} \nu^4 P_{12}^2 \, e^{-h\nu/kT}, \tag{43}$$

the sum being over all molecules in their lowest electronic state in a unit volume (the vibrational energy of the molecule being E_2), as well as over all vibrational levels E_1 of the upper electronic state, with $E_1 - E_2 = h\nu$. Now, the number of molecules per unit volume with vibrational energy E_2 is

$$\frac{\rho(1-\alpha)}{2m} e^{-E_2/kT} \left(1 - e^{-T_v/T}\right), \tag{44}$$

* The detailed optics of §§ 9 and 10 is unnecessary for obtaining (42), which simply states that the gas emits half its radiation towards the surface; but it is needed if more accurate estimates of heat transfer are to be attempted.

where T_v is 2230 °K for oxygen (Part 1, § 2.2). Hence the sum (43) can be replaced by

$$\hat{q} = \frac{32\pi^4 M^2 c}{3} \frac{\rho(1-\alpha)}{2m} (1 - e^{-T_v/T}) \sum_{E_1} \sum_{E_2} P_{12}^2 \left(\frac{E_1 - E_2}{hc} \right)^4 e^{-E_1/kT}, \tag{45}$$

where the summation is over all vibrational levels E_1 and E_2 of the excited and unexcited states.

Now, the values of P_{12}^2 are known (Fraser, Jarmain & Nicholls 1954) for the first four E_1 levels. For each one can obtain

$$\chi(E_1) = \sum_{E_2} P_{12}^2 \left(\frac{E_1 - E_2}{hc} \right)^4 \tag{46}$$

as in table 1; to estimate the small contribution from E_2 levels beyond the 25th (for which P_{12}^2 is not available) one may use the theoretical result that $\sum_{E_2} P_{12}^2 = 1$, which incidentally shows that $\chi(E_1)$ is a kind of average value of $(E_1/hc - E_2/hc)^4$—actually, it is found in each case to be equal to the value of this expression with the 15th-level value (21,000 cm^{-1}) of E_2/hc. It is reasonable to extrapolate the values in table 1 linearly right up to the 18th and last E_1 level, for which $E_1/hc = 56{,}870$ and the extrapolated value of $\chi(E_1)$ is 16·0; for this still agrees with the value of $(E_1/hc - E_2/hc)^4$ for $E_2/hc = 21{,}000$, the E_2 level under the minimum of the upper potential curve, and is therefore probably a close enough approximation, especially as $\hat{q}$ is not very sensitive to contributions from the higher E_1 levels.

E_1/hc	49,360	50,500	50,710	51,350
$\chi(E_1)$	$7{\cdot}0 \times 10^{17}$	$7{\cdot}5 \times 10^{17}$	$8{\cdot}0 \times 10^{17}$	$8{\cdot}5 \times 10^{17}$

TABLE 1

With these values of $\chi(E_1)$ it is possible to compute $\hat{q}$ for any values of ρ and T. Across such thin layers of gas as are of interest to us, T may vary substantially but the pressure p will be approximately constant. Accordingly we calculate the variation of $\hat{q}$ with T for fixed values of

$$p = \frac{k}{2m} \rho T (1 + \alpha). \tag{47}$$

In terms of p, (45) may be written

$$\hat{q} = p \frac{1-\alpha}{1+\alpha} \hat{Q}(T), \tag{48}$$

where

$$\hat{Q}(T) = \frac{32\pi^4 M^2 c}{3kT} (1 - e^{-T_v/T}) \sum_{E_1} \chi(E_1)\, e^{-E_1/kT}. \tag{49}$$

Table 2, which gives values of $\hat{Q}(T)$ obtained by summing the series with the values of $\chi(E_1)$ noted above, shows how rapidly the emissive power of molecules increases with temperature. However, at the higher temperatures, a much smaller proportion of molecules is present, that is, the $(1-\alpha)$ factor multiplying $\hat{Q}(T)$ in (49) reduced. Table 3 shows how much more slowly $\hat{q}$ itself varies with T, especially

at the lower pressures. The increase of $\hat{q}$ with p more rapidly than in strict proportion is due to the rapid increase with p in the said proportion $(1-\alpha)$ of undissociated molecules at these temperatures.

T (°K)	3000	4000	5000	6000
$\hat{Q}(T)$ (c.g.s. units)	0·041	13	400	3600

TABLE 2

	T (°K)			
p (atm)	3000	4000	5000	6000
1	0·0037	0·32	0·67	70·72
10	0·040	8	52	0
100	0·41	110	1900	5300

TABLE 3. Values of $\hat{q}$, the rate of radiative heat transfer to a surface from unit volume of gas near it, in the case when one neglects absorption by other gas en route, and reflexion scattering or re-emission by the surface. Units: W/cm³.

At the higher temperatures some addition is called for to the values of $\hat{Q}(T)$ and $\hat{q}$ in the above tables, due to emission not from true excited O_2 molecules, in discrete vibrational states, but from those at energy levels E_1 above their dissociation energy. Such emission occurs when an excited O atom has an encounter with an unexcited one, and during the process recombines into an unexcited O_2 molecule, emitting the extra energy as a photon. It is the inverse of the 'photodissociation' process discussed in § 12.

To help in estimating how much additional radiation is produced by this recombination process, we may use the experimental values of α_ν at room temperature (Ladenburg *et al.* 1932), which refer to absorption by molecules in their lowest E_2 state, leading to dissociation (§ 12), to write down the total contribution at high temperatures to α_ν from such molecules as are still in their lowest E_2 state. Substitution in (42) then gives the contribution to $\hat{q}$ from such recombinations as result in an unexcited O_2 molecule in this lowest E_2 state. The contribution to $\hat{Q}(T)$ turns out to be 11 at $T = 5000$ °K and 175 at $T = 6000$ °K. A comparison with the values 400 and 3600, respectively, given in table 2, shows among other things that room-temperature values of α_ν can give a seriously misleading ideal of high-temperature values, because the higher vibrational states present at high temperatures may absorb far more efficiently—particularly at the lower frequencies, which are the important ones for the deduction of emission rates.

We may now infer an estimate of the total correction to $\hat{Q}(T)$, due to transition from E_1 states above the dissociation energy, by supposing that significant contributions arise from approximately ten E_2 levels. It is reasonable to assume that these contributions remain fairly constant, since the increase with E_2 due to the expected increase in the relevant $e^{-E_1/kT}$ term in (45) is largely balanced by the decrease due to reduction in $(E_1 - E_2)^4$. [In estimating this part it is useful to

remember that $\sum_{E_1} P_{12}^2 = 1$, the sum being taken over all E_1 states, discrete and continuous; this strictly limits the possible contribution to (45) from any given E_2 state, and especially from the higher ones. Also, for $E_2 = 0$, the value of E_1/hc for maximum contribution to $\hat{Q}(T)$ is found to be 63,500, but at around the 9th-level value (13,200) of E_2/hc this value may be expected to decrease to 56,780 (the value for dissociation of the excited O_2 molecule).] Accordingly the values of $\hat{q}$ in table 3 may need to be increased, to allow for recombinative emission, by about 50 % at $T = 6000\,°\mathrm{K}$, 30 % at $T = 5000\,°\mathrm{K}$ and less still at the lower temperatures.

However, the actual radiative heat transfer to the surface will be much less affected than this theoretical value $\hat{q}$, since absorption values are high in the relevant range of frequencies (of the order of $100\,\mathrm{cm}^{-1}$ for densities of the order of $10^{-3}\,\mathrm{g/cm}^3$), so that little of the radiation associated with recombination would actually reach the surface. By contrast, the radiation whose emission intensity is exhibited in the above tables is of considerably lower frequency (only just ultraviolet, with wavelength around 3500 Å), and absorption values are accordingly much lower for given emission values.

Nevertheless, the upper bound $\tilde{q} = \int_0^\delta \hat{q}\,dz$ to the radiative heat transfer to the surface will certainly not be reached for large thicknesses of gas at high pressure. The greatest heat transfer, which can result from gas at a given temperature T radiating at given frequencies, is that proportion of the total 'equilibrium' heat transfer, $\frac{1}{4}acT^4$, discussed in § 8, which comes from those frequencies. At $T = 6000\,°\mathrm{K}$ the equilibrium heat transfer is $7400\,\mathrm{W/cm}^2$, and the Schumann–Runge bands discussed above, even with some pressure broadening assisting their already substantial degree of overlapping, cannot be expected to fill more than about a seventh of the area of the curve of equilibrium heat transfer against frequency. Accordingly, $1000\,\mathrm{W/cm}^2$ is about the maximum that will be found at this temperature; in particular, in the extreme case of table 3 ($p = 100\,\mathrm{atm}$, $q = 5300\,\mathrm{W/cm}^3$), only 0·2 cm of the layer would be effective, the rest being masked by absorption. However, much greater thicknesses of layer would contribute effectively at lower pressures.

REFERENCES

Beckwith, I. E. 1953 *J. Aero. Sci.* **20**, 645.

Chapman, S. & Cowling, T. G. 1952 *The Mathematical Theory of Non-Uniform Gases*, 2nd ed. Cambridge University Press.

Clarke, J. F. 1958 *J. Fluid Mech.* **4**, 441.

Fay, J. A. & Riddell, F. R. 1958 *J. Aero. Sci.* **25**, 73.

Fraser, P. A., Jarmain, W. R. & Nicholls, R. W. 1954 *Astrophys. J.* **119**, 286.

Freeman, N. C. 1958 *J. Fluid Mech.* **4**, 407.

Gaydon, A. G. 1953 *Dissociation Energies and Spectra of Diatomic Molecules*, 2nd ed. London: Chapman and Hall.

Grew, K. E. & Ibbs, T. L. 1952 *Thermal Diffusion in Gases*. Cambridge University Press.

Hirschfelder, J. O., Bird, R. B. & Spotz, E. L. 1948 *J. Chem. Phys.* **16**, 968.

Hirschfelder, J. O., Bird, R. B. & Spotz, E. L. 1949 *Chem. Rev.* **44**, 205.

Hirschfelder, J. O., Curtiss, C. F. & Bird, R. B. 1954 *Molecular Theory of Gases and Liquids*. New York: Wiley.

Kuo, Y. H. 1957 *J. Aero. Sci.* **24**, 345.
Ladenberg, R., Voorhis, C. C. van & Boyce, J. C. 1932 *Phys. Rev.* **40**, 1018.
Lees, L. 1956 *Jet Propulsion*, **26**, 259.
Lighthill, M. J. 1956 *Surveys in Mechanics* (ed. Batchelor & Davies), p. 250. Cambridge University Press.
Lighthill, M. J. 1957 *J. Fluid Mech.* **2**, 1.
Lighthill, M. J. 1959 *Proc. 1st Int. Cong. Aero. Sci.*, p. 120. London: Pergamon Press.
Moore, L. L. 1952 *J. Aero Sci.* **19**, 505.
Rose, P. H. & Stark, W. I. 1958 *J. Aero. Sci.* **25**, 86.
Stueckelberg, E. C. G. 1932 *Phys. Rev.* **42**, 518; with Errata in **44**, 234.
Weizel, W. 1931 *Bandenspektren*. Leipzig: Akad. Verlag.

On the tendency towards hexagonal cells in steady convection

By ENOK PALM
University of Oslo, Blindern, Norway

(Received 24 October 1959)

This paper attempts to explain theoretically the observed results that (1) the cells in steady convection approach a hexagonal form, and (2) the occurrence of ascent or descent in the middle of the cell depends on how the kinematical viscosity varies with temperature. The theory is based on non-linear equations and, of course, a variable coefficient of viscosity.

It is found that, due to the variation of viscosity with temperature, the non-linear terms contain a second-order term which is destabilizing. This second-order term regulates the development and leads to a final motion composed of regular hexagons with ascent or descent in the middle of the cell according as the viscosity decreases or increases with temperature.

The influence of a variable viscosity on Rayleigh's result concerning the initiation of convection is obtained as a by-product.

1. Introduction

This paper is a theoretical study of convection set up when a fluid is heated uniformly from below or cooled from above. The first experimental investigations of this phenomenon were made by Thomson (1881) and Bénard (1900). Later on their experiments were repeated and extended several times. The experimental results may be summarized briefly as follows.

(1) In order that convection should take place the (negative) temperature gradient must reach a critical value dependent on the depth and physical properties of the fluid.

(2) The convective motion tends towards a regular hexagonal pattern.

(3) The size of the cells is fixed by the depth and physical properties of the fluid.

The first and by far the most important contribution to the theory of convection is given by Rayleigh (1916). He succeeded in explaining the first and third experimental result just mentioned though some quantitative disagreement between theory and experiments existed, essentially due to the simplified boundary conditions applied by Rayleigh. The theory did not, however, explain the reason why the pattern finally consists of hexagonal cells. Actually, from his theory squares and triangles, for example, are just as likely forms of the cells as hexagons.

Rayleigh's theory has been refined by later investigators, notably by Jeffreys (1930) and Pellew & Southwell (1940). More realistic boundary conditions have been applied and a satisfactory numerical agreement between theory and the first and third experimental results has been obtained.

Little or no progress has, however, been made concerning the final form of the cells. It seems obvious that the effects determining this form are lost by the linearization of the equations in the papers mentioned above. The first work, to the author's knowledge, taking into account non-linear effects in this problem was published last year by Malkus & Veronis (1958). In this work the authors try to find the physically realized solution by examining the stability of the various solutions of the non-linear equations corresponding to stationary motion. However, their way of proceeding is not free from objection. In order to find the stable solution they add to the basic motion a disturbance of a very special form. Their disturbance is not a solution of the perturbation equations, and it seems hard to understand how any conclusion at all can be obtained by their method.

Experiments have revealed that the direction of circulation, i.e. ascent or descent in the middle of the cells, changes from fluid to fluid. Usually liquids and gases have opposite circulation, liquids having ascent and gases descent in the middle of the cell.

To the author's knowledge, no theoretical investigation on this phenomenon has been published. However, Graham (1933) has made the interesting suggestion that the different circulation may be a result of the fact that the kinematic viscosity varies with temperature in opposite manner in liquids and gases. This suggestion has not been followed up until the recent experiments performed by Tippelskirch (1956). Following an idea of Koschmieder he has investigated for different temperature-regions the direction of circulation in liquid sulphur. This substance has the peculiar property that the kinematic viscosity decreases or increases with temperature according as the temperature is less or greater than 153° C. It was found that Graham's suggestion was confirmed, the motion being ascending in the middle of the cell in the first temperature region and descending in the other.

2. The purpose of the present work

The principal purpose of this paper is to explain why hexagonal cells are preferred in laminar convection. According to the above, the variation of viscosity with temperature is the major effect determining the direction of circulation. We are therefore led to base our study on the non-linear equations with a variable viscosity.

3. Derivation of the differential equations

The equations of motion in the class of problems under consideration may be simplified somewhat, as shown by Boussinesq (1903). Thus the dependence of density on pressure is unimportant, and even the variation with temperature may be disregarded except in so far as it modifies the operation of gravity. The equations of fluid motion and the continuity equation may then be written

$$\rho_0 \mathbf{v}_t + \rho_0 \mathbf{v} \cdot \nabla \mathbf{v} = -\nabla p + \rho_0 (X\mathbf{i} + Y\mathbf{j} + Z\mathbf{k}) - \mathbf{g}\rho, \tag{3.1}$$

$$\nabla \cdot \mathbf{v} = 0. \tag{3.2}$$

Here x, y are horizontal co-ordinates, z is the vertical co-ordinate, measured positive upwards, $\mathbf{i}$, $\mathbf{j}$ and $\mathbf{k}$ are the respective unit vectors and t is the time. $\mathbf{v}$ is

the velocity with components u, v, w; ρ is the density, ρ_0 the standard density, p the pressure and g the acceleration of gravity. Subscripts t, x, y, z indicate differentiation. Furthermore,

$$X = \nu\nabla^2 u + \nu_z(u_z + w_x) + 2\nu_x u_x + \nu_y(v_x + u_y),$$
$$Y = \nu\nabla^2 v + \nu_x(v_x + u_y) + 2\nu_y v_y + \nu_z(w_y + v_z),$$
$$Z = \nu\nabla^2 w + \nu_y(w_y + v_z) + 2\nu_z w_z + \nu_x(u_z + w_x),$$

where ν denotes the kinematic coefficient of viscosity.

The two other equations employed by Boussinesq are the equation for conduction of heat,

$$\Theta_t + \theta_t + w\Theta_z + \mathbf{v}.\nabla\theta = \kappa(\nabla^2\Theta + \nabla^2\theta), \tag{3.3}$$

and the equation of state in the form

$$g\rho = g\rho_0(1 - \alpha(\Theta + \theta)). \tag{3.4}$$

Here Θ is the mean temperature, defined by integration over x and y, θ the departure from the mean temperature, κ the thermal diffusivity, and α the coefficient of expansion.

If ν is constant and the above equations are linearized, u, v, p and θ are easily eliminated and a sixth-order differential equation in w is obtained. It turns out to be convenient to base the present discussion on the corresponding equation. To derive this equation the x-component of (3.1) is differentiated with respect to x and z, the y-component of (3.1) with respect to y and z and the equations are added, applying (3·2). It is then found that

$$\rho_0(-w_{tzz} + (\mathbf{v}.\nabla u)_{xz} + (\mathbf{v}.\nabla v)_{yz}) = -\nabla_1^2 p_z + \rho_0(X_{xz} + Y_{yz}), \tag{3.5}$$

where

$$\nabla_1^2 = \frac{\partial^2}{\partial x^2} + \frac{\partial^2}{\partial y^2}.$$

Elimination of p between the y-component of (3.1) and (3.5) and use of (3·4) lead to

$$\nabla^2 w_t + \nabla_1^2(\mathbf{v}.\nabla w) - (\mathbf{v}.\nabla u)_{xz} - (\mathbf{v}.\nabla v)_{yz} = \nabla_1^2 Z - X_{xz} - Y_{yz} + g\alpha\nabla_1^2\theta. \tag{3.6}$$

Finally, elimination of θ between (3.3) and (3.6) gives

$$-\nabla^2 w_{tt} + \kappa\nabla^4 w_t - \left(\frac{\partial}{\partial t} - \kappa\nabla^2\right)(X_{xz} + Y_{yz} - \nabla_1^2 Z) - g\alpha\Theta_z\nabla_1^2 w$$
$$= -\left(\frac{\partial}{\partial t} - \kappa\nabla^2\right)((\mathbf{v}.\nabla u)_{xz} + (\mathbf{v}.\nabla v)_{yz} - \nabla_1^2(\mathbf{v}.\nabla w)) + g\alpha\nabla_1^2(\mathbf{v}.\nabla\theta). \tag{3.7}$$

It is seen that this equation contains beside w the four other unknown variables, u, v, θ and Θ. Four more equations are therefore needed. Two equations are found by combination of the x- and y-components of (3.1) with (3.2), which gives

$$\nabla_1^2 u_t + w_{xzt} - X_{yy} + Y_{xy} = (\mathbf{v}.\nabla v)_{xy} - (\mathbf{v}.\nabla u)_{yy}, \tag{3.8}$$
$$\nabla_1^2 v_t + w_{yzt} - Y_{xx} + X_{xy} = (\mathbf{v}.\nabla u)_{xy} - (\mathbf{v}.\nabla v)_{xx}. \tag{3.9}$$

Equation (3.3) may be considered as a third equation. The fourth equation is obtained by averaging (3.3), which results in

$$\left(\frac{\partial}{\partial t}-\kappa\frac{\partial^2}{\partial z^2}\right)\Theta = -\overline{\mathbf{v}.\nabla\theta}, \tag{3.10}$$

with a bar denoting the mean value.

The five equations (3.3, 3.7, 3.8, 3.9, 3.10) constitute, with proper boundary conditions, a complete set of equations for the five unknown variables, and are suitable for the present purpose. Apart from the terms resulting from the variation of ν these equations correspond to those applied by Malkus & Veronis (1959).

4. The model

Following Rayleigh (1916), we simplify the problem in considering a fluid of infinite lateral extent bounded vertically by two free boundaries, at $z = 0$ and $z = h$, say. The boundary conditions are then

$$\theta = w = u_z = v_z = 0, \tag{4.1}$$

or, from (3.2),

$$\theta = w = w_{zz} = 0 \tag{4.2}$$

for $z = 0$ and $z = h$.

In order to obtain a unique solution it is also necessary to know the flow of heat conveyed to the system. The investigations will be restricted to systems satisfying the following two requirements:

(1) The flow of heat is only slightly larger than the critical one corresponding to the onset of convection.

(2) The change of the flow of heat is slow.

Let us now return to (3.10). We divide Θ into two parts

$$\Theta = \Theta_1 + \Theta_2, \tag{4.3}$$

where Θ_2 is defined by

$$\left(\frac{\partial}{\partial t}-\kappa\frac{\partial^2}{\partial z^2}\right)\Theta_2 = 0. \tag{4.4}$$

According to the second requirement above the accumulation of sensible heat is small compared with the flux, and (4.4) reduces to

$$\frac{\partial^2\Theta_2}{\partial z^2} = 0, \quad \text{or} \quad \frac{\partial\Theta_2}{\partial z} = -\beta(t), \tag{4.5}$$

where $\beta(t)$ is positive and independent of the space co-ordinates. It is also convenient to divide $\beta(t)$ into two parts:

$$\beta(t) = \beta_0 + \Delta\beta(t), \tag{4.6}$$

where β_0 denotes the negative temperature gradient corresponding to the onset of convection. $\Delta\beta(t)$ is positive and, owing to the first requirement above, relatively small.

The form of the dependence of kinematic viscosity on temperature varies from fluid to fluid. The present investigations will be restricted to fluids for which ν may be approximated by

$$\nu = \nu_0 + \gamma\cos\mu(\Theta+\theta) \tag{4.7}$$

in the actual temperature region. Here, ν_0, γ, μ are constants and $(\gamma/\nu_0)^2$ is supposed small compared with unity. It is convenient to choose the scale of temperature so that Θ is zero for $z = 0$. It is then seen that in the actual temperature region γ positive corresponds to ν increasing with temperature and vice versa.

Neglecting second-order terms in θ, we may write (4.7) as

$$\nu = \nu_0 + \gamma \cos \mu\beta z + \gamma\mu\theta \sin \mu\beta z, \tag{4.8}$$

ν is a function of time through its dependence on β and θ. According to the above assumption concerning the flow of heat, however, β may be considered as a constant in this formula. Moreover, μ or h is supposed to be chosen so that

$$\mu\beta = \lambda, \tag{4.9}$$

where $\lambda = \pi/h$. Hence, finally,

$$\nu = \nu_0 + \gamma \cos \lambda z + \frac{\gamma\lambda}{\beta}\theta \sin \lambda z. \tag{4.10}$$

5. The onset of convection

We will now investigate the influence of a variable viscosity on the conditions for initiation of convection. It suffices in this problem to consider only linearized equations.

Inserting the expressions for X, Y, Z in (3.7) we obtain

$$\begin{aligned} -\nabla^2 w_{tt} + (\kappa+\nu)\nabla^4 w_t + 2\nu_z \nabla^2 w_{zt} - \nu_{zz}(\nabla_1^2 w_t - w_{zzt}) \\ + \kappa\nabla^2[-\nu\nabla^4 w - 2\nu_z \nabla^2 w_z + \nu_{zz}(\nabla_1^2 w - w_{zz})] + g\alpha\beta_0 \nabla_1^2 w = 0. \end{aligned} \tag{5.1}$$

Convection takes place when one of the solutions of (5.1) becomes unstable. At the transition from stable to unstable solutions (5.1) reduces to

$$\kappa\nabla^2[-\nu\nabla^4 w - 2\nu_z \nabla^2 w_z + \nu_{zz}(\nabla_1^2 w - w_{zz})] + g\alpha\beta_0 \nabla_1^2 w = 0. \tag{5.2}$$

A basic solution of this equation satisfying the boundary conditions has the form

$$\sum_m A_{11m} \cos kx \cos ly \sin m\lambda z. \tag{5.3}$$

For small values of γ/ν_0

$$\frac{A_{11m+1}}{A_{11m}} \propto \frac{\gamma}{\nu_0},$$

and to obtain a first approximation it suffices only to take the first two terms into account. Equation (5.2) then leads to

$$[\kappa\nu_0\sigma^3 - g\alpha\beta_0(k^2+l^2)]A_{111} + F\gamma A_{112} = 0, \tag{5.4}$$

where

$$\left.\begin{aligned} \sigma &= k^2 + l^2 + \lambda^2, \\ F &= \kappa\sigma[\tfrac{1}{2}(k^2+l^2+4\lambda^2)^2 + \tfrac{1}{2}\lambda^2(4\lambda^2 - k^2 - l^2) - 2\lambda^2(k^2+l^2+4\lambda^2)]. \end{aligned}\right\} \tag{5.5}$$

Correspondingly, from (5.2),

$$MA_{112} + H\gamma A_{111} = 0, \tag{5.6}$$

where

$$\left.\begin{aligned} M &= \kappa\nu_0(k^2+l^2+4\lambda^2)^3 - g\alpha\beta_0(k^2+l^2), \\ H &= \kappa(k^2+l^2+4\lambda^2)[\tfrac{1}{2}\sigma^2 + \lambda^2\sigma + \tfrac{1}{2}\lambda^2(\lambda^2 - k^2 - l^2)]. \end{aligned}\right\} \tag{5.7}$$

Consequently,

$$\kappa\nu_0\sigma^3 - g\alpha\beta_0(k^2+l^2) - \frac{FH}{M}\gamma^2 = 0. \tag{5.8}$$

β_0, being defined as the temperature gradient corresponding to the onset of convection, is obtained by combining (5.8) with the equation obtained by differentiating (5.8) with respect to k^2+l^2. It is found after some computation that the Rayleigh number, Ra, is

$$Ra = \frac{g\alpha\beta_0 h^4}{\kappa\nu_0} = \pi^4\left(6{\cdot}75 - 1{\cdot}3\frac{\gamma^2}{\nu_0^2}\right). \tag{5.9}$$

The corresponding wave numbers are found to be given by

$$k^2+l^2 = \left(0{\cdot}5 - 0{\cdot}024\frac{\gamma^2}{\nu_0^2}\right)\lambda^2. \tag{5.10}$$

For $\gamma = 0$, (5.9) and (5.10) reduce to the results found by Rayleigh. It is seen that the effect of a variable ν is to lower the critical temperature gradient and diminish the corresponding values of k^2+l^2. The magnitude of these effects is, however, small.

The approximation involved in the derivation of these results amounts to neglecting A_{113} compared with A_{111}, which implies that γ^2/ν_0^2 is small compared with unity. The ratio A_{112}/A_{111} is found to be $-0{\cdot}15\,\gamma/\nu_0$, indicating that the series (5.6) converges rapidly even for moderate values of γ/ν_0.

6. The tendency towares hexagonal cells

Formulation of the problem

We now proceed to consider the problem of determining the final form of the cells. According to the previous sections we know that when the temperature gradient has attained its critical value given by (5.9), a motion composed of waves of form (5.10) starts to grow. This motion is very complex and is mathematically described by a Fourier–Stieltjes integral. This phase of the motion lasts until the non-linear terms become appreciable. Observations reveal that from then on there is a marked tendency towards a cellular motion with cells approaching a hexagonal form.

The most natural interpretation of this regulating effect of the non-linear terms seems to be that they act in such a way as to destabilize selected wave components. These waves will therefore dominate the further development. The other waves satisfying (5.10) will finally decay, being more or less to be considered as 'noise' superimposed on a motion which gradually becomes stable. It will be our aim to show that a non-linear instability of this kind really exists.

The actual problem is characterized by lateral homogeneity and isotropy. The location and orientation of the cells therefore vary from experiment to experiment, dependent on the initial conditions. Here and below *initial* refers to the state of motion just before the non-linear terms become important. It seems reasonable to suppose that only the initial waves with the largest amplitudes decide the location and orientation of the cells. Therefore, and also to obtain

a tractable problem, we will consider the development of an initial motion consisting mainly of one single wave,

$$A'_{111}\cos(k'x'+l'y')\sin\lambda z, \tag{6.1}$$

or, more precisely,

$$\sum_m A'_{11m}\cos(k'x'+l'y')\sin m\lambda z. \tag{6.2}$$

The primes are here used for later convenience. (6.1) (or (6.2)) is not the total initial motion, which would have been an unrealistic assumption. In addition, the initial motion consists also of the other waves (5.10), though this part of the wave-spectrum has smaller amplitudes.

By rotation of the frame of reference so that the new x-axis becomes parallel to the lines of constant phase, (6.1) takes the form, with appropriate notation,

$$A_{021}\cos 2ly\sin\lambda z. \tag{6.3}$$

It is seen that the wave component

$$A_{111}\cos kx\cos ly\sin\lambda z \tag{6.4}$$

satisfies (5.10) if

$$k^2+l^2=4l^2 \quad \text{or} \quad k^2=3l^2. \tag{6.5}$$

It will now be demonstrated that this wave and the wave (6.3) are, due to the kind of instability mentioned above, preferred waves. Let us for example consider the term $\kappa\nabla^2 X_{xz}$ in (3.7). This term yields a term of the form

$$\gamma A_{111}A_{021}\cos kx\cos ly\sin\lambda z, \tag{6.6}$$

which obviously destabilizes the wave (6.4), provided the sign of γA_{021} has the proper value. This will, indeed, always be true since the sign of A_{021} may be changed by displacing the frame of references half a wavelength along the y-axis. Consequently, the wave (6.4) will increase more rapidly than all other waves except (6.3). This instability will be closer investigated in the mathematical discussion that follows.

The mathematical derivation

As a conclusion of the reasoning above we are led to consider a motion with (6.3) and (6.4) as the dominant waves. According to the assumptions introduced these terms are themselves small, so that an iteration process may be used. The non-linear terms will give rise to waves with wave numbers $2k$, $3k$, ..., $2l$, $3l$, ..., 2λ, 3λ, ... A solution of the system of non-linear equations satisfying the boundary conditions therefore is of the form

$$\left.\begin{aligned} w &= \sum_{ijm} A_{ijm}(t)\cos ikx\cos jly\sin m\lambda z,\\ u &= \sum_{ijm} B_{ijm}(t)\sin ikx\cos jly\cos m\lambda z,\\ v &= \sum_{ijm} C_{ijm}(t)\cos ikx\sin jly\cos m\lambda z, \end{aligned}\right\} \tag{6.7}$$

provided the series converge. When no misunderstanding is possible, the subscripts of the amplitudes will be neglected.

Insertion of (6.7) in (3.7) leads to an infinite number of equations. According to the previous discussion we first study the equation corresponding to $i=j=m=1$. In this case the linearized restoring term is small (proportional to $\Delta\beta$) and negative. Hence the non-linear terms contributing to the restoring term will be important.

The equation may be simplified somewhat. The term $-(\partial/\partial t)(X_{xz}+Y_{yz}-\nabla_1^2 Z)$ is essentially a damping term and does not influence the restoring term at all. It consists of one linear part, $\nu\nabla^4 w_z$, and terms of higher order. These higher-order terms, being of no interest in the actual problem, will be neglected. Correspondingly, the damping term

$$\frac{\partial}{\partial t}\{(\mathbf{v}.\nabla u)_{xz}+(\mathbf{v}.\nabla v)_{yz}-\nabla_1^2(\mathbf{v}.\nabla w)\}$$

will be neglected, since it consists entirely of higher-order terms.

In the restoring term, terms of higher order than the third will be cancelled. The non-linear part of the equation therefore will consist of products of type $A_{202}A_{111}$, $A_{022}A_{111}$, $A_{112}A_{021}$, $A_{132}A_{021}$ and the corresponding products with B, C, D instead of A. The amplitudes B and C may be expressed in terms of A by (3.8) and (3.9). Neglecting higher-order terms these equations may be written

$$\left(\frac{\partial}{\partial t}-\nu\nabla^2\right)\nabla_1^2 u+\left(\frac{\partial}{\partial t}-\nu\nabla^2\right)w_{zx}=(\mathbf{v}.\nabla v)_{xy}-(\mathbf{v}.\nabla u)_{yy}, \tag{6·8}$$

$$\left(\frac{\partial}{\partial t}-\nu\nabla^2\right)\nabla_1^2 v+\left(\frac{\partial}{\partial t}-\nu\nabla^2\right)w_{zy}=(\mathbf{v}.\nabla u)_{xy}-(\mathbf{v}.\nabla v)_{xx}. \tag{6.9}$$

It turns out that the right-hand sides of these equations do not give any contributions to the wave components to be considered here, and the equations reduce to

$$\nabla_1^2 u=-w_{zx}, \tag{6.10}$$

$$\nabla_1^2 v=-w_{zy}. \tag{6.11}$$

By elimination of B and C by these equations, and application of (4.5) and (5.10), it is found that

$$\begin{aligned}\sigma\ddot{A}_{111}&+(\kappa+\nu)\sigma^2\dot{A}_{111}+(\kappa\nu_0\sigma^3-4g\alpha\beta l^2)A_{111}\\&=-F\gamma A_{112}-\frac{13\kappa\sigma\lambda^5}{64\beta}\gamma(A_{111}D_{021}+A_{021}D_{111})-9\kappa l^2\lambda\\&\quad\times(A_{111}A_{202}+3A_{022}A_{111}+3A_{021}A_{112}+A_{021}A_{132})-\tfrac{1}{2}g\alpha\lambda l^2\\&\quad\times(8D_{002}A_{111}+A_{111}D_{202}+3A_{111}D_{022}+3A_{021}D_{112}+A_{021}D_{132}).\end{aligned} \tag{6.12}$$

The amplitude D may be expressed in terms of A by (3.3). Applying (4.4) and (4.5) we find that this equation may be written

$$\left(\frac{\partial}{\partial t}-\kappa\nabla^2\right)(\theta+\Theta_1)=-\mathbf{v}.\nabla\theta+\beta w-\frac{\partial\Theta_1}{\partial z}w. \tag{6.13}$$

According to the above $\partial/\partial t$ is small compared with $\kappa\nabla^2$, being proportional to $\Delta\beta$ or γA_{021}. Taking account of this, we find that

$$\left.\begin{aligned}D_{111}&=\frac{\beta}{\kappa\sigma}A_{111}, & D_{022}&=\frac{\beta}{4\kappa}\frac{A_{022}}{l^2+\lambda^2}-\frac{3}{64}\frac{\beta\lambda}{\kappa^2\sigma}\frac{A_{111}^2}{l^2+\lambda^2},\\D_{021}&=\frac{\beta}{\kappa\sigma}A_{021}, & D_{202}&=\frac{\beta}{4\kappa}\frac{A_{202}}{k^2+\lambda^2}-\frac{1}{64}\frac{\beta\lambda}{\kappa^2\sigma}\frac{A_{111}^2}{k^2+\lambda^2},\\D_{112}&=\frac{\beta A_{112}}{4\kappa(l^2+\lambda^2)}-\frac{3}{16}\frac{\beta\lambda}{\kappa^2\sigma}\frac{A_{111}A_{021}}{l^2+\lambda^2},\\D_{132}&=\frac{\beta A_{132}}{4\kappa(k^2+\lambda^2)}-\frac{1}{16}\frac{\beta\lambda}{\kappa^2\sigma}\frac{A_{111}A_{021}}{k^2+\lambda^2}, & D_{002}&=-\frac{1}{16}\frac{\beta A_{111}^2}{\lambda\kappa^2\sigma}.\end{aligned}\right\} \tag{6.14}$$

A_{202}, A_{022}, A_{112} and A_{132} are expressed in terms of A_{111}, A_{021} and γ by the respective equations obtained when (6.7) is inserted in (3.7) and higher-order terms neglected. As above, it is seen that the terms containing time differentiation may be neglected. In this way we find that

$$\left.\begin{aligned} -MA_{112} &= H\gamma A_{111} + GA_{111}A_{021}, \\ -MA_{022} &= H\gamma A_{021} + \tfrac{1}{4}GA_{111}^2, \\ A_{202} &= -P_1 A_{111}^2, \\ A_{132} &= -4P_1 A_{111}A_{021}. \end{aligned}\right\} \tag{6.15}$$

M and H are defined above, and G is defined by

$$G = 3\kappa(l^2+\lambda^2)\lambda\sigma + \frac{3\beta g\alpha\lambda l^2}{\kappa\sigma}. \tag{6.16}$$

P_1 is a positive quantity, whose form is irrelevant for the present purpose.

Inserting these values in (6.12) and applying (4.6), we find that

$$\sigma\ddot{A}_{111} + (\kappa+\nu_0)\sigma^2\dot{A}_{111} - 4g\alpha l^2\Delta\beta A_{111} = -\tfrac{1}{3}\tfrac{3}{2}\lambda^5\gamma A_{111}A_{021} - RA_{111}^3 - PA_{111}A_{021}^2, \tag{6.17}$$

where R and P are positive quantities. Correspondingly, the equation for A_{021} is found to be

$$\sigma\ddot{A}_{021} + (\kappa+\nu_0)\sigma^2\dot{A}_{021} - 4g\alpha l^2\Delta\beta A_{021} = -\tfrac{1}{4}\tfrac{1}{3}\tfrac{3}{2}\lambda^5\gamma A_{111}^2 - 4RA_{021}^3 - \tfrac{1}{4}PA_{111}^2A_{021}. \tag{6.18}$$

7. Discussion of the equations

We will first consider (6.17). It is seen that the linear terms, assembled on the left-hand side, correspond to an unstable motion. The non-linear terms consist of one second-order term and two third-order terms. The second-order term is destabilizing if

$$\gamma A_{021} < 0. \tag{7.1}$$

Since γ is determined by the properties of the fluid, (7.1) fixes the sign of A_{021}.

The two third-order terms are important when the amplitude has become relatively large. It is noted that they are always stabilizing, and these terms are responsible for the stationary character of the motion finally achieved.

Equation (6.18) is very much of the same form as equation (6.17). It is seen that condition (7.1) implies that the second-order term in (6.18) is also destabilizing. Hence A_{111} and A_{021} are coupled in such a manner that they mutually reinforce each other.

None of these equations fixes the sign of A_{111}. This means only that the sign of A_{111} is arbitrary, corresponding to the fact that the sign will be changed by moving the frame of references half a wavelength along the x-axis. In what follows the origin is chosen so that A_{111} has the same sign as A_{021}.

Let us now examine the final form of the motion when $t \to \infty$. The amplitudes A_{111} and A_{021} are found from (6.17) and (6.18) by neglecting terms containing time differentiation. It is readily found that, in this case,

$$A_{111} = 2A_{021}. \tag{7.2}$$

According to Christophersen (1940) hexagons are given analytically by

$$\cos\sqrt{3}\,lx\cos ly+\tfrac{1}{2}\cos 2ly. \tag{7.3}$$

Hence we have proved that when $t\to\infty$, the motion tends towards a pattern consisting of hexagons.

The direction of circulation in the hexagons is given by (7.1). It follows from (4.7) that ν increasing with temperature corresponds to a positive γ and ν decreasing with temperature corresponds to a negative γ. Therefore, for fluids in which ν increases with temperature (gases) the motion is descending in the middle of the cell and for fluids for which ν decreases with temperature (liquids) the motion is ascending in the middle of the cell.

These results are in agreement with the observations mentioned in the introduction.

8. Conclusion and final remarks

We have started with an initial motion which is essentially a harmonic wave and demonstrated that for large values of time hexagons are formed. The agency responsible for this has been shown to be the dependence of the kinematic viscosity on temperature.

We have in this paper only taken into account the variation of ν with temperature. Also κ varies considerably with temperature and it seems likely that for some fluids this variation may also be important.

Finally, it should be mentioned that waves with wave numbers which lie sufficiently near to (5.10) will also be initiated. When $\Delta\beta$ is small, however, this effect may be ignored. Altogether, a small change in k^2+l^2 is of no importance in this problem since the Rayleigh number has a minimum for the actual value of k^2+l^2.

The author is indebted to Prof. A. Eliassen and Prof. E. Höiland for valuable discussions. The research has been sponsored by the Norwegian Research Council for Science and the Humanities through the Institute for Weather and Climate Research, Oslo.

REFERENCES

Bénard, M. 1901 *Ann. Chim. Phys.* **23**, 62.
Boussinesq, J. 1903 *Théorie Analytique de la Chaleur*, vol. 2. Paris: Gauthier-Villars.
Christophersen, D. G. 1940 *Quart. J. Mech. Appl. Math.* **11**, 63.
Graham, A. 1933 *Phil. Trans.* A, **232**, 285.
Jeffreys, H. 1930 *Proc. Camb. Phil. Soc.* **26**, 170.
Malkus, W. V. R. & Veronis, G. 1958 *J. Fluid Mech.* **4**, 225.
Pellew, A. & Southwell, R. V. 1940 *Proc. Roy. Soc.* A, **176**, 312.
Rayleigh, Lord 1916 *Phil. Mag.* **32**. (Reprinted in *Collected Papers*, **6**, 432.)
Thomson, J. 1882 *Proc. Glasg. Phil. Soc.* **13**, 464.
Tippelskirch, H. V. 1956 *Beitr. Phys. frei. Atmos.* **29**, 37.

An improved perturbation theory for shock waves propagating through non-uniform regions

By M. P. FRIEDMAN
Institute of Mathematical Sciences, New York University.

(Received 9 October 1959)

This paper considers the problem of the propagation of a shock wave down a non-uniform tube. Linearized solutions to the problem (Chester 1954) do not hold when the velocity behind the shock is near or at the sonic speed. By retaining appropriate non-linear terms of the flow equations, a solution is obtained which holds for all conditions behind the shock, and reduces to the linearized solution for conditions away from sonic.

The behaviour of supersonic or subsonic flow entering regions of expanding or contracting area changes is discussed. It is found that subsidiary shocks may be formed; these can be located and described using the present solution. Explicit solutions are given for the cases of supersonic or subsonic flow entering a region of linearly expanding or contracting area. The point of shock formation as well as the path of the subsidiary shock is obtained for the case in which the area contracts.

1. Introduction

Chester (1954) studies the motion of a shock wave down a non-uniform tube on the basis of a linearized theory in which the changes in tube area and the consequent changes in shock strength are assumed to be small. In this linearized theory the solution breaks down when the flow behind the shock is nearly sonic. In this paper, a solution is obtained which holds for all conditions behind the shock. A similar situation arises in the study of the transients arising from the addition of heat to a gas flow (Stocker 1952), and the same techniques are used here.

Recently, it has been shown by Chisnell (1957) and Whitham (1958) that Chester's work could be simplified and extended. One minor simplification is that whereas Chester worked with the full three-dimensional equations and performed an averaging process in the course of the analysis, it is sufficient to work from the outset with the one-dimensional (hydraulic) formulation; i.e. all quantities are averaged over the cross-sectional area to give functions of time and distance down the tube only. Then Whitham shows that the motion of the shock can be found very simply, without solving the equations for the flow behind the shock in detail. The method can be given as the following rule: apply the differential relation which is to be satisfied by the flow quantities along a characteristic to the flow quantities just behind the shock. Using the shock relations which express these values in terms of the shock strength, the change in shock strength is then determined. This rule is easily proved to be correct for the small perturbation

theory. In fact it is found to be very accurate even when the total changes in shock strength are not small although a full understanding of this fact is still lacking.

Although the detailed solution of the small perturbation equations can be by-passed in this way, it is useful to consider also the full solution. Using the subscript 1 to denote unperturbed values behind the shock, the general solution of the linearized one-dimensional equations is (see § 2)

$$p-p_1=\frac{\rho_1 a_1^2 u_1^2}{a_1^2-u_1^2}\frac{A(x)-A_1}{A_1}+F(x-\{u_1+a_1\}t)+G(x-\{u_1-a_1\}t),$$

$$u-u_1=-\frac{a_1^2 u_1}{a_1^2-u_1^2}\frac{A(x)-A_1}{A_1}+\frac{1}{\rho_1 a_1}F(x-\{u_1+a_1\}t)-\frac{1}{\rho_1 a_1}G(x-\{u_1-a_1\}t),$$

$$\rho-\rho_1=\frac{p-p_1}{a_1^2}+H(x-u_1 t),$$

where p, ρ, a, u are the pressure, density, sound speed, and particle velocity; $A(x)$ is the cross-sectional area of the tube; and F, G, H are arbitrary functions to be fixed by initial and boundary conditions. In the present problem, it is assumed that the tube is uniform in $x<0$ with $A(x)=A_1$, and that the shock initially moves with uniform speed in this part of the tube (p_1, ρ_1, u_1 are the constant values behind the shock). Hence F is identically zero. The functions G and H are determined from the shock relations.

Now it is observed that the solution breaks down near sonic conditions when $u_1 \simeq a_1$, because the first term, depending on the area change, becomes infinite. The object of the present paper is to discuss the sonic case and provide a valid solution to deal with it. Small perturbations will still be assumed, but non-linear terms will be included to avoid the breakdown, which is essentially due to the linearization. It should be noted that Whitham's derivation for the motion of the shock is valid for all u_1 and a_1, since he assumes only that the disturbances are small and makes no use of the above expressions; thus only the treatment of the flow behind the shock requires correction. A related fact is that the motion of the shock is qualitatively the same whether the flow behind the shock is subsonic or supersonic. For example, $\delta M>0$ if $\delta A<0$ in both cases, M being the Mach number of the shock, whereas the sign of $u_1^2-a_1^2$ in the above solution changes for subsonic and supersonic flows.

The corrected solution depends on a more exact treatment of the negative characteristics, $dx/dt=u-a$, than is done in the linearized solution where they are approximated by lines $x-(u_1-a_1)t=$ constant. When u_1 is equal to or near a_1, the disturbance represented by these characteristics has very little motion relative to the tube. Hence small variations in the magnitude of $u-a$ become critically important and the linearization of this quantity is inadequate. If this is not corrected, the effect of the area change continually builds up (as shown by the linearized solution) because the disturbance does not move relative to the tube. In the true solution, some build up of the disturbance occurs, but this automatically changes $u-a$ away from zero and the disturbance moves up or down the tube, depending on the sign of $u-a$. This will be shown in detail in the im-

proved solution. Furthermore, an interesting feature of the non-linear treatment of the disturbances is that secondary shocks are formed in the flow, and they can be studied by means of the solution presented here.

The theory is developed for the problem of a shock moving in a non-uniform tube, but the same methods apply to analogous problems involving shock waves propagating through regions in which the gas has a non-uniform initial state.

2. Basic equations and small perturbation solution

One-dimensional, non-steady flow problems are described by the equations of motion

$$\rho_t + u\rho_x + \rho u_x + \frac{\rho u}{A} A_x = 0, \tag{1}$$

$$\rho u_t + \rho u u_x + p_x = 0, \tag{2}$$

$$p_t + u p_x - a^2(\rho_t + u\rho_x) = 0, \tag{3}$$

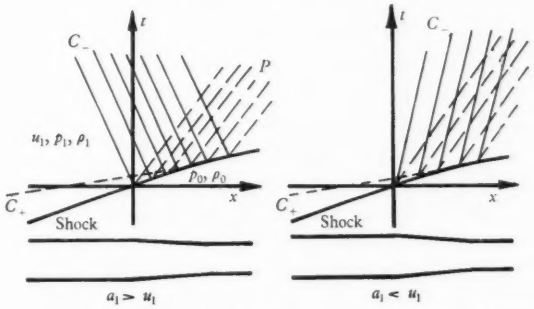

FIGURE 1. The (x, t) diagram showing the characteristics and particle paths.

where p is the pressure, ρ is the density, u is the particle velocity, and a is the sound speed; $a = (\gamma p/\rho)^{\frac{1}{2}}$ for a polytropic gas with ratio of specific heats equal to γ. In characteristic form, we have

$$p_t + \rho a u_t + (u+a)(p_x + \rho a u_x) + \frac{\rho a^2 u}{A} A_x = 0, \tag{4}$$

$$p_t - \rho a u_t + (u-a)(p_x - \rho a u_x) + \frac{\rho a^2 u}{A} A_x = 0, \tag{5}$$

in place of (1) and (2).

We consider the problem represented in figure 1 wherein a shock wave initially moves in the straight part of the tube $x < 0$, and then passes into the non-uniform part, $x > 0$, where the area $A(x)$ varies from the original value A_1. The flow ahead of the shock is assumed to be uniform and stationary. Conditions ahead of the shock will be denoted by a subscript 0; subscript 1 denotes the constant values behind the shock when it is uniform in $x < 0$. When the shock meets the area change at $x = 0$, disturbances are reflected along the negative characteristics C_- and entropy changes propagate along the particle paths P. Disturbances on the negative characteristics move backwards or forwards relative to the tube depending on whether $u_1 - a_1 < 0$ or $u_1 - a_1 > 0$.

In the linearized theory, the coefficients in equations (3)–(5) are replaced by the same quantities with subscripts 1 to give

$$(p+\rho_1 a_1 u)_t+(u_1+a_1)(p+\rho_1 a_1 u)_x+\frac{\rho_1 a_1^2 u_1}{A_1}A_x=0, \tag{6}$$

$$(p-\rho_1 a_1 u)_t+(u_1-a_1)(p-\rho_1 a_1 u)_x+\frac{\rho_1 a_1^2 u_1}{A_1}A_x=0, \tag{7}$$

$$p_t+u_1 p_x-a_1^2(\rho_t+u_1\rho_x)=0. \tag{8}$$

The solution may be written:

$$(p-p_1)+\rho_1 a_1(u-u_1)=-\frac{\rho_1 a_1^2 u_1}{u_1+a_1}\frac{A(x)-A_1}{A_1}+2F(x-(u_1+a_1)t), \tag{9}$$

$$(p-p_1)-\rho_1 a_1(u-u_1)=-\frac{\rho_1 a_1^2 u_1}{u_1-a_1}\frac{A(x)-A_1}{A_1}+2G(x-(u_1-a_1)t), \tag{10}$$

$$\rho-\rho_1=\frac{1}{a_1^2}(p-p_1)+H(x-u_1 t). \tag{11}$$

F gives the disturbances on C_+, G the disturbances on C_-, and H the disturbances on P. Since the shock was assumed to come undisturbed from $x=-\infty$, the contribution F on the positive characteristics vanishes. When F vanishes, (9) is the relation used by Whitham to determine the shock. Notice that it is independent of the disturbance G, and the area term is finite for all u_1 and a_1. This checks with the comment made earlier that the derivation for the shock motion is valid even when $u_1=a_1$. The perturbation solutions are, therefore,

$$p-p_1=G(x-(u_1-a_1)t)+\frac{\rho_1 u_1^2 a_1^2}{a_1^2-u_1^2}\frac{A(x)-A_1}{A_1}, \tag{12}$$

$$u-u_1=-\frac{1}{\rho_1 a_1}G(x-(u_1-a_1)t)-\frac{u_1 a_1^2}{a_1^2-u_1^2}\frac{A(x)-A_1}{A_1}, \tag{13}$$

$$\rho-\rho_1=\frac{1}{a_1^2}(p-p_1)+H(x-u_1 t). \tag{14}$$

The functions G and H are determined from the requirement that the solution given by (12)–(14) satisfies the shock conditions. At the shock

$$p=\frac{p_0}{\gamma+1}(2\gamma M^2-\gamma+1),$$

$$u=\frac{2a_0}{\gamma+1}\left(M-\frac{1}{M}\right),$$

$$\rho=\rho_0\frac{(\gamma+1)M^2}{2+(\gamma-1)M^2},$$

where $M=U/a_0$, U is the shock velocity, and subscript zero refers to values ahead of the shock. In terms of the changes in shock Mach number,

$$M-M_1=(U-U_1)/a_0,$$

we have

$$p-p_1=\frac{4\gamma p_0}{\gamma+1}M_1(M-M_1), \tag{15}$$

$$u-u_1=\frac{2a_0}{\gamma+1}\left(1+\frac{1}{M_1^2}\right)(M-M_1), \tag{16}$$

$$\rho-\rho_1=\frac{4(\gamma+1)\rho_0 M_1}{[2+(\gamma-1)M_1^2]^2}(M-M_1). \tag{17}$$

Substituting the values given by (12), (13) and (14) at $t = x/U_1$, we have

$$\frac{2M_1(M-M_1)}{(M_1^2-1)\,K(M_1)} = -\frac{A(x)-A_1}{A_1}, \tag{18}$$

$$G\left(\frac{x}{k_2}\right) = -\frac{\rho_1 u_1^2 a_1^2}{a_1^2-u_1^2} k_1 \frac{A(x)-A_1}{A_1}, \tag{19}$$

$$H\left(\frac{x}{k_3}\right) = k_4 \frac{A(x)-A_1}{A_1}, \tag{20}$$

where

$$K(M_1) = 2[(1+u_1/a_1)(1+M_1^{-2}+2\mu)]^{-1},$$

$$\mu^2 = \left(\frac{U_1-u_1}{a_1}\right)^2 = \frac{(\gamma-1)M_1^2+2}{2\gamma M_1^2-(\gamma-1)},$$

$$k_1 = 1+\frac{a_1^2-u_1^2}{u_1 a_1}\mu K(M_1),$$

$$k_2 = \frac{U_1}{U_1-u_1+a_1}, \quad k_3 = \frac{U_1}{U_1-u_1},$$

$$k_4 = \frac{\gamma-1}{2}\frac{u_1^2}{a_1^2}\rho_1 K(M_1)(1-M_1^{-2}).$$

Equation (18) gives the change in the shock Mach number and follows directly from (9), (15) and (16). From (19) and (20) the full solution behind the shock is

$$\left.\begin{aligned} p-p_1 &= -\frac{\rho_1 u_1^2 a_1^2}{a_1^2-u_1^2}\left\{k_1\frac{A(k_2[x-(u_1-a_1)t])-A_1}{A_1} - \frac{A(x)-A_1}{A_1}\right\}, \\ u-u_1 &= \frac{u_1 a_1^2}{a_1^2-u_1^2}\left\{\frac{u_1}{a_1}k_1\frac{A(k_2[x-(u_1-a_1)t])-A_1}{A_1} - \frac{A(x)-A_1}{A_1}\right\}, \\ \rho-\rho_1 &= \frac{1}{a_1^2}(p-p_1)+k_4\frac{A(k_3[x-u_1 t])-A_1}{A_1}. \end{aligned}\right\} \tag{21}$$

This is Chester's solution. As explained above the solution breaks down when $u_1 = a_1$.

In the next section we obtain an improved solution which will reduce to this one when $u_1 - a_1$ is not small, but is valid in the case when $u_1 - a_1$ is small or even zero.

3. Improvement of the solution along the negative characteristics

The cause of the breakdown when $u_1 = a_1$ is explained by examining (7), the equation holding along the negative characteristics. The original coefficient $u-a$ in (5) has been replaced by the unperturbed value $u_1 - a_1$. Near the sonic speed this approximation is not valid, and it is seen that this coefficient leads directly to the denominator $u_1 - a_1$ in (10). Notice that if the term with coefficient $u-a$ is left out altogether on the grounds that it is small, we get the solution

$$(p-p_1)-\rho_1 a_1(u-u_1) = -\frac{\rho_1 a_1^2 u_1}{A_1}A_x t + 2G(x)$$

which is again inadequate.

In this section we consider a more exact analysis of the negative characteristic equation. Since $u-a$ is the critical quantity, the differential equations will be rewritten so as to use u and a as dependent variables, in place of u and p. Then an equation with $u-a$ as dependent variable will be derived. With u and a as dependent variables the equations of motion (1)–(3) become

$$\frac{2}{\gamma-1}[a_t+ua_x]+au_x+\frac{ua}{A}A_x=0, \tag{22}$$

$$u_t+uu_x+\frac{2}{\gamma-1}aa_x-\frac{a^2S_x}{c_v\gamma(\gamma-1)}=0, \tag{23}$$

$$S_t+uS_x=0, \tag{24}$$

where it is convenient now to work with the entropy $S=c_v\log(p/\rho^\gamma)$. Taking the combinations (22) + (23) and (23) $-\frac{1}{2}(\gamma-1)\times$ (22), we have respectively

$$\frac{2}{\gamma-1}[a_t+(u+a)a_x]+[u_t+(u+a)u_x]=\frac{a^2S_x}{\gamma(\gamma-1)c_v}-\frac{ua}{A}A_x, \tag{25}$$

$$(u_t-a_t)+(u-a)(u_x-a_x)+\frac{3-\gamma}{2}a\left[\frac{2}{\gamma-1}a_x+u_x\right]=\frac{a^2S_x}{\gamma(\gamma-1)c_v}+\frac{\gamma-1}{2}\frac{ua}{A}A_x. \tag{26}$$

(To obtain (26), the quantity $a(u_x-a_x)$ has been added and subtracted.) Since there are no difficulties along the positive characteristics or the particle paths, we can linearize (25) and (24):

$$\left(\frac{2}{\gamma-1}a+u\right)_t+(u_1+a_1)\left(\frac{2}{\gamma-1}a+u\right)_x=\frac{a_1^2S_x}{\gamma(\gamma-1)c_v}-\frac{u_1a_1}{A_1}A_x, \tag{27}$$

$$S_t+u_1S_x=0. \tag{28}$$

Then

$$\left.\begin{aligned}\frac{2}{\gamma-1}(a-a_1)+(u-u_1)&=\frac{a_1}{\gamma(\gamma-1)c_v}(S-S_1)\\&\quad-\frac{u_1a_1}{u_1+a_1}\frac{A(x)-A_1}{A_1}+F(x-(u_1+a_1)t),\\S&=-\frac{c_va_1^2}{p_1}H(x-u_1t),\end{aligned}\right\} \tag{29}$$

the coefficient of H being chosen to agree with (11). The function F, constant along characteristics $dx/dt=u_1+a_1$, is set equal to zero as before since there is no incoming disturbance. The function H is determined from the shock condition and, as there is no change from the linearized theory, is given by equation (20). Now, the terms in (26) which do not involve $u-a$ can also be linearized. Letting $u-a=w$; and linearizing the remaining terms, we have

$$w_t+ww_x+\frac{3-\gamma}{2}a_1\left[\frac{2}{\gamma-1}a_x+u_x\right]=\frac{a_1^2}{\gamma(\gamma-1)c_v}S_x+\frac{\gamma-1}{2}\frac{u_1a_1}{A_1}A_x. \tag{30}$$

Substituting from (29), we have finally

$$w_t+ww_x=-\frac{a_1^2}{2\rho_1}H'(x-u_1t)+\beta\frac{A'(x)}{A_1}, \tag{31}$$

where

$$\beta=\frac{u_1a_1}{u_1+a_1}[\tfrac{1}{2}(\gamma-1)u_1+a_1].$$

Since $A(x)$ is prescribed and $S \propto H$ is known in terms of $A - A_1$ (see equation (20)), equation (31) is a quasi-linear partial differential equation with the right-hand side a known function of x and t. Equation (31) gives the change of w along the C_-; it must therefore be integrated along each C_- with initial values given at the shock, $x = U_1 t$. The initial condition for w is obtained in terms of $M - M_1$ from the shock relations (15)–(17). Finally, determining this value in terms of $A - A_1$ from (18), we have

$$w = -k\frac{A - A_1}{A_1} + (u_1 - a_1) \tag{32}$$

at the shock, where

$$k = \frac{a_0}{\gamma + 1}\left[1 + M_1^{-2} - \frac{\gamma\mu^2 M_1^2 - 1}{M_1^2\mu}\right]\frac{(M_1^2 - 1)\,K(M_1)}{M_1}.$$

Equation (31) can be reduced to a system of ordinary differential equations

$$dt : 1 = dx : w = dw : -\frac{a_1^2}{2\rho_1}H' + \beta\frac{A'}{A_1}.$$

It is convenient, however, to introduce a characteristic co-ordinate σ such that $\sigma_t + w\sigma_x = 0$, i.e. $(dx/dt)_{\sigma=\text{const}} = w$; then the equation becomes

$$\left(\frac{dw}{dt}\right)_{\sigma=\text{const}} = w_t + ww_x = -\frac{a_1^2}{2\rho_1}H' + \beta\frac{A'}{A_1}. \tag{33}$$

If we choose σ so that it is equal to x at the shock, we require

$$w = -k\frac{A(\sigma) - A_1}{A_1} + (u_1 - a_1) \quad \text{at} \quad x = \sigma, \quad t = \frac{\sigma}{U_1}. \tag{34}$$

Equation (33) will hold whether $u_1 - a_1$ is near zero or not. If we assume that the perturbation in $u - a$ is small compared with $u_1 - a_1$, (33) can be integrated immediately to give

$$w = \frac{a_1}{2\rho_1}H(x - u_1 t) + \frac{\beta}{u_1 - a_1}\frac{A(x) - A_1}{A_1} + G(x - (u_1 - a_1)t).$$

This, in combination with the positive characteristic result in (29), will reduce to Chester's solution (21).

It does not seem possible to find a convenient general expression for the solution to (33) when $A(x)$ is arbitrary. In §5 the solution is found for the special case $A(x) = A_1(1 + \epsilon x)$ for $x > 0$. However, a general solution can be obtained when the entropy term, $H(x - u_1 t)$, is neglected; and this will be considered first. If the shock is not too strong the error introduced by neglecting the entropy term is small. For sonic conditions this term is about 10% of the area term. It should also be noted that H will often be zero over a large part of the range of integration, since it is non-zero only to the right of the particle path $x = u_1 t$ (see figure 1). The entropy term does not affect the qualitative behaviour of the solution; and its effect on the magnitude of the disturbances is shown to be small in the special case of §5. Accordingly we drop this term in (33), for the present. Then

$$\left.\begin{aligned} &w_t + ww_x = \beta A'(x)/A_1, \\ \text{or} \quad &w\left(\frac{dw}{dt}\right)_{\sigma=\text{const}} = \frac{\beta}{A_1}\left(\frac{dA}{dt}\right)_{\sigma=\text{const}}, \end{aligned}\right\} \tag{35}$$

and the solution is

$$w^2 = 2\beta A(x)/A_1 + \phi(\sigma),$$

where $\phi(\sigma)$ is chosen to satisfy (34). The final solution for w is

$$w = \pm\sqrt{\left[\left\{k\frac{A_1 - A(\sigma)}{A_1} + (u_1 - a_1)\right\}^2 + 2\beta\left\{\frac{A(x) - A(\sigma)}{A_1}\right\}\right]}. \tag{36}$$

The sign in front of the radical is determined by whether the flow is supersonic ($w > 0$) or subsonic ($w < 0$). The characteristics and σ are given then by

$$t = \frac{\sigma}{U_1} + \int_\sigma^x \frac{dx}{w(\sigma, x)}.$$

It should be noted that on those characteristics originating at the shock in $x < 0$, $A(\sigma) = A_1$. If, however, $u_1 > a_1$ the characteristics slope downstream and will, sooner or later, encounter the area change, $x > 0$; then the shape of the characteristics is altered by the term $2\beta A_1^{-1}\{A(x) - A(\sigma)\}$ under the radical.

4. Discussion of the results for general $A(x)$, with entropy changes neglected

There are four cases to discuss depending on the signs of $A'(x)$ and $u_1 - a_1$. If $A'(x) < 0$ the shock strength increases in the area change as shown by (18); from (35), w decreases along the characteristics so that in the (x, t) plane characteristics bend in the upstream direction. If $A'(x) > 0$, the shock decreases in strength, and w increases along the characteristics so that they bend downstream.

Case (i): $u_1 > a_1$; $A'(x) < 0$ *for* $x > 0$ (*figure* 2)

We consider a monotonic decreasing area change and assume the incoming flow to be slightly supersonic; hence the plus sign is taken in front of the radical in (36). Since the area is decreasing the shock strength increases and the flow behind the shock becomes more supersonic. This is indicated in (36) by the fact that $k(A_1 - A(\sigma))/A_1$ increases with σ.

Characteristics 1 in figure 2 originating in the uniform flow region remain straight with slope $dt/dx = (u_1 - a_1)^{-1}$ until the area change is encountered. In $x > 0$ their slopes are given by $w^{-1} = \{(u_1 - a_1)^2 + 2\beta A_1^{-1}(A(x) - A_1)\}^{-\frac{1}{2}}$. It is to be noted that w takes this form along all characteristics originating in $x < 0$; therefore their behaviour in $x > 0$ is identical. (This is just the steady flow solution of the perturbed equations; the exact solution of the full equations could easily be found for this steady flow region.) Since the area is decreasing, $A(x) - A_1 < 0$ for $x > 0$, and w decreases along the characteristic as x increases; therefore, the characteristic slope $dt/dx = w^{-1}$ increases. If $u_1 - a_1$ is small enough the area decrease will cause w to vanish at some point; the characteristic will have a vertical tangent there, and will then begin to slope back upstream. Here the sign in front of the radical in (36) changes from plus to minus as the flow goes from supersonic to subsonic.

Characteristics 2 start initially with a slope $\{k(A_1 - A(\sigma)) + (u_1 - a_1)\}^{-1}$. Here again if the area change encountered is enough to overcome the initial value, the characteristics will curve around and head upstream. For characteristics 3 the

area change is not sufficient to overcome the initial value at the shock. Characteristics of this type continue downstream after passing through the perturbed area region; they form an expansion wave moving downstream. Characteristics 4 start after the area change and are straight, with a slope determined by the increased shock strength caused by the total area change.

Since $u_1 > a_1$ in the initial flow $x < 0$, the only disturbance which can be sent back into this region is a shock wave. Hence before emerging from the perturbed area region the reflected disturbances, represented by the characteristics which bend back, must form a shock. The shock formation corresponds to the intersection of the characteristics as indicated in figure 2. It is easy to see that they do

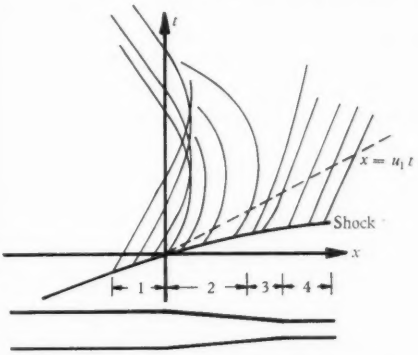

FIGURE 2. The (x, t) diagram for case (i): $u_1 > a_1$, $A'(x) < 0$.

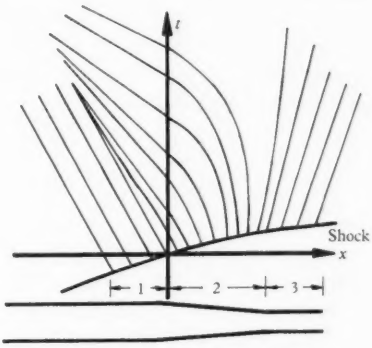

FIGURE 3. The (x, t) diagram for case (ii): $u_1 < a_1$, $A'(x) < 0$.

intersect. The characteristics 1 starting in $x < 0$ have the same shape in $x > 0$ but are successively displaced in the t-direction; clearly they have an envelope which is the locus of the points of vertical slope ($w = 0$). This envelope starts at the point of vertical slope on the characteristic through the origin and usually this will be the point of shock formation. However, it is possible for the later characteristics, 2, to form an envelope sooner, but this depends on the precise form of $A(x)$; for a linear change $A'(x) =$ constant, this is not the case. For the special problem of a linear area change, details of shock formation are given in the last section for all the cases: supersonic or subsonic incoming flow, and expanding or contracting area. If $u_1 - a_1$ is not small, any subsidiary shocks form far upstream or downstream and so have little importance. However, near sonic conditions the subsidiary shocks form in or near the area change, and may form immediately or soon after the main shock reaches the area change.

Case (ii): $u_1 < a_1$; $A' < 0$ *for* $x > 0$ (*figure* 3)

For this case with the incoming flow slightly subsonic, the minus sign is taken in front of the radical in (36). Characteristics 1 in figure 3 never enter the perturbed area region. Type 2 characteristics, which start at the shock in $x > 0$, have initial slopes which become closer to the vertical as the shock strengthens in the contraction. The area change in this case causes the characteristics to bend upstream. When a characteristic crosses into $x < 0$ it becomes a straight line whose slope is

equal to its slope at $x = 0$. It will be shown that for the special case considered in the next section these characteristics will merge upstream of the area change, forming a shock which will propagate upstream. For this case, as for the previous one, location of the point of shock formation depends on the precise form of $A(x)$. If the flow is still subsonic downstream of the area change, the characteristics starting there will point upstream and will reach the area change. But if the contraction is great enough and the shock strengthens sufficiently to make the flow supersonic, the characteristics will point downstream; this is the case shown in figure 3.

Case (iii): $u_1 > a_1$; $A' > 0$ *for* $x > 0$ (*figure* 4)

The incoming flow is supersonic and we again choose the positive sign in (36). However, as the area increases the shock strength decreases and hence so does $u - a$. We assume that the area change is sufficient to alter the shock strength so that the flow immediately behind the shock changes from supersonic to subsonic.

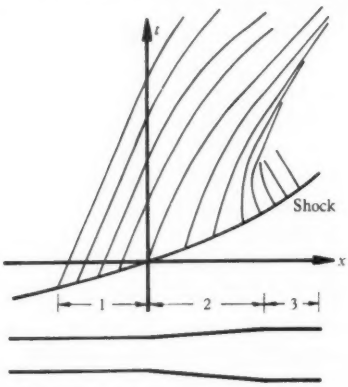

FIGURE 4. The (x, t) diagram for case (iii): $u_1 > a_1$, $A'(x) > 0$.

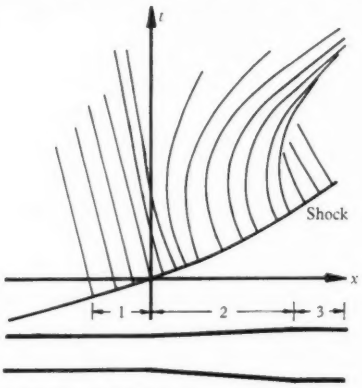

FIGURE 5. The (x, t) diagram for case (iv): $u_1 < a_1$, $A'(x) > 0$.

Characteristics 1 have constant slope $(u_1 - a_1)^{-1} = w^{-1}$ in $x < 0$. At the area change w increases, since $(A(x) - A_1) > 0$, and the characteristics bend downstream. Characteristics 2, starting in the perturbed area, have slopes at first pointing downstream, but as the shock is weakened they may eventually point upstream at the shock. In the latter case, however, $2\beta A_1^{-1}(A(x) - A(\sigma))$ decreases at first along the characteristics; therefore they become vertical and then bend back downstream. These characteristics will either merge with each other or with characteristics 3 from the uniform section downstream and again a shock will be formed. In this case the shock may move upstream or continue downstream.

Case (iv): $u_1 < a_1$; $A' > 0$ *for* $x > 0$ (*figure* 5)

For this case, as for case (ii), the characteristics 1, originating at the shock in $x < 0$, will head upstream, undisturbed. Type 2 characteristics start out more subsonic than type 1 as the shock is weakened in the expanding area. However, the effect of the area change is to bend these characteristics downstream. If a

characteristic meets $x = 0$ before it curves downstream it continues into $x < 0$ with constant slope. Those characteristics which do bend downstream will, as in the previous case, merge to form a shock.

It is interesting to note that in all cases the effect of the area change on the flow behind the shock and within the area change tends to counteract the effect on the shock. A contracting area strengthens the shock but then causes $u - a$ to decrease along the characteristics, while an expanding area weakens the shock and then causes $u - a$ to increase along the characteristics.

5. Solution of the equations for the case of a linear area change

The solution, including the contribution of the entropy term, will now be given for the relatively simple problem of a linear area change. We assume that

$$A(x) = A_1 \qquad (x \leqslant 0),$$
$$A(x) = A_1(1+\epsilon x) \quad (x > 0).$$

Hence, using (20),

$$-\frac{a_1^2}{2\rho_1} H(x-u_1 t) = \begin{cases} -b\epsilon(x-u_1 t) & \text{for} \quad x-u_1 t > 0, \\ 0 & \text{otherwise}, \end{cases} \tag{37}$$

where $$b = \tfrac{1}{4}(\gamma-1)(1-M_1^{-2})\,K(M_1)\,u_1^2 \frac{U_1}{U_1-u_1}.$$

At the shock $x = \sigma$, $t = \sigma/U_1$,

$$w = \begin{cases} u_1 - a_1, & \text{for} \quad \sigma \leqslant 0 \\ (u_1-a_1) - k\epsilon\sigma = w_s, \quad \text{say}, & \text{for} \quad \sigma > 0 \end{cases}. \tag{38}$$

The differential equation (31) becomes

$$\left(\frac{dw}{dt}\right)_{\sigma=\text{const}} = w_t + w w_x = (\beta - b)\,\epsilon, \tag{39}$$

where $$\beta = 0 \quad \text{for} \quad x < 0,$$
$$b = 0 \quad \text{for} \quad x - u_1 t < 0.$$

In connexion with the approximation of the last section in which the entropy change was omitted it is of interest to note that, for sonic conditions, $u_1 = a_1$, $\beta = 1{\cdot}04a_0^2$ and $b = 0{\cdot}109a_0^2$; also $k = 0{\cdot}238a_0$.

The integration of (39) is immediate but there are various regions to distinguish in each case.

Case (i): $u_1 > a_1$, $\epsilon < 0$ (*figure* 2)

For characteristics 1, starting in $x < 0$, we have

$$\left.\begin{aligned} w &= u_1 - a_1, \\ x &= (u_1-a_1)\left(t - \frac{\sigma}{U_1}\right) + \sigma, \end{aligned}\right\} \tag{40}$$

for $x \leqslant 0$, $\dfrac{\sigma}{U_1} \leqslant t \leqslant t_0 = \sigma\left(\dfrac{1}{U_1} - \dfrac{1}{u_1-a_1}\right)$;

$$\left.\begin{aligned} w &= \beta\epsilon(t-t_0) + (u_1-a_1), \\ x &= \frac{\beta\epsilon}{2}(t-t_0)^2 + (u_1-a_1)(t-t_0), \end{aligned}\right\} \tag{41}$$

for $x \geqslant 0$, $t \geqslant t_0$; where t_0 gives the time at which the characteristic σ passes $x = 0$.

For characteristics 2, starting in $x > 0$, we have

$$\left.\begin{aligned} w &= \epsilon(\beta-b)\left(t-\frac{\sigma}{U_1}\right)+w_s, \\ x &= \frac{\epsilon}{2}\left(t-\frac{\sigma}{U_1}\right)^2(\beta-b)+w_s\left(t-\frac{\sigma}{U_1}\right)+\sigma, \end{aligned}\right\} \tag{42}$$

for $x-u_1t \geqslant 0$;

$$\left.\begin{aligned} w &= \beta\epsilon\left(t-\frac{\sigma}{U_1}\right)+w_s+c_1, \\ x &= \frac{\beta\epsilon}{2}\left(t-\frac{\sigma}{U_1}\right)^2+(w_s+c_1)\left(t-\frac{\sigma}{U_1}\right)+c_2+\sigma, \end{aligned}\right\} \tag{43}$$

for $x-u_1t \leqslant 0$; where w_s is the value of w at the shock, given by (38), and

$$c_1(\sigma) = \frac{b}{b-\beta}\left[(u_1-w_s)-\sqrt{\left\{(u_1-w_s)^2+2\epsilon\sigma(\beta-b)\left(\frac{u_1}{U_1}-1\right)\right\}}\right],$$

$$c_2(\sigma) = -c_1^2/2\beta\epsilon.$$

The functions c_1 and c_2 are determined by connecting (42) and (43) at the line $x = u_1t$. A characteristic of the type given in (43) may meet the t-axis. If this occurs it continues upstream with a constant slope equal to its slope at the t-axis. These are given by

$$\left.\begin{aligned} w &= \beta\epsilon\left(t_1-\frac{\sigma}{U_1}\right)+w_s+c_1, \\ x &= \left\{\beta\epsilon\left(t_1-\frac{\sigma}{U_1}\right)+w_s+c_1\right\}(t-t_1), \end{aligned}\right\} \tag{44}$$

for $x \leqslant 0$, $t \geqslant t_1$, where

$$t_1 = \frac{\sigma}{U_1}-\frac{1}{\beta\epsilon}\{(w_s+c_1)+\sqrt{[(w_s+c_1)^2-2\beta\epsilon(\sigma+c_2)]}\}. \tag{45}$$

The solutions (42) or (43) can be put into the form of equation (36), used for the discussion of the previous section, by eliminating $t-\sigma/U_1$; from (42), for example

$$w = \sqrt{[\{(u_1-a_1)-k\epsilon\sigma\}^2+2\epsilon(\beta-b)(x-\sigma)]}. \tag{46}$$

The location of the point of shock formation in the perturbation region can be calculated from equations (41) to (43). We look for the first intersection of characteristics. The characteristics 1 which originate in $x < 0$, equation (41), have the same slope in $x > 0$; they form a one parameter family of parabolas with an envelope given by

$$x = \frac{(u_1-a_1)^2}{2\beta|\epsilon|}, \quad t \geqslant \frac{(u_1-a_1)}{\beta|\epsilon|}.$$

Those characteristics originating in $x > 0$ have initial slopes less than $(u_1-a_1)^{-1}$. Also in the region $u_1t < x \leqslant U_1t$ the rate of increase of their slope, $\epsilon(\beta-b)$, is less than that of the characteristics originating in $x < 0$, which is $\epsilon\beta$. For $x < u_1t$ the rate of increase of slope for both kinds of characteristics is the same. Hence those characteristics which originate in $x > 0$ fan out downstream more than

those from $x < 0$. The first intersection of characteristics will therefore be determined by the envelope given above and the point of shock formation will be

$$x = \frac{(u_1 - a_1)^2}{2\beta|\epsilon|}, \quad t = \frac{(u_1 - a_1)}{\beta|\epsilon|},$$

on the characteristic through $x = t = 0$.

The subsidiary shock formed at this point will stay relatively weak and its path and strength could be determined using the property that the path of a weak shock in the (x, t) plane bisects the angle between the characteristics on each side of it; but even for this special case of a linear area change the results take a complicated form. However, since the subsidiary shock is weak it will at first stay close to the characteristic through $x = t = 0$, and will emerge from the non-uniform region approximately where this characteristic does; i.e. after a time given by $t = 2(u_1 - a_1)(\beta|\epsilon|)^{-1}$. When the shock emerges into the uniform region $x < 0$, $t > 0$, its motion is given by relatively simple formulae; these will be discussed in § 6.

Case (ii): $u_1 < a_1$, $\epsilon < 0$ (*figure* 3)

For characteristics 1, which start and remain in $x < 0$, we have

$$\left.\begin{aligned} w &= u_1 - a_1, \\ x &= (u_1 - a_1)\left(t - \frac{\sigma}{U_1}\right) + \sigma, \end{aligned}\right\} \tag{47}$$

where $x \leqslant 0$, $(\sigma/U_1) \leqslant t$.

For characteristics 2, starting in $x > 0$, we have

$$\left.\begin{aligned} w &= \epsilon(\beta - b)\left(t - \frac{\sigma}{U_1}\right) + w_s, \\ x &= \frac{\epsilon}{2}(\beta - b)\left(t - \frac{\sigma}{U_1}\right)^2 + w_s\left(t - \frac{\sigma}{U_1}\right) + \sigma, \end{aligned}\right\} \tag{48}$$

for $x - u_1 t \geqslant 0$;

$$\left.\begin{aligned} w &= \beta\epsilon\left(t - \frac{\sigma}{U_1}\right) + w_s + c_1, \\ x &= \frac{\beta\epsilon}{2}\left(t - \frac{\sigma}{U_1}\right)^2 + (w_s + c_1)\left(t - \frac{\sigma}{U_1}\right) + \sigma + c_2, \end{aligned}\right\} \tag{49}$$

for $x - u_1 t \leqslant 0$; where c_1 and c_2 are given in equation (43). A characteristic of this type which crosses the t-axis is given by

$$\left.\begin{aligned} w &= \beta\epsilon\left(t_1 - \frac{\sigma}{U_1}\right) + w_s + c_1, \\ x &= \left\{\beta\epsilon\left(t_1 - \frac{\sigma}{U_1}\right) + w_s + c_1\right\}(t - t_1), \end{aligned}\right\} \tag{50}$$

for $x \leqslant 0$, $t \leqslant t_1$, where t_1 is defined in (45). By examining the expression for w in (50), it can be shown that as σ increases the slope of the characteristic,

$$dt/dx = 1/w,$$

becomes smaller in absolute value. These characteristics will therefore merge upstream. The point of shock formation will either be where characteristics (50)

merge or where they meet characteristics (47), whichever occurs first. If we rewrite (50) as

$$x = w(t_1)\,(t - t_1), \tag{51}$$

then, since t_1 increases monotonically with σ, we obtain for the envelope

$$x = \frac{w^2}{w'}, \quad t = t_1 + \frac{w}{w'}. \tag{52}$$

Note that for this case,

$$u_1 < a_1,\ t_1 = 0 \quad \text{when} \quad \sigma = 0;$$

whereas for case (i),

$$u_1 > a_1,\ t_1 = 2(u_1 - a_1)\,(\beta|\epsilon|)^{-1} \quad \text{when} \quad \sigma = 0.$$

Evaluating (52) at $t_1 = \sigma = 0$ we have

$$\left.\begin{aligned} x &= -\frac{(u_1-a_1)^2\left(\dfrac{|u_1-a_1|}{U_1}+1\right)}{|\epsilon|\left[\beta+|u_1-a_1|\left\{\dfrac{b}{a_1}\left(\dfrac{u_1}{U_1}-1\right)-k\right\}\right]}, \\ t &= \frac{|u_1-a_1|\left(\dfrac{|u_1-a_1|}{U_1}+1\right)}{|\epsilon|\left[\beta+|u_1-a_1|\left\{\dfrac{b}{a_1}\left(\dfrac{u_1}{U_1}-1\right)-k\right\}\right]}. \end{aligned}\right\} \tag{53}$$

This point also lies on the characteristic (47) through the origin. To show that this is the point of shock formation, it is necessary to see that the envelope (52) does not form for a value of x greater than that given in (53). This is determined by evaluating

$$\frac{dx}{dt_1} = 2w - \left(\frac{w}{w'}\right)^2 w''$$

at $t_1 = \sigma = 0$; it can be shown that this is negative and hence the envelope moves upstream as t_1 increases; therefore (53) is the first point of touching characteristics and is the point of shock formation. The details of the shock path will be obtained in the next section.

Cases (iii) and (iv)

For case (iii) ($u_1 > a_1$, $\epsilon > 0$ (figure 4)) and case (iv) ($u_1 < a_1$, $\epsilon > 0$ (figure 5)) the solutions are the same as for cases (i), equations (40)–(44), and (ii), equations (47)–(50), respectively. To locate the point of shock formation for cases (iii) and (iv) we first find the envelope of the characteristics arising in the non-uniform region. Equation (49) is used for this but to simplify the presentation entropy effects are neglected, so that $b = c_1 = c_2 = 0$. The envelope is given, with σ as parameter, by

$$\left.\begin{aligned} t &= \frac{\sigma}{U_1} + \frac{1 - \dfrac{u_1-a_1}{U_1} + \dfrac{k\epsilon\sigma}{U_1}}{\epsilon k\left(1+\dfrac{\beta}{kU_1}\right)}, \\ x &= \frac{\beta\epsilon}{2}\left(t-\frac{\sigma}{U_1}\right)^2 + [(u_1-a_1) - k\epsilon\sigma]\left(t-\frac{\sigma}{U_1}\right) + \sigma. \end{aligned}\right\} \tag{54}$$

It is seen, from (54), that at $\sigma = 0$ both x and t are $O(\epsilon^{-1})$. Since ϵ, the rate of area change, is assumed to be small, any shocks arising from the merging of characteristics of equation (49) will occur far downstream. A shock will form, however, when characteristics (type 3, figure 4) arising in the uniform region downstream of the area change meet characteristics arising in the non-uniform area region. Analysis of this situation, carried out at the end of the area change, is identical with that done for cases (i) and (ii) at the entrance to the area change.

6. Motion of the subsidiary shocks

In the previous section the point of shock formation for the cases of contracting area, (i) and (ii), was determined. We now discuss the determination of the subsequent shock path. The shock must be fitted in so that the shock relations are satisfied; for a weak shock, the shock conditions show that its slope at each point in the (x, t) plane is the average of the slopes of the characteristics meeting it and this property can be used to determine the motion of the shock (see Whitham 1952). For case (ii) of subsonic incoming flow, the shock forms upstream of the non-uniform region, and will have undisturbed characteristics ahead of it and characteristics of type 2 (which have turned back upstream) behind it. Owing to the simple form of the undisturbed characteristics (straight lines with slope $(u_1 - a_1)^{-1}$) it is relatively easy to determine the shock path for this case. However, for case (i) (supersonic incoming flow) the shock forms in the non-uniform region and both sets of characteristics meeting it are disturbed. As was noted in the previous section, the detailed motion of the shock, while in this region is given by complicated implicit formulae. It does not seem worth while to develop and explain these in detail. Instead we will use a rough estimate of the shock strength and the time when the shock emerges into the uniform region, and its path in the uniform region will then be found.

For case (ii), $u_1 < a_1$, $\epsilon < 0$, the shock forms upstream of the non-uniform region at the point (see (53))

$$\left.\begin{aligned} t_s &= \frac{|u_1 - a_1|\left(\dfrac{|u_1 - a_1|}{U_1} + 1\right)}{|\epsilon|\left[\beta + |u_1 - a_1|\left\{\dfrac{b}{a_1}\left(\dfrac{u_1}{U_1} - 1\right) - k\right\}\right]}, \\ x_s &= -|u_1 - a_1| t_s. \end{aligned}\right\} \tag{55}$$

Upstream of the area change, the characteristics which arise in $x < 0$ and $x > 0$ are given respectively by

$$\left.\begin{aligned} x &= (u_1 - a_1)\left(t - \frac{\sigma}{U_1}\right) + \sigma, \\ x &= w(t_1)\,(t - t_1), \end{aligned}\right\} \tag{56}$$

where $w(t_1) = \beta\epsilon(t_1 - (\sigma/U_1)) + w_s + c_1$, and t_1 is given in (45). Assuming the shock path to be given by $x = X(t)$, we have

$$X(t) = w(t_1)\,(t - t_1)$$

along the shock path. Also, as the shock slope is the average of the slope of the characteristics,

$$X'(t) = \tfrac{1}{2}\{w(t_1) + (u_1 - a_1)\}.$$

But, from the first relation $X'(t)$ can also be written

$$X'(t) = (t-t_1)\,w'(t_1)\frac{dt_1}{dt} + w(t_1)\left(1-\frac{dt_1}{dt}\right).$$

Hence
$$\frac{d}{dt_1}\{[w-(u_1-a_1)]^2\,(t-t_1)\} = w^2-(u_1-a_1)^2, \tag{57}$$

and this is the differential equation for the shock path. The solution to this equation, with initial conditions (55), is

$$\left.\begin{aligned} t &= t_1+[w-(u_1-a_1)]^{-2}\left\{\int_0^{t_1} w^2\,dt_1-(u_1-a_1)^2 t_1\right\},\\ X &= w[w-(u_1-a_1)]^{-2}\left\{\int_0^{t_1} w^2\,dt_1-(u_1-a_1)^2 t_1\right\}. \end{aligned}\right| \tag{58}$$

It can be shown, using (45) and (50), that as t_1 approaches zero, x and t tend to the initial conditions x_s and t_s in (55). The initial velocity $X'(t_s)$ of the shock is u_1-a_1 relative to fixed co-ordinates; that is, it is of magnitude a_1 relative to the upstream flow. Letting M^*-1 measure the shock strength, where M^* is the Mach number $|X'-u_1|/a_1$, we see that the shock starts initially with zero strength.

If the upstream velocity were sonic, $u_1 = a_1$, the shock would start at $x = t = 0$ with velocity u_1 relative to the incoming flow; its initial strength, $a_1^{-1}(u_1-a_1)$ would be zero. The equation for the path in this sonic case is given by (58) when (u_1-a_1) is set equal to zero.

For case (i), $u_1 > a_1$, $\epsilon < 0$, it was shown in the previous section that the shock forms within the non-uniform region at the point

$$x = \frac{(u_1-a_1)^2}{2\beta|\epsilon|}, \quad t = \frac{(u_1-a_1)}{\beta|\epsilon|}.$$

As the shock is weak it will follow, very nearly, the path of the characteristic through this point. Thus it is given approximately by

$$x = \tfrac{1}{2}(\beta\epsilon)\,t^2+(u_1-a_1)\,t,$$

which is obtained from (43) with $\sigma = 0$. At $t = 2(u_1-a_1)\,(\beta|\epsilon|)^{-1}$ this characteristic crosses the t axis into $x < 0$. It will therefore be assumed that the shock enters the uniform region near the point

$$x = 0, \quad t = \frac{2(u_1-a_1)}{\beta|\epsilon|}. \tag{59}$$

The strength of the shock depends on the small difference of its slope from the characteristic slope. At $x = 0$, the shock will have an undisturbed characteristic with slope $(u_1-a_1)^{-1}$ ahead of it, and a characteristic of type 2, which has turned back upstream, behind it. Characteristics of type 2 have slopes approximately equal to $-(u_1-a_1)^{-1}$ when they reach $x = 0$. Hence, initially, the slope of the shock (being the mean of these) is approximately vertical, in the (x,t) plane. Relative to the incoming flow the shock velocity is just u_1, so its strength, M^*-1, is $a_1^{-1}(u_1-a_1)$. Thus, according to this estimate, the strength at $x = 0$ is independent of ϵ; however, ϵ determines the time at which the shock emerges (see (59)).

In $x < 0$ the equations of the characteristics meeting the shock are given in (56) and the differential equation for the shock path is given in (57). The solution to the equation, with initial conditions (59), is

$$\left.\begin{aligned} t &= t_1 + [w-(u_1-a_1)]^{-2}\left\{\int_{t_i}^{t_1} w^2\,dt_1 - (u_1-a_1)^2(t_1-t_i)\right\}, \\ x &= w[w-(u_1-a_1)]^{-2}\left\{\int_{t_i}^{t_1} w^2\,dt_1 - (u_1-a_1)^2(t_1-t_i)\right\}, \end{aligned}\right\} \tag{60}$$

where $t_i = 2(u_1-a_1)(\beta|\epsilon|)^{-1}$. It should be remembered that the initial point, t_i, is approximate and that this equation is not intended to give the detailed behaviour near $t = t_i$.

However, for sonic upstream flow, $u_1 = a_1$, the initial condition (59) becomes $x = t = 0$, and the shock never enters the non-uniform region. Equation (60) is correct for this case when (u_1-a_1) and t_i are set equal to zero.

For the cases (iii) and (iv), the subsidiary shocks move downstream in general; if the area eventually becomes uniform downstream, similar expressions to the above can be found for the shock path.

This research was sponsored by the United States Air Force under Contract No. AV 49(638)-446 monitored by the A. F. Office of Scientific Research and Development Command.

The author wishes to thank Professor G. B. Whitham for suggesting this problem, and for his continued interest and helpful advice.

REFERENCES

Chester, W. 1954 *Phil. Mag.* (7), **45**, 1293.
Chisnell, R. F. 1957 *J. Fluid Mech.* **2**, 286.
Stocker, P. M. 1952 *Proc. Camb. Phil. Soc.* **48**, 482.
Whitham, G. B. 1952 *Commun. Pure App. Math.* **5**, 315.
Whitham, G. B. 1958 *J. Fluid Mech.* **4**, 337.

The forces on wing-fuselage combinations in supersonic flow

By JOSEPH H. CLARKE
Boeing Scientific Research Laboratories, Seattle, Washington†

(Received 5 October 1959)

Reverse-flow relations are used to provide convenient expressions for the aerodynamic forces which act on a general wing-fuselage combination in supersonic flow. The drag, lift, spanwise and chordwise lift distributions, and wing moments are treated. Consideration is given to available methods and results, including tables, which apply to the wing-fuselage interference problem, and reverse-flow relations are then employed to effect desirable changes in the defining force expressions by introducing wings or fuselages in the reverse flow. It is shown that the aerodynamic forces can be determined from a solution for the pressure on only the fuselage surface within the domain of dependence of the wing, this region being selected on the basis of relative ease of computation. In some cases the simplification achieved is quite substantial. Certain results in the literature arise naturally as special cases. The reverse-flow theorem is re-examined in the light of the procedure considered, and it is found to be inapplicable in one respect. The difficulty is circumvented by constructing an acceptable configuration which is equipollent to the prescribed one. It appears that the method given is applicable in other linear hyperbolic problems in mathematical physics when bulk or gross information is required and a suitable reciprocity relation can be constructed.

1. Introduction

This paper presents a method for the determination of the supersonic aerodynamic forces, particularly the drag, that act on the general wing-fuselage combination shown in figure 1. Upstream and downstream of the wing, the infinite fuselage surface is a cylinder with an arbitrary cross-section and an incidence α_1. Over the interval $x_i \leqslant x \leqslant x_f$, where x is a Cartesian co-ordinate in the direction of the incident stream, the fuselage surface exhibits arbitrary small deflexions in addition to the incidence; these might represent contours deduced from considerations of favourable interference, a canopy, etc. The fuselage considered is then described as an infinite quasi-cylinder. The boundary conditions and surface pressures are discussed, within the framework of linearized theory, on a reference surface Σ_1, which is a cylinder with generators parallel to the incident stream and with the cross-section mentioned. The wing has arbitrary planform, thickness distribution and warp, and is arbitrarily mounted on the fuselage. The reference

† Permanent address: Division of Engineering, Brown University, Providence, Rhode Island.

surface for thetwo panels is the plane Σ_2 which is taken to lie in the (x, y)-plane. The combination is symmetric about the (x, z)-plane. The disturbance field of these boundaries is conveniently written as the sum of four terms: the flow field of the isolated fuselage, the flow field of the isolated wing (arbitrarily extended through the body), the interference flow field produced on Σ_1 to cancel cross-flow originating on the wing, and the interference flow field produced on Σ_2 to cancel cross-flow originating on the fuselage.

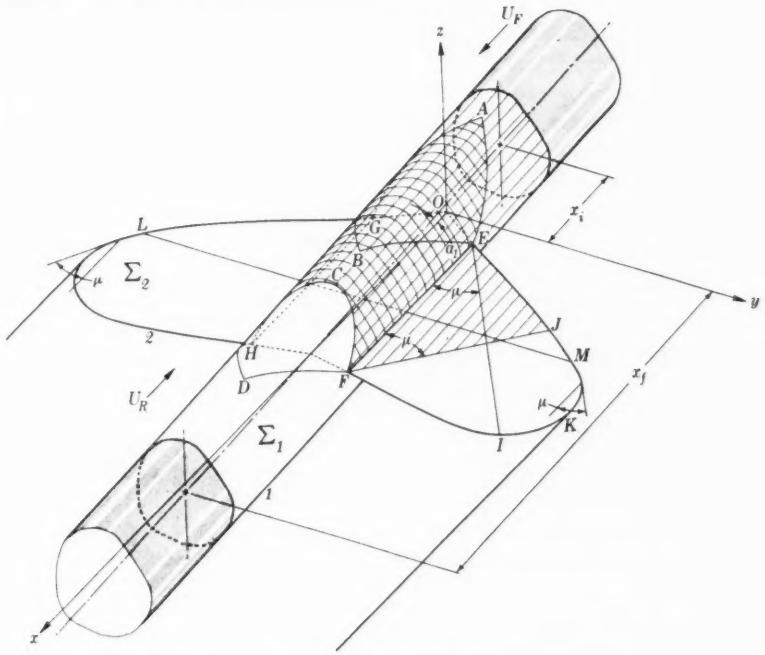

FIGURE 1. Wing-fuselage combination considered.

The determination of the disturbance field produced when the boundary values discussed (or special cases thereof) are prescribed has been considered extensively in the literature. The calculations required are, in general, difficult and extensive (cf. Lawrence & Flax 1954). Beginning with the two isolated flows, it is possible to cancel in turn the remote cross-flow induced on each surface by the other. This non-terminating process gives rise to an infinite number of boundary-value problems for isolated wings and isolated infinite quasi-cylinders; the convergence of the series has been established by Ferrari (1948, 1949), who proposed and used the method.

For field points upstream of the domain of influence of the trailing edge, a simpler formulation is sometimes possible. (Since the fuselage incidence may be treated separately by superposition, it is taken as zero for the present.) If the wing leading edge is supersonic over a sufficiently long segment and if the prescribed fuselage contours are suitable, the field point discussed is not influenced by

disturbances originating on the other side of the (x, y)-plane. The flow at the point is the same as that over the influencing geometry plus the image thereof in the (x, y)-plane. A portion of the field is then determined by mating two half-spaces, the process satisfying the boundary conditions of the problem. The lifting problem for the upstream region discussed is then reduced to two equivalent symmetric problems corresponding to the geometry above and below the (x, y)-plane, respectively. Now, when the combination in figure 1 is symmetric about the (x, y)-plane, the disturbance field may be found by a process which terminates in one step. The isolated fuselage does not induce a cross-flow on Σ_2. When the cross-flow induced on Σ_1 by the isolated wing is cancelled, the resulting interference flow does not flow across Σ_2. The symmetric problem is then reduced to solving two infinite quasi-cylindrical problems and one isolated wing problem: the latter requires no further discussion.

The above formulation was proposed by Lagerstrom & Van Dyke (1949), and has subsequently been employed by a number of writers, particularly Nielson (1955) and Randall (1955) for the case of the infinite quasi-cylinder with almost circular section. The several approaches to this last problem suggest that the most satisfactory procedure in practice is one straightforward in principle which employs a Fourier expansion of the surface deflexions in the meridian angle, and solution of the resulting boundary-value problem by Laplace transforms. The formidable difficulty here is in evaluating a set of characteristic functions $W_n(x, r), n = 0, 1, 2, \ldots$, in the streamwise co-ordinate x and the cylindrical co-ordinate r, the functions being defined as inverse Laplace transforms of modified Bessel functions. An extensive set of tables of these functions has now been prepared jointly by Nielson (1957) and Mersman (1954). The tables are given for very small intervals in x, so that the surface pressure on $r = 1$ may be computed with a simple, routine calculation. Only a very small number of values of r appear, however, so that calculation of the flow induced on Σ_2 (i.e. off Σ_1) remains necessarily extensive in most cases. The complication is compounded in the case of the interference flow by the fact that wing-induced cross-flow on Σ_1 will generally be discontinuous, so that the Fourier series in the characteristic functions which gives the interference flow component will be slowly convergent. A discussion of this state of affairs has been given by Lock (1958) whose extension is mentioned below. Fuselages with polygonal cross-sections have been considered for the equivalent symmetric problem by Lagerstrom & Van Dyke (1949), and the almost rectangular cross-section has been treated by Ting (1957).

In the present paper, reverse-flow relations are used to provide useful expressions for the supersonic aerodynamic forces acting on the configuration described. The drag, lift, spanwise and chordwise lift distributions, and wing moments are considered. Such relations are obtained by choosing in the reverse flow either a wing alone, a fuselage alone, or a wing and a fuselage which interfere in the absence of interference flows so that mutual distortion occurs. The geometry of these bodies is so chosen to produce the desired force expressions in the reverse-flow relations. Prominent in the results are mixed-drag expressions that require the integration of the pressure in forward flow over the slopes of the stream surfaces of the reverse flow which are near the reference surface. The technique

was introduced by Clarke (1959*a*) in connexion with arrangements of separated interfering finite bodies which are not necessarily quasi-cylindrical. The expressions obtained for the aerodynamic forces require that the solution for the perturbation flow be determined only on the region of Σ_1 that is influenced by the wing in reverse flow (the region is assumed throughout not to extend downstream of the wing-fuselage junction in forward flow). This is the hatched and cross-hatched portion of Σ_1 shown in figure 1. The result appears to introduce an essential simplification, no matter what method is used to compute the flow. When fuselage contouring is absent, the results are particularly simple.

Again considering that the fuselage incidence is suppressed, suppose further that the leading edge of the wing is supersonic along the segments, denoted on the right panel by EJ, which are within the region of dependence of the cited portion of Σ_1. Also suppose that the contours either vanish or are vertically symmetric on the portion of Σ_1 within the region of dependence of EJ and its counterpart on the left. This is the hatched surface bounded on the upper side by curve EAG. Then the required perturbation pressure on Σ_1 may be determined by solving two equivalent symmetric problems, although the presence of an afterbody and any subsonic edge segments would exclude this formulation for the full problem.† In the case of quasi-cylinders of almost circular cross-section, the calculation of this pressure is then a routine matter, with use of the tables discussed, since it is required only on the surface of the cylinder.

The reverse-flow field of at least the afterbody of the isolated fuselage is required on Σ_2 (i.e. off Σ_1) in certain of the drag expressions, however, and this introduces additional labour unless the few values in the table suffice for this purpose. But a convenient drag expression is obtained for the case where the prescribed configuration is immediately reducible to equivalent symmetric problems which eliminates the need to calculate the flow of any infinite quasi-cylinder off its surface. Most of the results discussed require the introduction of the reverse-flow fields of certain isolated wings. Consideration of the complexity of the wing-fuselage interference problem suggests that this exchange of labour is a highly desirable one, since the wing problems have received extensive study. In fact, the supersonic flow fields of certain wings are now tabulated in the literature. In all cases the simplification achieved in the forward flow has to be compared with the calculations introduced in the reverse flow. And the advantage of the expressions obtained is, of course, assessed by comparison with the corresponding direct calculation.

A number of theorems concerning the lift of wing-fuselage combinations appear in the literature. Reverse-flow considerations have been used to relate the lift on a prescribed configuration to that on a simpler one (Lawrence & Flax 1954); these results can be used to arrive at the configuration to be actually analysed with the present lift results. Flax (1953) has given a Trefftz plane theorem for the fuselage lift; this arises naturally in the present work in a slightly more general form. When the flow field of the wing in reverse flow is two-dimensional, there appears, as an important special case of the transverse force expression, the

† When the given combination fulfils these geometric requirements in the reverse flow instead of the forward flow, the simplifications still obtain in the case of the drag.

integral relation which was obtained by Ferri, Clarke & Ting (1957) for a fuselage of quasi-rectangular cross-section by physical reasoning. This was generalized by Ting (1959) to an arbitrary cross-section by a method that amounts to application of the hyperbolic divergence theorem to the region enclosed by the trailing edge Mach planes in reverse flow and the foremost Mach surface in forward flow. Lawrence & Flax (1954) had deduced a special version of this integral relation earlier from reverse-flow considerations. For the case of quasi-cylinders of almost circular section, Lock has tabulated the values of cylinder-pressure integrals which extend over lateral lines from the cylinder surface to the limit of disturbance. These tables can be used to compute the forces on certain simple wings without need for the functions $W_n(x, r)$ for $r > 1$. But the wing lift and pitching moment are otherwise given by the integral relation discussed; the tables are, however, useful in the determination of rolling moment.

The reverse-flow theorem for finite bodies with cylindrical reference surfaces was given by Ursell & Ward (1950). Flax (1953) established that the theorem still holds for a wing-fuselage combination with an infinite fuselage at incidence if the latter is a true cylinder. Lawrence & Flax (1954) state the theorem in reference to a combination with an infinite cylinder at zero incidence which may be contoured in addition near the wing. In the present paper, necessary and sufficient conditions for the reverse-flow theorem to hold are derived for the case of boundaries composed of a wing mounted on an infinite quasi-cylinder. For the reverse flows of interest herein, the wing cross-flow on Σ_1 produces distortions which extend to infinity unattenuated; it is found that the reverse-flow theorem fails to apply unless the important fuselage incidence in forward flow is suppressed. This obstacle to the investigation just outlined is removed by constructing a configuration which is equipollent† to the prescribed one and which has zero fuselage incidence and extra wing warp; the two configurations differ by a two-dimensional cylinder flow. The given and equipollent configurations are shown to support identical aerodynamic forces, hence the name.

The first two sections of the paper are concerned, respectively, with the reverse-flow theorem for an infinite quasi-cylinder in combination with a wing, and with the construction of the equipollent configuration. The next section deals with lift, the spanwise and chordwise lift distribution, and wing moments. The final, most extensive section treats the drag, the aerodynamic force of principal interest in the paper.

2. Reverse-flow relation for infinite quasi-cylinder in combination with wing

Let $\mathbf{i}$, $\mathbf{j}$, and $\mathbf{k}$ be unit vectors in the directions of the streamwise co-ordinate x, the lateral co-ordinate y, and the transverse co-ordinate z, respectively. Let the remote stream have a uniform velocity $\mathbf{U} = U\mathbf{i}$, where $U \gtrless 0$, a density ρ_0, and a Mach number $M > 1$. If the steady fluid velocity is written $\mathbf{U} + \mathbf{V}$, then the small perturbation velocity $\mathbf{V} = u\mathbf{i} + v\mathbf{j} + w\mathbf{k}$ is governed by the linear equations

$$\nabla . \mathbf{W} = 0, \quad \nabla \times \mathbf{V} = 0, \tag{1}$$

† For the definition of this term, see e.g. *Principles of Mechanics*, by Synge & Griffith, 2nd ed., p. 260.

where

$$\mathbf{W} = \Phi.\mathbf{V}, \quad \Phi = \begin{bmatrix} -B^2 & 0 & 0 \\ 0 & 1 & 0 \\ 0 & 0 & 1 \end{bmatrix}, \tag{2}$$

and $B = \sqrt{(M^2-1)}$. The boundary condition on the body surface may be written

$$\mathbf{V}.\mathbf{N} = -\mathbf{U}.\mathbf{n} \quad \text{on } \Sigma, \tag{3}$$

where $\Sigma = \Sigma_1 + \Sigma_2$ is the reference surface of the combination, $\mathbf{N}$ is the outward unit normal to the reference surface, and $\mathbf{n}$ is the outward unit normal to the body surface. The perturbation pressure p is related to $\mathbf{V}$ by

$$p = -\rho_0 \mathbf{U}.\mathbf{V}. \tag{4}$$

Using the approach of Ursell & Ward (1950; see also, Ward 1955), we now consider the conditions under which a useful reverse-flow relation can be written when combinations of the type discussed appear in both forward and reverse flow. In accord with previous remarks, we admit the additional possibility here that interference flows are not used in one or both directions, so that the boundaries are those associated with only the isolated flows; the consequence of present interest is that the wing-induced cross-flow produces additional distortions on the fuselage which extend downstream unattenuated. Far downstream in the Trefftz plane of two-dimensional flow, a trailing vortex system streams past an inclined cylinder, possibly distorting it. We then bear in mind two classes of boundaries in each flow direction. Let $U_F > 0$ denote a forward flow incident upon a combination with surface normal $\mathbf{n}_F$, and let $U_R = -U_F < 0$ denote a reverse flow (with equal values of ρ_0 and M) incident upon a combination with surface normal $\mathbf{n}_R$. The bodies have the same reference surface. The perturbation velocities and pressures satisfy (1) to (4), written with subscript F and R, respectively.

We begin with the volume-surface integral identity

$$\int_S (\mathbf{V}_F \mathbf{W}_R.\mathbf{n} + \mathbf{V}_R \mathbf{W}_F.\mathbf{n} - \mathbf{V}_F.\mathbf{W}_R\mathbf{n})\,dS$$
$$= \int_T [\mathbf{V}_F \nabla.\mathbf{W}_R + \mathbf{V}_R \nabla.\mathbf{W}_F - \mathbf{W}_F \times (\nabla \times \mathbf{V}_R) - \mathbf{W}_R \times (\nabla \times \mathbf{V}_F)]\,dT, \tag{5}$$

where T is the region interior to a closed surface S with outward normal $\mathbf{n}$. We enclose Σ by two right circular semi-cylinders which are separated by the (x, y)-plane. We apply (5) separately to two regions T and add the result; the upper region is interior to the cylindrical surface, the reference surface Σ_1, the upper side of the (x, y)-plane, and the annular parts of the cylinder bases exterior to Σ_1; the lower region is similar. The annular bases $S(x = +\infty)$ and $S(x = -\infty)$ are located infinitely far from the wing; the radius of the semi-cylinders is regarded as indefinitely large. The right-hand side of (5) vanishes because of (1). The scalar product of (5) and $\mathbf{U}_F$ then gives

$$\int_S (\mathbf{U}_F.\mathbf{V}_F \mathbf{W}_R.\mathbf{n} - \mathbf{U}_R.\mathbf{V}_R \mathbf{W}_F.\mathbf{n} - \mathbf{V}_F.\mathbf{W}_R \mathbf{U}_F.\mathbf{n})\,dS = 0. \tag{6}$$

The integrations in (6) over the cylindrical surfaces vanish, as do those over the portion of the (x, y)-plane which is free of discontinuities. It is noted that the

initial flow in each direction is two-dimensional. After using (3) and (4), we obtain

$$\int_{\Sigma}(p_F\mathbf{n}_R.\mathbf{i}+p_R\mathbf{n}_F.\mathbf{i})\,dS=\rho_0\int_{S(x=+\infty)}(v_Fv_R+w_Fw_R)\,dS$$
$$-\rho_0\int_{S(x=-\infty)}(v_Fv_R+w_Fw_R)\,dS. \tag{7}$$

It is important to note that the wing planforms in the two directions over the common reference plane may be different; Σ_2 then refers to the composite planform. We may regard each wing to be extended outward over a surface which is free of thickness and loading in order to fill Σ_2. The additional terms which can arise at singular wing edges have been disregarded in (7); for a discussion of this matter from the present point of view, see Clarke (1959*b*). When the right-hand side of (7) vanishes, it then assumes the form of the Ursell–Ward reverse-flow theorem for finite quasi-cylinders.

In order to effect a rearrangement of the right-hand side of (7), we introduce a variant of a well-known decomposition of boundaries (Lagerstrom & Van Dyke 1949; Flax 1953). Let

$$\mathbf{V}_F=\mathbf{V}_{1\alpha F}+\mathbf{V}_F^*, \tag{8}$$

and

$$\mathbf{V}_R=\mathbf{V}_{1\alpha R}+\mathbf{V}_R^*, \tag{9}$$

where $\mathbf{V}_{1\alpha F}$ is the two-dimensional perturbation velocity in forward flow induced by the cylinder obtained from a rotation of the reference surface Σ_1 through an angle α_{1F}, the fuselage incidence in forward flow. When the latter is zero, (8) is trivial. The perturbation flow $\mathbf{V}_F^*$, actually defined by (8), is seen to satisfy the boundary conditions for the combinations discussed for the case $\alpha_{1F}=0$, except that the wing has an extra warp which is just sufficient to cancel the upwash on Σ_2 from $\mathbf{V}_{1\alpha F}$ when $\mathbf{V}_{1\alpha F}$ is added to $\mathbf{V}_F^*$ to obtain $\mathbf{V}_F$. The discussion of the reverse flows introduced in (9), involving the fuselage incidence α_{1R}, is analogous. The flows $\mathbf{V}_F^*$ and $\mathbf{V}_R^*$ include any fuselage distortions resulting from the wing cross-flow; for reasons that will appear below, we shall refer to the boundaries associated with these flows as the equipollent configurations.

Substituting (8) and (9) into the right-hand side of (7), we obtain

$$\rho_0\int_{S(x=+\infty)}(v_F^*v_{1\alpha R}+w_F^*w_{1\alpha R})\,dS-\rho_0\int_{S(x=-\infty)}(v_{1\alpha F}v_R^*+w_{1\alpha F}w_R^*)\,dS$$
$$+\rho_0\int_{S(x=+\infty)}(v_{1\alpha F}v_{1\alpha R}+w_{1\alpha F}w_{1\alpha R})\,dS-\rho_0\int_{S(x=-\infty)}(v_{1\alpha F}v_{1\alpha R}+w_{1\alpha F}w_{1\alpha R})\,dS, \tag{10}$$

where the sum of the last two integrals vanishes. The first integral can be rewritten as a line integral with use of the two-dimensional form of Green's theorem by noting that

$$\frac{\partial v_F^*}{\partial y}+\frac{\partial w_F^*}{\partial z}=0 \quad \text{on } S(x=+\infty),$$

and by introducing the perturbation potential defined by $\mathbf{V}_{1\alpha R}=\nabla\phi_{1\alpha R}$. The treatment of the second integral is analogous. Equation (7) finally becomes

$$\int_{\Sigma}(p_F\mathbf{n}_R.\mathbf{i}+p_R\mathbf{n}_F.\mathbf{i})\,dS$$
$$=-\rho_0\oint_{\Sigma_1(x=+\infty)}\phi_{1\alpha R}\mathbf{V}_F^*.\mathbf{N}\,d\sigma+\rho_0\oint_{\Sigma_1(x=-\infty)}\phi_{1\alpha F}\mathbf{V}_R^*.\mathbf{N}\,d\sigma, \tag{11}$$

where $d\sigma$ is an element of the inner bounding curve of $S(x = \pm\infty)$ denoted by $\Sigma_1(x = \pm\infty)$.

The condition for the existence of the required reverse-flow relation is that the right-hand side of (11) vanish. If fuselage distortion due to wing-induced cross-flow is not present in forward flow, the equipollent combination exhibits an undeflected cylinder downstream and $\mathbf{V}_F^*.\mathbf{N} = 0$ on $\Sigma_1(x = +\infty)$. If the analogous situation also prevails in reverse flow, then, under these conventional conditions, the right-hand side of (11) does, in fact, vanish. But if, for example, distortion appears in reverse flow, $\mathbf{V}_R^*.\mathbf{N} \neq 0$ on $\Sigma_1(x = -\infty)$ and the last integral in (11) vanishes only if α_{1F}, and therefore $\phi_{1\alpha F}$, is zero; a restriction on the choice of forward flows therefore arises which bears on the subsequent development. If $\alpha_{1F} = \alpha_{1R} = 0$, distortions may occur in both flow directions. Equation (11) still holds if the reference surface for the wing is not a plane.

3. Relation between forces acting on prescribed combination and its equipollent combination

We have seen that if fuselage distortions are permitted in the reverse flow, whatever the combination chosen, then fuselage incidence in forward flow cannot be treated. In this regard, let us relate the drag in forward flow of the prescribed combination to the drag of its equipollent combination. If the drag D is defined as the component of the force in the direction of the incident stream, then, in general,

$$D \equiv -(U/|U|)\int_\Sigma p\mathbf{n}.\mathbf{i}\,dS \tag{12}$$

in the absence of wing-edge forces. For the prescribed configuration in forward flow, we then have, using (3),

$$D_F = \frac{1}{U_F}\int_\Sigma p_F \mathbf{V}_F.\mathbf{N}\,dS. \tag{13}$$

From the decomposition (8),

$$p_F = p_{1\alpha F} + p_F^*, \tag{14}$$

where, significantly,

$$p_{1\alpha F} \equiv 0. \tag{15}$$

With use of (8), (14), and (15), (13) becomes

$$D_F = \frac{1}{U_F}\int_\Sigma p_F^* \mathbf{V}_F^*.\mathbf{N}\,dS + \frac{1}{U_F}\int_\Sigma p_F^* \mathbf{V}_{1\alpha F}.\mathbf{N}\,dS. \tag{16}$$

We now show that the last term vanishes.

We take for the forward flow in (11)

$$\mathbf{V}_F = \mathbf{V}_F^*. \tag{17}$$

The flow $\mathbf{V}_{1\alpha F}$ induced on the inclined cylinder, whose normal is $\mathbf{n}_{1\alpha F}$, satisfies the boundary condition

$$\mathbf{V}_{1\alpha F}.\mathbf{N} = -U_F \mathbf{n}_{1\alpha F}.\mathbf{i} \quad \text{on } \Sigma_1. \tag{18}$$

Then let $\mathbf{V}_R$ in (11) satisfy

$$\mathbf{V}_R.\mathbf{N} = -U_R \mathbf{n}_{1\alpha F}.\mathbf{i} \quad \text{on } \Sigma_1. \tag{19}$$

The solution for $\mathbf{V}_R$ satisfying (19) and the boundary conditions at infinity is

$$\mathbf{V}_R = -\mathbf{V}_{1\alpha F}. \tag{20}$$

The combination in reverse flow has for its wing on Σ_2 the stream surface of the two-dimensional cylinder flow chosen. When (17) and (20) are used in (11), the last three terms vanish, and we obtain

$$\int_\Sigma p_F^* \mathbf{n}_{1\alpha F} . \mathbf{i}\, dS = 0,$$

or

$$\frac{1}{U_F} \int_\Sigma p_F^* \mathbf{V}_{1\alpha F} . \mathbf{N}\, dS = 0. \tag{21}$$

Equations (16) and (21) give

$$D_F = D_F^*. \tag{22}$$

Thus, the drag of the prescribed configuration and the drag D_F^* of the equipollent configuration are equal. The boundaries of each produce the same pressure field, from (14); the equipollent configuration has zero fuselage incidence but a greater angle-of-attack distribution over the wing, and the two deviations in slope are seen to balance. The surface inclination does not enter into the calculation of the remaining aerodynamic forces and moments on Σ, so that these will certainly be the same for both configurations, by virtue of (14). The equipollent combination is readily found from any prescribed combination by determining the associated cylinder upwash field of the latter on Σ_2. We shall hereafter concern ourselves with determining forces and moments on the equipollent combination. Otherwise stated, the fuselage incident α_{1F} in the combination of interest may subsequently be considered to be zero without loss in generality. We also discard in this connexion the designation ( )*, which we shall later use differently.

4. Transverse forces and moments supported by wing in combination of interest

In order to obtain convenient expressions for the transverse forces and the moments supported on the wing panels in forward flow, it is convenient to consider an isolated wing, which passes through Σ_1 arbitrarily, for the reverse flow. The geometry of the wing is so chosen to produce the desired expression in the reverse-flow relation. The boundary of the region of influence on Σ_1 of the reverse flow is indicated by the curve *FCH* on the upper side of Σ_1 in figure 1 and a similar curve on the lower side. To apply (11) we consider that the reverse flow includes a fictitious fuselage constructed from a stream surface of the isolated wing flow which begins as the cylinder Σ_1 in the undisturbed stream. Our reverse flow is then a special case of that considered in connexion with the reverse-flow relation. Since the right-hand side vanishes, (11) gives, with use of (3), the relation

$$\frac{1}{U_F} \int_{\Sigma_1} p_F \mathbf{V}_R . \mathbf{N}\, dS = -\frac{1}{U_F} \int_{\Sigma_1} p_F \mathbf{V}_R . \mathbf{N}\, dS - \int_\Sigma p_R \mathbf{n}_F . \mathbf{i}\, dS. \tag{23}$$

Suppose that the isolated wing is a lifting surface without thickness. Then the boundary condition which defines the reverse flow is conveniently written

$$w_R = -U_R \alpha_R(x, y) \quad \text{on the } (x, y)\text{-plane}, \tag{24}$$

where $\alpha_R(x, y)$ is the angle-of-attack distribution. With use of (24), (23) provides the following expression for the transverse forces and moments on the wing

$$\int_{\Sigma_2'} l_F \alpha_R(x,y)\, dS = \int_{\Sigma_1} p_R \mathbf{n}_F.\mathbf{i}\, dS + \int_{\Sigma_2} p_R \mathbf{n}_F.\mathbf{i}\, dS - \frac{1}{U_R}\int_{\Sigma_1} p_F \mathbf{V}_R.\mathbf{N}\, dS, \quad (25)$$

where Σ_2' is one side of Σ_2, and l_F is the lift distribution across Σ_2' in forward flow.

Consider the left-hand side of (25). To construct the lift over any portion $\Sigma_2'^*$ of Σ_2', let the reverse planform be the same as the forward planform, and take

$$\alpha_R = \begin{cases} k & \text{on } \Sigma_2'^* \\ 0 & \text{on } \Sigma_2' - \Sigma_2'^*, \end{cases} \quad (26)$$

where k is a constant. The left-hand side is then k times the required lift. The spanwise or chordwise lift distribution follows from two such results by subtraction. The pitching moment about the y-axis, produced over any portion $\Sigma_2'^*$ of Σ_2' is constructed by replacing k by $-kx$ in (26). The left-hand side of (25) is then k times the required moment. The treatment of rolling moment is similar.

Following choice of α_R, the first and second integrals on the right-hand side of (25) are to be evaluated as indicated. Note that the slope $-\mathbf{n}_F.\mathbf{i}$ vanishes on Σ_1 for $x < x_i$. Evaluation of the third integral requires, in addition to the cross-flow $\mathbf{V}_R.\mathbf{N}$, the solution for p_F on Σ_1 upstream of the bounding curve FCH and its lower counterpart. This is the hatched and cross-hatched region of Σ_1 (figure 1). We have already mentioned that (i) if the wing leading edge and upstream fuselage contours are appropriate† (as suggested by the hatching on Σ_2 and Σ_1), the problem can be reduced to two equivalent symmetric problems, and (ii) in the case of infinite quasi-cylinders of almost circular cross-section, the calculation of p_F is then a routine matter, because the solution is not required off Σ_1.

The advantage in the use of (25) appears by comparing the procedure required to evaluate the right-hand side with the procedure required to evaluate the left-hand side straightforwardly. Notice that the half-space formulation is possible in the former case for a much broader class of wing planforms than in the latter case.

An interesting special case occurs when the reverse flow is two-dimensional on Σ_2 and on the portion of Σ_1 where $\mathbf{n}_F.\mathbf{i} \neq 0$. In the choice of the planform in reverse flow, care must be used to avoid pressure integrations on Σ_2 over deflected forward-flow stream surfaces which are off the forward-flow planform, since these are unknown. Thus, take the straight unswept leading edge of the reverse-flow planform to lie upstream of the trailing edge and any subsonic leading edges of the forward-flow planform. Take the reverse-flow trailing edge to lie along the remaining forward-flow leading edge. Let $\alpha_R = \alpha_R(x)$ over $\Sigma_2'^*$, the planform constructed (LMO in figure 1). The reverse flow will then be two-dimensional upstream of its trailing edge. Assume $\mathbf{n}_F.\mathbf{i} = 0$ within the domain of influence of the reverse-flow trailing edge (this gives bounding curves like EAG in figure 1).

† It might sometimes be possible to relax the restriction that no unsymmetrical contours appear within the domain of dependence of EJ and its counterpart on the left panel. If the cross-flow from these contours in the plane of the wing forward of its leading edge can be evaluated, the wing can be extended forward along the computed stream surface with no change in the forces. The restriction is then fulfilled for the new boundary.

This special case, which simplifies (25), arises naturally in the procedure outlined when it is applicable. We have

$$\left.\begin{aligned} u_R &= -\frac{z}{|z|}\frac{U_R}{B}\alpha_R(x+B|z|), \\ w_R &= -U_R\alpha_R(x+B|z|). \end{aligned}\right\} \tag{27}$$

Since the left-hand side vanishes on $\Sigma_2' - \Sigma_2'^*$, (25) gives

$$\begin{aligned} \int_{\Sigma_1'^*} l_F \alpha_R(x)\,dS = (\rho_0 U_F^2/B)\int_{\Sigma_1^*}\frac{z}{|z|}\alpha_R(x+B|z|)\,\mathbf{n}_F.\mathbf{i}\,dS \\ + (\rho_0 U_F^2/B)\int_{\Sigma_1^*}\frac{z}{|z|}\alpha_R(x)\,\mathbf{n}_F.\mathbf{i}\,dS + \int_{\Sigma_1^*}\alpha_R(x+B|z|)\,p_F\mathbf{N}.\mathbf{k}\,dS, \end{aligned} \tag{28}$$

where Σ_1^* is the part of Σ_1 influenced by the reverse flow.

The chordwise lift distribution on the wing is found by taking $\alpha_R(x)$ as an impulse function, so that the reverse-flow disturbance vanishes except between two pairs of adjacent Mach planes. The left-hand side is proportional to the wing lift on the lateral strip. The first two terms on the right-hand side are proportional to the integral of the included slope along both sides of Σ, and the third integral is proportional to the fuselage lift between the four Mach planes. To find the lift on Σ_2', take $\alpha_R = k$. Equation (28) becomes

$$\int_{\Sigma_1'^*} l_F\,dS = \int_{\Sigma_1^*} p_F\mathbf{N}.\mathbf{k}\,dS + (\rho_0 U_F^2/B)\int_{\Sigma_1^*+\Sigma_2^*}\frac{z}{|z|}\mathbf{n}_F.\mathbf{i}\,dS. \tag{29}$$

The left-hand side is the required lift. As just noted, it happens that the first term on the right-hand side is the negative of the forward-flow fuselage lift over Σ_1^*. This term is to be evaluated, as before, from the partial solution for p_F (given here by equivalent symmetric problems). But if we want the lift over both wing and fuselage forward of the Mach planes attached to the reverse-flow leading edge, then this sum is given at once in (29) by a surface integral of the prescribed slope over $\Sigma_1^* + \Sigma_2^*$. To find the pitching moment about the y-axis produced by the distribution l_F over Σ_2', let $\alpha_R = -kx$ in (28). The left-hand side of (28) is k times the required moment, but the last term in (28) is not the pitching moment produced over Σ_1^*.

Further results using a wing which induces a two-dimensional reverse flow can be obtained from (23); the integral relation for the chordwise lift distribution, together with certain associated results, has been given by Ferri *et al.* (1957) and by Ting (1959) using other methods.

Having found the lift, as well as other information, for the wing by using an isolated wing in reverse flow, it is only natural to inquire whether a useful expression for the lift on the fuselage can be obtained by using an isolated fuselage in reverse flow. Since forward fuselage incidence is admissible in (11) in this case, we may then work with the original prescribed combination, as well as with its equipollent combination. The calculation is virtually the same as the one in § 3. We take for the boundary in reverse flow the infinite cylinder, with normal $\mathbf{n}_{1\alpha R}$, which can be obtained from rotation of the reference surface Σ_1 through an incidence α_{1R}. Thus

$$\mathbf{n}_{1\alpha R} = \mathbf{N} + \alpha_{1R}\mathbf{j}\times\mathbf{N} \quad \text{and} \quad \mathbf{n}_{1\alpha R}.\mathbf{i} = \alpha_{1R}\mathbf{N}.\mathbf{k}. \tag{30}$$

The reverse flow $\mathbf{V}_{1\alpha R}$ satisfies the boundary condition

$$\mathbf{V}_{1\alpha R}.\mathbf{N} = -U_R \mathbf{n}_{1\alpha R}.\mathbf{i} \quad \text{on } \Sigma_1. \tag{31}$$

Equation (11) gives

$$\int_{\Sigma_1} p_F \mathbf{n}_{1\alpha R}.\mathbf{i}\, dS - \frac{1}{U_R}\int_{\Sigma_2} p_F \mathbf{V}_{1\alpha R}.\mathbf{N}\, dS = 0. \tag{32}$$

With use of (30), we obtain from (32)

$$-\int_{\Sigma_1} p_F \mathbf{N}.\mathbf{k}\, dS = \frac{1}{U_R \alpha_{1R}}\int_{\Sigma_1'} l_F w_{1\alpha R}\, dS. \tag{33}$$

The left-hand side is the fuselage lift L_{1F}. Noting that $(\partial/\partial x)\, w_{1\alpha R} = 0$, and letting $\mathbf{V}_F = \nabla\phi_F$, we can also write (33) as

$$L_{1F} = (\rho_0/\alpha_{1R})\int \Delta\phi_F w_{1\alpha R}\, dy. \tag{34}$$

where $\Delta\phi_F$ is the difference in the velocity potential from the upper to the lower side of the wing, evaluated at the trailing edge. The integration extends from left tip to right tip along the exposed trailing edge. But it may also be evaluated along the wing traces in the Trefftz plane (since the integrand is independent of x in the wake), and we then recognize (34) as the Trefftz plane theorem of Flax (1953), extended slightly here to admit fuselage incidence, but written for a planar wing. We have already discussed how to calculate the spanwise lift distribution required in (33) and (34); the calculation of the two-dimensional reverse cross-flow $w_{1\alpha R}$ is no problem.

5. Drag of combination of interest

Combination not reducible to equivalent symmetric problems

We now seek to obtain useful expressions for the drag of the combination of interest, and, in this connexion, consider first the general case where the planform and contours are such that the problem cannot, in the first instance, be reduced to two equivalent symmetric problems—especially because of downstream contouring or trailing edges with subsonic segments. Since the drag of this combination is, according to (11), the same in each direction (aside from edge force considerations), the direction chosen as the forward flow is a matter of convenience in the light of what follows. We note that, in accordance with the remarks made in the first paragraph of the introduction, the forward flow can be written as the sum of four flows as follows, in the order named

$$\mathbf{V}_F = \mathbf{V}_{1F} + \mathbf{V}_{2F} + \mathbf{V}'_{1F} + \mathbf{V}'_{2F}. \tag{35}$$

The direct computation of the last two terms would probably be carried out using the non-terminating process discussed in the third paragraph. Equation (35) suggests the choice for the reverse flow

$$\mathbf{V}_R = \mathbf{V}_{1R} + \mathbf{V}_{2R}, \tag{36}$$

where the reverse flow past the isolated fuselage $\mathbf{V}_{1R}$ satisfies the boundary condition

$$\mathbf{V}_{1R}.\mathbf{N} = -\mathbf{U}_R.\mathbf{n}_F \quad \text{on } \Sigma_1. \tag{37}$$

and the reverse flow past the isolated wing $\mathbf{V}_{2R}$ satisfies the boundary condition

$$\mathbf{V}_{2R}.\mathbf{N} = -\mathbf{U}_R.\mathbf{n}_F \quad \text{on } \Sigma_2. \tag{38}$$

Here $\mathbf{n}_F$ is the normal to the combination of interest in forward flow. The two isolated wings would normally be extended inside Σ_1 in the same way. It is apparent that the reverse flow exhibits distortion of the type discussed.

Substituting (36) into (11), rearranging, and using (37) and (38), the drag in forward flow appears in the relation; we obtain

$$D_F \equiv -\int_\Sigma p_F \mathbf{n}_F.\mathbf{i}\,dS = \int_{\Sigma_1} p_{1R}\mathbf{n}_F.\mathbf{i}\,dS + \int_{\Sigma_2} p_{2R}\mathbf{n}_F.\mathbf{i}\,dS$$
$$+\int_{\Sigma_1} p_{2R}\mathbf{n}_F.\mathbf{i}\,dS - \int_{\Sigma_1} p_F \frac{1}{U_R}\mathbf{V}_{2R}.\mathbf{N}\,dS + \int_{\Sigma_2} p_{1R}\mathbf{n}_F.\mathbf{i}\,dS - \int_{\Sigma_2} p_F \frac{1}{U_R}\mathbf{V}_{1R}.\mathbf{N}\,dS, \tag{39}$$

where $p_R = p_{1R} + p_{2R}$. Equation (39) for the drag in forward flow requires determination of p_F on the now established hatched and cross-hatched region of Σ_1. In addition, p_F is also required over the portion of Σ_2 on which the cross-flow from the isolated fuselage in reverse flow is different from zero; but we shall shortly see that this term can be eliminated if desired. If the upstream contouring and the wing edges are suitable, p_F on Σ_1 and Σ_2 can then be determined by solving two equivalent symmetric problems, since the solution is required only upstream of the trailing edge. Further, the cross-flow and pressure induced by the isolated fuselage in reverse flow is required by (39) off Σ_1; however, the next to last integral, involving p_{1R}, vanishes when the wing thickness is zero. While still requiring a complex calculation, (39) permits, with suitable geometry, a reduction of the full problem to a (finite) number of isolated quasi-cylinders and isolated wings. In the case of quasi-cylinders of almost circular section, the particular difficulty is in finding the flow off Σ_1.

Equation (39) is particularly useful when the fuselage contours extend downstream but are limited in type or extent upstream. An interesting application is illustrated in figure 2, which shows a fuselage which is contoured for favourable interference upstream, and which terminates at a base along the wing trailing edge. Equation (22) does not apply, since the fuselage is only semi-infinite, but suppose the prescribed fuselage incidence is zero. The drag is unchanged by extending the fuselage cylindrically downstream, and then reversing the flow direction. If the latter is regarded as the forward flow, the combination then exhibits the features just discussed.

As a commonly treated special case, suppose $\mathbf{n}_F.\mathbf{i} = 0$ on Σ_1, so that $\mathbf{V}_{1R} \equiv 0$. Equation (39) reduces to the simple result

$$D_F = \int_{\Sigma_1} p_{2R} n_F.\mathbf{i}\,dS - \int_{\Sigma_1} p_F \frac{1}{U_R}\mathbf{V}_{2R}.\mathbf{N}\,dS. \tag{40}$$

The integral containing the required p_F extends over the portion of the cross-hatched surface labelled *EBGHDFE* in figure 1; the curve *EBG* bounds the region of influence on Σ_1 of the forward flow. The condition for the reduction of the problem of finding p_F to equivalent symmetric problems is merely that the

leading edge segment EJ and its left-hand counterpart be supersonic. Equation (40) is much simpler than a direct calculation, even when the latter can be made with equivalent symmetric problems. The drag D_F is, of course, supported solely on the wing panels, and (40) resembles (25) because we now have only a wing in the reverse flow; when the reverse flow is two-dimensional, similar considerations can be applied to (40) as well.

We now show that it is possible to eliminate the last integral in (39), which requires determination of p_F on Σ_2. The situation will then revert to that discussed in the introduction. First, the elimination of this term greatly weakens the conditions for a half-space formulation for the forward flow, these conditions

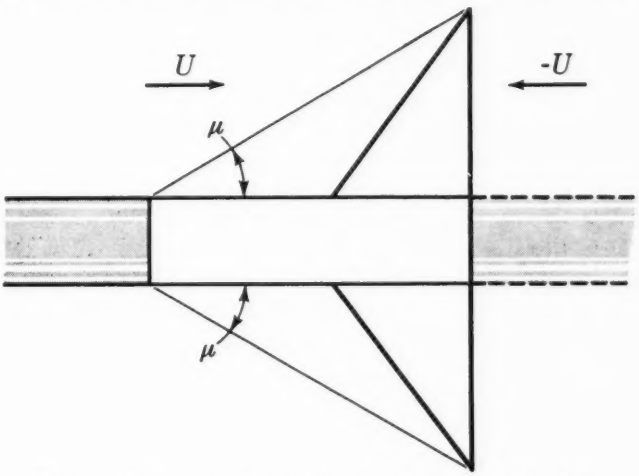

FIGURE 2. Example of combination with contoured fuselage.

reverting to those initially given. Secondly, within the half-space formulation, the two quasi-cylinder flow calculations on each side of the (x, y)-plane off Σ_1 are no longer necessary; two of these four are apt to be slowly convergent. The necessity of finding the reverse flow induced by the isolated fuselage on Σ_2 will, however, remain. The last term in (39) is readily rewritten as

$$\int_{\Sigma_1} p_F \frac{1}{U_R} \mathbf{V}_{1R} . \mathbf{N} \, dS = -\int_{\Sigma_1'} l_F \frac{w_{1R}}{U_R} dS. \tag{41}$$

Introduce a planar wing over Σ_2, with flow field $\mathbf{V}^*_{2R}$, which satisfies the boundary condition

$$\frac{w^*_{2R}}{U_R} = -\alpha^*_{2R} \quad \text{on } \Sigma_2 \tag{42}$$

and the relation

$$w^*_{2R} = w_{1R} \quad \text{on } \Sigma_2. \tag{43}$$

This defines α^*_{2R}. The wing is extended through Σ_1 arbitrarily. Substituting (42) and (43) into (41), we obtain for the right-hand side of (41)

$$\int_{\Sigma_1'} l_F \alpha^*_{2R} dS.$$

We have already evaluated this expression in (25). Inserting (25) in (41) and (41) in (39), we now obtain for the drag of the combination of interest in forward flow

$$D_F = \int_{\Sigma_1} p_{1R}\mathbf{n}_F.\mathbf{i}\,dS + \int_{\Sigma_2} (p_{2R}-p^*_{2R})\,\mathbf{n}_F.\mathbf{i}\,dS + \int_{\Sigma_1} (p_{2R}-p^*_{2R})\,\mathbf{n}_F.\mathbf{i}\,dS + \int_{\Sigma_1} p_{1R}\mathbf{n}_F.\mathbf{i}\,dS + \int_{\Sigma_1} p_F \frac{1}{U_R}(\mathbf{V}^*_{2R}-\mathbf{V}_{2R}).\mathbf{N}\,dS. \quad (44)$$

Combination symmetric or reducible to equivalent symmetric problems

We next discuss the drag of the combination of interest for the case where the planform and contours permit reduction to equivalent symmetric problems in the first instance. Thus all wing edges are supersonic. On Σ_1, $\mathbf{n}_F.\mathbf{i} = 0$ downstream of curve FDH and its counterpart below, where FDH is the bounding curve of the region of influence on Σ_1 of the wing trailing edges. Similarly $\mathbf{n}_F.\mathbf{i} = 0$ forward of a pair of curves like EAG. The case where the original prescribed combination is symmetric about the (x, y)-plane is also included. In this case, much simpler than the preceding one, the forward flow for either equivalent symmetric problem is given by (35), where

$$\mathbf{V}'_{2F} = 0. \quad (45)$$

By definition, the drag in forward flow is

$$D_F = -\int_{\Sigma_1} p_F\mathbf{n}_F.\mathbf{i}\,dS - \int_{\Sigma_2} p_F\mathbf{n}_F.\mathbf{i}\,dS, \quad (46)$$

where the pressure on each side of the wing is given by a different expression of the form $p_F = p_{1F} + p'_{1F} + p_{2F}$. It is generally true that the determination of the first two pressures on Σ_1 is easier than on Σ_2; for quasi-cylinders of almost circular section, this is certainly the case, for the reasons discussed. If we regard as immaterial the flow direction in which the self-induced wing drag is computed, it is then desirable to eliminate the last integral in (46) entirely with the technique used for transverse forces on the wing. Therefore, choose $\mathbf{V}_F$ for the forward flow, and take for the reverse flow the flow past the same isolated wing $\mathbf{V}_{2R}$, so that (38) is satisfied. Equation (23), together with the remarks which precede it, applies to the last integral in (46), where $\mathbf{V}_R$ becomes $\mathbf{V}_{2R}$. Equation (46) assumes the form

$$D_F = \int_{\Sigma_2} p_{2F}\mathbf{n}_F.\mathbf{i}\,dS + \int_{\Sigma_1} p_{2R}\mathbf{n}_F.\mathbf{i}\,dS - \int_{\Sigma_1} p_F\mathbf{n}_F.\mathbf{i}\,dS - \int_{\Sigma_1} p_F \frac{1}{U_R}\mathbf{V}_{2R}.\mathbf{N}\,dS. \quad (47)$$

To use (47), the pressure and cross-flow induced on Σ_1 by the wing must be known in both forward and reverse flow. The pressures p_{1F} and p'_{1F} are required only on Σ_1, as intended. This solves Lock's problem (1958). Because of the next to last integral, we have deviated somewhat from the general statement in the introduction that the solution in forward flow is required only on the hatched and cross-hatched parts of Σ_1; however, the extra integration downstream of FCH introduces no particular complication in this case. No reverse quasi-cylinder flows appear in (47). If $\mathbf{n}_F.\mathbf{i} = 0$ on Σ_1, (47) reduces to (40) because the distinction

between the two approaches then vanishes. Generally, the first approach can be applied to the second case considered as well as to the first, but is considerably less convenient, since it evidently requires a reverse-flow quasi-cylinder calculation both on Σ_2 and Σ_1.

A synthetic approach

Suppose that asymmetric contours vanish on the hatched portion of Σ_1 and that the wing leading edges are supersonic at least along EJ and its counterpart on the left. Then we can determine p_F on Σ_1 from the equivalent symmetric problems downstream at least to curve FCH and its counterpart below. If all wing edges are supersonic, we might be able to find p_F on Σ_1 in this way downstream to FDH and its counterpart below. Take a closed curve C on Σ_1 which lies between FCH, FDH, and their counterparts below; suppose C to bound the region of Σ_1 over which p_F can be computed from equivalent symmetric problems. A re-examination of (47) shows that it applies to the present case as well, but p_F in the next to the last integral is very difficult to evaluate on Σ_1 downstream of C. Let

$$D_F = D_{CF} + D^*_{1F}, \tag{48}$$

where D_{CF} is given by (47), the next to last integral thereof being carried downstream only to C; as has been discussed, this is a convenient expression. The term D^*_{1F} is the remainder of the drag, which is supported only on Σ_1 downstream of C. We shall evaluate D^*_{1F} with a variant of the first approach given.

Take as the forward flow the combination of interest with the boundary condition

$$\mathbf{V}_F.\mathbf{N} = -\mathbf{U}_F.\mathbf{n}_F \quad \text{on } \Sigma. \tag{49}$$

Take the reverse flow $\mathbf{V}^*_{1R}$ as that past an infinite quasi-cylinder, and such that

$$\mathbf{V}^*_{1R}.\mathbf{N} = \begin{cases} -\mathbf{U}_R.\mathbf{n}_F & \text{on } \Sigma^*_1 \\ 0 & \text{on } \Sigma_1 - \Sigma^*_1, \end{cases} \tag{50}$$

where Σ^*_1 is the part of Σ_1 between C and the plane $x = x_f$. Using (49) and (50) in (11), we obtain

$$D^*_{1F} \equiv -\int_{\Sigma^*_1} p_F \mathbf{n}_F.\mathbf{i}\, dS = \int_{\Sigma_1} p^*_{1R}\mathbf{n}_F.\mathbf{i}\, dS + \int_{\Sigma_2} p^*_{1R}\mathbf{n}_F.\mathbf{i}\, dS - \int_{\Sigma_2} p_F \frac{1}{U_R}\mathbf{V}^*_{1R}.\mathbf{N}\, dS. \tag{51}$$

We may eliminate the last integral in (51) with the same method used in the first approach. Introduce a planar wing over Σ_2, with flow field $\mathbf{V}^*_{2R}$, which satisfies the boundary condition

$$\frac{w^*_{2R}}{U_R} = -\alpha^*_{2R} \quad \text{on } \Sigma_2 \tag{52}$$

and the relation

$$w^*_{2R} = w^*_{1R} \quad \text{on } \Sigma_2. \tag{53}$$

With use of (25), (51) may then be written

$$D^*_{1F} = \int_{\Sigma_1} (p^*_{1R} - p^*_{2R})\,\mathbf{n}_F.\mathbf{i}\, dS + \int_{\Sigma_2} (p^*_{1R} - p^*_{2R})\,\mathbf{n}_F.\mathbf{i}\, dS + \int_{\Sigma_1} p_F \frac{1}{U_R}\mathbf{V}^*_{2R}.\mathbf{N}\, dS. \tag{54}$$

Equation (54) requires p_F only on the now established region of Σ_1. But p_F has already been evaluated on this region in connexion with D_{CF}. In eliminating the need for p_F on Σ_1^*, we have introduced the flow fields of one infinite quasi-cylinder and one wing.

Applied to the present problem, (44) and the sum of (47) and (54) are seen to employ essentially the same devices, although in a somewhat different manner. Both introduce two isolated wings in reverse flow. From the point of view taken in this investigation, both suffer the residual disadvantage of requiring the pressure and cross-flow of one infinite quasi-cylinder on Σ_2 (i.e. off Σ_1). But it is in this respect that the third approach excels the first. First, the geometry of its quasi-cylinder is apt to be simpler. Secondly, and more important, its quasi-cylinder flow on Σ_2 enters only the second part of the drag, so that the result is less sensitive to approximation.

Finally, let us reconsider the general case where the planform is arbitrary and the contours on Σ_1 are arbitrary as well over the interval $x_i \leqslant x \leqslant x_f$. Setting aside considerations of reduction to equivalent symmetric problems, we see, upon re-examination, that (48), (47), and (54) are still applicable expressions for D_F. If we want to minimize the region of Σ_1 on which p_F must be found, and also reduce the importance in (48) of the reverse flow of the infinite quasi-cylinder on Σ_2 (in accordance with the remarks in the last paragraph), we choose the curve C to be coincident with FCH and its counterpart below. The resulting relation (48) is then preferable to (44).

REFERENCES

Clarke, J. H. 1959*a* *J. Fluid Mech.* **6**, 272.

Clarke, J. H. 1959*b* *J. Aero/Space Sci.* **26**, 535.

Ferrari, C. 1948 *J. Aero. Sci.* **15**, 317.

Ferrari, C. 1949 *J. Aero. Sci.* **16**, 542.

Ferri, A., Clarke, J. H. & Ting, L. 1957 *J. Aero. Sci.* **24**, 791.

Flax, A. H. 1953 *J. Aero. Sci.* **20**, 483.

Lock, R. C. 1958 *J. Fluid Mech.* **4**, 33.

Lagerstrom, P. A. & Van Dyke, M. D. 1949 *Douglas Aircraft Company, Rep.* no. SM-13432.

Lawrence, H. R. & Flax, A. H. 1954 *J. Aero. Sci.* **21**, 289.

Mersman, W. A. 1954 *Proc. Int. Cong. Math.*, Amsterdam, **2**.

Nielson, J. N. 1955 *Nat. Adv. Comm. Aero., Wash., Rep.* no. 1252.

Nielson, J. N. 1957 *Nat. Adv. Comm. Aero., Wash., Tech. Note* no. 3873.

Randall, D. G. 1955 *Roy. Air. Est. Tech. Note Aero.* no. 2404. (Also *Aero. Res. Coun., Lond., Tech. Note* no. 18492.)

Ting, L. 1957 *J. Aero. Sci.* **24**, 821.

Ting, L. 1959 *Quart. Appl. Math.* **16**, 373.

Ursell, F. & Ward, G. N. 1950 *Quart. J. Mech. Appl. Math.* **3**, 326.

Ward, G. N. 1955 *Linearized Theory of Steady High-Speed Flow.* Cambridge University Press.

Laminar convection in uniformly heated vertical pipes

By B. R. MORTON
Department of Mathematics, Manchester University

(Received 15 October 1959)

An exact solution is presented in this paper for the problem of laminar convective flow under a pressure gradient along a vertical pipe, the walls of which are heated or cooled uniformly; the solution is based on the assumption that velocity and buoyancy profiles far from the pipe entrance do not change with height, and entry-length effects are ignored. Two different types of behaviour are found accordingly as the pressure gradient and buoyancy forces act together or in opposition near the centre of the pipe.

When an upflow is heated (or a downflow cooled) the velocity near the walls is increased relatively and that near the axis decreased until, for sufficiently large Rayleigh numbers, definite velocity and thermal boundary layers are formed.

In the case of cooled upflow (or heated downflow) there is an increase in the velocity across the whole profile for small Rayleigh numbers. As the Rayleigh number is increased the velocity and buoyancy increase, slowly at first and then rapidly, and the solution 'runs away' at a Rayleigh number of about 33. For higher Rayleigh numbers, laminar Poiseuille flow of an increasingly complicated profile is theoretically possible, but is unlikely to be found in practise.

1. Introduction

Thermal convection consists of the transport of heat by a moving fluid in which local variations of temperature (and hence of density) produce a distributed buoyancy force that itself modifies the pattern of flow. This interaction of velocity and density fields is the essential feature of convection: hence, to find the convective flow in a heated pipe, both the velocity and temperature fields must be determined together throughout the whole region of flow.

Solutions of this kind are usually difficult to find, and so only the specially simple categories of forced and natural convection have been studied theoretically in any detail. In *forced convection* the density of the flow is regarded as entirely unaffected by the heat transported, which therefore acts only to 'mark' parts of the fluid passing near certain boundaries. These marked elements are then swept away in the flow produced by externally applied forces, and are distributed throughout the region by convection and diffusion without affecting the field of flow in any way. Mathematically the problem reduces to finding the temperature distribution due to heated or cooled boundaries in a specified velocity field. The analysis is particularly simple for the case of Poiseuille flow in a straight pipe of circular section with walls maintained at a uniform temperature gradient (which corresponds very nearly with uniform heating), and

this solution was given by Nusselt (1910; see also, Goldstein 1938, p. 622). The solution is, of course, independent of the orientation of the pipe, and it predicts a Nusselt number of 6 based on pipe diameter and mean temperature across a section (or 48/11 if based on a mean temperature weighted with respect to velocity). The motion of a fluid in *natural convection* is caused solely by buoyancy forces due to the action of some field of force on the unevenly unheated fluid. In a gravitational field the velocities established are generally small, but there may be vigorous motion in other fields (notably in rotating systems, e.g. the use of the thermosyphon for cooling turbine blades). A power series solution in terms of the Rayleigh number can be obtained for natural convection in a vertical pipe when the rate of heating is low.

Neither of these solutions can be expected to give an adequate idea of 'mixed' thermal convection in a vertical pipe. The forced convection solution essentially represents a limit for vanishingly small heat transfer, and it can be used effectively only for small values of the ratio (*characteristic buoyancy force*)/(*characteristic inertia force*) for the system; in pipe convection this ratio may take large values. The natural convection solution predicts a weak flow which will in general show some dependence on time, and this would be dominated completely by the flow due to quite small superimposed pressure gradients along the pipe. Thus, neither forced nor natural convection solutions can be expected to give any real indication of the character of laminar convection in flow under a pressure gradient along a vertical, uniformly heated pipe. However, for this case a direct analysis of the problem is possible.

The related two-dimensional problem of flow between vertical heated plates has been discussed by Ostrach in a number of reports (e.g. 1954, 1957), in which he has taken into account the effects due to frictional heating and to distributed heat sources in the fluid. The corresponding problem of laminar convection in a uniformly heated *horizontal* pipe has a very different solution with a secondary circulation in planes normal to the axis (see Morton 1959).

2. Equations for steady laminar convection in vertical pipes

If it is assumed that the kinematic viscosity ν and the thermometric conductivity κ are independent of temperature, and that variations in density are important only in so far as they give rise to buoyancy forces, then it seems reasonable to expect that a specially simple type of similarity solution will exist for laminar flow under a pressure gradient in a uniformly heated vertical pipe. The velocity profile for this solution will be the same at all sections sufficiently far from the pipe entrance, but all temperatures will increase linearly with distance along the pipe (though the buoyancy profile will remain unchanged); also, there will be no component of velocity in sections normal to the axis. Although for real fluids there can be large temperature variations in ν, and rather smaller ones in κ, the solution which will be obtained is still of interest because an important part of the flow behaviour arises from the combination of pressure gradient and buoyancy forces. If the temperature changes in diffusivity were taken into account also, there would be a progressive small modification of the similar profile shapes, but this would be a secondary effect.

There will be a linear temperature gradient along a uniformly heated vertical pipe carrying a convecting fluid stream, and either a constant rate of heat input per unit area of pipe wall, or a constant temperature gradient along the pipe wall may be taken as the thermal boundary condition at the pipe. Each can be important experimentally, but the latter condition will be chosen as it is slightly more convenient in the analysis.

In Ostrach's earlier work he calculated buoyancy forces on the fluid within the pipe relative to cool fluid at the same level outside the pipe. This was presumably intended to model the case of a vertical pipe open at top and bottom; however, even in Ostrach's case, it seems better to regard the fluid in the pipe as moving under an over-all pressure difference between the ends and the relative buoyancy forces within. For the idea of a buoyancy force is essentially related with immediate fluid contact in horizontal levels (for gravity-induced buoyancy). Although it is true that there will be a pressure difference between the open ends of a vertical pipe (with heated inner wall) due to the gross density difference of the fluid within and without, this will be distributed uniformly along the pipe only if the flow is the same at all levels. This cannot be the case in entry-length regions or in unheated or differently heated sections of the pipe; and in a pipe closed at one or both ends the local density of the external fluid is important only at an opening. Thus, it is better to divide buoyancy effects into 'gross buoyancy', which is more likely to be interpreted correctly when incorporated as a pressure distribution due to forces applied at particular parts of the system, and local buoyancy which is a force tending to cause relative rearrangement of neighbouring elements of fluid.

Consider the steady flow of fluid with density ρ under a constant pressure gradient along a vertical pipe of radius a, the walls of which are maintained at a uniform temperature gradient τ/a in the direction of the axis. The system will be referred to cylindrical polar coordinates (x, r, ϕ) with the x-axis directed vertically upwards along the pipe axis, and as there is axial symmetry the convection will be independent of ϕ; the velocity components can be taken as $u(r), 0, 0$ for the solution envisaged. Let the absolute temperature of the inner wall of the pipe be $T_w = T_0 + \tau(x/a)$, and the temperature within the fluid $T = T_w - \theta(r)$; T_0 is the temperature of the pipe at the level of the origin and may be regarded as representative for the region of flow considered, so that ν and κ and the coefficient of cubical expansion β are evaluated at temperature T_0. The rate of heat flow through the wall per unit area is proportional to $(\partial T/\partial r)_{r=a} = -(d\theta/dr)_{r=a}$, and this is independent of x so that there is uniform heating or cooling.

The equation of continuity is now satisfied identically, and the equations of motion and energy reduce to

$$\left.\begin{aligned} 0 &= -\frac{1}{\rho}\frac{\partial p}{\partial x} + \nu\nabla_1^2 u - g, \\ 0 &= -\frac{1}{\rho}\frac{\partial p}{\partial r}, \\ u\frac{\partial T}{\partial x} &= \kappa\nabla_1^2 T, \end{aligned}\right\} \tag{1}$$

where p is the pressure and $\nabla_1^2 \equiv \partial^2/\partial r^2 + r^{-1}\partial/\partial r + \partial^2/\partial x^2$. The first of these equations (in which the only approximation that has been made is that the coefficient of viscosity, μ, is independent of temperature) can be written

$$0 = -\left(\frac{\partial p}{\partial x} + \rho_w g\right) + \mu\nabla_1^2 u + (\rho_w - \rho)\, g,$$

and from the equation of state $\rho = \rho_w\{1 + \beta(T_w - T)\}$,

$$0 = -\left(\frac{\partial p}{\partial x} + \rho_w g\right) + \mu\nabla_1^2 u - \rho_w \beta g (T_w - T),$$

where the suffix w refers to conditions at the pipe wall. According to the assumptions stated above, ρ_w is replaced now by ρ_0, the reference density at the pipe wall at $x = 0$; and hence

$$0 = -\left(\frac{1}{\rho_0}\frac{\partial p}{\partial x} + g\right) + \nu\nabla_1^2 u - \beta g\theta. \tag{2}$$

From equations (1) and (2) it follows that the pressure varies only in the direction of flow, and

$$\left.\begin{aligned}\left(\frac{d^2}{dr^2} + \frac{1}{r}\frac{d}{dr}\right) u &= \frac{1}{\nu}\left(\frac{1}{\rho_0}\frac{\partial p}{\partial x} + g\right) + \frac{\beta g}{\nu}\theta,\\ \left(\frac{d^2}{dr^2} + \frac{1}{r}\frac{d}{dr}\right)\theta &= -\frac{\tau}{\kappa a}u.\end{aligned}\right\} \tag{3}$$

The transformations $r = aR$, $x = aX$, $u = (\kappa/a)\, U$, $\theta = \tau\Theta$ reduce equations (3) to the dimensionless form

$$\left.\begin{aligned}\left(\frac{d^2}{dR^2} + \frac{1}{R}\frac{d}{dR}\right) U &= -\gamma + A\Theta \operatorname{sgn}\tau,\\ \left(\frac{d^2}{dR^2} + \frac{1}{R}\frac{d}{dR}\right)\Theta &= -U,\end{aligned}\right\} \tag{4}$$

where A is the Rayleigh number $\beta g\,|\tau|\, a^3/\kappa\nu$ based on the pipe radius and the change in temperature along the pipe in a length equal to the radius, and $\gamma = (a^3/\kappa\nu)\,[(1/\rho_0)\,(\partial p/\partial x) + g]$; $\operatorname{sgn}\tau = \pm 1$ according as $\tau \gtrless 0$, respectively. The non-dimensional parameter γ has the general form of a Reynolds number for the flow (a normal Reynolds number based on the mean velocity across a section of the pipe and on pipe-diameter is $-(a^3/4\rho\nu^2)\,\partial p/\partial x$) but with the important difference that it is based on the net upwards force at the pipe wall (the resultant of the pressure gradient and gravitational forces). Unlike the Reynolds number for ordinary pipe flow, there will be circumstances in which the *sign* of $\rho^{-1}\partial p/\partial x + g$ will change in passing from the wall to the axis of the pipe, and these should result in a reversed flow near the axis. If Θ is eliminated from equations (4), the result is

$$\left(\frac{d^2}{dR^2} + \frac{1}{R}\frac{d}{dR}\right)^2 U + AU \operatorname{sgn}\tau = 0. \tag{5}$$

When U has been determined, Θ can be found from the first equation of (4).

It can be seen from equation (5) that the character of the solution depends on the direction in which the pipe temperature increases. The heating of cold fluid flowing upwards is basically the same as the cooling of hot fluid flowing downwards—in each case the pressure and buoyancy forces oppose one another near the axis and reinforce near the wall. A different pattern of convection results when these forces reinforce near the axis, as in the cooling of hot fluid flowing upwards and the heating of cold fluid flowing downwards.

Equation (5) is satisfied by the Bessel functions of zero order $J_0(\alpha R)$ and $Y_0(\alpha R)$ and by the modified Bessel functions of zero order $I_0(\alpha R)$ and $K_0(\alpha R)$, where $\alpha^4 = -A \operatorname{sgn} \tau$. Hence the general solution is of the form

$$U = c_1 J_0(\alpha R) + c_2 Y_0(\alpha R) + c_3 I_0(\alpha R) + c_4 K_0(\alpha R), \tag{6}$$

where c_1, c_2, c_3, c_4 are arbitrary constants. This solution and the corresponding expressions for Θ must satisfy the boundary conditions

$$T = T_w \quad \text{and} \quad u = 0, \quad \text{on} \quad r = a;$$
$$\frac{\partial T}{\partial r} = 0 \quad \text{and} \quad \frac{\partial u}{\partial r} = 0, \quad \text{on} \quad r = 0;$$

or in non-dimensional form

$$\Theta = 0 \quad \text{and} \quad U = 0, \quad \text{on} \quad R = 1;$$
$$\frac{d\Theta}{dR} = 0 \quad \text{and} \quad \frac{dU}{dR} = 0, \quad \text{on} \quad R = 0.$$

The corresponding non-dimensional boundary conditions for the solution of equation (5) in U are obtained with the aid of the first equation of (4):

$$\left.\begin{aligned} U = 0 \quad &\text{and} \quad \left(\frac{d^2}{dR^2} + \frac{1}{R}\frac{d}{dR}\right) U = -\gamma, \quad \text{on} \quad R = 1; \\ \frac{dU}{dR} = 0 \quad &\text{and} \quad \frac{d}{dR}\left(\frac{d^2}{dR^2} + \frac{1}{R}\frac{d}{dR}\right) U = 0, \quad \text{on} \quad R = 0. \end{aligned}\right\} \tag{7}$$

The form taken by the solution depends on the sign of the temperature gradient ($\operatorname{sgn} \tau$) along the pipe wall, the two possible cases will now be treated separately.

3. Convection when the pipe temperature increases with height

The steady heating of ascending cool fluid and the steady cooling of descending hot fluid in a pipe are both included in the case $\operatorname{sgn} \tau = 1$, and $\alpha = (-A)^{\frac{1}{4}} = i^{\frac{1}{2}} A^{\frac{1}{4}}$. (The choice of $i^{\frac{1}{2}}$ for $(-1)^{\frac{1}{4}}$ does not affect the generality of the solution.) For this case the general solution (6) takes the form

$$U = c_1 J_0(i^{\frac{1}{2}} A^{\frac{1}{4}} R) + c_2 Y_0(i^{\frac{1}{2}} A^{\frac{1}{4}} R) + c_3 I_0(i^{\frac{1}{2}} A^{\frac{1}{4}} R) + c_4 K_0(i^{\frac{1}{2}} A^{\frac{1}{4}} R). \tag{8}$$

This can also be written in the form

$$U = c_1 \operatorname{ber}(A^{\frac{1}{4}} R) + c_2 \operatorname{bei}(A^{\frac{1}{4}} R) + c_3 \operatorname{ker}(A^{\frac{1}{4}} R) + c_4 \operatorname{kei}(A^{\frac{1}{4}} R), \tag{9}$$

where
$$\operatorname{ber} x + i \operatorname{bei} x = J_0(x e^{\frac{3}{4}\pi i}) = I_0(x e^{\frac{1}{4}\pi i})$$

and
$$\operatorname{ker} x + i \operatorname{kei} x = \tfrac{1}{2}\pi K_0(x e^{\frac{1}{4}\pi i}) = \tfrac{1}{2}\pi i H_0^{(1)}(x e^{\frac{3}{4}\pi i})$$

(see, for example, Jeffreys & Jeffreys 1950, Ch. 21), and the constants c_i are different from (but related to) those of solutions (8). The advantage of using the ber, bei, ker and kei functions is that they are real in argument and real in value; they are tabulated adequately for this purpose.

For small values of x,

$$\operatorname{ber} x = 1 - \frac{x^4}{2^4(2!)^2} + \ldots, \quad \operatorname{bei} x = \frac{x^2}{2^2(1!)^2} - \frac{x^6}{2^6(3!)^2} + \ldots,$$

$$\ker x = -\left(1 - \frac{x^4}{2^4(2!)^2} + \ldots\right)\log\frac{x}{2} + \frac{\pi}{4}\left(\frac{x^2}{2^2(1!)^2} - \ldots\right) + \left(F(0) - F(2)\frac{x^4}{2^4(2!)^2} + \ldots\right),$$

$$\operatorname{kei} x = -\left(\frac{x^2}{2^2(1!)^2} - \ldots\right)\log\frac{x}{2} - \frac{\pi}{4}\left(1 - \frac{x^4}{2^4(2!)^2} + \ldots\right) + \left(F(1)\frac{x^2}{2^2(1!)^2} - \ldots\right),$$

where $F(n)$ is the digamma function of argument n. Hence, applying the boundary conditions (7) at $R = 0$, it follows that c_3 and c_4 in solution (9) must be zero. And from the conditions at $R = 1$

$$c_1 = \gamma A^{-\frac{1}{2}} \frac{\operatorname{bei} A^{\frac{1}{2}}}{\operatorname{ber}^2 A^{\frac{1}{2}} + \operatorname{bei}^2 A^{\frac{1}{2}}} \quad \text{and} \quad c_2 = -\gamma A^{-\frac{1}{2}} \frac{\operatorname{bei} A^{\frac{1}{2}}}{\operatorname{ber}^2 A^{\frac{1}{2}} + \operatorname{bei}^2 A^{\frac{1}{2}}};$$

so that

$$\gamma^{-1} A^{\frac{1}{2}} U = \frac{\operatorname{bei} A^{\frac{1}{2}} \operatorname{ber} A^{\frac{1}{2}} R - \operatorname{ber} A^{\frac{1}{2}} \operatorname{bei} A^{\frac{1}{2}} R}{\operatorname{ber}^2 A^{\frac{1}{2}} + \operatorname{bei}^2 A^{\frac{1}{2}}}, \tag{10}$$

and

$$\gamma^{-1} A \Theta = 1 - \frac{\operatorname{ber} A^{\frac{1}{2}} \operatorname{ber} A^{\frac{1}{2}} R + \operatorname{bei} A^{\frac{1}{2}} \operatorname{bei} A^{\frac{1}{2}} R}{\operatorname{ber}^2 A^{\frac{1}{2}} + \operatorname{bei}^2 A^{\frac{1}{2}}}. \tag{11}$$

In order to display the significance of this solution a set of cases has been worked numerically with values of $A^{\frac{1}{2}}$ of 0, 1, 2, 3, 4, 5, 7, 10 and the velocity and buoyancy profiles, respectively, are drawn in sets (figures 1 and 2) to illustrate the changes in profile with increasing Rayleigh number. Figure 1 shows velocity profiles, which are plotted as the ratio of the non-dimensional velocity U to the effective Reynolds number γ against the non-dimensional distance from the axis R. The curve for zero Rayleigh number is the parabolic profile for normal Poiseuille flow at uniform temperature. With increase in the Rayleigh number the flow velocities decrease over the whole section of the pipe and the upflow is concentrated progressively more closely towards the walls; in fact when the Rayleigh number exceeds about 600 there is reversed flow near the axis, and for rather larger Rayleigh numbers the solution predicts annular regions of slow up and down flow near the axis. Such regions of reversed flow are to be expected wherever $\rho^{-1}\partial p/\partial x + g$ changes sign. It is unlikely that these more complicated flows for Rayleigh numbers above about 600 would be found experimentally since conditions will seldom arise which might produce them (and so this behaviour has not been stressed in figure 1), however, the solution up to the stage of reversed flow at the axis should certainly be observable physically. Figure 2 shows the corresponding curves for non-dimensional profiles of the difference between wall and interior temperature plotted as $\gamma^{-1}\Theta$ against R. The most striking feature of these sets of curves is the progressive development of velocity and thermal

boundary layers at the pipe wall with increasing values of the Rayleigh number. The (relative) widths of the two boundary layers do not depend on the Prandtl number. These figures demonstrate how buoyancy effects may be able to upset the conception of forced convection.

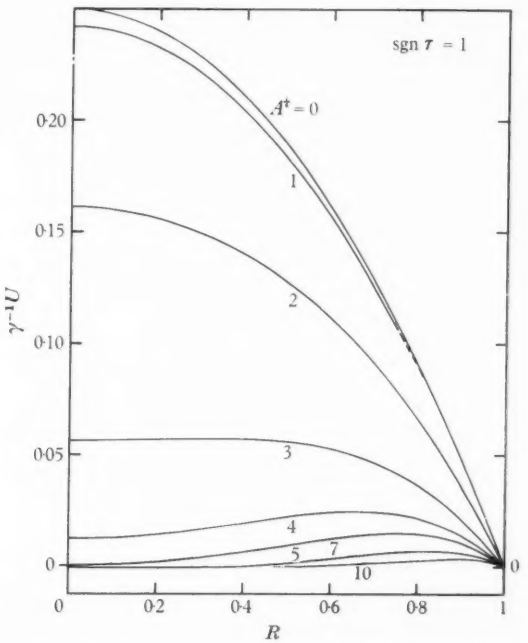

FIGURE 1. The profiles for dimensionless velocity ($\gamma^{-1}U$) against dimensionless distance from the axis (R) for rising convection under a specified pressure gradient in a uniformly heated vertical pipe. The curve $A^{\frac{1}{4}} = 0$ corresponds with normal Poiseuille parabolic flow, and the other curves are for increasing values of the Rayleigh number A.

The rate of heat transfer through the pipe walls to the fluid per unit area of pipe surface is

$$k\left(\frac{\partial T}{\partial r}\right)_{r=a} = -\frac{\tau k}{a}\left(\frac{d\Theta}{dR}\right)_{R=1} = \frac{\gamma\tau k}{a}A^{-\frac{1}{4}}\frac{\mathrm{ber}\,A^{\frac{1}{4}}\,\mathrm{ber}'\,A^{\frac{1}{4}} + \mathrm{bei}\,A^{\frac{1}{4}}\,\mathrm{bei}'\,A^{\frac{1}{4}}}{\mathrm{ber}^2\,A^{\frac{1}{4}} + \mathrm{bei}^2\,A^{\frac{1}{4}}}, \tag{12}$$

where the accents imply differentiation with respect to the argument, and k is the thermal conductivity.

The rate of volume flow through the pipe is

$$\int_0^a 2\pi r u\,dr = 2\pi a\kappa\gamma A^{-\frac{1}{4}}\frac{\mathrm{ber}\,A^{\frac{1}{4}}\,\mathrm{ber}'\,A^{\frac{1}{4}} + \mathrm{bei}\,A^{\frac{1}{4}}\,\mathrm{bei}'\,A^{\frac{1}{4}}}{\mathrm{ber}^2\,A^{\frac{1}{4}} + \mathrm{bei}^2\,A^{\frac{1}{4}}}. \tag{13}$$

The non-dimensional volume flux (volume flux/$a\kappa\gamma$) is plotted against $A^{\frac{1}{4}}$ as curve 1 of figure 3; there is little effect on the flux for small Rayleigh numbers,

but there is then a rapid decrease in the flow rate with increasing Rayleigh number. Curve 2 shows the non-dimensional heat transfer per unit area of pipe surface plotted against $A^{\frac{1}{4}}$.

A measure for the effectiveness of heat transfer is provided by the Nusselt number

$$N = \frac{\textit{rate of heat transfer per unit area of pipe wall} \times \textit{pipe diameter}}{k \times \textit{characteristic temperature difference in main direction of conduction}}.$$

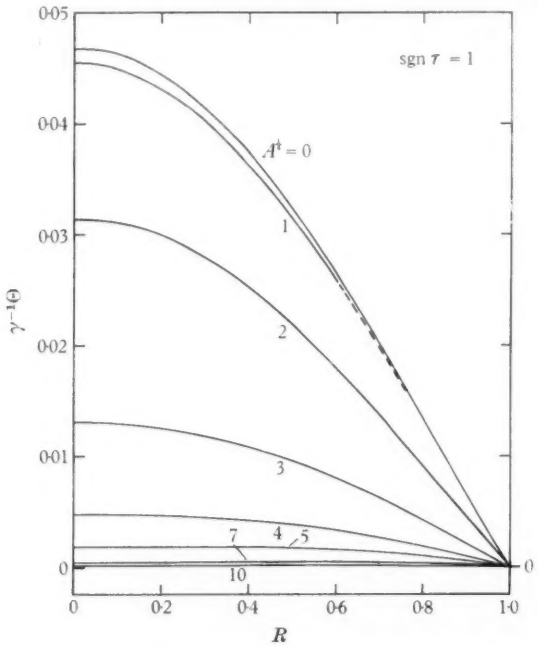

FIGURE 2. The profiles for dimensionless temperature deficiency ($\gamma^{-1}\Theta$) between the fluid and the pipe wall against dimensionless distance from the axis (R) for rising convection in a uniformly heated vertical pipe (or downflow in a cooled pipe). The curve $A^{\frac{1}{4}} = 0$ corresponds with the forced thermal convection solution.

This temperature difference can be taken in various ways; here, partly for ease of comparison with the results quoted above, it will be taken as the difference between the wall temperature and the mean temperature across a section of the pipe, which is

$$\frac{1}{\pi a^2}\int_0^a 2\pi r\theta\, dr = \frac{2\tau\gamma}{A}\left[\frac{1}{2} + \frac{\operatorname{bei} A^{\frac{1}{4}} \operatorname{ber}' A^{\frac{1}{4}} - \operatorname{ber} A^{\frac{1}{4}} \operatorname{bei}' A^{\frac{1}{4}}}{A^{\frac{1}{4}}(\operatorname{ber}^2 A^{\frac{1}{4}} + \operatorname{bei}^2 A^{\frac{1}{4}})}\right]. \tag{14}$$

Hence the Nusselt number is

$$N = \frac{A^{\frac{1}{4}}(\operatorname{ber} A^{\frac{1}{4}} \operatorname{ber}' A^{\frac{1}{4}} + \operatorname{bei} A^{\frac{1}{4}} \operatorname{bei}' A^{\frac{1}{4}})}{(\operatorname{bei} A^{\frac{1}{4}} \operatorname{ber}' A^{\frac{1}{4}} - \operatorname{ber} A^{\frac{1}{4}} \operatorname{bei}' A^{\frac{1}{4}}) + \frac{1}{2}A^{\frac{1}{4}}(\operatorname{ber}^2 A^{\frac{1}{4}} + \operatorname{bei}^2 A^{\frac{1}{4}})}. \tag{15}$$

The appropriate curve (marked sgn $\tau = 1$) of figure 4 shows the Nusselt number plotted against (Rayleigh number)$^{\frac{1}{4}}$. When $A = 0$ the Nusselt number takes the

value $N = 6$ for forced convection which has been calculated previously; small increases in the Rayleigh number have little effect on the Nusselt number, and for this particular flow the forced convection solution is still accurate to 1 % at $A = 10$. However, for larger Rayleigh numbers the Nusselt number increases

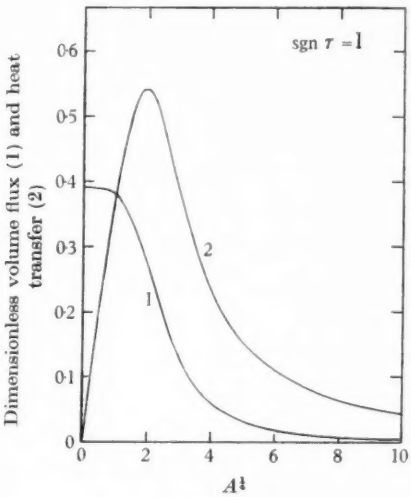

FIGURE 3

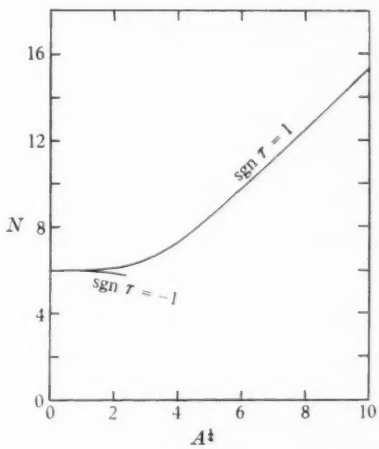

FIGURE 4

FIGURE 3. The dimensionless volume flux (actual flux $\times\, 1/a\kappa\gamma$) (curve 1) and the dimensionless heat flux per unit area from the pipe surface (actual flux $\times\, 2\pi\beta g a^4/\gamma k\kappa\nu$) (curve 2) shown as functions of the (Rayleigh number)$^{\frac{1}{4}}$.

FIGURE 4. The variation of Nusselt number with $A^{\frac{1}{4}}$ for the two possible types of convection; the Nusselt number varies little from its value 6 for forced convection at small Rayleigh numbers.

steadily, and for $A > 1000$ a very good approximation to the Nusselt number can be taken from the results shown as

$$N \doteq 1{\cdot}30 + 1{\cdot}40 A^{\frac{1}{4}}. \tag{16}$$

It should be noted that the normal physical application of the solution will not usually lie in this range of A.

When the Rayleigh number is small, the results stated above can be expanded in series form, and these approximate series will be useful for later reference. From (10) and (11),

$$\left.\begin{aligned} U &= \frac{\gamma}{4}(1-R^2)\left\{1 - \frac{1}{576}A(19 - 8R^2 + R^4)\right. \\ &\qquad \left. + \frac{1}{3{,}686{,}400}A^2(3{,}651 - 1{,}624R^2 + 276R^4 - 24R^6 + R^8) + \ldots\right\}, \\ \Theta &= \frac{\gamma}{64}(1-R^2)\left\{(3-R^2) - \frac{1}{2{,}304}A(211 - 93R^2 + 15R^4 - R^6) + \frac{1}{33{,}177{,}600}\right. \\ &\qquad \left. \times A^2(90{,}921 - 40{,}515R^2 + 6{,}960R^4 - 640R^6 + 35R^8 - R^{10}) + \ldots\right\}. \end{aligned}\right\} \tag{17}$$

When $A\ (=\beta g\tau a^3/\kappa\nu)=0$ the solution for the velocity reduces to the Poiseuille velocity profile for laminar pipe flow; if $\tau=0$ the temperature is uniform throughout the fluid, but if A is zero because the gravitational force (i.e. g) vanishes, then $\Theta=\frac{1}{64}\gamma(1-R^2)(3-R^2)$ gives the forced convection solution. For small values of A the velocity is decreased across the whole profile (see figure 1), and the effect of a temperature gradient (or steady rate of heating) is to reduce the volume flow obtained for a given pressure gradient to the value

$$\frac{\pi}{8}\frac{a^4}{\nu}\left(\frac{1}{\rho_0}\frac{\partial p}{\partial x}+g\right)\left\{1-\frac{11}{384}A+\frac{473}{552{,}960}A^2-\ldots\right\}. \tag{18}$$

The rate of heat transfer through the pipe walls per unit area of surface is

$$-\frac{1}{16}\frac{k}{\beta g a}\left(\frac{1}{\rho_0}\frac{\partial p}{\partial x}+g\right)A\left\{1-\frac{11}{384}A+\frac{473}{552{,}960}A^2\ldots\right\}, \tag{19}$$

and the Nusselt number based on the mean temperature is

$$6\left(1+\frac{1}{960}A+\frac{5}{1{,}548{,}288}A^2+\ldots\right). \tag{20}$$

4. Convection when the pipe temperature decreases with height

The steady cooling of ascending hot fluid or the steady heating of descending cold fluid correspond with $\operatorname{sgn}\tau=-1$, and $\alpha=A^{\frac{1}{4}}$. The general solution (6) now takes the form

$$U=c_1J_0(A^{\frac{1}{4}}R)+c_2Y_0(A^{\frac{1}{4}}R)+c_3I_0(A^{\frac{1}{4}}R)+c_4K_0(A^{\frac{1}{4}}R). \tag{21}$$

From boundary conditions (7) at $R=0$, it follows that c_2 and c_4 must be zero; and from the conditions at $R=1$,

$$c_1=\frac{\gamma}{2A^{\frac{1}{4}}J_0(A^{\frac{1}{4}})} \quad \text{and} \quad c_3=-\frac{\gamma}{2A^{\frac{1}{4}}I_0(A^{\frac{1}{4}})}.$$

Hence

$$\gamma^{-1}A^{\frac{1}{4}}U=\frac{1}{2}\left\{\frac{J_0(A^{\frac{1}{4}}R)}{J_0(A^{\frac{1}{4}})}-\frac{I_0(A^{\frac{1}{4}}R)}{I_0(A^{\frac{1}{4}})}\right\}, \tag{22}$$

$$\gamma^{-1}A\Theta=\frac{1}{2}\left\{\frac{J_0(A^{\frac{1}{4}}R)}{J_0(A^{\frac{1}{4}})}+\frac{I_0(A^{\frac{1}{4}}R)}{I_0(A^{\frac{1}{4}})}\right\}-1. \tag{23}$$

In the previous solution for $\operatorname{sgn}\tau=1$, the extent of the modification to the normal isothermal laminar pipe flow with increasing Rayleigh number was considerable, but here the solutions for both velocity and buoyancy (or temperature difference) actually become infinite at values of A which are roots of $J_0(A^{\frac{1}{4}})=0$, the smallest root of which is $A^{\frac{1}{4}}=2{\cdot}405$. Non-dimensional profiles of velocity are shown in figure 5 and of temperature difference in figure 6 for values of $A^{\frac{1}{4}}$ of 0, 1, 1·5, 2, 2·3, all of which are below the first critical Rayleigh number. It can be seen that both velocity and temperature difference increase across the whole profile, at first slowly with increasing Rayleigh number, and then extremely rapidly as the critical value of A is approached. Above this first critical Rayleigh number there are theoretically possible flows of a more com-

plicated character which are rather unlikely to be found in practice since they would require improbable end conditions. For example, the cooling of an upwards hot stream for Rayleigh numbers lying between the first two critical values produces a downflow of cold fluid in a layer at the wall, and for higher Rayleigh numbers there will be a succession of annular regions of up and down flow between the rising stream near the axis and the wall. The striking feature of

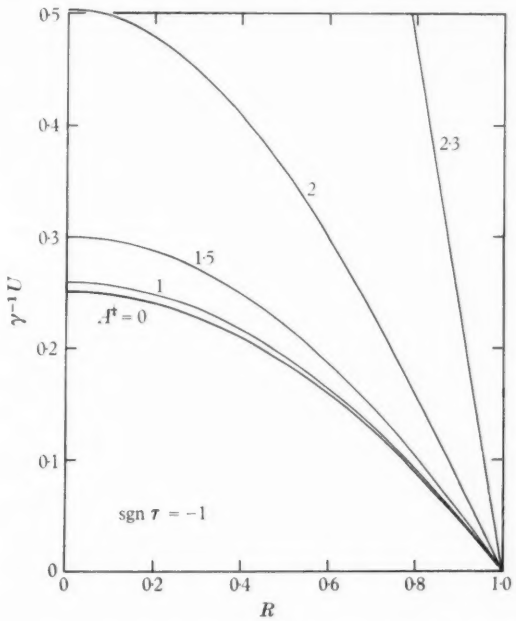

FIGURE 5. The non-dimensional velocity profiles ($\gamma^{-1}U$ against R) for falling convection under a specified pressure gradient in a uniformly heated vertical pipe. The curve $A^{\frac{1}{2}} = 0$ corresponds with normal Poiseuille flow at uniform temperature and the first critical state is for $A^{\frac{1}{2}} = 2{\cdot}405$.

this solution is that the laminar Poiseuille flow which is found for small Rayleigh numbers begins to 'run away' as the Rayleigh number approaches 33, and just above this value there is a state of affairs in which laminar Poiseuille flow is no longer possible until there has been a rearrangement of the flow profile. It is almost certain that the flow would become unsteady and then turbulent as the first critical Rayleigh number is approached. This 'runaway' occurs in the solution because higher values of temperature gradient along the pipe produce larger buoyancy forces leading to higher fluid velocities, which in their turn give rise to greater buoyancy forces. The character of the flow after rearrangement is such as to produce smaller buoyancy forces which can be offset by viscous forces from a more rapidly changing velocity profile.

Near the critical Rayleigh number the similarity solution calculated above will be increasingly in error, but it may be expected to provide a reasonable

solution over the greater part of the range $0 < A < 33$. The corresponding rate of heat transfer to the fluid per unit area of pipe wall is in this case

$$-\frac{\gamma k\kappa\nu}{2\beta g a^4} A^{\frac{1}{4}}\left(\frac{J_0'(A^{\frac{1}{4}})}{J_0(A^{\frac{1}{4}})}+\frac{I_0'(A^{\frac{1}{4}})}{I_0(A^{\frac{1}{4}})}\right), \tag{24}$$

the rate of volume flow through the pipe is

$$-\pi\kappa a\gamma A^{-\frac{3}{4}}\left(\frac{J_0'(A^{\frac{1}{4}})}{J_0(A^{\frac{1}{4}})}+\frac{I_0'(A^{\frac{1}{4}})}{I_0(A^{\frac{1}{4}})}\right), \tag{25}$$

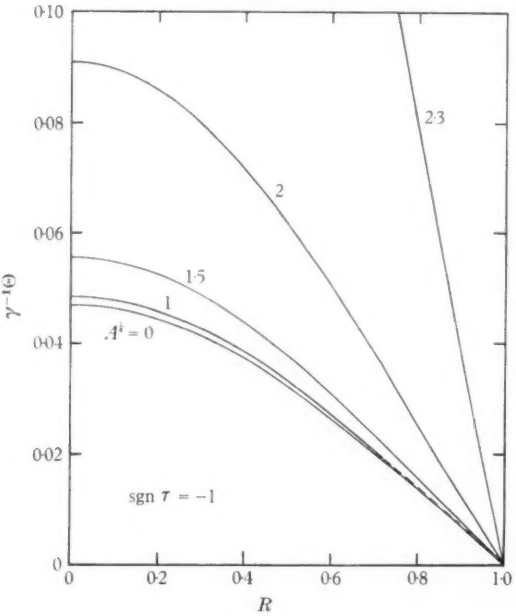

FIGURE 6. The non-dimensional buoyancy profiles (plotted as $\gamma^{-1}\Theta$ against R) for falling convection in a uniformly heated pipe (or upflow in a cooled pipe). The curve $A^{\frac{1}{4}} = 0$ corresponds with the forced convection solution.

the mean temperature difference across a pipe section is

$$\frac{\gamma\kappa\nu}{\beta g a^3} A^{-\frac{1}{4}}\left(A^{\frac{1}{4}}+\frac{J_0'(A^{\frac{1}{4}})}{J_0(A^{\frac{1}{4}})}-\frac{I_0'(A^{\frac{1}{4}})}{I_0(A^{\frac{1}{4}})}\right), \tag{26}$$

and the Nusselt number is

$$N = \frac{A^{\frac{1}{4}}\left(\frac{J_0'(A^{\frac{1}{4}})}{J_0(A^{\frac{1}{4}})}+\frac{I_0'(A^{\frac{1}{4}})}{I_0(A^{\frac{1}{4}})}\right)}{A^{\frac{1}{4}}+\frac{J_0'(A^{\frac{1}{4}})}{J_0(A^{\frac{1}{4}})}-\frac{I_0'(A^{\frac{1}{4}})}{I_0(A^{\frac{1}{4}})}}. \tag{27}$$

Figure 7 shows curves for (1) the non-dimensional volume flow and (2) the non-dimensional heat transfer per unit area of pipe surface, plotted against $A^{\frac{1}{4}}$, for

the range of Rayleigh numbers up to the first (and important) critical value. The variation of Nusselt number for the same range is shown on figure 4, marked $\operatorname{sgn}\tau = -1$; within this range N is very nearly constant at the value 6.

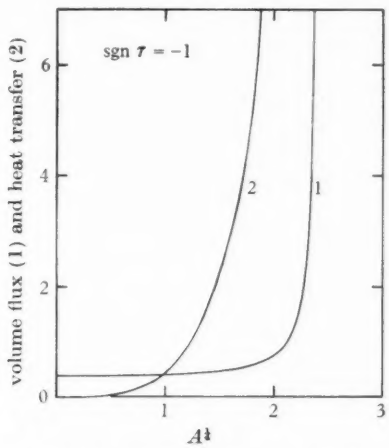

FIGURE 7. The non-dimensional volume flux (curve 1) and heat flux per unit area of pipe surface (curve 2) shown as functions of $A^{\frac{1}{4}}$ up to the first critical Rayleigh number.

The series forms of the solutions for small Rayleigh numbers are

$$\left.\begin{aligned} U &= \frac{\gamma}{4}(1-R^2)\left\{1+\frac{A}{576}(19-8R^2+R^4)\right. \\ &\qquad \left.+\frac{1}{3{,}686{,}400}A^2(3{,}651-1{,}624R^2+276R^4-24R^6+R^8)+\ldots\right\}, \\ \Theta &= \frac{\gamma}{64}(1-R^2)\left\{(3-R^2)+\frac{1}{2{,}304}A(211-93R^2+15R^4-R^6)+\frac{1}{33{,}177{,}600}\right. \\ &\qquad \left.\times A^2(90{,}921-40{,}515R^2+6{,}960R^4-640R^6+35R^8-R^{10})+\ldots\right\}. \end{aligned}\right\} \tag{28}$$

The volume flow is

$$\frac{\pi}{8}\frac{a^4}{\nu}\left(\frac{1}{\rho_0}\frac{\partial p}{\partial x}+g\right)\left\{1+\frac{11}{384}A+\frac{473}{552{,}960}A^2+\ldots\right\}; \tag{29}$$

the rate of heat transfer per unit area of wall surface is

$$-\frac{1}{16}\frac{k}{\beta g a}\left(\frac{1}{\rho_0}\frac{\partial p}{\partial x}+g\right)A\left\{1+\frac{11}{384}A+\frac{473}{552{,}960}A^2+\ldots\right\}; \tag{30}$$

and the Nusselt number based on the mean temperature is

$$6\left(1-\frac{1}{960}A+\frac{5}{1{,}548{,}288}A^2-\ldots\right). \tag{31}$$

All of these pipe flows will show a tendency to become unsteady and turbulent as the Reynolds number is increased, although the changes in profile make it difficult to relate critical Reynolds numbers with those for isothermal pipe flow. When $\operatorname{sgn}\tau = 1$ there is the additional effect of stable thermal stratification, so that in this case the laminar flow régime is likely to be of some practical importance, especially for high rates of heating (or large values of A). On the other hand, when $\operatorname{sgn}\tau = -1$ the fluid is unstably stratified in density so that for all A (< 33) the critical Reynolds numbers will be smaller than for isothermal flow, and as A approaches 33 the flow is likely to become unsteady at Reynolds numbers far below the usual critical value. Turbulent convection will minimize the difference in temperature between pipe and fluid and will reduce the effects of buoyancy forces for this reason. Because the flow is less stable when $\operatorname{sgn}\tau = -1$ it should be most effective to heat fluid by passing it down a hot pipe or to cool an upwards flowing stream.

REFERENCES

Goldstein, S. (Ed.) 1938 *Modern Developments in Fluid Dynamics*, Vol. 2. Oxford University Press.

Jeffreys, H. & Jeffreys, B. S. 1950 *Methods of Mathematical Physics*, 2nd ed. Cambridge University Press.

Morton, B. R. 1959 *Quart. J. Mech. Appl. Math.*, **12**, 410.

Nusselt, H. 1910 *Z. Ver. dtsch. Ing.* **54**, 1154.

Ostrach, S. 1954 *N.A.C.A. Tech. Note* 3141.

Ostrach, S. 1957 50 *Jahre Grenzschichtforschung*. Görtler and Tollmien (Eds.), Vieweg, Braunschweig.

On the collapse of an empty cavity in water

By C. HUNTER
Trinity College, Cambridge

(Received 14 December 1959)

This paper is concerned with the spherically symmetric collapse of an empty cavity in water. The effects of viscosity and surface tension are neglected, but the compressibility of the water is allowed for and a suitable equation of state for the water assumed. The object of this is to clarify the effect of compressibility on the flow by considering it in isolation and thus to describe the formation of a pressure pulse by the collapse and its subsequent propagation.

The exact flow equations are integrated numerically and it is found that very high flow speeds develop in the neighbourhood of the collapse point. The radius of the cavity is found to be proportional to $(-t)^n$ for small t, where $t = 0$ is the instant of collapse, and n is some positive number less than unity.

The flow in the neighbourhood of the collapse point can be described by means of a similarity solution, and the value of n is determined by regularity properties of the similarity solution (the value of n depends on the equation of state assumed for the water). The similarity theory, which is valid only at very high pressures and velocities, can be continued beyond the instant of collapse to describe the formation of a shock wave after the collapse is completed, and the initial propagation of this shock.

1. Introduction

Cavitation is a phenomenon of great practical importance, and has been the subject of many scientific investigations. In normal circumstances a liquid will contain a large number of minute nuclei containing undissolved gas and/or vapour, and if the local liquid pressure falls to vapour pressure, these nuclei will grow in size to become clearly visible cavities. The internal pressures of these cavities will be made equal to the liquid vapour pressure by the evaporation of some of the liquid into them. If the ambient liquid pressure then increases to a value greater than the vapour pressure after a cavity has been formed, the cavity is forced to collapse. This situation can arise when a cavity has been formed in a flowing liquid in a region of low pressure, and is then swept by the flow into a region of higher pressure. The resulting collapse can have serious effects on hydraulic machinery. For, although the typical maximum size of a cavity in water is only of the order of a centimetre, the cavity may collapse with great violence and generate high pressures. A pressure wave is then propagated outwards in the form of a shock wave, and serious damage to nearby solid surfaces may be caused, with small fragments of their material being torn away from them.

To account for these observed phenomena, many workers have studied the collapse of a single spherical cavity in an otherwise undisturbed liquid. An early theoretical investigation was made by Lord Rayleigh (1917) who discussed the collapse of an empty spherical cavity, that is one with zero internal pressure, which is initially at rest in an otherwise undisturbed mass of incompressible liquid at positive pressure p_0. Let R' be the radius of the cavity at time t', and let r' be the radial distance from the origin O at the centre of the cavity. Then, if the flow is assumed to be spherically symmetric, the distribution of velocity throughout the liquid must, by continuity, be given by

$$u' = \frac{R'^2 \dot{R}'}{r'^2}. \tag{1}$$

(Here and subsequently dots denote differentiation with respect to time.) Conservation of the total energy of the flow then yields an equation for the motion of the cavity wall

$$\dot{R}'^2 = \frac{2p_0}{3\rho'}\left(\frac{R_0^3}{R'^3} - 1\right), \tag{2}$$

where R_0 is the initial radius of the cavity and ρ' is the density.

The $R' - t'$ curves obtained experimentally for cavities agree well with those predicted by (2) until R' becomes very much less than R_0. During this latter stage, however, detailed observation is extremely difficult, since by this time the cavity is usually minute in size and events are taking place very rapidly. Equation (2) gives rise to some physically unrealistic features associated with this rapid final part of the collapse, which suggest that it ceases to be valid during this part of the motion. It predicts that the pressure p' is infinite for finite r' when $R' = 0$, and also that $\dot{R}' = -\infty$ at this instant. Further, $u' = 0$ for $r' > 0$ at the instant when $R' = 0$, and the whole kinetic energy of the flow is concentrated at the origin O.

A number of physical processes which are neglected in the above theory become important in the late part of the collapse, and these have been the subject of many subsequent investigations. Lord Rayleigh himself recognized the fact that at the high liquid velocities that probably occur during the collapse of a cavity, the compressibility of the liquid should be taken into account, and it is with this factor that the present paper is concerned. Another basic assumption in the derivation of (2) is that the cavity is empty. In practice a cavity will contain liquid vapour and probably a small amount of permanent gas. At the start of the collapse vapour will condense back into the liquid so that the internal pressure in the cavity remains equal to the liquid-vapour pressure. The work of Zwick & Plesset (1955) on the collapse of a vapour cavity in water suggests that this will not always be the case, and that the final part of the collapse takes place so rapidly that some of the vapour does not have time to condense. This remnant of vapour, together with any gas there may be in the cavity, will then be compressed to a high pressure which will eventually become large enough to halt the inrushing liquid and cause the cavity to rebound. If σ is the ratio of the specific heats of the cavity contents which are compressed adiabatically, then their

pressure is proportional to $R'^{-3\sigma}$. The ratio σ is always greater than unity, and so the effect of this pressure will be small over a long period and will then build up very suddenly when the flow is moving inwards at high speed. The cavity will thus be in effect empty until this build-up of the internal cavity pressure occurs, since the vapour pressure is usually small compared with the external pressure causing the cavity to collapse.

Two other mechanisms neglected by Lord Rayleigh are the liquid viscosity and the tension of the cavity surface, though it can be shown that these do not have an appreciable effect on the collapse of a cavity in water before the late part of the collapse. Their magnitude increases as $R' \to 0$, but, in the case of an empty cavity collapsing in an incompressible liquid at least, the surface tension and viscous forces are of a lesser order of magnitude than pressure and inertia forces as $R' \to 0$. Yet another factor is instability, which destroys the spherical symmetry of the flow. It is known that the collapse of an empty cavity in an incompressible liquid is unstable (Birkhoff 1954).

A complete description of all these processes would be a very considerable task, and we shall here seek only to clarify the effect of compressibility on the flow by considering it in isolation. We shall therefore discuss the symmetric collapse of a spherical cavity in a compressible liquid, neglecting surface tension and viscosity and retaining the simplifying assumption that the cavity is empty. It is indeed plausible to assume that liquid velocities of the order of the velocity of sound in water occur before effects such as those of the cavity contents become important, so that this model is physically sensible. The liquid compressibility is a mechanism which will slow down the collapse, though the more important object of taking compressibility into account is to describe accurately the formation of a pressure pulse as a result of the collapse and its subsequent propagation.

For practical purposes it is the behaviour of a cavity in water that is of interest, and an appropriate equation of state is therefore assumed. The collapse of an empty cavity in water assuming an equation of state of this type has been studied by Gilmore (1952) who made use of an approximation concerning the outward propagation of a finite-amplitude wave suggested by Kirkwood & Bethe (1942). In the present paper the exact partial differential flow equations are integrated numerically (§ 3) and, from the results of this numerical integration, an analytical theory in the form of a similarity solution is developed to describe the flow in the neighbourhood of the collapse point (§ 4). The flow immediately after the collapse, in which a shock wave is formed at the collapse point and travels outwards, is then discussed (§ 5) and it is found that another similarity solution describes the flow behind the shock, the two similarity solutions being matched at the shock. The whole analytical theory is valid only at very high pressures, and for typical values of the relevant parameters the size of the region in which it applies is of the order of a hundredth of a centimetre, although roughly 20 % of the total energy of the flow is contained therein.

2. The formulation of the problem

To describe the collapse of an empty spherical cavity in water, it is necessary to solve the equations of conservation of momentum and mass for a spherically symmetric flow

$$\frac{\partial u'}{\partial t'} + u' \frac{\partial u'}{\partial r'} + \frac{1}{\rho'} \frac{\partial p'}{\partial r'} = 0, \tag{3}$$

$$\frac{\partial \rho'}{\partial t'} + u' \frac{\partial \rho'}{\partial r'} + \rho' \left(\frac{\partial u'}{\partial r'} + \frac{2u'}{r'} \right) = 0. \tag{4}$$

In addition, an equation of state for water is necessary. There is no simple theoretical law to describe the thermodynamic properties of water, but it has been found that experimental thermodynamic data for water can be described by a caloric equation of state of the modified Tait form (Cole 1948),

$$\frac{p' + B}{B} = \left(\frac{\rho'}{\rho_0} \right)^{\gamma}, \tag{5}$$

where, if S is the specific entropy, $\rho' = \rho'(p', S)$, $\rho_0 = \rho'(0, S)$, and B is some function of S which is dimensionally a pressure. The index γ is a constant, and both B and ρ_0 are slowly varying functions of S. The values quoted for γ vary from 7 to 7·5, and the value of B lies in the neighbourhood of 3 kilobars.

When there are no shocks present, the usual assumption of homentropic flow can be made. An important property of water is that even when very strong shocks are present, the entropy changes are small and have little effect on the p'–ρ' relation. In the present paper therefore B and ρ_0 are both taken as constant, and the p'–ρ' relation given by (5) is assumed to hold everywhere even when shocks occur. This means that we are neglecting the effect of the entropy changes produced by shocks on the liquid motion and are assuming that, as far as the equations of conservation of mass and momentum are concerned, the flow is everywhere homentropic. This approximation has usually been made hitherto in underwater explosion research. A detailed justification of it in the special case of a spherical shock pulse initially of 50 kilobars has been made by Penney & Pike (1950) who showed that the radial expansion terms in the equations of motion were very much greater than the entropy gradient terms. They did conclude, however, that this may not be a good approximation for shock pulses of very much greater strength. However, there is considerable disagreement between the results of different experimenters for pressures in excess of about 100 kilobars (Rice & Walsh 1957). The degree of accuracy of the homentropic approximation is probably as much as is either justified or necessary in the present case.

We shall take the constant value of B as 3 kilobars and that of γ as 7 and, when this is done, the thermodynamic data for water is fitted to within, at most, a few percent for pressures less than 100 kilobars.

The velocity of sound c' is defined as usual by

$$c'^2 = \left(\frac{dp'}{d\rho'} \right)_S = \frac{\gamma B \rho'^{\gamma - 1}}{\rho_0^{\gamma}}. \tag{6}$$

If $c' = c_0$ when $\rho' = \rho_0$, then

$$\rho_0 c_0^2 = \gamma B. \tag{7}$$

We shall need later an expression for the specific internal energy $\mathscr{E}'$ of the water. Thus

$$\mathscr{E}' = \int_{\rho'}^{\rho_0} p' dv' + \mathscr{E}'_0(S) = \frac{c'^2 - c_0^2}{\gamma(\gamma-1)} + B\left(\frac{1}{\rho'} - \frac{1}{\rho_0}\right) + \mathscr{E}'_0(S), \tag{8}$$

where v' is the specific volume. The specific internal energy $\mathscr{E}'$ is here measured relative to its value when $p' = 0$, and $\mathscr{E}'_0(S)$ is some function of entropy alone.

We next consider the boundary conditions to be applied to the solutions of (3) and (4). The pressure is zero at the cavity wall and is p_0 far from the cavity, and these two pressure conditions, together with the condition that the cavity wall is a free surface (so that $u' = \dot{R}'$ when $r' = R'$), must always be satisfied. To determine the liquid flow completely, it is necessary in addition to specify the entire velocity and pressure distribution in the liquid at some initial instant. This difficulty does not arise in the incompressible treatment, since disturbances are propagated instantaneously and the whole flow field at any instant is determined by the cavity-wall motion at that instant. The choice of any particular distribution as an approximation to a physically realistic one is necessarily arbitrary. In particular, if the initial conditions are chosen to be the same as in the incompressible problem with an empty cavity initially at rest in a liquid at positive pressure, there would be a discontinuity in the motion at the initial instant, and this discontinuity would persist in the flow. However, this difficulty about the initial conditions is not physically relevant. The liquid compressibility will be important only in the final high-speed part of the collapse, and the precise form of the initial low-speed flow will not influence this appreciably.

A way of overcoming this difficulty about initial conditions is suggested by a re-examination of the incompressible theory. According to this, in the last part of the collapse when $R' \ll R_0$,

$$\dot{R}'^2 \sim \frac{2p_0 R_0^3}{3\rho' R'^3}. \tag{9}$$

The liquid motion therefore does not depend on the scales p_0 and R_0 separately, but only on their combination $p_0 R_0^3$ which is equal to $3E/4\pi$, where E is the initial potential energy of the system. When $R' \ll R_0$, almost all this potential energy has been converted into the kinetic energy of the liquid motion. Formally the whole flow is determined by the parameter E alone if we make $p_0 \to 0$ and $R_0 \to \infty$ in such a way that E is unaltered. This means that we are considering a cavity of initially infinite size which has been collapsing for an infinite time. There is now no difference between the pressure in the cavity and that in the liquid far from it, and there is a constant and finite energy E associated with the flow. Equation (2) for the cavity wall motion now becomes

$$E = 2\pi\rho R'^3 \dot{R}'^2, \tag{10}$$

which can be integrated to give

$$R'^{\frac{5}{2}} = \frac{5}{2}\sqrt{\left(\frac{E}{2\pi\rho'}\right)}(t'_0 - t'), \tag{11}$$

where $t' = t'_0$ is the instant of collapse.

This model of the initially infinite cavity can be used when the liquid is assumed compressible. The expression (11) is now asymptotically exact as $t' \to -\infty$ in the compressible theory, since the effect of compressibility is negligible for large $(t_0 - t')$ when liquid velocities are much less than the velocity of sound in the liquid. Initial conditions are now specified for the liquid flow with all the essential features of the final part of the collapse being retained.†

It is convenient to use the velocity of sound c' as the single thermodynamic variable needed to describe the state of the liquid. With the boundary conditions in the form just discussed, c' is equal to c_0 at the cavity wall and also tends to this value as $r' \to \infty$. From the three dimensional scales E, ρ_0 and c_0, non-dimensional variables (without dashes) can be defined as follows:

$$\left.\begin{aligned} u' &= uc_0, \quad c' = cc_0, \quad \rho' = \rho\rho_0, \quad r' = r\left[\frac{5}{2c_0}\sqrt{\left(\frac{E}{2\pi\rho_0}\right)}\right]^{\frac{2}{3}}, \\ t' &= \frac{t}{c_0}\left[\frac{5}{2c_0}\sqrt{\left(\frac{E}{2\pi\rho_0}\right)}\right]^{\frac{2}{3}}, \quad \mathscr{E}' = \mathscr{E}c_0^2. \end{aligned}\right\} \tag{12}$$

Using the thermodynamic relations (5) and (6), we find that the governing equations (3) and (4) become, in terms of these scaled variables,

$$\frac{\partial u}{\partial t} + u\frac{\partial u}{\partial r} + \frac{1}{(\gamma-1)}\frac{\partial c^2}{\partial r} = 0, \tag{13}$$

$$\frac{\partial c^2}{\partial t} + u\frac{\partial c^2}{\partial r} + (\gamma-1)c^2\left(\frac{\partial u}{\partial r} + \frac{2u}{r}\right) = 0. \tag{14}$$

The boundary conditions are

$$\left.\begin{aligned} &c = 1 \quad \text{and} \quad u = \dot{R} \quad \text{at the cavity wall} \quad r = R, \\ &c \to 1 \quad \text{as} \quad r \to \infty, \\ R \sim (t_0 - t)^{\frac{2}{5}}, &\quad u \sim \frac{-2(t_0-t)^{\frac{1}{5}}}{5r^2}, \\ c^2 = 1 + \frac{2(\gamma-1)(t_0-t)^{-\frac{6}{5}}}{25}&\left[\frac{(t_0-t)^{\frac{8}{5}}}{r} - \frac{(t_0-t)^{\frac{8}{5}}}{r^4}\right]. \end{aligned}\right\} \quad \text{as} \quad (t_0 - t) \to \infty. \tag{15}$$

The problem now has a universal form. Since the incompressible theory is valid when liquid velocities are small compared with that of sound in the liquid, one way of attacking this compressible problem is by way of a perturbation theory of the incompressible solution. This approach is complicated by the fact that to take account of non-linear effects, the expanded solution of the governing equations must be made uniformly valid in space. It has been used by both Proudman (unpublished) and Brooke Benjamin (1958). Since this method is a perturbation one on the incompressible theory, there is some uncertainty about the value of any of its predictions concerning the final high-speed flow in which sonic and supersonic velocities occur.

† This treatment of the boundary conditions is due to Dr Ian Proudman.

3. The numerical integration of the governing equations

To investigate the flow as $R \to 0$, a numerical integration of equations (13) and (14) for u and c was carried out. These equations can be written in the characteristic form

$$\left(\frac{\partial}{\partial t} + (u \pm c)\frac{\partial}{\partial r}\right)\left(u \pm \frac{2c}{(\gamma - 1)}\right) = \mp \frac{2uc}{r}. \tag{16}$$

Equations (16) were integrated for the case $\gamma = 7$ using a form of the method of characteristics due to Hartree (1958, pp. 260–3). In this method the integration of the whole flow field is advanced successively by prescribed steps in time, and the characteristics are not explicitly determined. As starting values formulae (15) were taken at the instant when $\dot{R} = -0{\cdot}1$ and at each step u and c were evaluated at a fixed set of values of r/R ranging from 1 at the cavity to just over 10. The outer limit was so chosen that at each step forward in the integration,

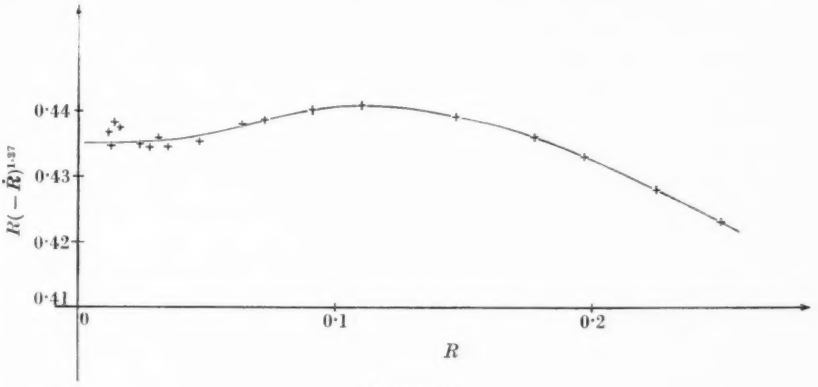

FIGURE 1

the solution was advanced only to points that lay within the domain of dependence of the solution already determined. In the most accurate calculations a grid of 109 such points was used, and the results were checked by carrying out a similar integration on an 82-point grid. The 109-point calculations were taken up to the stage at which $\dot{R} = -17{\cdot}65$ and showed two important features by this time:

(1) The velocity $(-\dot{R})$ appears to be increasing in such a way that

$$R(-\dot{R})^{\tau} \to \text{constant} \quad \text{as} \quad R \to 0,$$

where τ is some constant. The $\log R - \log(-\dot{R})$ curve is approximately straight for $-\dot{R} > 3$, and the estimated value of τ is 1·27. More sensitive evidence for this estimate is given in figure 1 where $R(-\dot{R})^{1\cdot27}$ is plotted as a function of R.

(2) For each fixed value of r/R both $-u \to \infty$ and $c \to \infty$ as $R \to 0$, and in such a way that $u/\dot{R}$ and $c^2/\dot{R}^2$ become functions of r/R only.

These results were confirmed by calculations on the coarser grid up to $\dot{R} = -10{\cdot}6$, the estimate for τ in this case being 1·28. The agreement between

these two sets of results, and the agreement between both of them and the asymptotic theory developed below, indicate that numerical errors in the overall calculation were probably not more than one or two percent at most.

4. The flow as $R \to 0$

4.1. *The nature of the solution as* $R \to 0$

We saw in the last section that the numerical solution suggests that the flow in the neighbourhood of the collapse point is of the form

$$u = \dot{R}f(r/R), \quad c^2 = \dot{R}^2 g(r/R). \tag{17}$$

There are other reasons for supposing that the flow in this region should be of the above form. When the cavity is very small, any length scale for the flow in its neighbourhood which can be derived from the boundary conditions will become orders of magnitude too large to be relevant as $R \to 0$. Thus the only suitable length scale for the flow is the cavity radius R. Similarly, fluid velocities become very much larger than any velocity scale provided by the boundary conditions, and we can look to the velocity of the cavity wall $\dot{R}$ to provide a velocity scale for the flow. This velocity $\dot{R}$ also provides a scale for the velocity of sound c which tends to infinity for finite r/R everywhere except at the cavity wall. These dimensional arguments therefore also suggest that the asymptotic form of the flow in the neighbourhood of the collapse point is of the form (17).

When the forms (17) are substituted into the governing equations (13) and (14), the resulting equations involve functions of r/R only except for terms with the factor $R\ddot{R}/\dot{R}^2$. If we put $R\ddot{R}/\dot{R}^2 = \text{const.} = 1 - n^{-1}$ say, then on integration we get $R = A(-t)^n$, where A is a constant and $t = 0$ is the instant of collapse. (The exponential solution for R corresponding to infinite n cannot represent a collapse in which $R = 0$ at some finite time.) A power law of this sort has already been suggested by the numerical results. The index n has yet to be determined precisely, though we know that $0 < n < 1$ since $R \to 0$ and $\dot{R} \to -\infty$ as $(-t) \to 0$.

The aim now is to determine the power n and the functions f and g. First, let us consider the boundary conditions on these functions. The condition $u = \dot{R}$ when $r = R$ requires $f(1) = 1$. The condition $c = 1$ when $r = R$ cannot be satisfied exactly when c^2 has the form given by (17). The approximation $c^2 \gg 1$ is implicit in the dimensional argument given above and the similarity theory can be valid only when this approximation holds. It is never true actually at the cavity, but it is true for values of r/R arbitrarily close to unity as $R \to 0$. The boundary condition to be satisfied by c^2 at the cavity should therefore be taken as $c^2 = 0$ to within the degree of accuracy of the theory, and so $g(1) = 0$. The solution we are seeking therefore, which is only an asymptotically exact solution of our equations and boundary conditions, is the exact solution for a fluid obeying an adiabatic law of the more familiar perfect gas form $p \propto \rho^\gamma$ advancing into a vacuum. When $c^2 \gg 1$, $p' \gg B$, so that the equation of state (5) becomes of this form.

If we revert to unscaled variables, we see that the flow does not now depend on the scales c_0 and E/ρ_0 separately, but only on the combination $(c_0)^{\frac{1}{3}(5n-2)}(E/\rho_0)^{\frac{1}{3}(1-n)}$ which occurs in the R'–t' relation for the cavity wall.

In the theory that follows we shall discuss only the case $\gamma = 7$ for which the numerical work was carried out. A similar investigation could be carried out for some other value of γ greater than unity, should another value be chosen to fit the thermodynamic properties of water or some other fluid. It is necessary though that the equation of state of the fluid should be of the form (5) for a theory of this sort to apply.

4.2. *The similarity solution equations*

At $t = 0$, r/R becomes infinite for $r > 0$. We shall later be interested in the region $t \geqslant 0$ as well as $t < 0$, so that it is more convenient to work in terms of the similarity variable ξ defined by

$$\xi = -\left(\frac{R}{r}\right)^{1/n} = \frac{\alpha t}{r^{1/n}}, \quad \alpha = A^{1/n}. \tag{18}$$

A variable of this type has been used by Butler (1954) for the case of a spherical shock wave converging on a point. It is easily seen that $R^{(1/n)-1}\dot{R} = -n\alpha$, and we now look for a similarity solution of the form

$$u = -n\alpha r^{1-(1/n)}F(\xi), \quad c^2 = n^2\alpha^2 r^{2-(2/n)}G(\xi). \tag{19}$$

Substitution of (19) in the governing equations (13) and (14) gives two ordinary differential equations

$$6(1+\xi F)F' + \xi G' + 2(1-n)(3F^2+G) = 0, \tag{20}$$

$$6\xi GF' + (1+\xi F)G' + 4(2-5n)FG = 0. \tag{21}$$

Dashes here denote differentiation with respect to ξ.

The problem of determining the flow for $t \leqslant 0$ now requires a solution of (20) and (21) for F and G in the range $-1 \leqslant \xi \leqslant 0$. The boundary conditions at the cavity are now $F(-1) = 1$ and $G(-1) = 0$. A straightforward investigation shows that there exist unique regular expansions for F and G about $\xi = -1$ subject to these conditions, which are

$$\left.\begin{aligned} F &= 1 + \frac{(9-20n)}{7}(\xi+1) + O[(\xi+1)^2], \\ G &= 6(1-n)(\xi+1) + O[(\xi+1)^2]. \end{aligned}\right\} \tag{22}$$

Apart from a solution with $G = 0$ everywhere, this regular solution is the only one which is bounded at $\xi = -1$. Consider now the outer boundary conditions to be applied to our similarity solution. When the complete flow is considered, it is necessary that $u \to 0$ and $c \to 1$ as $r \to \infty$. The similarity solution, however, is valid only when $c^2 \gg 1$ and so cannot hold for indefinitely large r. In some region where the approximation $c^2 \gg 1$ breaks down, it must be matched to some solution of the flow equations for which u and c remain finite as $(-t) \to 0$. The similarity variable $\xi = 0$ for $t = 0$ and $r > 0$. The forms (19) show that

$$u \propto (-t)^{n-1}(-\xi)^{1-n}F(\xi), \quad c^2 \propto (-t)^{2n-2}(-\xi)^{2-2n}G(\xi), \tag{23}$$

and so it is necessary that both $(-\xi)^{1-n}F(\xi)$ and $(-\xi)^{2-2n}G(\xi)$ are zero at $\xi = 0$ for a region in which u and c remain finite as $(-t) \to 0$ to exist.

The integration of (20) and (21) in the range $-1 \leqslant \xi \leqslant 0$ meets with difficulties. These equations may be re-arranged in the form

$$3[(1+\xi F)^2 - G\xi^2]F' = 2(2-5n)\xi FG - (1-n)(1+\xi F)(3F^2+G), \quad (24)$$

$$[(1+\xi F)^2 - G\xi^2]G' = 2(1-n)(3F^2+G)\xi G - 4(2-5n)(1+\xi F)FG, \quad (25)$$

which shows that they have singular points at the roots of $(1+\xi F)^2 = G\xi^2$, and also at $\xi = \pm\infty$. Now the expression $(1+\xi F)^2 - G\xi^2$ vanishes at the cavity, and it is a simple matter to see that it must vanish again in the physically relevant range $-1 \leqslant \xi \leqslant 0$. The expansions (22) show that it becomes negative as ξ increases from -1, but its value is unity at $\xi = 0$, since we have seen that both ξF and $\xi^2 G$ are zero there. It will later transpire that $(1+\xi F)^2 - \xi^2 G$ in fact vanishes only once in the range $-1 < \xi \leqslant 0$, at $\xi = \xi_0$ say.

We shall next show that both F and G must be regular functions of ξ at $\xi = \xi_0$, and hence everywhere in $-1 \leqslant \xi \leqslant 0$, for a solution of our problem. It follows from the definitions of ξ, F and G that, if $(1+\xi F)^2 = \xi^2 G$ for a particular value $\xi = \xi^*$, then $dr/dt = u \pm c$ on the curve $\xi = \xi^*$ in the r–t plane. Such a curve would therefore be a characteristic through O, and so the singular point ξ_0 corresponds to the incoming characteristic through O in the r–t plane. The singular point $\xi = -1$ is a consequence of the fact that $c = 0$ and $dr/dt = u$ at the cavity (figure 2). If F and G are not regular at $\xi = \xi_0$, their irregularities are propagated along the incoming characteristic through O. Now it is well known that discontinuities in the derivatives of any order of u and c propagate along characteristics, and either exist in the flow from the start or never occur in it except possibly as the result of some external agency. There is no reason, however, for there to be any such discontinuities in the flow when the similarity solution becomes valid.

The remainder of § 4 is concerned with the determination of F and G. Once n is given, the solutions of (20) and (21) are completely determined by the boundary conditions at $\xi = -1$, and in general this solution is not regular at $\xi = \xi_0$. However, n is still a free parameter and we shall show that it is possible to choose n so that F and G are regular in $-1 \leqslant \xi \leqslant 0$. The value of the power n is dependent on γ and so its value only for the case $\gamma = 7$ is calculated in this paper.

This method of determining a power-law parameter in a similarity solution by regularity considerations was first used by Guderley (1942) in his treatment of a spherical shock converging on a point, and the work in the present paper is similar to his work and that of Butler (1954).

4.3. *A transformation of the similarity solution equations*

The solutions of (20) and (21) are best investigated by means of a change of variables. New variables are defined by the relations

$$X = \log(-\xi), \quad Y = -\xi F, \quad Z = \xi^2 G. \quad (26)$$

Equations involving X, Y and Z only are obtained when these relations are substituted in (20) and (21), and can be arranged in the form

$$dX : dY : dZ = (Y-1)^2 - Z : [Y(Y-1)(nY-1) - \tfrac{1}{3}Z(9nY+n-1)] : 2Z[-nZ+7nY^2+2Y(1-5n)+1]. \quad (27)$$

The ratios of the second to the third terms give a first-order differential equation involving Y and Z only, and it is this equation that we shall seek to integrate. This integration must be carried out numerically as no analytical integral is known for general values of n. The problem of integrating (20) and (21) as already outlined can be reduced to solving a corresponding problem in the Y–Z plane. The boundary conditions $F = 1$, $G = 0$ at the cavity wall $\xi = -1$ correspond to the point $C(1, 0)$ in the Y–Z plane. This point C is a saddle-point singularity

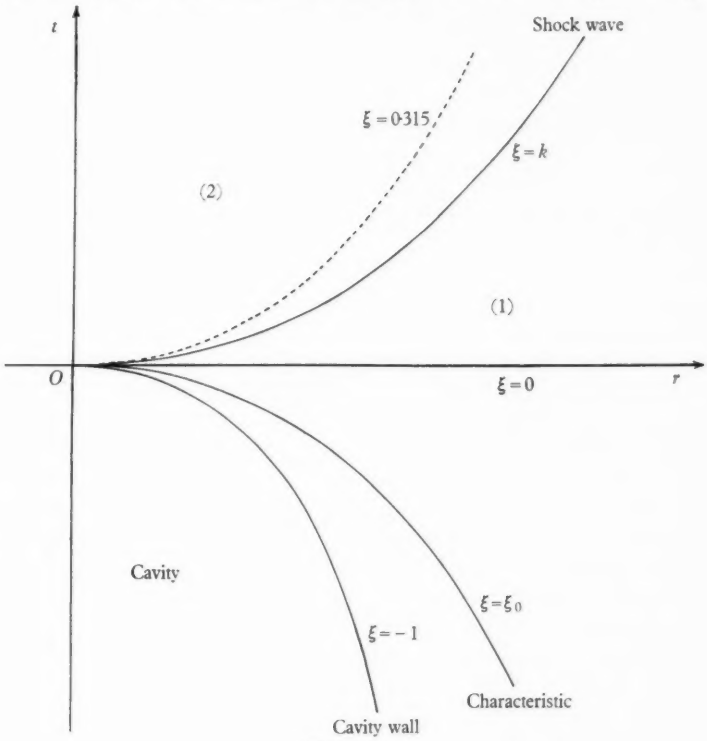

FIGURE 2

of the Y–Z equation, the two integral curves passing through it being $Z = 0$ and a solution tangent to the line $21(1-n)(Y-1) = (1-10n)Z$. This second integral curve in the Y–Z plane corresponds to the regular expansion (22) about $\xi = -1$. The origin O in the Y–Z plane is a nodal singular point. A single integral curve enters it along the line $3Y = (1-n)Z$, and all the other integral curves through it touch the Y-axis, which is itself an integral curve. Equation (27) shows that $dX : dZ = 1 : 2Z$ near the origin to the first order of small quantities, and so $X \to -\infty$ as $Z \to 0$. The origin therefore represents the r-axis ($\xi = 0$) in the physical plane. It is not a physically relevant singularity since it is not a singular point of (20) and (21), but only of the Y–Z relation. In the Y–Z plane, the integral curve that we require must therefore leave C along a known path and go to O.

To discuss the paths of the integral curves in the Y–Z plane, it is necessary to know some of the basic properties of integrals of (27). It is evident from (27) that $dZ = 0$ on the line $Z = 0$, which is an integral curve, and on the parabola

$$nZ = 7nY^2 + 2(1-5n)\,Y + 1. \tag{28}$$

The curve on which $dY = 0$ is the cubic

$$Z(9nY + n - 1) = 3Y(Y-1)(nY-1). \tag{29}$$

Singular points of the $Y - Z$ differential equation arise when both the second and third terms of the right-hand side of (27) vanish. These points are therefore the common points of the curves listed above, and neither dY nor dZ need be zero at them. There are six such points: the origin O, the points

$$A(1/n, 0), \quad B(1/10n,\ 27/100n^2), \quad C(1,\ 0),$$

and the two points of the parabola $Z = (Y-1)^2$ given by the roots of

$$6nY^2 + 2(1-4n)\,Y + (1-n) = 0. \tag{30}$$

These will be denoted, when they exist, by D and E, where E is given by the larger root. All the singular points except A for the special case $n = 0{\cdot}5552$, together with the integral curve from C in this case, are shown in figure 5.

The parabola $Z = (Y-1)^2$ is an important curve in the Y–Z plane since it corresponds to the curve $(1+\xi F)^2 = G\xi^2$ at which (20) and (21) are singular. We see from (27) that $dX/dY = dX/dZ = 0$ at a point of $Z = (Y-1)^2$ other than C, D and E. It follows that $d\xi/dF = d\xi/dG = 0$ and so ξ attains a turning value at such a point. This means that F and G are not single-valued functions of ξ for an integral curve that passes through such a point in the Y–Z plane, and so such an integral curve cannot be physically relevant. Another necessary property of the integral curve that we are seeking in the Y–Z plane is now apparent. It clearly must cross $Z = (Y-1)^2$ in its path from C to O, and the point of intersection corresponds to the characteristic of inward propagation $\xi = \xi_0$ through the origin O in the r–t plane. The single-valuedness condition requires that it crosses only at D or E.

Equation (30) shows that D and E do not exist if $7 + 3\sqrt{3} > 22n > 7 - 3\sqrt{3}$. The case $22n \leqslant 7 - 3\sqrt{3}$ corresponds to a collapse that is more rapid than that predicted by the incompressible theory when $n = 0{\cdot}4$. It will be shown in § 6 below that energy considerations require $n > 0{\cdot}4$ and so only the case

$$22n \geqslant 7 + 3\sqrt{3} \quad (n \geqslant 0{\cdot}55437)$$

is of interest. The points D and E coincide for $22n = 7 + 3\sqrt{3}$ and form a singular point which is the confluence of a saddle-point and a node. They separate as n increases from this value, E becoming a node and D a saddle-point. For some value of n in the neighbourhood of $0{\cdot}56$, E becomes a spiral point and remains so as it moves down the parabola $Z = (Y-1)^2$, as n increases, until it coincides with C for $n = 1$. For the present problem it is only necessary to discuss E, since it is found that the integral curve emanating from C always goes to E when it exists. We therefore seek an integral curve from C which crosses $Z = (Y-1)^2$ at

E only and goes to O. A further condition is that this curve should be such that Y is a regular function of Z at E. This is necessary since F and G are both regular functions of ξ at ξ_0 ($\xi_0 \neq 0$).

The next step in the argument therefore is to investigate the regularity of solutions of the Y–Z equation at E. Let us suppose that $Y = Y_0$ and $Z = Z_0$ at E, and define $y = Y - Y_0$, $z = Z - Z_0$. The Y–Z equation then becomes

$$\frac{dy}{dz} = \frac{a_{10}z + a_{01}y + \text{higher-order terms}}{b_{10}z + b_{01}y + \text{higher-order terms}}. \tag{31}$$

The a's and b's will be constants involving n, expressions for which can be found straightforwardly from (27). For the integral curve to be regular at E therefore, we require a regular expansion $y = y(z)$ about $y = 0$, $z = 0$. Writing $y = vz$ we have

$$z\frac{dv}{dz} = \frac{a_{10} + a_{01}v - b_{10}v - b_{01}v^2 + z\psi_1(v,z)}{b_{10} + b_{01}v + z\psi_2(v,z)}, \tag{32}$$

where ψ_1 and ψ_2 are polynomial expressions. Both sides must vanish for $z = 0$ so that v ($z = 0$) is a root of

$$a_{10} + (a_{01} - b_{10})v - b_{01}v^2 = 0. \tag{33}$$

Suppose v_1 is a root of this equation, then putting $v = V + v_1$, and expanding (32) gives

$$z\frac{dV}{dz} - A_{01}V = A_{10}z + A_{20}z^2 + A_{11}Vz + A_{02}V^2 + \text{higher-order terms}, \tag{34}$$

where

$$A_{01} = \frac{a_{01} - b_{10} - 2b_{01}v_1}{b_{10} + b_{01}v_1}, \tag{35}$$

provided $b_{10} + b_{01}v_1 \neq 0$. The A's too will be functions of n. Equation (34) is of the well-known Briot–Bouquet form (Goursat 1917, pp. 173–8) and its properties are as follows. It has a unique regular integral about $z = 0$, $v = 0$, if A_{01} is not a positive integer. If A_{01} is a positive integer it will in general have no regular integrals unless some particular additional relation exists between certain of the A's. This additional relation will depend on the particular integral value of A_{01}, and, if it is satisfied, there will be an infinite number of regular integrals.

Equation (33) is equivalent to

$$(a_{10}v^{-1} + a_{01})^2 - (a_{01} + b_{10})(a_{10}v^{-1} + a_{01}) + (a_{01}b_{10} - a_{10}b_{01}) = 0. \tag{36}$$

The conditions for E to be a node imply that both (33) and (36) have two real and distinct roots. It can be seen that the value of A_{01} corresponding to the root of (36) for $(a_{10}v^{-1} + a_{01})$ which is smaller in absolute magnitude is a positive integer if and only if the ratio of the roots is N or $1/N$ for some positive integer N. The value of A_{01} corresponding to the larger root is never a positive integer.

We are now in a position to discuss the integral curves in the y–z plane in the neighbourhood of the node E, which will be as shown in figure 3. There will be a curve EP which every curve except the single curve EQ will touch at E. Three possibilities as to the regularity of the functions $y = y(z)$ represented by these integral curves exist and are listed below.

(i) The general case is that in which n is such that the ratio of the roots of (36) is not equal to N or $1/N$. The roots then give rise to two distinct values of v_1, and hence to two regular integrals of the y–z relation. The curve EQ is the regular solution $y = y(z)$ arising from the value of v_1, given by the root of (36) which is larger in magnitude. The curve EP is similarly the regular solution arising from the other root, and the remaining solutions which touch EP at E are not regular at E.

(ii) The second case is that in which the ratio of the roots of (36) is N or $1/N$. The value of v_1 corresponding to the root of (36) which is smaller in magnitude now makes A_{01} a positive integer, but the additional relation between the A's

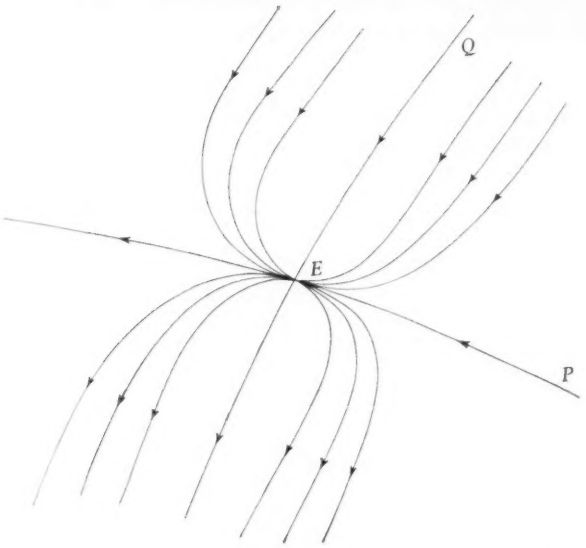

FIGURE 3

which is necessary to make all the integrals of (34) regular at E is not satisfied. The curve EQ thus represents a regular solution as before, but all the remaining solutions, including EP, are not regular at E.

(iii) There is finally the exceptional case when the additional relation mentioned in (ii) is satisfied. All the integral curves through E now represent regular functions $y = y(z)$. Given N, this relation between the A's and consequently the condition on n which must be satisfied in this exceptional case could be determined. The fact that the ratio of the roots of (36) is N or $1/N$ imposes yet another condition on n, and so n would have to satisfy two different relations for this exceptional case to arise.

The discussion of the regularity of solutions at E is now complete, and we go on to consider the numerical integrations of the Y–Z equation for different values of n. We saw earlier that $22n \geqslant 7 + 3\sqrt{3}$. When equality occurs, D and E coincide and there is a single regular solution through this point which does not go through C. For slightly larger values of n, the course of the integral curve

from C is as in case (a) in figure 4. (The diagram is schematic only. The position of E varies with n and the three cases have been superimposed in the figure.) Several reasons can be given for rejecting curves of this type. The discussion given above shows that such an integral curve represents a regular solution $y = y(z)$ only in the exceptional case (iii). In the present problem there is an enumerable infinity of values of n and hence of positions of E for which the ratio of the roots of (36) is N or $1/N$ and the course of the integral curve is as in case (a). Since this infinity is enumerable, it is still unlikely that the exceptional case will

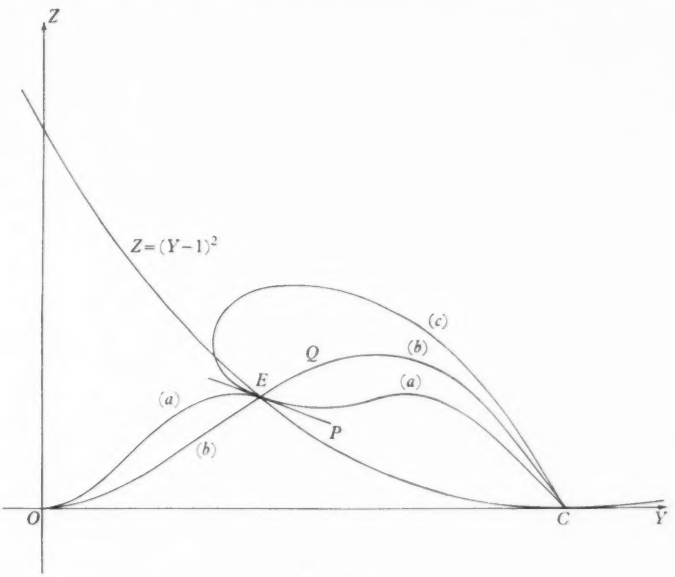

FIGURE 4

occur, but the possibility of it doing so exists. Again, if the exceptional case did arise, it would only be because of the particular value of γ chosen. The two conditions that n must satisfy for case (iii) to arise are really two relations between γ and n, and so, if both conditions were satisfied for one value of γ, they would not be satisfied for a neighbouring value of γ. The resulting special solution which depended on a special value of γ could hardly be expected to be physically relevant. A final reason for rejecting these curves is that when the graph of c^2 as a function of r at any given time derived from one of these curves is plotted, it has a point of inflexion between the cavity wall and the maximum value of c^2. The graphs obtained from the numerical integration of the partial differential equations do not have this feature.

When n attains the value 0·5552, the integral curve from C passes through E along the regular path QE and goes to O (case (b) in figure 4). This curve therefore represents a regular function $Y = Y(Z)$ and it can be seen from (27) that in this case $X = X(Z)$ is also regular. For this curve therefore $F(\xi)$ and $G(\xi)$ are regular for $-1 \leqslant \xi \leqslant 0$ and so we have a solution of our physical problem.

For larger values of n, the curves from C behave as in case (c) of figure 4, and so must be rejected since they cross $Z = (Y-1)^2$ at points other than D and E.

Once the Y–Z equation has been integrated, equation (27) can be integrated to give X, and so $F(\xi)$, $G(\xi)$, $f(r/R)$ and $g(r/R)$ can be calculated. Figure 5 shows the regular integral curve passing from C through E to O, and figure 6 shows the functions f and g.

The results obtained from the numerical integration of the partial differential equations fit in well with this similarity theory. The estimates obtained for n

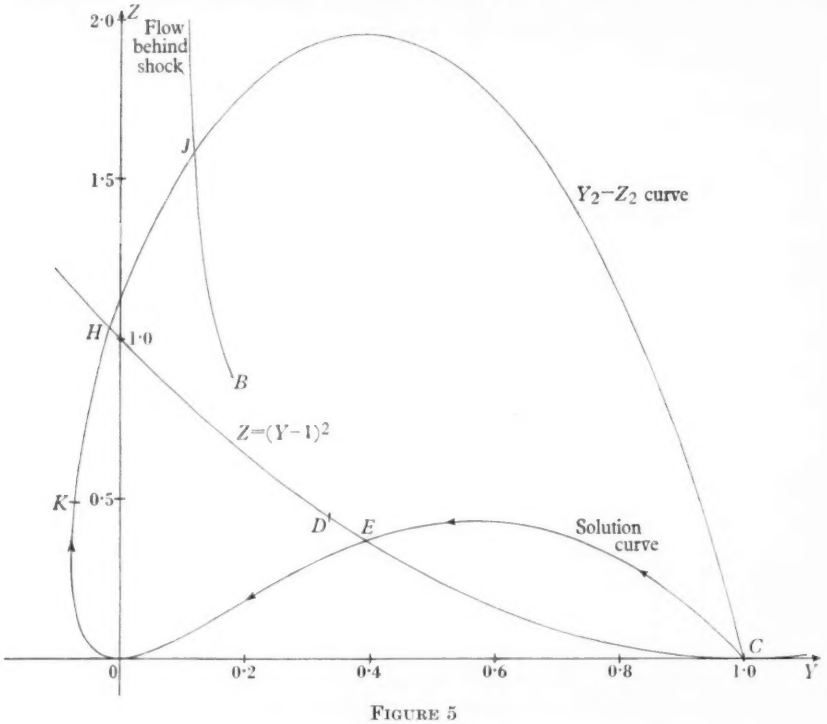

FIGURE 5

were 0·560 and 0·561 compared with the true value of 0·5552. By the time $-\dot{R} = 10$ was reached, $u/\dot{R}$ and $c^2/\dot{R}^2$ were well within 0·01 of their limiting forms f and g. When $(-\dot{R})$ increased still further, the values of $u/\dot{R}$ and $c^2/\dot{R}^2$ oscillated about these limiting values. This oscillation is probably a purely numerical effect due to using a finite difference approximation for the partial differential-equations.

5. The flow after the collapse

The cavity vanishes at $t = 0$, but the collapse similarity solution does not cease to be valid everywhere at this instant. The information that the cavity has collapsed takes a finite time to propagate outwards and only the flow actually at $r = 0$ is immediately affected. We should therefore expect, for $r > 0$, to be able

to continue the collapse solution valid for $t \leqslant 0$ into the region $t > 0$, that is from negative to positive values of ξ. In the last section we integrated equations (20) and (21) for F and G in the range $-1 \leqslant \xi \leqslant 0$, and since both F and G are finite at $\xi = 0$ and the equations are not singular there, the integration can be continued to positive values of ξ. When we continue the solution for $\xi > 0$, a singularity is reached at $\xi = 0{\cdot}315$ when once again $(1+\xi F)^2 = \xi^2 G$. This singularity, which corresponds to the outgoing characteristic through O (figure 2),

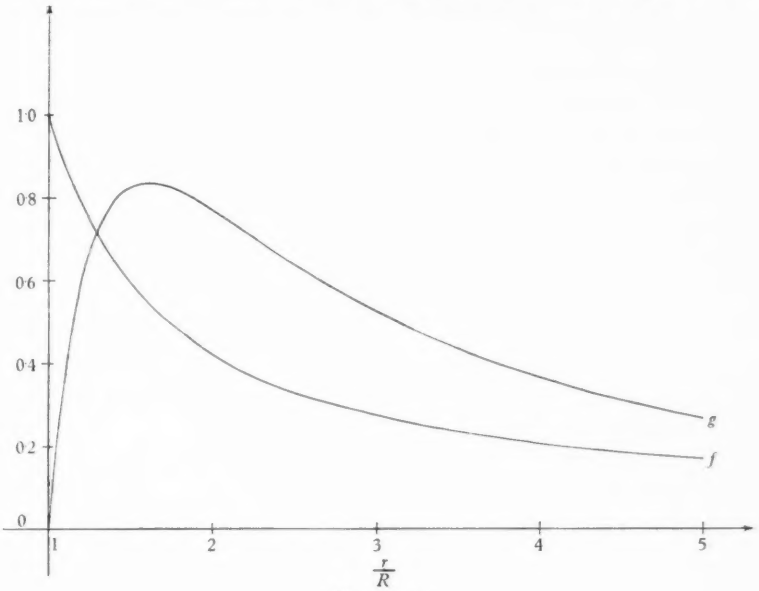

FIGURE 6

must be avoided and the only way this can be done is to have discontinuities in the values of F and G at some value k of ξ less than 0·315. Physically this means that a shock wave is formed at $r = 0$, $t = 0$ and propagates outwards along the path $kr^{1/n} = \alpha t$. Formally the integral curve in the Y–Z plane passes through the origin and continues in the region $Y < 0$, $Z > 0$ until it cuts the parabola $Z = (Y-1)^2$ at H (figure 5). This integral cannot be physically relevant beyond H since F and G must be single-valued functions of ξ. Since a shock wave travels out from O in the r–t plane, there will be no characteristic of outward propagation emanating from O and so $(1+\xi F)^2 - \xi^2 G$ changes sign discontinuously at $\xi = k$. Correspondingly the integral curve in the Y–Z plane jumps discontinuously across the parabola $Z = (Y-1)^2$.

When, as in the present problem, a single p–ρ relation holds throughout the flow, the two mechanical conditions at the shock, those of conservation of mass and momentum, are sufficient to determine the shock motion (Courant & Friedrichs 1948, p. 132). Energy is of course still conserved at the shock, and the energy conservation relation relates the values of $\mathscr{E}_0(S)$, the entropy part of the internal energy $\mathscr{E}$ in (8), on the two sides of the shock. This shock relation can

therefore be used to calculate the energy transformed irreversibly into heat by the shock.

If the suffix 1 refers to the flow in front of the shock and 2 to that behind it, the mechanical shock relations can be written in the form

$$c_1^{2/(\gamma-1)}(u_1-v) = c_2^{2/(\gamma-1)}(u_2-v), \tag{37}$$

$$c_1^{2/(\gamma-1)}[c_1^2+\gamma(u_1-v)^2] = c_2^{2/(\gamma-1)}[c_2^2+\gamma(u_2-v)^2], \tag{38}$$

where v is the velocity of the shock. These shock conditions must be satisfied on $\xi = k$.

We have now to determine the form of the flow in the region $\xi \geqslant k$ behind the shock wave. This region is of zero size at $t = 0$ and, for the same reasons as were given in § 4.1 for the flow near the cavity to be of a similarity form, we could expect a similarity solution to apply here also. The radial distance of the shock from O provides a length scale for this region of the flow, and the shock velocity provides a velocity scale. It is therefore natural to look for a similarity solution of the same form as before using, for convenience, a different form of the similarity variable

$$u = nAt^{n-1}\lambda(\eta), \quad c^2 = n^2A^2t^{2n-2}\mu(\eta), \quad \eta = \frac{r}{At^n} = \xi^{-n}. \tag{39}$$

Such a solution is of the right form for satisfying the shock conditions at $\xi = k$, and it will be shown below that a unique solution of this type satisfies all the required conditions.

Substituting the expressions (39) in the flow equations (13) and (14), we obtain two ordinary differential equations

$$6(n-1)\lambda + 6n(\lambda-\eta)\lambda' + n\mu' = 0, \tag{40}$$

$$2(n-1)\mu + n(\lambda-\eta)\mu' + 6n\mu\left\{\lambda' + \frac{2\lambda}{\eta}\right\} = 0. \tag{41}$$

(Dashes denote differentiation with respect to η.) Corresponding to the singular points of equations (20) and (21) for the collapse, these equations have singular points when $(\lambda-\eta)^2 = \mu$ and when $\eta = 0$. The first case is that of curves $\eta =$ constant on which $dr/dt = (u \pm c)$, but we have already seen that there is no characteristic through O in the region behind the shock.

Two possibilities still remain for the flow behind the shock while the similarity solution is valid. The first is that the cavity remains closed for $t > 0$ so that at $\eta = 0$, $\lambda = 0$ and $\mu =$ const. $= \beta$ (say). The second is that the cavity re-opens. In this latter case, there will again be a free surface on which $c = 0$. (The approximation $c^2 \gg 1$ still applies for the same reasons as before.) The form of the similarity solution (39) restricts the re-opening cavity path to be of the form $\eta =$ const. $= \delta$ (say). The similarity solution will in this case be subject to boundary conditions $\eta = \delta$, $\lambda = \delta$, $\mu = 0$. Both sets of boundary conditions represent singular points of (40) and (41), though in both cases unique regular series solutions about the singular points exist. The constants β and δ are as yet unspecified so that we have two one-parameter solutions which could represent the flow behind the shock.

Once again it is more convenient to work in the Y–Z plane, and we have the relations

$$Y = \frac{ut}{nr} = -\xi F = \frac{\lambda}{\eta}, \quad Z = \frac{c^2t^2}{n^2r^2} = \xi^2 G = \frac{\mu}{\eta^2}. \tag{42}$$

The two one-parameter solutions define unique curves in the Y–Z plane since if the values (λ, μ, η) satisfy (40) and (41), so too do $(\kappa\lambda, \kappa^2\mu, \kappa\eta)$ for any constant κ. The integral curve in the Y–Z plane in the first case is a curve from the point $Y = (1-n)/9n$, $Z = \infty$ to the singular point B, a node (figure 5). The similarity

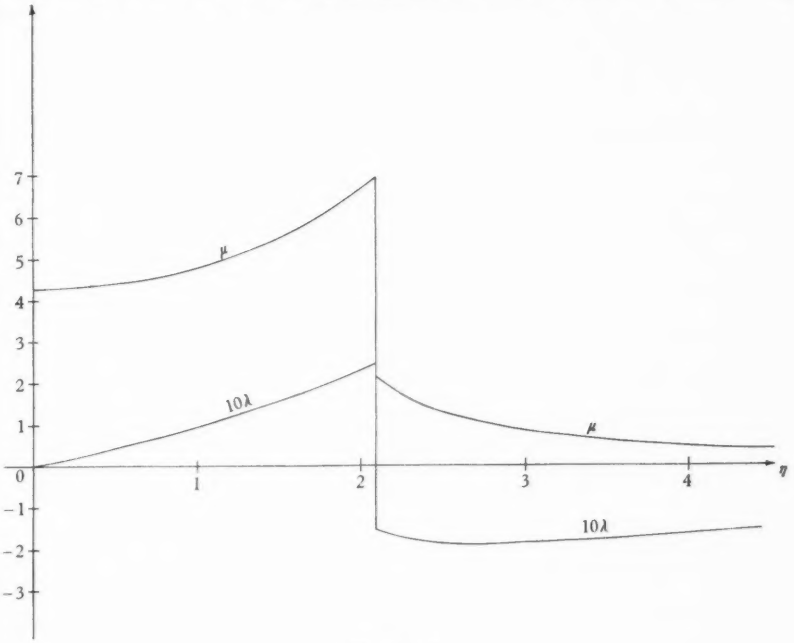

FIGURE 7

variable η is infinite at this point, and so ξ is zero and λ and μ are both infinite there. In the second case the boundary conditions $\eta = \delta, \lambda = \delta, \mu = 0$ correspond to C, and the integral curve in the Y–Z plane is that already determined for the flow before collapse. We are now interested in it only on the one side of the parabola $Z = (Y-1)^2$.

In the Y–Z plane the shock conditions (37) and (38) become

$$Z_1^{\frac{1}{2}}(Y_1 - 1) = Z_2^{\frac{1}{2}}(Y_2 - 1), \tag{43}$$

$$Z_1^{\frac{1}{2}}[Z_1 + 7(Y_1-1)^2] = Z_2^{\frac{1}{2}}[Z_2 + 7(Y_2-1)^2]. \tag{44}$$

For each point of the section OH of the integral curve in the Y–Z plane, we can calculate Y_2 and Z_2, the values of Y and Z that would pertain to the flow just behind a shock, should one occur at that point. The curve of possible values of Y_2 and Z_2 leaves C along the line $Z = 7(1-Y)$, and then bends round to meet $Z = (Y-1)^2$ at H (figure 5). The point C would arise from a shock at O, and H

from a shock at itself. In its path the $Y_2 - Z_2$ curve cuts the integral curve for the flow behind the shock with the cavity remaining closed at a single point J, and does not meet the other integral curve CE other than at C. The intersection at C does not give rise to a physically possible flow as it requires that the line $t = 0$ in the r–t plane is the path along which the cavity re-opens. The intersection at J does give rise to a physically possible flow in which the cavity remains closed for $t > 0$, and the matching of the two similarity solutions is now straightforward. We know the point K of the OH-section of the integral curve in the Y–Z plane which gives rise to J and the values of ξ, F and G at it. These values determine those of η, λ and μ at J and therefore their values throughout the region behind the shock. The latter are shown in figure 7.

6. Some properties of the similarity solution

We now consider some general aspects of the similarity solution. We have derived the similarity solution to describe the flow in the neighbourhood of the collapse point where flow velocities and the local velocity of sound are large. Let us examine the form of the similarity solution at $t = 0$. When $t = 0$, $\xi = 0$ for $r > 0$ and

$$u = -n\alpha r^{1-(1/n)}F(0), \quad c^2 = n^2\alpha^2 r^{2-(2/n)}G(0), \quad \rho = [n^2\alpha^2 r^{2-(2/n)}G(0)]^{1/(\gamma-1)}. \tag{45}$$

Consider now the amount of energy associated with the similarity solution. The internal energy per unit mass of the water is given by (8), and since $c^2 \gg 1$ when the similarity solution applies, then to the same degree of approximation

$$\mathscr{E} = \frac{c^2}{\gamma(\gamma-1)}. \tag{46}$$

The total energy contained within a sphere of radius r at $t = 0$ is

$$\int_{r=0}^{r} \rho[\mathscr{E} + \tfrac{1}{2}u^2]\, 4\pi r^2 dr. \tag{47}$$

The condition that this integral does not diverge at $r = 0$, and therefore that there is not an infinite amount of energy associated with the similarity solution is

$$3n(\gamma-1) > 2\gamma(1-n). \tag{48}$$

This inequality can also be written as

$$n > \frac{2}{5-3\gamma^{-1}}, \tag{49}$$

which shows that $n > 0{\cdot}4$. This result substantiates the statement made in § 4.3 that, in the compressible case, the velocity of collapse must be of lesser order than that predicted by the incompressible theory. The inequality (49) is satisfied for $\gamma = 7$ and the corresponding value $0{\cdot}5552$ of n determined above.

In the present problem $F(0) = 0{\cdot}568$, $G(0) = 3{\cdot}859$ and the energy integral (47) can be evaluated as

$$0{\cdot}893\alpha^{\frac{7}{3}}r^{1{\cdot}13}. \tag{50}$$

The coefficient α is not determined by the similarity theory and so must be estimated from the numerical integration of the partial differential equations: the estimate obtained being $\alpha = 0{\cdot}93$. The total energy possessed by the whole flow is finite and equal to 1·005, as can be calculated from (15). Initially this is all in the form of kinetic energy. We saw earlier in § 1 that the incompressible theory predicted that all this energy would be concentrated at $r = 0$ at the instant of collapse. This singular energy distribution does not occur in the compressible solution which is therefore more realistic physically. The expression (50) shows that the energy contained within a sphere of radius r is an increasing function of r, but (50) is not valid for indefinitely large r since the total energy is finite. It is only valid in the region in which $c^2 \gg 1$ and the similarity solution applies. The form of c at $t = 0$ therefore enables us to estimate the size of this region, and the energy in it can then be calculated from (50). The table given below shows the amount of energy contained within the sphere in which c is greater than the given limiting value. It can be seen from this table that roughly 20 % of the energy of the flow is contained within the similarity solution region. The remainder of the energy of the flow lies outside this region at larger values

Limiting value of c	Pressure in kilobars at limiting value	Energy within sphere
10	643·2	0·030
8	381·0	0·041
6	193·3	0·062
4	73·2	0·109
3	35·9	0·164
2·5	22·4	0·211
2	12·1	0·290

of r, and its exact distribution cannot be discussed by the similarity theory. As is to be expected, the physical size of the region in which the similarity solution is valid is small. If we estimate the parameter E by taking p_0 as atmospheric pressure and R_0 as half a centimetre, then the radius of the region in which the similarity solution applies at $t = 0$ is about 0·01 cm. It seems likely that a substantial part of the remaining energy is contained in the region adjacent to the similarity solution region where there are pressures of the order of kilobars, so that a large amount of the energy is contained within a small region in which high liquid pressures occur. The ratio of the internal energy to the kinetic energy at any point in the similarity solution region at $t = 0$ is 0·57.

The question of the physical relevance of the similarity solution still remains. It has been shown to be the mathematical solution to the problem of the high-speed motion caused by the symmetrical collapse of an empty cavity. The predicted final velocity of the collapse is infinite even when liquid compressibility is taken into account, although this infinity occurs only at a single point in space and time. The infinite velocity occurs only at a single point in the incompressible solution, but infinite pressures occur for all r at $t = 0$ in this case. The similarity solution exhibits the slowing-down effect of compressibility on the flow and gives

a physically more realistic description of the formation and initial propagation of a pressure pulse from the collapse.

It was explained in § 1 that our model of a collapsing empty cavity was chosen for the purpose of studying the effect of compressibility in isolation and to this end, the effects of all the other mechanisms listed in that section were neglected. The effects will not of course all be negligible, and the effect of cavity contents for one will ultimately become important. As to the other mechanisms, if constant surface tension is assumed, the surface tension force at the cavity is still of a lesser order of magnitude as $R \to 0$ than pressure and inertia forces when compressibility is taken into account. The possible effect of viscosity on the compressible flow problem is more difficult to assess, since the flow is no longer homentropic when viscosity is taken into account, and since the coefficient of viscosity varies considerably with pressure and temperature. The other mechanism that has been mentioned is instability, but we do not as yet know whether the collapse of an empty cavity in a compressible liquid is stable or not. It is indeed possible that the collapse solution might be unstable while the flow after collapse with an expanding shock wave is stable, the total net result being a loss of energy relative to the spherically symmetric solution.

It is clear that there are many possible and reasonable objections to the empty cavity theory. However, if our empty cavity formulation is a sensible overall approximation to what happens in practice, and this is something that still remains to be seen, then the predictions that may be obtained from the empty cavity theory for some overall feature, such as the strength of the shock propagated from the collapse after it has travelled a considerable distance from the cavity, should be in reasonable agreement with practice. This shock wave is a property of the collapse which is amenable to observation and measurement, whereas a phase of the motion which occupies lengths of the order of tenths of a millimetre and times of the order of microseconds is not. As the empty cavity theory now stands, the flow in the neighbourhood of the collapse point has been determined, and the flow when velocities are small can be described by a small Mach number expansion. To advance the theory, it is necessary to develop correction terms to the similarity theory and then to match the expansion so derived to the small Mach-number expansion. The development of correction terms to the similarity theory meets with difficulties since, although expansions for u and c^2 in increasing powers of r with functions of ξ as coefficients can be made to satisfy the flow equations (13) and (14), it is found that each successive function of ξ has a singularity of increasing order at $\xi = -1$. Another possibility is a numerical integration of the governing equations covering all regions of the flow and not just concentrating on the flow near the cavity as did the numerical integration described in § 3. The similarity solution theory deals with the flow in the neighbourhood of $R = 0$ which is the only region of the flow for which numerical integration is not straightforward.

The author is very grateful to Dr I. Proudman for suggesting this problem, and to him and Dr T. Brooke Benjamin for many helpful and interesting discussions. He is also very grateful to the Director and Staff of the Cambridge Univer-

sity Mathematical Laboratory for the facilities of EDSAC II, on which all the numerical work was carried out. This numerical work was in part paid for by the Royal Naval Scientific Service. During the period in which this work was done, the author was a Research Student of the Department of Scientific and Industrial Research.

REFERENCES

BIRKHOFF, G. 1954 *Quart. J. Appl. Math.* **12**, 306.

BROOKE BENJAMIN, T. 1958 *Proc. 2nd Symposium on Naval Hydrodynamics, Washington.*

BUTLER, D. S. 1954 *A.R.D.E. report* 54/54.

COLE, R. H. 1948 *Underwater Explosions.* Princeton University Press.

COURANT, R. & FRIEDRICHS, K. O. 1948 *Supersonic Flow and Shock Waves.* Interscience.

GILMORE, F. R. 1952 *Cal. Tech. Hydromechanics Lab. Rep.* 26–4.

GOURSAT, E. 1917 *A Course in Mathematical Analysis*, Vol. II, part II. (English translation.) Ginn and Co.

GUDERLEY, G. 1942 *Luftfahrtforschung.* **19**, 302.

HARTREE, D. R. 1958 *Numerical Analysis*, 2nd ed. Oxford University Press.

KIRKWOOD, J. G. & BETHE, H. A. 1942 *O.S.R.D. Report*, no. 588.

PENNEY, W. G. & PIKE, H. M. M. 1950 *Rep. Progr. Phys.* **13**, 46.

LORD RAYLEIGH. 1917 *Phil. Mag.* **34**, 94.

RICE, N. H. & WALSH, J. M. 1957 *J. Chem. Phys.* **26**, 824.

ZWICK, S. A. & PLESSET, M. S. 1955 *J. Math. Phys.* **33**, 308.

Multiple shock compression using a piston of finite weight

By D. F. T. WINTER

Armament Research and Development Establishment, Fort Halstead, Sevenoaks, Kent

(Received 29 October 1959)

This paper describes a theory for a piston-operated compressor in which shock waves are used to heat the gas being compressed. Detailed calculations are given showing the use of such a compressor to heat air for use in a hypersonic wind tunnel. The effect of real gas properties on the compression process is included in this discussion.

1. Introduction

When air is used in a hypersonic wind tunnel, it is necessary to start with hot compressed air in order to obtain reasonable static conditions in the expanded flow. For a given maximum pressure, the air will be heated to the highest temperature if there is the maximum increase of entropy during compression.

It is well known that the passage of air through a strong shock wave produces a large entropy rise, and the discussion which follows considers a process in which air is heated by successive shock waves generated between the face of a moving piston and a fixed wall.

2. The piston-operated compressor

Let us consider a long tube filled with gas and closed at one end. At the other end there is a piston, separated by a diaphragm from a reservoir of high-pressure gas which may differ from the gas in the tube, as shown in figure 1. When the diaphragm is burst, the high-pressure gas drives the piston down the tube. A shock wave is formed in the gas ahead of the piston at some position determined

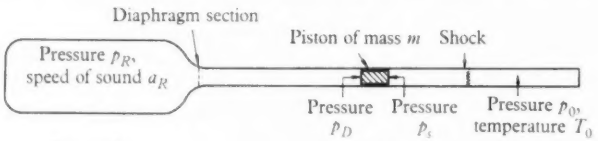

FIGURE 1. Schematic diagram of compressor.

by the initial piston acceleration. As the piston continues to gain speed, the shock wave will become stronger. When the shock reaches the end of the tube, it is reflected and moves back into the gas following it, and is then reflected again from the piston. A number of reflected shocks occur, and meanwhile the piston decelerates because of the pressure increase through each shock wave. The

deceleration causes expansion waves which tend to weaken the shock, and after several reflexions the shock wave will have degenerated to an isentropic wave. There is then a period during which all pressure differences are damped out, and finally the gas comes to rest with a uniform pressure throughout the system, but with the gas in the tube having been compressed and heated. Let us now consider each stage of the motion in detail. We shall assume that there are no friction or heat losses, and for §§ 2 and 3 we shall assume that the gases are perfect.

2.1. *Initial piston motion*

To determine the motion of the piston, the pressures on its front and rear faces must first be known. However, the pressure acting on the front face depends on the motion of the piston and on the compression waves generated by it. It is therefore impossible to obtain a closed solution for the motion when shock waves occur in the system. As a first approximation, the pressure on the front face may be obtained by using a method analogous to the tangent wedge approximation in steady supersonic flow. It is assumed that at any instant this pressure is equal to that which would act on a piston moving with constant velocity equal to the actual instantaneous velocity of the piston.

This pressure, p_s, may be calculated from the normal shock equations. For a normal standing shock wave, using standard notation,

$$\rho_1 v_1 = \rho_2 v_2 \tag{1}$$

$$\frac{\gamma}{\gamma-1}\frac{p_1}{\rho_1}+\frac{v_1^2}{2}=\frac{\gamma}{\gamma-1}\frac{p_2}{\rho_2}+\frac{v_2^2}{2}, \tag{2}$$

$$p_1+\rho_1 v_1^2 = p_2+\rho_2 v_2^2; \tag{3}$$

also

$$\frac{\gamma p_1}{\rho_1} = a_1^2. \tag{4}$$

By eliminating ρ_1, ρ_2 and v_1 and writing $u = v_1 - v_2$, $p_s = p_2$ and $p_0 = p_1$, $a_0 = a_1$, we obtain

$$p_s = p_0\left[1+\frac{\gamma_0}{2}\frac{u}{a_0}\{x+\sqrt{(4+x^2)}\}\right], \tag{5}$$

where $x = \frac{1}{2}(\gamma_0+1)(u/a_0)$, u is the piston velocity, and a_0, γ_0 and p_0 are quantities appertaining to the undisturbed gas in the tube.

To calculate the pressure driving the piston, it is assumed that there is steady subsonic flow from the reservoir into the tube, and an unsteady expansion between the diaphragm section and the piston. Sonic flow will be established at the diaphragm section when the pressure ratio across it becomes greater than 2. The equations governing this flow are then

$$\frac{a_R^2}{\gamma_R+1} = \frac{a_*^2}{2}, \tag{6}$$

$$\frac{a_*}{2}\left(\frac{\gamma_R+1}{\gamma_R-1}\right) = \frac{u}{2}+\frac{a_D}{\gamma_R-1}, \tag{7}$$

$$\frac{p_D}{p_R} = \left(\frac{a_D}{a_R}\right)^{2\gamma_R/(\gamma_R-1)}, \tag{8}$$

which, when combined, give

$$p_D = p_R \left\{ \sqrt{\left(\frac{\gamma_R + 1}{2}\right)} - \frac{\gamma_R - 1}{2} \frac{u}{a_R} \right\}^{2\gamma_R/(\gamma_R - 1)}, \tag{9}$$

where γ_R, a_R and p_R denote quantities in the reservoir vessel and a_* is the speed of sound at the diaphragm section.

We now introduce the non-dimensional variables

$$\bar{s} = \frac{p_R A s}{m a_R^2}, \tag{10}$$

$$\bar{t} = \frac{p_R A t}{m a_R}, \tag{11}$$

where A is the cross-sectional area of the tube, m is the piston mass, and s is the distance which the piston has moved in time t. Then the equation for the piston motion is

$$(p_D - p_s) A = m \frac{d^2 s}{dt^2} = p_R A \frac{d^2 \bar{s}}{d\bar{t}^2}, \tag{12}$$

or

$$\frac{p_D - p_s}{p_R} = \frac{d^2 \bar{s}}{d\bar{t}^2}, \tag{13}$$

and the piston motion may be calculated in terms of the four parameters p_R/p_0, a_R/a_0, γ_R and γ_0 only.

2.2. *Shock formation*

Once the piston motion has been calculated, the position of the shock is determined graphically using the method of characteristics. The strength of the shock at different positions is calculated from the pressure increments across the compression characteristics. Figure 2 shows a typical example of the calculation. It will be seen that the rate at which the shock wave strengthens (as given by the rate of change of the slope of the shock curve, for example) is not uniform, and that the shock strength tends to a steady value as $\bar{s}$ becomes large.

As a second approximation it would be possible to calculate the pressures at the piston from the characteristics network described above. This has been done for one example, but the pressures were found to differ by only a few per cent from those calculated using the first approximation outlined in § 2.1. The shock strength is determined mainly by the initial piston motion, when the pressure on the front of the piston is small, and so it seems unnecessary to use the second approximation.

The greatest shock strength for a given length of tube will result from a light piston and a high driving pressure as may be seen from equation (12). A high driving pressure is attained by using a high pressure in the reservoir and a gas of low density (see equation (9)). For practical purposes, however, the piston must be strong enough to withstand the high pressures generated during compression and so cannot be made very light. A design criterion based on the parameters discussed in § 2.1 may be obtained by requiring that the shock wave should reach a certain percentage of its asymptotic strength before it reaches the end of the

tube. (The strength of a shock wave is defined for this purpose as the ratio of pressures across it.) In practical cases this strength is about 90 % of its asymptotic value.

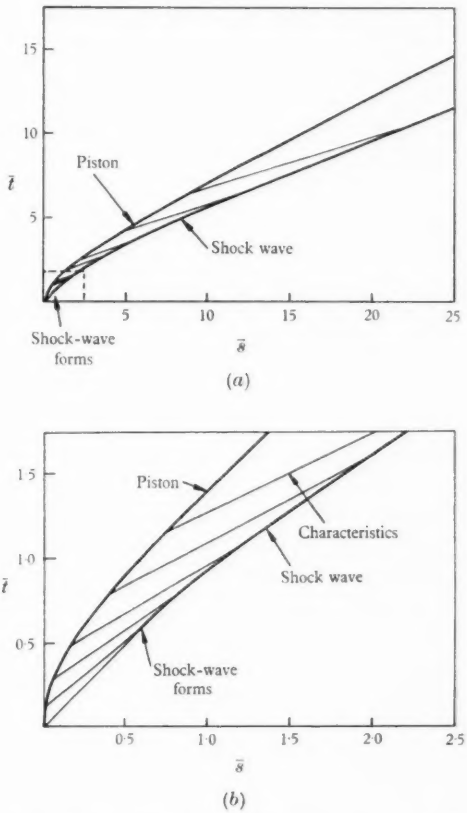

FIGURE 2. (*a*) Illustration of shock formation. (*b*) Details of starting process. $p_R/p_0 = 120$, $a_R/a_0 = 1$, $\gamma_R = \gamma_0 = 1{\cdot}4$.

2.3. *Shock reflexions and deceleration of the piston*

When the shock wave reaches the end of the tube, it will be reflected and move back into the gas which was following it (see figure 3). When it reaches the face of the piston it will again be reflected and the shock wave will return to the closed end. Because of the shock reflexion at the piston face, the pressure there is increased from p_s to p_3. An expression for this has been given by Glass (1958, p. 93) and when written in the present notation is

$$p_3 = p_s r \left\{ \frac{(3\gamma-1)r-(\gamma-1)}{(\gamma-1)r+(\gamma+1)} \right\}, \tag{14}$$

where r is the pressure ratio across the shock wave reaching the piston.

The increased pressure on the front of the piston now causes it to decelerate. Expansion waves are propagated forward, and those which catch up the shock before it reaches the end of the tube will weaken it. At the same time compression waves are being formed in the driver gas. The pressure at the two faces of the

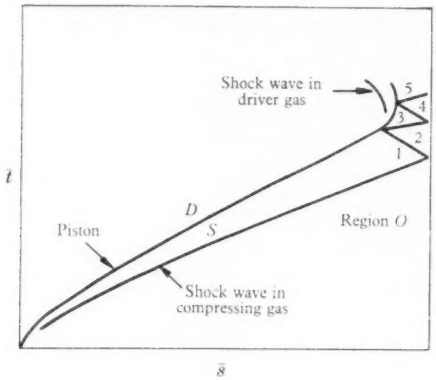

FIGURE 3. Sketch showing reflected shocks.

piston may be calculated by a method somewhat similar to that used for the initial piston motion. The pressure on the front face, p_3', is found by assuming an unsteady expansion from the point where the shock wave was reflected. Thus

$$p_3' = p_3\left(1-\frac{\gamma_0-1}{2}\frac{\Delta u}{a_3}\right)^{2\gamma_0/(\gamma_0-1)}, \tag{15}$$

where Δu is the change in velocity during deceleration, and a_3 corresponds to p_3 (after shock reflexion).

The pressure on the rear face, p_D', is found by assuming that a shock wave forms as before. Thus

$$p_D' = p_D\left[1+\frac{\gamma_D}{2}\frac{\Delta u}{a_D}\{x_1+\sqrt{(x_1^2+4)}\}\right], \tag{16}$$

where $x_1 = \frac{1}{2}(\gamma_R+1)(\Delta u/a_D)$, p_D and a_D are quantities in the driver gas just before the piston starts to decelerate.

Then from (15) and (16)

$$(p_3'-p_D')A = m\frac{d^2s}{dt^2} \tag{17}$$

and, as in equation (13),

$$\frac{p_3'-p_D'}{p_R} = \frac{d^2\bar{s}}{d\bar{t}^2}. \tag{18}$$

From this expression the piston motion may be calculated as described in § 2.1.

Having determined the piston motion, the method of characteristics is again used, as in § 2.2, to plot the strength and position of the shock wave, and the calculation proceeds until the shock wave again reaches the piston. Values for

p_3 and a_3 are then calculated and the process is repeated for the next deceleration period. After a number of reflexions, usually two from the end of the tube and two from the face of the piston, the shock wave is so weak that no further entropy change occurs in the gas.

2.4. *Final stages of the motion*

Because of the complex wave system generated in the motion described above, some time will elapse before steady conditions are established in the compressed gas. However, all oscillations will eventually be damped out, and a steady pressure will exist throughout the system. Because the reservoir gas now fills the tube as well, the pressure will be somewhat lower than p_R, and it will be denoted by p_F.

The temperature in the final steady state, T_F, is

$$T_F = T_0 \left(\frac{p_F}{p_0}\right)^{(\gamma_0-1)/\gamma_0} e^{s/c}\, p, \tag{19}$$

where $s = \sum_{\text{all shocks}} (\delta s)$, is the total entropy change during compression.

3. Simplified calculation procedure

The detailed calculation described in § 2.3 is laborious, since it requires alternate use of numerical integration and a graphical procedure. An approximate method of determining the final temperature is to assume that the shock wave is never affected by the deceleration of the piston, but continues to reflect as though the piston were moving with constant velocity until the shock is so weak that no further entropy change occurs. Evans & Evans (1956) have studied this problem and concluded that there is very little change in entropy after three shock reflexions. Since in any case the shock wave is not affected by the piston deceleration until after the second reflexion, it is to be expected that the (estimated) temperature given by this method will agree well with the calculations of § 2.

The formulae given by Evans & Evans (1956) are

$$\frac{p_4}{p_0} = \frac{(\lambda+\mu+4)(\lambda+\mu+3)(\lambda+\mu+2)(\lambda+\mu+1)}{(\lambda+3)(\lambda+2)(\lambda+1)\lambda}, \tag{20}$$

$$\frac{T_4}{T_0} = \frac{(\lambda+\mu+4)(\lambda+4)}{(\lambda+\mu)\lambda}, \tag{21}$$

where

$$\lambda = \frac{\mu+1}{p_1/p_0-1}, \quad \mu = \frac{\gamma+1}{\gamma-1},$$

and p_1/p_0 is the pressure ratio across the initial shock wave when it reaches the end of the tube.

The final temperature, T_F, is

$$T_F = T_4 \left(\frac{p_F}{p_4}\right)^{(\gamma-1)/\gamma}. \tag{22}$$

The temperatures derived in this way are plotted in figure 4 for different values of u/a_0 and various compression ratios.

3.1. *Comparison of methods*

Four sample calculations were performed using the procedure described in § 2 and also using the simplified method of § 3. The final temperatures calculated by each method are shown in table 1, and it may be seen that the maximum discrepancy is

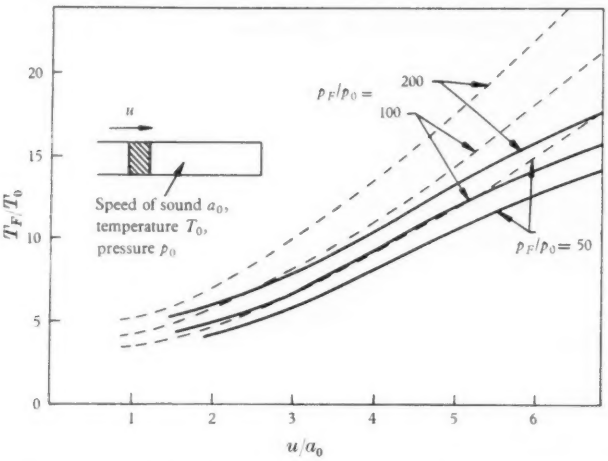

FIGURE 4. Temperature after compression by four shocks with isentropic expansion to various compression ratios. —, real gas; - - - -, perfect gas.

Initial shock strength (p_s/p_0)	Final temperature (T_F) °K: Characteristic method (§ 2)	Final temperature (T_F) °K: Approximate method (§ 3)
3·48	1150	1085
6·37	1310	1315
8·73	1940	1945
23·2	3330	3270

TABLE 1. Comparison of characteristic method and approximate calculations for shock heating.

only 6 %. In the range of variables so far considered, the approximate method thus appears to be adequate so long as no intermediate values of pressure and temperature are required. If, for example, the peak pressures generated during compression are wanted, the full calculation procedure of § 2 must be used.

3.2. *Calculation for a typical compressor*

As an example of the methods described above, calculations were performed for the No. 1 hypersonic gun tunnel at A.R.D.E. This tunnel had a tube of 20 mm diameter and was 60 in. long. For this example the chamber contained air at 1000 p.s.i. and the tube initially contained air at 14·7 p.s.i. The piston mass was

2g. The method described in § 2 was used to compute the variation of pressure with time at the closed end of the tube and the result is plotted in figure 5. For an experimental comparison, a strain-gauge-type pressure transducer was mounted

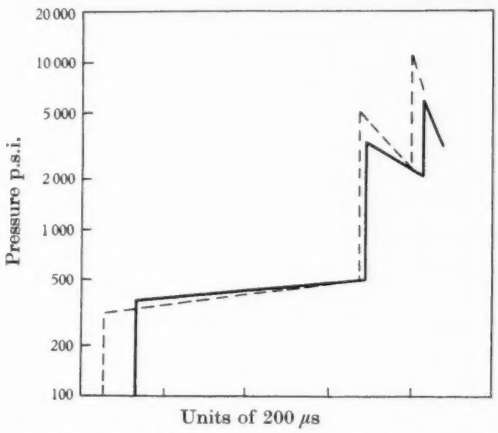

FIGURE 5. Variation of pressure with time at the closed end of the tube. Initial pressure of air in chamber 1000 p.s.i., in tube 14·7 p.s.i. Piston mass 2 g, tube length 5 ft., tube diameter 20 mm. —, theory; - - - -, mean of experiment.

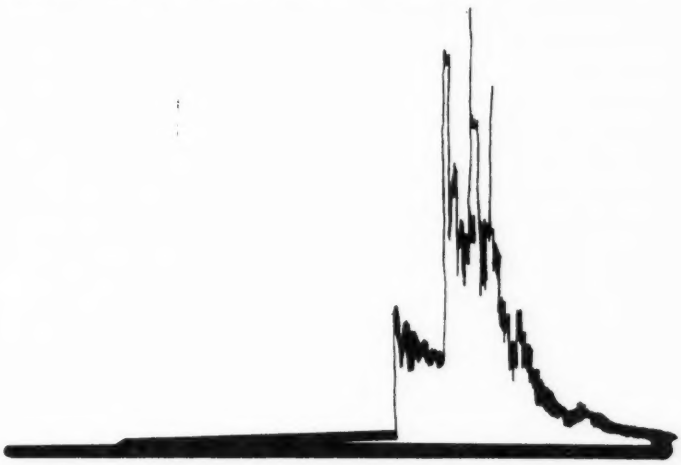

FIGURE 6. Copy of oscilloscope trace showing the pressure at the closed end of the tube.

flush with the closed end of the tube, and the tunnel was fired at the conditions used for calculation. The resulting pressure record is shown in figure 6.* The measured pressures are plotted in figure 5, which is drawn to a logarithmic scale for convenience.

* The oscilloscope trace was started at a convenient time to display the shock compression process. The high frequency oscillation is due to the gauge ringing at its natural frequency of 200 kc/s.

4. The use of a real gas

So far we have dealt only with the case of an ideal gas having a constant ratio of specific heats, for which the formulae of Evans & Evans (1956) hold. Although the inclusion of real gas effects may lead to a different final temperature, it must be remembered that for most applications the requirements will specify a particular value of enthalpy, and enthalpy for a given gas pressure is only weakly dependent on real gas effects.

Such properties as heat transfer by radiation are, however, dependent directly on temperature and the effect of variations in the gas properties must be discussed. Values of the internal energy and compressibility of air have been tabulated by Hilsenrath & Beckett (1955) and the method of application of the tables follows that used by Mary Romig (1956). Stollery & Maull (1958) have discussed a similar calculation, and they show that for a given enthalpy the real gas temperatures are lower than the ideal values, which is advantageous because radiative heat losses are reduced. The results of calculations for a real gas are also shown in figure 4.

5. Conclusions

The effect of the finite mass of a piston on the multiple shock compression process has been calculated using a method analogous to the tangent-wedge approximation to determine the initial motion (acceleration period) of the piston, and using the method of characteristics to determine the position and strength of the shock wave ahead of the piston. This shock strength was then used to obtain the subsequent piston motion (deceleration period) again using the method of characteristics, and it was found that there was a significant change of entropy through the first four shock waves. The final temperature (after expansion of the gas to a given pressure) was calculated by summing the entropy changes. It was also found that a good approximation to the final temperature could be obtained by assuming that the shock wave reflects three times while the piston moves at constant speed, and that the gas then expands to its final pressure. Experiments carried out at A.R.D.E. using an air-operated piston compressor have confirmed some of the calculated values of shock strength.

The author wishes to thank Dr R. N. Cox of A.R.D.E. for suggesting the basis of this study, and for his helpful criticism.

REFERENCES

Evans, C. & Evans, F. 1956 Shock compression of a perfect gas. *J. Fluid Mech.* **1**, 4.

Glass, I. I. 1958 Shock tubes. Part I: Theory and performance of simple shock tubes. *U.T.I.A. Rev.*, no. 12.

Hilsenrath, J. & Beckett, C. W. 1955 Thermodynamic properties of argon-free air to 15,000 °K. *N.B.S. Rep.*, no. 3991 (Revised).

Romig, M. F. 1957 The normal shock properties for air in dissociation equilibrium. *J. Aero. Sci.* **23**, 2.

Stollery, J. L. & Maull, D. J. 1958 A note on the compression of air through repeated shock waves. *J. Fluid Mech.* **4**, 6.

On the effect of the molecular diffusivity in turbulent diffusion

By P. G. SAFFMAN
Department of Applied Mathematics and Theoretical Physics, University of Cambridge

(Received 3 October 1959)

It is shown that the dispersion of a substance, with molecular diffusivity κ, in a stationary, homogeneous, turbulent velocity field can be formulated in terms of a 'substance auto-correlation function', this being a generalization of the well-known Lagrangian correlation between the velocity of a fluid particle at different times. It is found that the interaction between the molecular diffusion and the turbulent motion reduces the dispersion from the value it would have if the processes of molecular and turbulent diffusion were independent and additive. The conflict, between the results obtained in this paper and previous results which implied that the interaction increases the dispersion, is resolved. The ratio, of the contributions to the dispersion from the interaction term and the turbulent diffusion term, is obtained for comparatively large times by the use of intuitive arguments, and is found to be inversely proportional to the Prandtl number and a Reynolds number of the turbulence.

1. Introduction

Taylor (1921) showed that the mean-square displacement or dispersion, in a given direction, of infinitesimal fluid particles from their original position in a turbulent velocity field is

$$\overline{Y^2(t)} = 2\int_{t_0}^{t} dt' \int_{t_0}^{t'} \overline{v(t')\,v(t'')}\,dt'', \tag{1.1}$$

where $v(t)$ is the velocity of a fluid element or particle in the given direction. The integrand

$$\overline{v(t')\,v(t'')} = R_p(t', t''), \text{ say,} \tag{1.2}$$

is the covariance of the velocity of a fluid element at time t'' and later time t', and is a Lagrangian auto-correlation function. When the velocity of a fluid element is statistically stationary in time,

$$R_p(t', t'') = \overline{v^2} S_p(t' - t'') \tag{1.3}$$

and

$$\overline{Y^2} = 2\overline{v^2}\int_0^{t-t_0} (t - t_0 - \tau)\, S_p(\tau)\,d\tau \tag{1.4}$$

(see the review article by Batchelor & Townsend (1956); this is referred to hereafter as I).

When the quantity or substance being dispersed is subject to molecular diffusion (e.g. mass or heat) with a diffusivity κ, it can be shown (see I) that, provided $t-t_0$ is sufficiently small that

$$t-t_0 \ll (\overline{\boldsymbol{\omega}^2})^{-\frac{1}{2}}, \quad \frac{\kappa}{\nu}(t-t_0) \ll (\overline{\boldsymbol{\omega}^2})^{-\frac{1}{2}}, \tag{1.5}$$

the effects of turbulent and molecular diffusion are linearly additive in the first approximation, giving a total dispersion

$$D^2 = \overline{Y^2} + 2\kappa(t-t_0), \tag{1.6}$$

where $\boldsymbol{\omega}$ is the vorticity of the turbulent motion and ν is the kinematic viscosity. (Henceforth, for brevity, we shall write $\omega = (\overline{\boldsymbol{\omega}^2})^{\frac{1}{2}}$.) For larger values of $t-t_0$, there is an interaction between the turbulent and molecular diffusion. Arguments are presented in I (due originally to Townsend 1954) which give the improved approximation

$$\Delta = D^2 - \overline{Y^2} - 2\kappa(t-t_0) = \tfrac{28}{45}\kappa\omega^2(t-t_0)^3 \tag{1·7}$$

to $O(t-t_0)^3$ for times such that (1.5) is satisfied. That is, the effect of the interaction is initially, and by implication for later times, to increase the dispersion over and above that due to the turbulent and molecular diffusions acting independently.

It is the purpose of the present note to show that there is a fallacious step in the deduction of (1.7) ,and that in fact for stationary homogeneous turbulence

$$\Delta = -\tfrac{1}{9}\kappa\omega^2(t-t_0)^3 \tag{1.8}$$

to $O(t-t_0)^3$ when (1.5) is satisfied. Intuitive arguments are also given to show that, for larger values of $t-t_0$, Δ is a decreasing function of $t-t_0$ and inversely proportional to the Prandtl number ν/κ. This is in qualitative agreement with measurements by Mickelsen (1960) of the width of the diffusion wake behind a source emitting helium ($\kappa = 0{\cdot}725\,\mathrm{cm}^2/\mathrm{s}$) and carbon dioxide ($\kappa = 0{\cdot}167\,\mathrm{cm}^2/\mathrm{s}$) in the turbulent air stream downstream of a grid in a wind tunnel. He found for values of $t-t_0$ comparable with a time characteristic of the energy containing eddies that the values of $D^2 - 2\kappa(t-t_0)$ were 5 % or more smaller for helium than for carbon dioxide.

2. The substance auto-correlation coefficient

The reason why the dispersion of a substance differs from that of infinitesimal fluid particles is because the molecules of the substance do not move with the velocity of the fluid continuum (which can be regarded as a continuous function of position and time), but have relative to this velocity a random thermal or Brownian velocity, whereas the infinitesimal fluid particles are points which by definition move with the local fluid velocity. When the fluid velocity is zero, this Brownian velocity manifests itself as the molecular diffusivity.

The dispersion of a mass-like substance released from a source in a turbulent flow (e.g. a gas in a turbulent air stream) is the ensemble or stochastic average of the displacement (squared) of a marked molecule of the substance, where the average is over the ensemble of all Brownian motions and the ensemble of all

realizations of the turbulent velocity field. The velocity of the molecule in a given direction is $V(t)+q(t)$, where $V(t)$ is the velocity of the fluid at the point occupied by the molecule and $q(t)$ is the Brownian velocity. Hence, by analogy with (1.1),

$$D^2(t) = 2\int_{t_0}^{t} dt' \int_{t_0}^{t'} \mathfrak{R}(t', t'')\, dt'', \tag{2·1}$$

where

$$\mathfrak{R}(t', t'') = \langle \overline{\{V(t')+q(t')\}\{V(t'')+q(t'')\}} \rangle, \tag{2.2}$$

the angle brackets denoting an average over the Brownian ensemble and the overbar an average over the turbulent ensemble, and $V(t)+q(t)$ is the total (component of) velocity at time t of a marked molecule released from the source, at $\mathbf{x}_0$ say, at time t_0.

In the absence of fluid velocity, in a homogeneous medium, $q(t)$ is a stationary random function of t with zero mean, so that

$$\langle q(t')\, q(t'') \rangle = Q(t'-t''), \tag{2.3}$$

and since in this case $D^2 = 2\kappa(t-t_0)$, it follows (see (1.3) and (1.4)) that

$$\int_0^\infty Q(\tau)\, d\tau = \kappa, \tag{2.4}$$

where κ is the molecular diffusivity. Moreover, it is known that $Q(\tau)$ is negligible when $\tau \gg \tau_c$, where τ_c is the mean time between molecular collisions, so that (2.4) holds when the upper limit of integration is any time large compared with τ_c.

We now suppose that the ambient fluid is in turbulent motion, and in particular we shall assume that the turbulence is statistically stationary and homogeneous*. In this case, $q(t)+V(t)$ is a stationary random function of t with zero mean, and $\mathfrak{R}$ is a function of $t'-t''$, i.e.

$$\begin{aligned} \mathfrak{R}(t', t'') &= \langle \overline{\{V(t)+q(t)\}\{V(t+\tau)+q(t+\tau)\}} \rangle \\ &= \mathfrak{S}(\tau), \quad \text{say}, \end{aligned} \tag{2.5}$$

where $\tau = t'-t''$. Then D^2 is given by (1·4) with $\overline{v^2}S_p$ replaced by $\mathfrak{S}$.

Now the statistical distribution of $q(t)$ is determined by the molecular collisions with a time scale τ_c, whereas the time scale of the macroscopic motion is at least of order ω^{-1}. Now $\omega\tau_c \ll 1$, since otherwise it is not meaningful to regard the fluid as a continuum, and since the two time scales are so different, the Brownian motion and the macroscopic motion will be statistically uncorrelated (for a fuller discussion of this point see the Appendix). Hence, with error of order $\omega\tau_c$,

$$\begin{aligned} \mathfrak{S}(\tau) &= \langle \overline{V(t)\, V(t+\tau)} \rangle + \langle \overline{q(t)\, q(t+\tau)} \rangle \\ &= \overline{v^2} S_d(\tau) + Q(\tau), \quad \text{say}, \end{aligned} \tag{2.6}$$

where $Q(\tau)$ has the value it would have in the absence of fluid motion, and $\overline{v^2}$ is the mean square of a component of the turbulent velocity. It now follows that

$$D^2 = 2\overline{v^2} \int_0^{t-t_0} (t-t_0-\tau)\, S_d(\tau)\, d\tau + 2\kappa(t-t_0), \tag{2.7}$$

* It can be shown that the analysis given below is valid if the turbulence is homogeneous in the direction of the dispersion only (e.g. longitudinal dispersion in a pipe). However, for the sake of simplicity of exposition, we restrict the discussion to completely homogeneous turbulence.

and it can be shown (see the Appendix) that the error in (2.7) is of order $\kappa\omega\tau_c(t-t_0)$. $S_d(\tau)$ may be called the 'substance auto-correlation coefficient'.

Note that $S_d(\tau) \neq S_p(\tau)$, since the former is the correlation coefficient of the fluid velocity at two points which lie on the trajectory of a molecule, and the latter is the correlation at two points on the trajectory of an infinitesimal fluid particle.

An expression for $S_d(\tau)$ can be obtained as follows. Let $\theta(\mathbf{x}, t \,|\, \mathbf{x}_0, t_0)$ denote the solution of

$$\left.\begin{aligned} \frac{\partial\theta}{\partial t} + \mathbf{u}.\nabla\theta &= \kappa\nabla^2\theta, \\ \theta(\mathbf{x}, t_0 \,|\, \mathbf{x}_0, t_0) &= \delta(\mathbf{x}-\mathbf{x}_0). \end{aligned}\right\} \tag{2.8}$$

(It is assumed throughout that the substance is dynamically passive so that the distribution of θ has no effect on the turbulent velocity field $\mathbf{u}(\mathbf{x}, t)$.) Then $\theta\, d\mathbf{x}$ is the probability, for one realization of the turbulence, that a marked molecule is in the element of volume $d\mathbf{x}$ at time t, given that it was at $\mathbf{x}_0$ at time t_0. Let $u_2(\mathbf{x}, t)$ be the turbulent velocity component in the same direction as V. Then $V(t_0) = u_2(\mathbf{x}_0, t_0)$, and

$$\langle V(t)\rangle = \int u_2(\mathbf{x}, t)\, \theta(\mathbf{x}, t \,|\, \mathbf{x}_0, t_0)\, d\mathbf{x}. \tag{2.9}$$

so that

$$\begin{aligned} \overline{v^2} S_d(\tau) &= \langle \overline{V(t)\, V(t_0)}\rangle \\ &= \int \overline{u_2(\mathbf{x}, t)\, u_2(\mathbf{x}_0, t_0)}\, \theta(\mathbf{x}, t \,|\, \mathbf{x}_0, t_0)\, d\mathbf{x}, \end{aligned} \tag{2.10}$$

where $t = t_0 + \tau$. In the next section, we shall calculate $S_d(\tau)$ for small τ, and in § 5 obtained an estimate of its value for large τ.

Incidentally, to put $\kappa = 0$ is equivalent to saying that $q \equiv 0$ and that a molecule and an infinitesimal fluid particle always coincide. In this case, $V(t) = v(t)$, where $v(t)$ refers to the velocity of a fluid particle (in contrast to $V(t)$ which is the velocity of the fluid following a molecule), and $S_d(\tau) = S_p(\tau)$.

The expression (2.7) for D^2 involves only the fluid velocity and the molecular diffusivity κ, and should presumably describe the dispersion of a non mass-like quantity like heat, whose diffusion is not readily identifiable with the dispersion of a marked molecule. This could be verified if it were possible to derive (2.7) and (2.10) from formal manipulation of the diffusion equation (2.8) and the expression

$$D^2 = \int x_2^2\, \theta\, d\mathbf{x},$$

but an argument given in the Appendix implies that this may not be possible.

3. Calculation of $S_d(\tau)$ for small τ

When the second of the conditions (1.5) is satisfied, the size of an element of substance released at $\mathbf{x}_0, t_0$ is small compared with the length scale of the rotational and straining motions of the turbulence. The diffusion equation (2.1) for $\theta(\mathbf{x}, t \,|\, \mathbf{x}_0, t_0)$ can then be written approximately as

$$\frac{\partial\theta}{\partial t} + x_j' \frac{\partial\theta}{\partial x_i'} \left(\frac{\partial u_i}{\partial x_j}\right)_p = \kappa\nabla'^2\theta, \tag{3.1}$$

where $\mathbf{x}'$ is the position vector relative to the fluid particle with which the element of substance originally coincided, and the suffix p denotes that quantities are evaluated at the fluid particle (and are therefore functions of t only). It is easily verified that a solution of (3.1) exists of the form

$$\theta = \theta_m(t) \exp\{-\tfrac{1}{2}\alpha_{ij}x_i'x_j'\} \tag{3.2}$$

(see Townsend 1951), and that

$$\alpha_{ij} = \{\kappa(t-t_0)\}^{-1}[\delta_{ij} + O\{\omega(t-t_0)\}]. \tag{3.3}$$

To evaluate S_d, we note that

$$u_2(\mathbf{x}, t) = v(t) + x_j'\left(\frac{\partial u_2}{\partial x_j}\right)_p + \tfrac{1}{2}x_j'x_k'\left(\frac{\partial^2 u_2}{\partial x_j \partial x_k}\right)_p + O\left(x'^3\frac{\partial^3 u_2}{\partial x^3}\right), \tag{3.4}$$

where $v(t)$ is the (component of) velocity of the fluid particle which was at $\mathbf{x}_0$ at time t_0. Substituting into (2.9) and making use of (3.2), (3.3) and (3.4), we obtain

$$\langle V(t)\rangle = v(t) + \kappa(t-t_0)\,(\nabla^2 u_2)_p\,[1 + O\{\omega(t-t_0)\}]. \tag{3.5}$$

Hence, from (2.10) and the fact that $V(t_0) = v(t_0)$,

$$\overline{v^2}S_d(t, t_0) = \overline{v^2}S_p(t, t_0) + \kappa(t-t_0)\,\overline{v(t_0)\,(\nabla^2 u_2)_p}\,[1 + O\{\omega(t-t_0)\}]. \tag{3·6}$$

The second term in (3.6) arises from the interaction, but it involves what is essentially a Lagrangian–Eulerian correlation. However, if $t - t_0$ is small compared with ω^{-1}, then

$$\overline{v(t_0)\,(\nabla^2 u_2)_p} \doteq \overline{u_2 \nabla^2 u_2}, \tag{3.7}$$

since $\nabla^2 u_2$ is determined by the small-scale components of the turbulence which have a time scale ω^{-1}, and the time scale of $v(t)$ will be that of the energy containing eddies. Moreover,

$$\overline{u_2\,\nabla^2 u_2} = \overline{\nabla.(u_2 \nabla u_2)} - \overline{(\nabla u_2)^2};$$

where the first term is zero when the small-scale motion is homogeneous, and

$$\overline{(\nabla u_2)^2} = \tfrac{1}{3}\omega^2$$

if it is also isotropic.

It now follows from (3.6) that,

$$S_d(\tau) = S_p(\tau) - \frac{1}{3}\frac{\kappa\omega^2}{\overline{v_2^2}}\tau + O(\tau^2), \tag{3.8}$$

and substitution in (2.7) then gives

$$D^2 = \overline{Y^2} + 2\kappa(t-t_0) - \tfrac{1}{9}\kappa\omega^2(t-t_0)^3, \tag{3.9}$$

correct to order $(t-t_0)^3$. The initial effect of the interaction between the turbulence and the molecular diffusion is thus to *reduce* the dispersion relative to the origin.*

In view of the fact that this conclusion differs from that reached previously, it is perhaps worthwhile repeating qualitatively the present argument. An element

* Since we are concerned here with the initial stages of the diffusion, it would in fact suffice for the present argument if only the small-scale components of the turbulence were stationary and isotropic.

of substance spreads initially due to molecular diffusion like $\delta = \{\kappa(t-t_0)\}^{\frac{1}{2}}$. The order of magnitude of the difference between the velocities with which different parts of the element are convected is $\delta(\partial u_2/\partial x) + \frac{1}{2}\delta^2(\partial^2 u_2/\partial x^2) +$ smaller terms. For homogeneous turbulence, the covariance of u_2 and $\partial u_2/\partial x$ is zero, but that of u_2 and $\partial^2 u_2/\partial x^2$ is negative. Thus on average, the speed at which the substance is convected away from the source is less than that of the (originally coincident) fluid particle, and the dispersion is thereby reduced.

Another way of phrasing the argument is to note that from (3.8) $S_d(\tau) < S_p(\tau)$, at least initially. That is, the effect of molecular diffusion is, so to speak, to make the molecules of the diffusing substance forget more quickly than infinitesimal fluid elements what their original velocity of convection was. Since we should intuitively expect this effect to become more marked as τ increases, we conclude that S_d/S_p is a decreasing function of τ, and that Δ continues to decrease as $t-t_0$ increases.* We shall return to this point in § 5.

It remains to discuss why the results given here differ from those obtained in I by a somewhat different analysis. Light is thrown on this by consideration of the dispersion of a small amount of the substance released instantaneously, i.e. a spot.

4. Dispersion of a spot

A corollary of the present argument is that the centroid of the spot will lag behind, on average, the fluid particle released at the same instant. To calculate by how much, we multiply (2.8) by y and integrate over all space, obtaining

$$\frac{d}{dt}\int (y-y_p)\,\theta\,d\mathbf{x} = \int (u_2 - v)\,\theta\,d\mathbf{x}, \tag{4.1}$$

where y_p and v are the displacement and velocity of the fluid particle. To the same order of approximation as in § 3, the right-hand side of (4.1) can be evaluated to give

$$\int (u_2 - v)\,\theta\,d\mathbf{x} = \kappa(t-t_0)\,(\nabla^2 u_2)_p. \tag{4.2}$$

The left-hand side of (4.1) is the rate of change of the distance (in the y-direction) between the centroid of the heat spot and the fluid particle. The displacement of the centroid relative to the origin is therefore $Y + \frac{1}{2}\kappa(t-t_0)^2\,(\nabla^2 u_2)_p$, correct to order $(t-t_0)^2$. Since $Y \doteq v(t_0)\,(t-t_0)$ for small values of $t-t_0$, it follows that the dispersion of the centroid is, relative to the point of release,

$$\overline{Y^2} - \tfrac{1}{3}\kappa\omega^2(t-t_0)^3, \tag{4.3}$$

where $\overline{Y^2}$ is the dispersion of the fluid particle.

Moreover, it is easy to calculate the shape of the spot for small values of $t-t_0$ (see Townsend 1951), and it follows from his results that the dispersion in a given direction of the heat spot *relative to its centroid* is

$$2\kappa(t-t_0) + \tfrac{4}{3}\kappa(t-t_0)^3\,(\overline{\alpha^2} + \overline{\beta^2} + \overline{\gamma^2}), \tag{4.4}$$

* A very similar argument was put forward independently by Dr T. H. Ellison in a private communication in 1956.

where α, β and γ are the principal rates of strain, and $\overline{\alpha^2}+\overline{\beta^2}+\overline{\gamma^2} = \frac{1}{2}\omega^2$. Notice that the interaction term in (4.4) is positive, so that the interaction increases the dispersion of the spot relative to its centroid and, as a consequence, increases the rate at which the maximum concentration in the spot decreases, as was verified experimentally by Townsend (1951). However, combining (4.4) and (4.3), we find that the dispersion of the spot relative to the point of release is given by (3.9). That is to say, although the dispersion of the spot relative to its centroid is increased by the interaction, the dispersion of the centroid of the spot is reduced by a greater amount so that the total dispersion relative to the point of release is reduced.

We can now account for the difference between the present result and that given previously in I. In that work, the width of the contorted diffusing wake behind a continuous source moving (rapidly) through a turbulent velocity field was calculated, and it was shown that the effect of the interaction is to make this greater than $2\kappa(t-t_0)$. The present work in no way contradicts this result. However, it was tacitly assumed in the previous work that the instantaneous axis of the diffusing wake coincides with the locus of the fluid particles coming from the source. The present work shows that this assumption is unjustified, and that on average the displacement of the instantaneous axis is less than that of the fluid particles by an amount which more than compensates for the increase in the instantaneous wake width due to the interaction.

5. The interaction for large times

All the available evidence indicates strongly that $\overline{Y^2} \propto (t-t_0)$ when $t-t_0$ is comparable with t_e, a time characteristic of the energy containing eddies, and that we can write

$$\overline{Y^2} \sim C\overline{v^2}t_e(t-t_0), \tag{5.1}$$

where C is a constant of order unity. (For definiteness, we may suppose t_e is given by $\nu\omega^2 t_e/\overline{v^2} = \frac{3}{2}$; then for the decaying homogeneous turbulence downstream of a grid $t_e = t_0$, where t_0 is the time from a vertical origin at which the energy of the turbulence is infinite.) The expression (3.9) can be written

$$D^2 = \overline{Y^2} + 2\kappa(t-t_0) - \frac{\kappa}{\nu}\overline{v^2}\frac{(t-t_0)^3}{t_e}, \tag{5.2}$$

and is therefore clearly of limited value since it becomes negative as $t-t_0$ increases. In fact, (5.2) is unlikely to hold far outside its theoretical range of validity as given by (1.5). This is in practice so small (see I) that it is desirable to make an estimate of D^2 for larger values of $t-t_0$. The following discussion is intuitive and somewhat speculative, but seems worth giving in the absence of anything better, and the conclusions should be amenable to experimental investigation.

We still consider stationary, homogeneous turbulence, although later we shall apply the conclusions to cover decaying homogeneous turbulence behind a grid. The general argument presented at the end of §3 shows that $S_p(\tau) > S_d(\tau)$, and moreover the argument implies that S_p/S_d is an increasing function of τ. Now this ratio is determined primarily by an interaction between the molecular diffusion and the small-scale straining motions, so that when $\tau \gg \omega^{-1}$ the interaction will

cease to have any further effect and S_p/S_d should tend to a value independent of τ. We can express this argument formally as follows.

It follows from (2.10) that

$$S_d(\tau)-S_p(\tau)=(\overline{v^2})^{-1}\int\overline{\theta\{u_2-v(t)\}\,v(t_0)}\,d\mathbf{x}, \tag{5.3}$$

where $\tau=t-t_0$. Now the value of $\theta\{u_2-v(t)\}$ is determined mainly by the small-scale motion, whereas $v(t)$ is determined by the energy containing eddies, which suggests that

$$\overline{\theta\{u_2-v(t)\}\,v(t_0)}\doteq S_p(\tau)\,\overline{\theta\{u_2-v(t)\}\,v(t)}$$

when the Reynolds number of the turbulence is sufficiently large, where the term with the overbar is determined mainly by the molecular diffusivity, the rate of strain, and τ. Hence, from dimensional considerations,

$$S_d(\tau)-S_p(\tau)=-(\overline{v^2})^{-1}S_p(\tau)\,\kappa\omega f(\omega\tau), \tag{5.4}$$

where $f(\omega\tau)$ is a positive increasing function of τ to express the idea that the interaction continues to grow with τ. When $\tau\gg\omega^{-1}$, $f(\omega\tau)$ either tends to a constant or infinity; the latter is impossible since it would make D^2 negative, so we come to the conclusion that

$$S_d(\tau)-S_p(\tau)=-a\kappa\omega(\overline{v^2})^{-1}S_p(\tau) \tag{5.5}$$

when $\omega\tau\gg1$, where a is a (positive) constant, of order unity, depending on the structure of the turbulence.

The relation (5.5) suggests that an appropriate expression valid for all τ is

$$S_d(\tau)-S_p(\tau)=-a\kappa\omega(\overline{v^2})^{-1}S_p(\tau)\{1-e^{-b\omega\tau}\} \tag{5.6}$$

which agrees with (3.8) for $\omega\tau\ll1$ if $ab=\frac{1}{3}$, and reduces to (5.5) when $\omega\tau\gg1$.

The derivation of (5.5) or (5.6) is intuitive and far from watertight, but the argument is supported by the fact that these expressions have the properties which we should intuitively associate with S_d-S_p; e.g. the contribution to the interaction from the energy containing eddies is independent of the contribution from the small-scale motion, and the greater κ and ω, the greater the interaction. (Moreover, multiplying (5.5) or (5.6) by any function with a time scale comparable with t_e, to take account of any possible effect of the energy containing eddies on the interaction in addition to that represented by $S_p(\tau)$, can be shown to have insignificant effect.)

It now follows from substitution into (2.7) that, for $\omega(t-t_0)\gg1$,

$$\Delta=-a\kappa\omega\frac{\overline{Y^2}}{\overline{v^2}}=-a\sqrt{15}\frac{\kappa}{\nu}R_\lambda^{-1}\overline{Y^2}, \tag{5.7}$$

where R_λ is the Reynolds number based on $(\overline{v_2})^{\frac{1}{2}}$ and the dissipation length parameter $\lambda=\sqrt{(15\overline{v^2}/\omega^2)}$. Thus $\Delta/\overline{Y^2}$ is inversely proportional to the Prandtl number and R_λ. The ratio of $|\Delta|$ and the direct effect of molecular diffusion is

$$\frac{|\Delta|}{2\kappa(t-t_0)}=\frac{2}{4\sqrt{15}}aCR_\lambda, \tag{5.8}$$

where we have used (5.1) for $\overline{Y^2}$. Thus if the Reynolds number of the turbulence is sufficiently large, the direct effect of molecular diffusion is small compared with the interaction term.

For decaying homogeneous turbulence downstream of a grid, it is known that R_λ is constant during the initial period of decay, and that

$$R_\lambda^2 = \frac{10}{A}\frac{UM}{\nu}, \tag{5.9}$$

where U is the mean velocity, M is the spacing length of the grid, and A is a constant depending on the grid shape ($A = 135$ for the grids employed by Mickelsen 1960). We can therefore obtain an estimate of a from the data presented in figure 2 of his paper. Taking a rough mean of his measurements for

$$(t-t_0)/t_0 > 0{\cdot}6,$$

we obtain (neglecting one pair of points which appear inconsistent and which may be due to experimental error)

$$\frac{\Delta_{CO_2}-\Delta_{He}}{\overline{Y^2}} \doteq 0{\cdot}18 \quad \text{for} \quad R_\lambda = 20$$
$$\doteq 0{\cdot}07 \quad \text{for} \quad R_\lambda = 40,$$

whereas (5.7) predicts that this ratio should be $13{\cdot}5a/R_\lambda$. The experimental measurements are therefore in rough quantitative agreement if $a = 0{\cdot}23$. Incidentally, for these comparatively low values of R_λ, the interaction and the direct effect of molecular diffusion are of the same order of magnitude.

Appendix

We shall now discuss the covariances $\overline{\langle q(t)\, V(t+\tau)\rangle}$ and $\overline{\langle q(t+\tau)\, V(t)\rangle}$, which are functions of τ. Let $p(\mathbf{x}, \mathbf{q}, t \,|\, \mathbf{x}_0, t_0)$ denote the probability, for $t - t_0 \gg \tau_c$ and for one realization of the turbulence, that a marked molecule of the substance is in the element of phase space $d\mathbf{x}\, d\mathbf{q}$, given that it was at $\mathbf{x}_0$ at time t_0 with Brownian velocity $\mathbf{q}_0$, where the function p is a random variable over the ensemble of the possible turbulent motions. The assumption of the independence of the Brownian and macroscopic velocities is here made use of explicitly by saying that p is independent of $\mathbf{q}_0$ when $t - t_0 \gg \tau_c$. We have

$$\theta(\mathbf{x}, t \,|\, \mathbf{x}_0, t_0) = \int p(\mathbf{x}, \mathbf{q}, t \,|\, \mathbf{x}_0, t_0)\, d\mathbf{q}, \tag{A 1}$$

where θ is the solution of the diffusion equation (2.8), and moreover

$$\int q_i p(\mathbf{x}, \mathbf{q}, t \,|\, \mathbf{x}_0, t_0)\, d\mathbf{q} = -\kappa \frac{\partial \theta}{\partial x_i}(\mathbf{x}, t \,|\, \mathbf{x}_0, t_0), \tag{A 2}$$

where the suffix i denotes the component in the i-direction.

If f is any function of the marked molecule,

$$\langle f \rangle = \iint f p\, d\mathbf{x}\, d\mathbf{q},$$

and

$$\overline{\langle f \rangle} = \lim_{V \to \infty} \frac{1}{V} \int_V \langle f \rangle\, d\mathbf{x}_0,$$

since the turbulence is homogeneous and an average over the turbulent ensemble is equivalent to integrating with respect to $\mathbf{x}_0$ over a large region of space.

It now follows that

$$\langle q_i(t)\rangle = -\kappa \int \frac{\partial \theta}{\partial x_i}\, d\mathbf{x} = 0, \tag{A 3}$$

and that $\langle \overline{q_i(t)}\rangle = -\langle \overline{V_i(t)}\rangle = 0.$

The covariances are given by (no summation implied and writing $t' = t+\tau$)

$$\langle q_i(t)\, V_i(t+\tau)\rangle = \iiint \left[\iint u_i(\mathbf{x}', t')\, p(\mathbf{x}', \mathbf{q}', t' \,|\, \mathbf{x}, t)\, d\mathbf{x}'\, d\mathbf{q}'\right] q_i\, p(\mathbf{x}, \mathbf{q}, t \,|\, \mathbf{x}_0, t_0)\, d\mathbf{x}\, d\mathbf{q}$$

$$= -\kappa \iint u_i(\mathbf{x}', t')\, \theta(\mathbf{x}', t' \,|\, \mathbf{x}, t) \frac{\partial}{\partial x_i}\theta(\mathbf{x}, t \,|\, \mathbf{x}_0, t_0)\, d\mathbf{x}\, d\mathbf{x}', \tag{A 4}$$

and

$$\langle q_i(t+\tau)\, V_i(t)\rangle = \iiint \left[\iint q_i' p(\mathbf{x}', \mathbf{q}', t' \,|\, \mathbf{x}, t)\, d\mathbf{x}'\, d\mathbf{q}'\right] u_i(\mathbf{x}, t)\, p(\mathbf{x}, \mathbf{q}, t \,|\, \mathbf{x}_0, t_0)\, d\mathbf{x}\, d\mathbf{q}$$

$$= -\kappa \iint \frac{\partial}{\partial x_i'}\theta(\mathbf{x}', t' \,|\, \mathbf{x}, t)\, u_i(\mathbf{x}, t)\, \theta(\mathbf{x}, t \,|\, \mathbf{x}_0, t_0)\, d\mathbf{x}\, d\mathbf{x}', \tag{A 5}$$

where we have made use of (A 1) and (A 2). We note that (A 5) is zero, since the integral with respect to $\mathbf{x}'$ vanishes, but that (A 4) is not in general zero for one particular realization of the turbulence. (The physical interpretation of this result is that, by (A 2), the value of q_i at a point $\mathbf{x}$ is correlated with $\mathbf{x}$ if the molecule has come from $\mathbf{x}_0$, and the continuum velocity at $\mathbf{x}'$ is also correlated with $\mathbf{x}$.) However, the average of (A 4) over the turbulent ensemble vanishes since

$$\int \frac{\partial}{\partial x_i}\theta(\mathbf{x}, t \,|\, \mathbf{x}_0, t_0)\, d\mathbf{x}_0 = 0.$$

Hence (dropping the suffix i)

$$\langle \overline{q(t)\, V(t+\tau)}\rangle = \langle \overline{q(t+\tau)\, V(t)}\rangle = 0,$$

provided, of course, $\tau \gg \tau_c$.

If this last condition is not satisfied, the covariances will not in general vanish. We can obtain an estimate of this effect as follows. The covariance does not vanish in a time of order τ_c because the molecule still remembers, so to speak, that it has come from a region where the fluid velocity differed by an amount of order $\lambda\omega$, where λ is the mean free path. (It is only differences in the fluid velocity that matter.) Thus,

$$\langle \overline{V(t)\, q(t+\tau)}\rangle = \lambda\omega\bar{q} f(\tau/\tau_c),$$

where $\bar{q}$ is the root-mean-square Brownian velocity and f is dimensionless, and similarly for the other covariance. A contribution of this type to $\mathfrak{S}(\tau)$ gives a contribution to D^2 of amount

$$2\lambda\omega\bar{q}\tau_c (t-t_0) \int_0^\infty f(\xi)\, d\xi,$$

when $t - t_0 \gg \tau_c$. Remembering that $\lambda\bar{q}/\kappa = O(1)$, we see that this is negligible compared with $2\kappa(t-t_0)$, the direct effect of molecular diffusion. Similarly, the difference between $\langle q(t)\, q(t+\tau)\rangle$ and the value it would have in a fluid at rest gives rise to an effect of the same order of magnitude.

Finally, a comment seems appropriate on the difficulty of deriving the expression (2.7) from formal manipulation of the diffusion equation. The point seems to be that the θ in (2.10) is really a probability, whereas the θ in the diffusion equation is a concentration. The two are the same only if $\omega\tau_c \ll 1$, and so it appears that formal manipulation of the diffusion equation, without explicit use in some way (not yet clear) of the condition $\omega\tau_c \ll 1$, will not give (2.7).

I wish to thank Dr T. H. Ellison for the benefit of a lengthy correspondence, in which a fallacy in earlier arguments, in particular the non-vanishing of the covariance $\langle q(t)\, V(t+\tau)\rangle$, was made clear to me.

REFERENCES

Batchelor, G. K. & Townsend, A. A. 1956 Article in *Surveys in Mechanics*, p. 352. Cambridge University Press.

Mickelsen, W. R. 1960 *J. Fluid Mech.* **7**, 397.

Taylor, G. I. 1921 *Proc. Lond. Math. Soc.* **20**, 196.

Townsend, A. A. 1951 *Proc. Roy. Soc.* A, **209**, 418.

Townsend, A. A. 1954 *Proc. Roy. Soc.* A, **224**, 487.

The compressible viscous heat-conducting vortex

By LESLIE M. MACK

Jet Propulsion Laboratory, California Institute of Technology, Pasadena, California

(Received 12 November 1959)

The plane, steady, laminar vortex flow of a viscous, heat-conducting perfect gas is treated. Simple relations are obtained for the flow quantities in the irrotational vortex, for arbitrary Prandtl numbers. When the Prandtl number is $\frac{1}{2}$, the irrotational vortex is also isentropic. When the temperature dependence of the viscosity coefficient is taken into account, the vortex flow is rotational. An exact solution for the rotational vortex is obtained which is suitable for numerical evaluation by successive approximations. Distributions of velocity, temperature, pressure, density, and stagnation temperature through the rotational vortex are given for a typical case.

1. Introduction

This paper treats the generalization of the potential vortex to a vortex in a viscous, heat-conducting, perfect gas. Such a vortex can be generated by a circular cylinder rotating in a fluid of infinite extent initially at rest. The final steady-state flow is a vortex. This vortex is to be distinguished from one driven by a radial flow carrying angular momentum inward.

When the rotational speed of the driving cylinder is low, the temperature variation across the vortex is small and the viscosity coefficient can be assumed constant. Then the flow is irrotational even in a viscous fluid, but is not, in general, isentropic. The irrotational isentropic solution is a special case of the spiral flow of Taylor (1930). Taylor gave an expression for the minimum radius of the vortex. However, even for irrotational flow, viscosity and heat conduction influence the temperature distribution, and the question to be answered is whether or not an isentropic vortex is possible in a real gas.

When the rotational speed of the driving cylinder is high, the temperature variation across the vortex is large and the temperature dependence of the viscosity coefficient must be taken into account. With a variable viscosity coefficient, the vortex is no longer irrotational. The details of the rotational vortex, and particularly the manner in which the distribution of the flow quantities differs from the irrotational vortex, are investigated in the following sections.

2. Equations of motion

The equations of motion for the two-dimensional vortex flow will now be developed. The streamlines are concentric circles. There is a single co-ordinate, r, the radius, and a single velocity component, v, the tangential velocity. The

flow is laminar and the tangential momentum equation has no inertia terms or pressure-gradient term. This equation is

$$\frac{d}{dr}\left[r^3\mu\frac{d}{dr}\left(\frac{v}{r}\right)\right] = 0, \tag{2.1}$$

where μ is the viscosity coefficient, a function of temperature. The shear stress is

$$\tau = \mu r\frac{d}{dr}\left(\frac{v}{r}\right), \tag{2.2}$$

and the first integral of (2.1) can be written

$$G = 2\pi r^2\tau = \text{const.} \tag{2.3}$$

G is the viscous torque for unit length normal to the plane of flow. From (2.1) it is apparent that for constant μ the irrotational velocity distribution $v \sim 1/r$ is still a solution. However, when μ varies along the radius, an irrotational solution is no longer possible.

The radial momentum equation equates the force resulting from the pressure gradient to the centrifugal force, and is

$$\frac{dp}{dr} = \frac{\rho v^2}{r}, \tag{2.4}$$

where p is the pressure and ρ is the density.

In the absence of convection terms the only two terms left in the energy equation are the work done by the shear stress and the heat transferred by conduction. The equation is

$$\frac{d}{dr}\left[kr\frac{dT}{dr} + \mu r^2 v\frac{d}{dr}\left(\frac{v}{r}\right)\right] = 0, \tag{2.5}$$

where T is the temperature, and k is the coefficient of thermal conductivity, a function of temperature. The first integral of (2.5) can be written

$$\frac{di}{dr} + \sigma v r\frac{d}{dr}\left(\frac{v}{r}\right) = -\frac{\text{const.}}{2\pi\mu r}\sigma, \tag{2.6}$$

where $\sigma = c_p\mu/k$, the Prandtl number, has been introduced. The temperature has been replaced by i, the specific enthalpy, and c_p, the specific heat at constant pressure, by use of the perfect gas relation $i = \int c_p dT$. The heat transfer rate per unit length normal to the plane of flow is

$$q = -2\pi r k\frac{dT}{dr}. \tag{2.7}$$

With (2.7) and (2.3), (2.6) can be written

$$q = \omega G + \text{const.}, \tag{2.8}$$

where ω is the angular velocity. For the vortex, $\omega \to 0$ at infinity and the integration constant in (2.6) and (2.8) is identified as the heat transfer at infinity. The term with the integration constant in (2.6) also appears in steady-state heat transfer through a solid and leads to a logarithmic temperature distribution. Consequently, the steady-state vortex extending to infinity must have zero heat

transfer at infinity. Then $q = \omega G$ at every radius, and at the cylinder driving the flow an amount of heat must be withdrawn per second just equal to the power required to maintain the flow.

The system of equations is completed by the equation of state for a perfect gas

$$p = \rho RT, \tag{2.9}$$

where R is the gas constant per unit mass.

The boundary conditions are as follows

$$v = 0 \quad \text{at} \quad r = \infty. \tag{2.10}$$

This condition eliminates the solid-body solution. The requirement of zero heat transfer at infinity is met by setting the integration constant in (2.6) equal to zero. At some radius, r_1, the velocity and temperature are given,

$$v = v_1, \quad T = T_1 \quad \text{at} \quad r = r_1. \tag{2.11}$$

Alternatively, the Mach number M_1 and temperature can be given. Two convenient choices for r_1 are the radius of the cylinder that drives the flow, and the sonic radius.

3. Irrotational solution

When μ is a constant, the tangential momentum equation (2.1) can be integrated to give, with (2.10) and (2.11),

$$v = \frac{v_1 r_1}{r}. \tag{3.1}$$

This is the familiar irrotational-vortex velocity distribution. With the introduction of dimensionless quantities, (3.1) can be written

$$v^* = \frac{1}{r^*}, \tag{3.2}$$

where the asterisk means that the quantity is divided by its value at $r = r_1$.

With the velocity distribution known, the energy equation (2.6) can be integrated. The result, with the integration constant in (2.6) zero and Prandtl number constant, is

$$i + \sigma v^2 = i_1 + \sigma v_1^2. \tag{3.3}$$

With the further assumption of constant specific heat, (3.3) can be written in terms of the temperature. The result, in dimensionless form, is

$$T^* = 1 + (\gamma - 1)\,\sigma M_1^2 \left(1 - \frac{1}{r^{*2}}\right), \tag{3.4}$$

where γ is the specific heat ratio. It can be noted from (3.4) and (3.2) that only the Mach number at r_1 has to be specified for the irrotational solution. This is true as long as both c_p and σ are constant.

The pressure-temperature, density-pressure, stagnation-temperature, and stagnation-pressure relations can all be readily obtained. They are:

$$p^* = T^{*\gamma/(\gamma-1)\,\gamma/2\sigma(\gamma-1)} \tag{3.5}$$

$$\rho^* = p^{*(1/\gamma)[\gamma-(\gamma-1)\,2\sigma]}, \tag{3.6}$$

$$\frac{T_0}{T_\infty} = \frac{1+\frac{1}{2}(\gamma-1)\,M^2}{1+(\gamma-1)\,\sigma M^2}, \tag{3.7}$$

$$\frac{p_0}{p_\infty} = \left(\frac{T_0}{T_\infty}\right)^{\gamma/(\gamma-1)} \left(\frac{T_\infty}{T}\right)^{[\gamma/(\gamma-1)][1-(1/2\sigma)]}. \tag{3.8}$$

The subscript ∞ refers to conditions at $r = \infty$. The stagnation temperature and pressure are defined in the usual manner. Since the gas is at rest at infinity, both p_∞ and T_∞ are also local stagnation values.

These results being out the strong dependence of the flow quantities on the Prandtl number. The case of $\sigma = \frac{1}{2}$ is of particular interest because for this value of the Prandtl number (3.5) and (3.6) reduce to the isentropic relations, and p_0 and T_0 are constant. This result identifies the isentropic solution as a special case of the irrotational vortex flow of a viscous, heat-conducting perfect gas.

For a given M_1 the solution obtained applies only outside of a minimum radius given by (3.4) for $T = 0$. By (3.5) and (3.6), p and ρ (for $\sigma < \frac{1}{2}\gamma/(\gamma-1)$) are also zero at this radius. The expression for $r^*_{\min}$ is

$$r^*_{\min} = \sqrt{\left(\frac{(\gamma-1)\,\sigma M_1^2}{1+(\gamma-1)\,\sigma M_1^2}\right)}. \tag{3.9}$$

If r_1 is the sonic radius, $r^*_{\min}$ depends only on γ and σ. With $\gamma = 1{\cdot}40$ and $\sigma = 0{\cdot}70$, $r^*_{\min} = 0{\cdot}468$; for the isentropic vortex $r^*_{\min} = 0{\cdot}408$. The supersonic region of a vortex is, therefore, restricted to an annulus not much wider than the diameter of the driving cylinder. The existence of this limiting radius does not, of course, mean that a steady vortex flow with a hole in the middle actually exists. The vortex must be associated with a means of producing it, which in the absence of a radial flow carrying angular momentum inward can only be a rotating cylinder. The vortex flow then is always outside of a solid boundary. Any size rotating cylinder will produce a vortex. It is only when a Mach number is specified at a fixed radius that there is a lower limit to the size of the cylinder that can satisfy this condition.

4. Rotational solution

The irrotational solution can be expected to be accurate only for low Mach numbers where the temperature variation across the vortex is not large. For the higher Mach numbers the temperature dependence of μ must be taken into account. The variable μ solution will be set up in such a way that μ enters essentially as a correction factor to the irrotational solution. For this purpose a new variable, ξ, is introduced to replace r. This transformation permits the integration of (2.1), the tangential momentum equation, for the angular velocity. It is apparent that this variable is

$$d\xi = -\frac{dr}{\mu r^3}. \tag{4.1}$$

The expression for r in terms of ξ is

$$\frac{1}{2r^2} = \int_0^{\xi} \mu \, d\xi, \tag{4.2}$$

where the lower integration limit has been chosen so that $\xi = 0$ at $r = \infty$.

When μ is constant, ξ equals the inverse square of the radius except for a constant factor. The dimensionless irrotational velocity and temperature in terms of ξ are

$$v^* = \sqrt{\xi^*}, \tag{4.3}$$

and

$$T^* = 1 + (\gamma - 1)\sigma M_1^2(1 - \xi^*), \tag{4.4}$$

where ξ has been made dimensionless with respect to ξ_1, which is defined by (4.2) at $r = r_1$.

The rotational correction factors to (4.3) and (4.4) are readily found. Integration of (2.1) yields

$$\frac{v^*}{r^*} = \xi^*. \tag{4.5}$$

If now the circulation, $\Gamma = 2\pi r v$, is introduced, (4.5) and (4.2) give the result that

$$\Gamma^* = \frac{\displaystyle\int_0^1 \mu^* d\xi^*}{\dfrac{1}{\xi^*}\displaystyle\int_0^{\xi^*} \mu^* d\xi^*}. \tag{4.6}$$

The circulation then varies inversely with the average value of μ^* between infinity and ξ^*, the average being taken over ξ^*. Since the temperature increases monotonically from the driving cylinder to infinity, μ does likewise. Therefore, the average μ^* increases away from the cylinder and the circulation decreases. The integral $\displaystyle\int_0^{\xi^*} \mu^* d\xi^*$ will be referred to as the μ^* integral.

The relation between ξ and r, (4.2), can be written in dimensionless form in terms of Γ^* as

$$\xi^* = \frac{\Gamma^*}{r^{*2}}. \tag{4.7}$$

The velocity, from (4.5) and (4.7), is

$$v^* = \sqrt{\xi^*}\sqrt{\Gamma^*}, \tag{4.8}$$

and the rotational velocity is just the irrotational velocity at the same ξ^* multiplied by $\sqrt{\Gamma^*}$.

The energy equation (2.6), with the integration constant zero, can be manipulated into the following form

$$\frac{di}{d\xi} + \sigma \frac{v^2}{\xi} = 0. \tag{4.9}$$

With constant specific heat and Prandtl number, (4.9) gives, with the use of (4.8),

$$T^* = 1 + (\gamma - 1)\sigma M_1^2(1 - \xi^*)\left(\frac{1}{1 - \xi^*}\int_{\xi^*}^1 \Gamma^* d\xi^*\right). \tag{4.10}$$

The correction factor to the irrotational temperature distribution is the average circulation. The average here is taken between the reference point and ξ^*.

Because (4.8) and (4.10) contain μ, the rotational solution is, in general, dependent on T_1 in addition to M_1.

With the velocity and temperature known, the pressure can be obtained from (2.4), the radial momentum equation, and the equation of state. The result is

$$\log p^* = \tfrac{1}{2}\gamma M_1^2 \int_{\xi^*}^1 \frac{v^{*2}}{T^*} \frac{\mu^*}{\int_0^{\xi^*} \mu^* d\xi^*} d\xi^*. \tag{4.11}$$

From (2.3), (4.5) and (4.2) the expression for the torque is found to be

$$G = -4\pi\mu_1 v_1 r_1 \int_0^1 \mu^* d\xi^*, \tag{4.12}$$

where the negative sign appears because the cylinder exerts torque on the gas. If (4.12) is written as

$$G = -4\pi\bar{\mu} v_1 r_1, \tag{4.13}$$

where

$$\bar{\mu} = \mu_1 \int_0^1 \mu^* d\xi^*, \tag{4.14}$$

then (4.13) is identical in form to the expression for the torque of an irrotational vortex. Consequently, the torque required to maintain a rotational vortex is equal to that required for a related irrotational vortex. If r_1 is the radius of the driving cylinder, the related vortex has circulation equal to that of the rotational vortex at the cylinder, and has a constant viscosity coefficient equal to the average rotational viscosity coefficient, the average being taken over ξ^*.

The solution of the rotational vortex has been reduced to the evaluation of the circulation, which, by (4.6), means the evaluation of the μ^* integral. The method of successive approximations is very appropriate here for a numerical solution since the irrotational solution is available for the initial approximation. For supersonic Mach numbers, the irrotational solution is not a close first approximation, and something better would be useful. Since the irrotational temperature varies linearly with ξ and $\mu \sim T$ is often a useful approximation, the assumption of a linear relation between μ and ξ is suggested. Therefore, let

$$\mu^* = \mu_\infty^* - (\mu_\infty^* - 1)\,\xi^*. \tag{4.15}$$

With (4.15) the μ^* integral can be evaluated and the velocity and temperature distributions obtained. The results are

$$\frac{1}{r^{*2}} = \xi^* \left(\frac{1-\delta\xi^*}{1-\delta}\right), \quad v^* = \sqrt{\xi^*}\left(\frac{1-\delta}{1-\delta\xi^*}\right)^{\frac{1}{2}}, \tag{4.16}$$

$$T^* = 1 + (\gamma-1)\,\sigma M_1^2 \frac{1-\delta}{\delta} \log \frac{1-\delta\xi^*}{1-\delta}, \tag{4.17}$$

where δ is defined by

$$\delta = \frac{1}{2}\frac{\mu_\infty - \mu_1}{\mu_\infty}.$$

The use of δ as a parameter is equivalent to the specification of T_1 and T_∞ as the boundary conditions rather than T_1 and M_1. M_1 is determined from (4.18) at $\xi^* = 0$. If T_1 and M_1 are retained as the boundary conditions, then a trial-and-error process involving (4.17) and the viscosity law is necessary to find δ.

5. Numerical results and discussion

The numerical computations have been performed for air using the Sutherland viscosity law,

$$\mu \times 10^7 = \frac{145{\cdot}8T^{\frac{3}{2}}}{T + 110{\cdot}4}, \tag{5.1}$$

where T is in °K, and μ is in poises. The constants are those given by Hilsenrath *et al.* (1955). For $T < 110{\cdot}4$ °K, μ is taken proportional to T. The ratio of specific heats, γ, is 1·40, and the Prandtl number is 0·70 unless otherwise noted.

A convenient way of presenting the distribution of flow quantities through the vortex is to fix the temperature at the sonic radius and then calculate the temperature, pressure, etc., as functions of the radius from the minimum radius to infinity. The temperature distribution according to the exact solution is shown

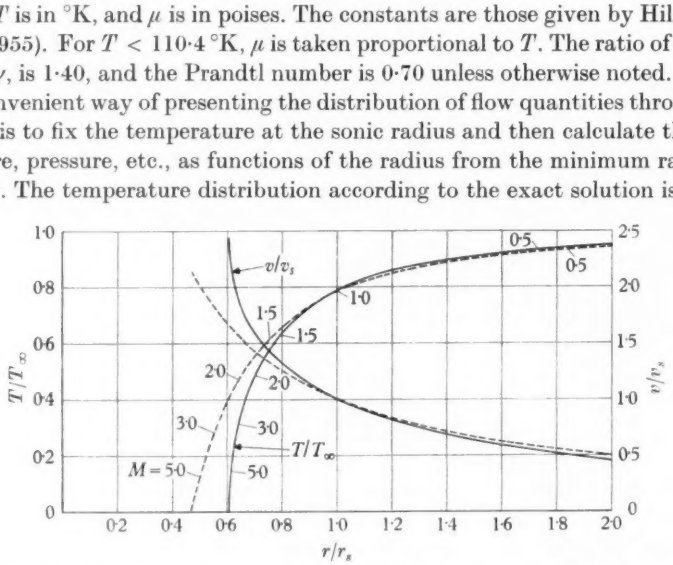

FIGURE 1. Vortex temperature and velocity distribution. $\sigma = 0{\cdot}70$, $\gamma = 1{\cdot}40$. ——, Exact rotational solution, $T_s = 800$ °K; – – –, irrotational solution.

in figure 1 for a sonic temperature of 800 °K. The subscript s refers to sonic conditions. Also shown is the irrotational solution with the same Prandtl number. This solution is independent of the temperature. The local Mach numbers are also shown in the figure. It can be seen that although for $r/r_s < 0{\cdot}8$ the two curves diverge considerably, at the same Mach number the temperatures are roughly the same. The minimum radius obtained from the rotational solution is larger than obtained from the irrotational solution, even further narrowing the supersonic region of the vortex.

The velocity distributions are also shown in figure 1. The rotational velocity distribution is characterized by having a steeper slope than the irrotational distribution. This is a result of the necessity to maintain constant torque even though the viscosity coefficient decreases with decreasing radius. Ultimately, at the minimum radius where $\mu = 0$, the velocity slope is infinite.

The pressure distributions are shown in figure 2. In contrast to the situation with the temperature, the irrotational pressure is much lower than the rotational pressure at the same Mach number. Since the irrotational isentropic pressure is still lower, the stagnation pressure of the rotational vortex must increase sharply with decreasing radius in the supersonic region. The exact solution has the interesting feature that at the minimum radius, where T is zero, p is not zero.

This follows directly from (4.11). When μ is constant near $T = 0$, p is also zero because the integral has a logarithmic singularity there. However, when μ goes to zero with any power of T, the singularity is not present and p does not go to zero. A consequence of this situation is that the density must become infinite as shown in figure 2. Since the assumption of a perfect gas is not valid under this circumstance, the solution is physically meaningless near the minimum radius. However, the density minimum occurs in a region where the solution is valid. For instance, with the sonic temperature of 800 °K, the density minimum is at 168 °K. The reason for the density minimum can be found by examining the equation of state. Logarithmic differentiation of (2.9) gives

$$d(\log \rho^*) = d(\log p^*)\left[1 - \frac{d(\log T^*)}{d(\log p^*)}\right]. \tag{5.2}$$

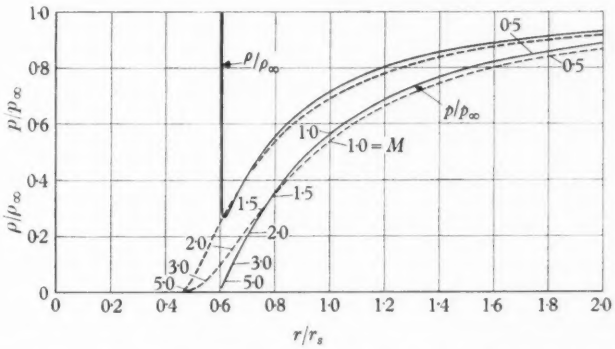

FIGURE 2. Vortex pressure and density distribution. $\sigma = 0{\cdot}70$, $\gamma = 1{\cdot}40$. ——, Exact rotational solution, $T_s = 800$ °K; – – –, irrotational solution.

Therefore, the sign of the density change is opposite to the sign of the pressure change if

$$\frac{d(\log T^*)}{d(\log p^*)} > 1. \tag{5.3}$$

From (4.10), (4.11) and (4.8) this criterion can be written

$$\mu^*\xi^* \Big/ \int_0^{\xi^*} \mu^* d\xi^* < 2\sigma \frac{\gamma - 1}{\gamma}. \tag{5.4}$$

The left-hand side of (5.4) is zero at the minimum radius and unity at infinity ($\xi^* = 0$). The right-hand side is always less than one for a gas. For the irrotational vortex (5.4) can never be satisfied, and the density decreases with the pressure throughout the vortex as shown in figure 2. However, for the rotational vortex, as the radius decreases, a point is reached below which (5.4) is always satisfied and the density increases, even though the pressure is decreasing.

The importance of the Prandtl number in this type of vortex flow is emphasized by the results shown in figure 3 where stagnation temperature distributions outside of a cylinder rotating with $M_1 = 2{\cdot}75$ and $T_1 = 100$ °K are shown for Prandtl numbers between 0·50 and 0·80. The linear μ solution was used for the calculation as it gives a result within 1 % of the exact solution for these conditions.

The quantity plotted is T_0/T_∞, and with T_1 fixed, T_∞ increases about 30% as the Prandtl number increases from 0·50 to 0·80. The abscissa is taken as $1/r^{*2}$ in order to include the entire flow on the plot, and also because this variable equals ξ^* for irrotational flow. The location of the T_0 minimum can be related directly to the Prandtl number. From the definition of T_0 and (4.10), an expression for T_0^* is

$$T_0^* = 1 + \frac{\gamma - 1}{2} M_1^2 \left(v^{*2} + 2\sigma \int_{\xi^*}^{1} \Gamma^* d\xi^* \right), \tag{5.5}$$

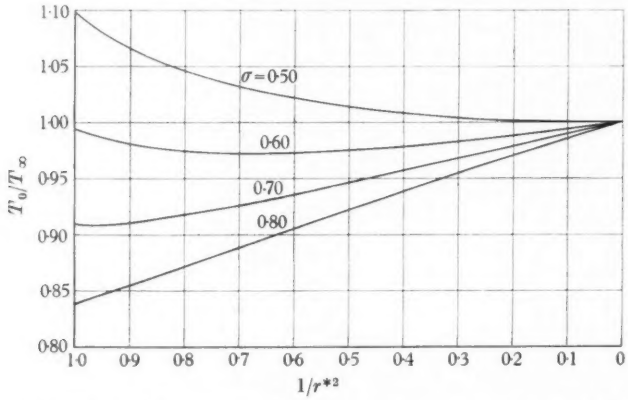

FIGURE 3. Effect of Prandtl number on stagnation temperature distribution. $M_1 = 2{\cdot}75$, $T_1 = 100$ °K.

and with (4.8) and (4.6) the derivative can be written

$$\frac{dT_0^*}{d\xi^*} = \frac{\gamma - 1}{2} M_1^2 \Gamma^* \left[2(1-\sigma) - \mu^* \xi^* \Big/ \int_0^{\xi^*} \mu^* d\xi^* \right]. \tag{5.6}$$

The second quantity in brackets has already appeared in (5.4). The first quantity varies from unity at $\sigma = \frac{1}{2}$ to zero at $\sigma = 1$. Therefore, T_0^* has a minimum at some radius of the complete vortex for $\frac{1}{2} < \sigma < 1$, and the location of this minimum depends directly on the Prandtl number. Whether or not the minimum occurs in the actual flow field depends on the surface conditions of the driving cylinder. For $\sigma = \frac{1}{2}$, T_0^* has zero slope at infinity; for $\sigma = 1$, it has zero slope at the minimum radius. The $\sigma = \frac{1}{2}$ result is just another version of the irrotational, isentropic solution. It is apparent that there is no special value of the Prandtl number for which the rotational vortex has constant stagnation temperature. Likewise there is no Prandtl number for which the rotational vortex is isentropic.

This paper presents of one phase of research carried out at the Jet Propulsion Laboratory, California Institute of Technology, under joint sponsorship of the Department of the Army, Ordnance Corps, and the Department of the Air Force.

REFERENCES

HILSENRATH, J. *et al.* 1955. *Tables of Thermal Properties of Gases.* Circular no. 564, National Bureau of Standards, Washington.

TAYLOR, G. I. 1930 Recent work on the flow of compressible fluids. *J. Lond. Math. Soc.* **5**, 224–40.

Mass transport in the boundary layer at a free oscillating surface

By M. S. LONGUET-HIGGINS
National Institute of Oceanography, Wormley, Surrey

(Received 24 November 1959)

In a previous paper (1953*b*) it was shown theoretically that just below the boundary layer at the surface of a free wave the mass-transport gradient should be exactly twice that given by Stokes's irrotational theory. The present paper describes careful experiments which confirm the higher value of the gradient.

The results have an implication for any oscillatory boundary layer at the free surface of a fluid; such a boundary layer must generate a second-order mean vorticity which diffuses inwards into the interior of the fluid.

1. Introduction

Although it was Stokes (1847) who first theoretically predicted the existence of a mean forwards velocity of the particles (mass transport) in a water wave, only since the experimental work of Bagnold (1947) has it been realized that the mass-transport velocities may be very different quantitatively from those given by Stokes's irrotational theory. For example, Bagnold observed a strong forwards 'jet' close to the bottom, a phenomenon unaccountable on the hypothesis of irrotational motion. The whole distribution of the mass transport is in fact strongly influenced by viscous boundary layers both at the bottom and at the free surface, as was shown by the present author (1953*b*; this paper will be referred to as (I)).

The boundary-layer theory of (I) yielded two surprising results; first, that just above the boundary layer at the bottom the forward mass-transport velocity is independent of the viscosity and has the value

$$U = \frac{5}{4}\frac{a^2\sigma k}{\sinh^2 kh}, \tag{1.1}$$

where a denotes the amplitude of the waves at the surface, $2\pi/\sigma$ the wave period, $2\pi/k$ the wavelength and h the mean depth. This value is quite different from that obtained on the non-viscous theory of Stokes (1847).*

Secondly, just below the boundary layer at the *free surface* the vertical gradient of the mass-transport velocity is given by

$$\frac{\partial U}{\partial z} = -4a^2\sigma k^2 \coth kh, \tag{1.2}$$

* Stokes's theory is given partially in Lamb's *Hydrodynamics* (1932, Ch. 9); the mass-transport velocity is there derived only in the case of deep water ($kh \gg 1$).

z being measured vertically downwards. This is also independent of the viscosity and moreover is exactly twice the value given by Stokes.

The value (1.1) has been well verified by the recent experimental studies of Vincent & Ruellan (1957), Russell & Osorio (1958) and Allen & Gibson (1959), though with a considerable scatter of observations in the last case.*

On the other hand no careful verification has yet been attempted of the gradient (1.2), which may be no less important in determining the distribution of mass transport throughout the fluid. Partly, no doubt, this is due to the greater experimental difficulty in making measurements close to a moving surface, and partly also to the weak stability of the motion near the surface, which can be easily disturbed by external influences, as will be explained in § 4.

Our purpose is to describe some experiments designed to measure the velocity gradient near the free surface. These do in fact confirm equation (1·2) as against Stokes's prediction.

The opportunity is taken to correct a theoretical calculation of Harrison (1908) on the same subject. Harrison's corrected calculation leads also to equation (1.2) but over a more restricted range of the amplitude a.

The validity of (1.2) implies that a second-order vorticity is generated by the oscillatory boundary layer and is diffused inwards into the fluid, as described in § 5 below. Moreover, a similar phenomenon must occur in any fluid motion where there is a free oscillating boundary, even though the mean velocity is zero to the first order. The value of the vorticity ω generated by any free surface in this way is given by equation (6.12).

2. Theory of the boundary layer

A general theory for an oscillating free boundary has been given in § 8 of (I). Here we shall present a simplified version, relying however on (I) for some of the results quoted.

On account of the thinness of the boundary layer in relation to the usual amplitude of the waves it is desirable to take co-ordinates (s, n) measured along and normal to the free surface itself (and therefore moving with the fluid). The co-ordinate n is supposed to be directed normally inwards into the fluid. In the notation of (I) the components of velocity tangential and normal to the surface are written q_s, q_n and these are related to the stream function ψ by

$$(q_s, q_n) = \left(\frac{\partial \psi}{\partial n}, -\frac{1}{\eta}\frac{\partial \psi}{\partial s}\right), \tag{2.1}$$

where $\eta = 1 - n\kappa$ and κ denotes the curvature of the surface. The vorticity is equal to $\nabla^2\psi$ where

$$\nabla^2 \equiv \frac{1}{\eta}\left[\frac{\partial}{\partial s}\left(\frac{1}{\eta}\frac{\partial}{\partial s}\right) + \frac{\partial}{\partial n}\left(\eta\frac{\partial}{\partial n}\right)\right]. \tag{2.2}$$

* Vincent & Ruellan, as well as Allen & Gibson, actually compared their observations with the predicted *maximum* velocity in the boundary layer, which is about 10 % greater than (1·1).

An extension of the result (1·1) to the case of turbulent flow is given by the author in an appendix to the paper of Russell & Osorio (1958).

It is supposed that q_s, q_n and ψ can be expanded asymptotically in the series

$$\left.\begin{aligned} q_s &= \epsilon q_{s1} + \epsilon^2 q_{s2} + \ldots, \\ q_n &= \epsilon q_{n1} + \epsilon^2 q_{n2} + \ldots, \\ \psi &= \epsilon \psi_1 + \epsilon^2 \psi_2 + \ldots, \end{aligned}\right\} \tag{2.3}$$

where ϵ is a small parameter which may tend to zero and where the mean values of q_{s1}, q_{n1} are identically zero. The mass-transport velocity is then shown in (I) § 6 to be of order ϵ^2; its stream function is denoted by $\epsilon^2\Psi$.

The case when the stresses vanish at the surface $n = 0$ is included in the discussion in (I) § 8. By applying a 'boundary-layer' approximation it is shown that ψ_1 satisfies the differential equation

$$\left(\frac{\partial}{\partial t} - \nu \frac{\partial^2}{\partial n^2}\right) \nabla^2 \psi_1 = 0. \tag{2.4}$$

Assuming that the tangential stress at the surface vanishes we have the boundary condition

$$\nabla^2 \psi_1 = -2 \frac{\partial q_{n1}}{\partial s} \quad (n = 0) \tag{2.5}$$

(derived from (220) of (I) by setting $p_{ns}^{(0)} = 0$ and $\kappa_0 = 0$). When the motion is simple-harmonic with angular frequency σ the appropriate solution of (2.4) and (2.5) is

$$\nabla^2 \psi_1 = -2 \frac{\partial q_{n1}^{(0)}}{\partial s} e^{-\alpha n}, \tag{2.6}$$

where $q_{n1}^{(0)}$ denotes the value of q_{n1} at $n = 0$ and

$$\alpha = \frac{1+i}{\delta}, \qquad \delta = (2\nu/\sigma)^{\frac{1}{2}}. \tag{2.7}$$

It is understood that in (2.6) the real part of the right-hand side is to be taken. So the first-order vorticity $\nabla^2\psi_1$ vanishes exponentially inwards, in a distance of order δ.

The differential equation satisfied by Ψ is given by (211) of (I) (in which V_{s1} is to be set equal to zero). We have

$$\frac{\partial^4 \Psi}{\partial n^4} = 4 \int \frac{\partial^2}{\partial n^2} \nabla^2 \psi_1 \, dt \, \frac{\partial q_{s1}^{(0)}}{\partial s}, \tag{2.8}$$

where a bar denotes mean values with respect to the time. On integrating from outside the boundary layer, where $\partial^3\Psi/\partial n^3$ is assumed to be relatively small, we have

$$\frac{\partial^3 \Psi}{\partial n^3} = 4 \int \frac{\partial}{\partial n} \nabla^2 \psi_1 \, dt \, \frac{\partial q_{s1}^{(0)}}{\partial s}. \tag{2.9}$$

At the free surface $n = 0$, the boundary condition for Ψ is that

$$\frac{\partial^2 \Psi}{\partial n^2} = 0 \quad (n = 0) \tag{2.10}$$

(see equation (218) of (I)), and so from (2.9) and (2.10)

$$\frac{\partial^2 \Psi}{\partial n^2} = 4 \int (\nabla^2 \psi_1)_0^n \, dt \, \frac{\partial q_{s1}^{(0)}}{\partial s}. \tag{2.11}$$

In the case of simple-harmonic motion, when $\nabla^2\psi_1$ is given by (2.6) we have

$$\frac{\partial^2\Psi'}{\partial n^2} = \frac{4}{i\sigma}\frac{\partial q_{n1}^{(0)}}{\partial s}\frac{\partial q_{s1}^{(0)*}}{\partial s}(1-e^{-\alpha n}), \tag{2.12}$$

where a star denotes the complex conjugate quantity and the real part of the product is to be taken. Hence, just beyond the boundary layer ($n \gg \delta$) we have

$$\frac{\partial^2\Psi'}{\partial n^2} = \frac{4}{i\sigma}\frac{\partial q_{n1}^{(0)}}{\partial s}\frac{\partial q_{s1}^{(0)*}}{\partial s} \quad (n \gg \delta), \tag{2.13}$$

a value independent of the viscosity.

Now in the case of progressive gravity waves in water of uniform depth the orbital velocities at the surface are given by

$$\left.\begin{aligned} \epsilon q_{s1}^{(0)} &= a\sigma\coth kh\, e^{i(\sigma t-ks)}, \\ \epsilon q_{n1}^{(0)} &= ia\sigma\, e^{i(\sigma t-ks)}, \end{aligned}\right\} \tag{2.14}$$

approximately, so that (2.12) and (2.13) become

$$\epsilon^2\frac{\partial^2\Psi'}{\partial n^2} = 4a^2\sigma k^2\coth kh(1-e^{-n/\delta}\cos n/\delta) \tag{2.15}$$

and

$$\epsilon^2\frac{\partial^2\Psi'}{\partial n^2} = -4a^2\sigma k^2\coth kh \quad (u \gg \delta). \tag{2.16}$$

Since $\epsilon^2\partial\Psi'/\partial n$ is equal to the mean tangential component of mass transport ((I), § 6) and since n is approximately vertical, equation (2.16) is equivalent to (1.2).

As already remarked, this result represents exactly twice the gradient given by the irrotational theory of Stokes (1847).

3. Digression on a result of Harrison

It was pointed out to me by Professor P. S. Eagleson that a conclusion apparently different from the above was obtained by Harrison (1908). Harrison's method consisted of a direct expansion of the equations of motion and boundary conditions in terms of rectangular co-ordinates (x, z). This method has the disadvantage of being valid only for waves whose amplitude a is small compared with the thickness δ of the boundary layer. Nevertheless, since the range of validity of equation (2.16) certainly includes such small amplitudes, one would expect Harrison's result to agree with equation (2.16) over the restricted range.

Another formal difference between Harrison's solution and ours is that we have assumed the motion to be periodic in time, whereas Harrison allows for a slight exponential decrement proportional to $\nu k^2 t$. It can, however, be shown that such a slight decrement, or one proportional to $(\nu/\sigma)^{\frac{1}{2}}k^2x$, does not affect the boundary-layer theory outlined in § 2.

Translated into our notation, Harrison's expression for the elevation of the free surface in waves on deep water is

$$\begin{aligned} -z = {} & a\, e^{-2\nu k^2 t}\cos(kx-\sigma t) \\ & + a^2 k\, e^{-4\nu k^2 t}[\tfrac{1}{2}\cos 2(kx-\sigma t) - k(\nu^2/4gk)^{\frac{1}{4}}\sin 2(kx-\sigma t)] \end{aligned} \tag{3.1}$$

and for the mass-transport velocity (p. 115)

$$U = a^2\sigma k\, e^{-4\nu k^2 t} \times [e^{-2kz} + \tfrac{1}{2}k\delta\{4(\cos z/\delta - \sin z/\delta)\, e^{-(k+\delta^{-1})z} - \sin 2kz\} + \nu k^2/\sigma\{4\sin z/\delta\, e^{-(k+\delta^{-1})z} - 3e^{-2z/\delta}\}] \tag{3.2}$$

terms of higher order in ν being neglected. (Harrison's $\beta, \lambda, \mu, p, y$ are equivalent to our a, δ^{-1}, δ^{-1}, $-\sigma$, $-z$.) On differentiation with respect to z this gives us for the terms of highest order

$$\frac{\partial U}{\partial z} = -2a^2\sigma k^2(1 - 2\, e^{-z/\delta}\cos z/\delta) \tag{3.3}$$

which is not in agreement with (2.15). (The slight exponential decrement $e^{-4\nu k^2 t}$ is ignored.)

An examination of Harrison's analysis reveals the source of the discrepancy. For his second boundary condition on p. 111 he has assumed that the stress component p_{xy} vanishes at the free surface. This is incorrect, for in fact it is not p_{xy} but p_{ns} which must vanish, and the two differ by the second-order quantity

$$4\mu\frac{\partial\eta}{\partial x}\frac{\partial^2\psi}{\partial x\,\partial y}, \tag{3.4}$$

where $z = -\eta$ denotes the equation of the free surface. Hence to the left-hand side of his equation (12) should be added a term

$$2pk^2\beta^2\, e^{2\alpha t}. \tag{3.5}$$

This would add to his expression for U on p. 115 a term

$$-pk\beta^2\sin 2ky\, e^{2\alpha t}, \quad \sim -a^2\sigma k\, e^{-4\nu k^2 t}\sin 2kz, \tag{3.6}$$

whence the gradient of U, for values of z comparable with δ, would be

$$\frac{\partial U}{\partial z} = -2a^2\sigma k^2(2 - 2e^{-z/\delta}\cos z/\delta) \tag{3.7}$$

in agreement with (2.15).

Doubtless the reason why Harrison overlooked his algebraical slip was that it happens by chance to bring the value for $(\partial U/\partial z)_{z\gg\delta}$ into exact agreement with the irrotational theory of Stokes, as might at first sight have been expected.

4. Observations

The actual measurement of velocity gradients near the free surface is a somewhat delicate matter owing not only to the movement of the surface itself but to the external influences by which it is easily affected. The presence of grease or other impurity in the form of a thin surface film may completely alter the gradient by restricting the free tangential motion of the particles and producing a forwards jet, as in the boundary layer at the bottom. Turbulent currents in the air may have a disturbing influence; and very slight temperature changes can produce strong velocity gradients associated with density currents; for if the length of the tank or wave system is restricted, the forwards mass transport at

one level must be compensated by a backwards flow at other levels; hence any temperature stratification will tend to intensify the horizontal shearing.

Further, the presence of obstacles in the water, even the vertical walls of a measuring tank, will alter the distribution of mass transport in the neighbourhood. The observations must therefore be made far enough from such obstacles for their effect to be negligible.

Lastly, it is extremely important to ensure that the wave motion is purely sinusoidal. In relatively deep water, for example ($\coth kh \doteqdot 1$) equation (1.2) shows that $\partial U/\partial z$ is proportional to $a^2\sigma k^2$, that is to σ^5 since $\sigma^2 \doteqdot gk$. If any second harmonic, of amplitide a', is present in the wave motion its effect on the velocity gradient will be in the ratio

$$32a'^2/a^2. \tag{4.1}$$

Even if a'/a is as little as 1/10 this will be sufficient to increase the observed velocity gradient by 32 %. In shallow water waves, however, the relative effect is correspondingly less.

For the purpose of the experiments the wind-wave tank at the Hydraulics Research Station, Wallingford, was kindly made available. A full description of the apparatus is given in the paper by Russell & Osorio (1958). The tank is 185 ft. long, 4 ft. wide and has a maximum depth of 22 in. The wave generator is of a paddle type with a fixed or movable hinge at the bottom. The wave absorber consists of a shingle beach, at a slope of about 1 in 10. All the present observations were made from the centre window of the tank, which is about 90 ft. from the wave generator. The tank is covered, and is fitted with a fan capable of drawing air over the surface in the direction of the beach, at a mean speed of about 25 ft./s.

In preliminary trials of the wavemaker it was found that on switching off the motor, and after the main group of waves had passed the point of observation half-way down the tank, there persisted a train of waves of twice the frequency but of smaller amplitude, until their group-velocity in turn has carried them past the point of observation. The existence of this second harmonic was attributed to the form of linkage used in the wave generator which had in fact been designed so as to increase the velocity of the forward stroke compared with that of the backward stroke. The linkage was therefore modified with the result that the amplitude of the second harmonic at the point of observation was reduced to about 4 % of that of the first harmonic. The error corresponding to (4.1) was thus reduced to about 5 %.

Method of observation

A grid of lines was drawn (see figure 1) at an angle $\tan^{-1} 2$ to the vertical, and was attached to a metal sheet on the far side of the tank, in the plane of motion. A drop of black ink (Waterman's ink, diluted 3 : 1) was let fall from a syringe at a height of about 18 in. above the surface, between the viewer and the grid of lines. The drop penetrated about 1 cm below the surface, leaving a nearly vertical streak. Owing to the velocity gradient the streak gradually became inclined (figure 1), and the time τ taken for its mean inclination to become parallel to

the grid of lines was measured with a stop-watch. The velocity gradient was then taken to be

$$\frac{\partial U}{\partial z} = \frac{2}{\tau}. \tag{4.2}$$

The height $2a$ of the waves was measured against a grid on the near window of the tank, and the wave period was measured over 20 cycles with a stop-watch.

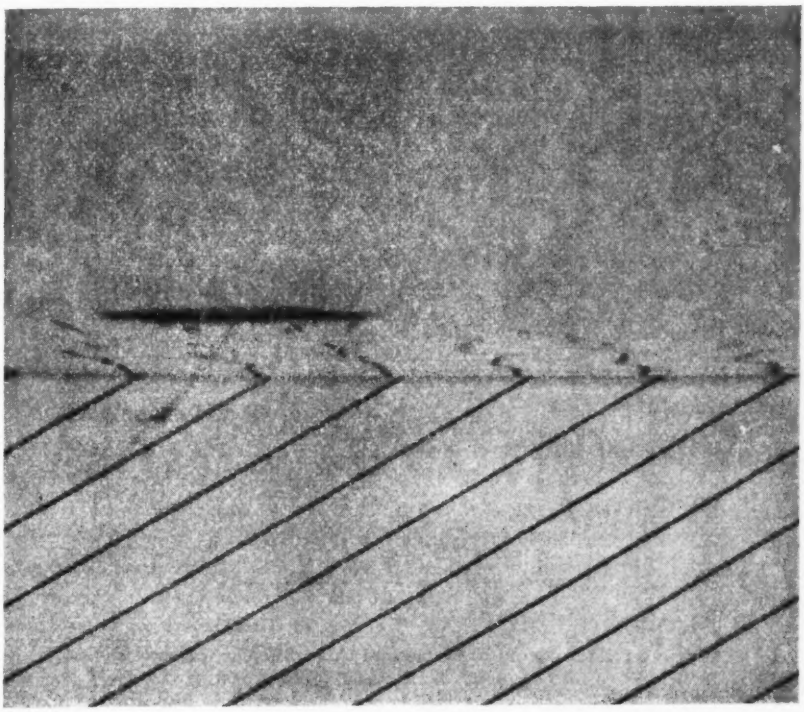

FIGURE 1. A photograph taken through the window of the tank from a point just below the surface of the wave. This shows the streak left by a drop of dilute ink, inclined after the passage of a few waves. (Some ink is left on the surface.) The lines in the background were drawn at an angle $\tan^{-1} 2$ to the vertical. The vertical separation of the lines was $\frac{1}{2}$ in.

Precautions

It was found that a thin film of oil or grease was nearly always present on the surface. In order to remove this, the fan was switched on for about 15 min, so that the surface film was driven up to the far end of the tank. Without further precautions the film would quickly have returned and covered the surface of the tank (at a rate of several cm/s). Accordingly, when the wind ceased a plastic curtain was immediately inserted in the tank at about 15 ft. from the beach. This prevented the return of the surface film, while allowing the transmission of waves from the generator to the beach.

The vigorous action of the wind also had the effect of thoroughly stirring the water, so that suspended particles were observed to be carried quickly from near

the bottom to the surface and back again. In this way any temperature gradient present in the tank was temporarily destroyed.

After switching off the wind, a period of 30–45 min was allowed for the tank to become quiet again, until a drop of ink or dye inserted in the water showed that the velocity gradients were negligible. The wave generator was then started and allowed to run for 5 min before observations were begun. This period gave time for the vorticity generated in the boundary layer to penetrate at least the upper 5 mm below the free surface (see § 5 below). Only those observations were

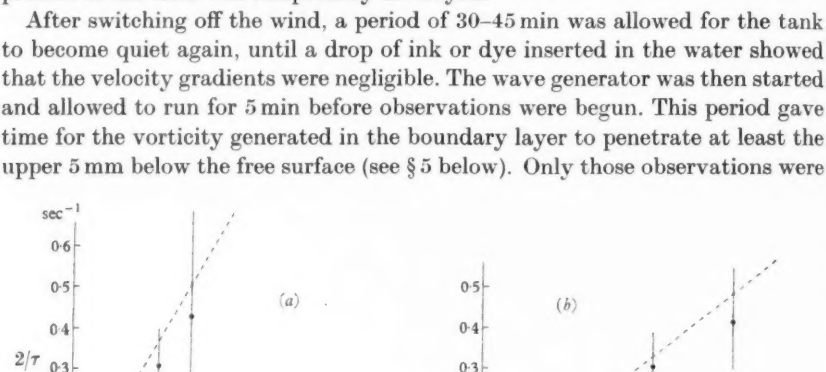

FIGURE 2. Results of observations at three different wave periods: (*a*) $kh = 2{\cdot}81$, (*b*) $kh = 1{\cdot}54$, (*c*) $kh = 1{\cdot}06$.

accepted in which the ink trace was initially vertical and remained in a practically straight line from 2 to 10 mm below the surface. At each run, ten acceptable observations were recorded: these were completed between 5 and 15 min after switching on the wave generator.

The choice of parameters for the experiments was limited: first, by the design of the wavemaker, which could not run safely at periods much less than 0·7 sec; secondly, by the method of observation, which is satisfactory only if the time of observation τ contains a sufficient number of wave cycles (about 10), for otherwise it is hard for the observer to judge accurately the moment when the mean inclination of the ink trace becomes parallel with the grid of lines; thirdly, by the presence of very weak gradients due to turbulent air movements and to residual effects of the stirring process described above: these last set the lower limit to the observed gradients.

Finally, three periods were chosen: $T = 0{\cdot}65$, 0·925 and 1·20 sec corresponding to $kh = 2{\cdot}81$, 1·54 and 1·06, respectively, and a number of runs were made at

different amplitudes a, while the wave period was kept constant. The mean depth h was kept at 29·7 cm throughout the experiments.

The observed results are shown in figure 2, plotted in each case against the square of the wave amplitude a^2. At each wave period, according to equation (1.2) the plotted points would be expected to lie on a straight line through the origin, as has been indicated in the figure. Each plotted point represents the mean of just ten consecutive observations, and the vertical lines through the points represent the total range of the same ten observations.

The most obvious feature of the results is the very wide scatter of observations, but this is in fact not much greater than would be expected considering the method of observation. It is perhaps puzzling that in figures 2(*a*) and (*b*) the mean values tend to lie slightly below the theoretical value while in figure 2(*c*) they lie somewhat above it; but this could be brought about by quite a small error in the measurement of wave period.

Two fairly definite conclusions may be drawn: (1) over the ranges of T, a and kh covered by the experiments the velocity gradient does tend to increase proportionally to a^2 approximately; and (2) the constant of proportionality is not far from that given by equation (1.2), and is certainly closer to (1.2) than to half this value.

5. Consequences for the interior of the fluid

Some implications of these results for the motion in the main body of the fluid may be briefly mentioned here.

Before the waves are started the vorticity is everywhere zero, and since vorticity cannot be generated within the fluid it follows that immediately after starting the waves the motion *beyond* the boundary layer is irrotational and will be given by Stokes's theory approximately. The difference between (1.2) and Stoke's value corresponds to a vorticity

$$\omega = -2a^2\sigma k^2 \coth kh, \tag{5.1}$$

which can be regarded as having been generated in the boundary layer itself, that is, within a distance of order $(\nu/\sigma)^{\frac{1}{2}}$ from the free surface. This vorticity will then begin to diffuse into the interior of the fluid.

Now it was shown in (I) that in a quasi-steady (that is, perfectly periodic) state of motion the vorticity ω in the interior of the fluid ($n \gg (\nu/\sigma)^{\frac{1}{2}}$) satisfies the equation

$$\mathbf{U}.\nabla\omega - \nu\nabla^2\omega = 0, \tag{5.2}$$

where $\mathbf{U}$ denotes the mass-transport velocity.* The first term in (5.2) represents the transport of vorticity by convection with the mass-transport velocity, and the second term represents the transport of vorticity by viscous conduction. This result might also be expected on physical grounds (cf. Lamb 1932, § 328); the motion being two-dimensional, there is no stretching of the vortex lines.

Before the vorticity in the interior is fully established the motion is not

* ω is of second order; the first-order vorticity vanishes in the interior; see (I), equation (50).

exactly periodic beyond the first order; but similar arguments suggest that the differential equation governing the distribution of vorticity in the interior is

$$\frac{\partial \omega}{\partial t} + \mathbf{U} \cdot \nabla \omega - \nu \nabla^2 \omega = 0. \tag{5.3}$$

In a regular progressive wave the mass-transport velocity is almost horizontal, apart from effects at the ends of tank. Any decrease in amplitude with distance also produces small vertical mass transports, but since the third term in (5.3) initially predominates near the surface it can be seen that most of the transport of vorticity in the layers nearest the free surface will take place by viscous 'conduction'.

Thus the equation governing the initial distribution of the vorticity just beyond the boundary layer is

$$\frac{\partial \omega}{\partial t} = \nu \nabla^2 \omega = \nu \frac{\partial^2 \omega}{\partial z^2}. \tag{5.4}$$

The solution of this equation with initial conditions

$$\omega = \begin{cases} 0, & z = 0, \quad t < 0, \\ \omega_0, & z = 0, \quad t > 0, \end{cases} \tag{5.5}$$

is well known:

$$\omega(z,t) = \frac{2\omega_0}{\sqrt{\pi}} \int_{z/2(\nu t)^{\frac{1}{2}}}^{\infty} e^{-\theta^2} d\theta, \tag{5.6}$$

which may also be written

$$1 - \frac{\omega}{\omega_0} = \frac{2}{\sqrt{\pi}} \int_0^z e^{-\theta^2} d\theta \equiv f(Z), \tag{5.7}$$

where

$$Z = \frac{z}{2(\nu t)^{\frac{1}{2}}}. \tag{5.8}$$

For a fixed value of z, as $t \to \infty$ so $Z \to 0$ and $f(Z) \to 0$; hence $\omega \to \omega_0$. The following table gives some typical values of $f(Z)$

$2Z$	$f(Z)$
0·0018	0·001
0·0035	0·002
0·0089	0·005
0·0177	0·01
0·0355	0·02
0·095	0·05
0·178	0·01

Thus to ensure that the vorticity is within 10 % of its value ω_0 at $z = 0$ we must have

$$\frac{z}{(\nu t)^{\frac{1}{2}}} \leqslant 0{\cdot}178. \tag{5.9}$$

Taking $\nu = 0{\cdot}013\ \mathrm{cm^2/s}$ and $t = 5$ min we find $z \leqslant 0{\cdot}47$ cm.

However, the *mean* value of ω between O and z, defined by

$$\frac{\omega_{\text{mean}}}{\omega_0} = \frac{1}{Z} \int_0^z f(Z)\, dZ, \tag{5.10}$$

is much closer to unity, as may be seen from the series expansion

$$\frac{\omega_{\text{mean}}}{\omega_0} = 1 - \frac{1}{\sqrt{\pi}}\left(Z - \frac{Z^3}{6} + \frac{Z^5}{30} - \frac{Z^7}{180} + \ldots\right). \tag{5.11}$$

With the same values: $t = 5$ min, $z = 0{\cdot}47$ cm, we find

$$\frac{\omega_{\text{mean}}}{\omega_0} = 0{\cdot}950, \tag{5.12}$$

so that the mean velocity gradient in the upper 5 mm is within 5 % of its ultimate value. It was this mean value which was measured in the experiments of § 4.

Generally, the width of the upper region influenced by the diffusion of vorticity from the oscillatory boundary layer will be of order $(\nu t)^{\frac{1}{2}}$, within the first few minutes. This region constitutes an outer 'boundary layer' of a different type from the oscillatory layer, the thickness of the latter being of order $(\nu T)^{\frac{1}{2}}$ only.*

At later times the fluid may be influenced by vorticity diffused in a similar way from the boundary layers at the bottom and sides of the tank. However, in most wave tanks it seems likely that the transport of vorticity by convection from the ends of the tank will intervene and ultimately predominate, so that conditions beyond the first few cm of fluid at the surface and bottom may depend somewhat on the type of wave generator or wave absorber which is used. The time required for vorticity to be convected from the ends of the tank through a distance x is clearly of order x/U. In the experiments described above this time was considerably greater than the time taken for the observations.

All the above predictions rely upon the assumption that the motion is laminar and the mass-transport current is predominantly horizontal and parallel to the wave velocity. Even slight winds may completely alter the character of the circulation (except near the bottom, where the motion is controlled by the bottom boundary layer). The possibility of the shearing motion becoming unstable of its own accord when the waves are sufficiently short and steep has also to be borne in mind. Indeed, this mechanism may contribute to the very marked turbulence that is present in all waves under the action of wind.

6. General implications

The analysis of § 2 shows that the effects just described are by no means peculiar to water waves, but will occur whenever there is an oscillatory fluid motion with a free boundary.

Thus from equation (2.11) we have just beyond the boundary, where $\nabla^2\psi_1 \to 0$,

$$\frac{\partial^2 \Psi}{\partial n^2} = -4\int (\nabla^2\psi_1)_0 \, dt \, \frac{\partial q_{s1}^{(0)}}{\partial s} \quad (n \gg \delta), \tag{6.1}$$

which combined with (2.5) becomes

$$\frac{\partial^2 \Psi}{\partial n^2} = 8\int \frac{\partial q_{n1}^{(0)}}{\partial s} \, dt \, \frac{\partial q_{s1}^{(0)}}{\partial s} \quad (n \gg \delta). \tag{6.2}$$

* Harrison's solution for the interior (equation (3.2)) contains a term in $\sin kz$. It is hard to see how such a motion, not tending to zero as $z \to \infty$, could be realized in practice.

Since we are now dealing with the part of the fluid beyond the inner boundary layer, we may, to the present order in ϵ, replace the velocity q_{s1}, q_{n1} by $\partial\psi_1/\partial z$, $-\partial\psi_1/\partial x$, where (x, z) are rectangular co-ordinates tangential and normal to the mean boundary. Thus

$$\frac{\partial^2\Psi}{\partial z^2} = -8\overline{\int \frac{\partial^2\psi_1}{\partial x^2}\,dt\,\frac{\partial^2\psi_1}{\partial x\,\partial t}}. \tag{6.3}$$

Since the mean boundary forms a streamline for the mass transport we must have also

$$\frac{\partial\Psi}{\partial x} = 0, \quad \frac{\partial^2\Psi}{\partial x^2} = 0, \tag{6.4}$$

so that the left-hand side of (6.3) can be replaced by $\nabla^2\Psi$. Now the mass-transport velocity is given in terms of ψ_1 and ψ_2 by

$$\Psi = \overline{\psi}_2 + \overline{\int \frac{\partial\psi_1}{\partial z}\,dt\,\frac{\partial\psi_1}{\partial x}} \tag{6.5}$$

(see (I) § 3), and since by equation (85) of (I)

$$\nabla^2\overline{\int \frac{\partial\psi_1}{\partial z}\,dt\,\frac{\partial\psi_1}{\partial x}} = -4\overline{\int \frac{\partial^2\psi_1}{\partial x^2}\,dt\,\frac{\partial^2\psi_1}{\partial x\,\partial z}}, \tag{6.6}$$

it follows, on operating on both sides of (6.5) with ∇^2, that

$$-8\overline{\int \frac{\partial^2\psi_1}{\partial x^2}\,dt\,\frac{\partial^2\psi_1}{\partial x\,\partial z}} = \nabla^2\overline{\psi}_2 - 4\overline{\int \frac{\partial^2\psi_1}{\partial x^2}\,dt\,\frac{\partial^2\psi_1}{\partial x\,\partial z}}. \tag{6.7}$$

Hence

$$\nabla^2\overline{\psi}_2 = -4\overline{\int \frac{\partial^2\psi_1}{\partial x^2}\,dt\,\frac{\partial^2\psi_1}{\partial x\,\partial z}}. \tag{6.8}$$

This last expression, multiplied by ϵ^2, represents the vorticity just in the interior of the fluid, for, beyond the boundary layer,

$$\nabla^2\psi_1 \to 0, \quad \nabla^2\psi_2 \to \nabla^2\overline{\psi}_2 \tag{6.9}$$

(see (I) § 4) and therefore

$$\omega = \nabla^2\psi \to \epsilon^2\nabla^2\overline{\psi}_2 + \ldots. \tag{6.10}$$

Now write

$$\epsilon\frac{\partial\psi_1}{\partial z} = u, \quad -\epsilon\frac{\partial\psi_1}{\partial x} = w, \tag{6.11}$$

for the components of velocity tangential and normal to the mean position of the boundary (these differ from their corresponding values at the boundary by quantities of order ϵ^2). Our result can thus be written

$$\omega = 4\overline{\frac{\partial u}{\partial x}\int \frac{\partial w}{\partial x}\,dt}. \tag{6.12}$$

In other words, the presence of the free boundary produces a mean vorticity in the interior given by (6.12). The modifications of this result needed to take account of any arbitrary tangential stresses applied at the surface may be deduced from the general formulae of (I) § 8.

It is interesting to note that so far as the distributon of mass transport in the interior is concerned the presence of the boundary is equivalent to a virtual stress

$$4\mu \overline{\frac{\partial u}{\partial x} \int \frac{\partial w}{\partial x} dt}. \tag{6.13}$$

Since $\int w dt$ is equal to the surface elevation η, this last expression may be written

$$4\mu \overline{\frac{\partial u}{\partial x} \frac{\partial \eta}{\partial x}} \tag{6.14}$$

which, as we saw in § 3, is equal to the difference between the stress components p_{xz} and p_{ns}. It is p_{ns} that vanishes and p_{xz} generally differs from zero on account of the tilting of the surface through an angle $\partial\eta/\partial x$. Thus we might say that the virtual stress (6.13) was due simply to the corrugation of the free surface; but this would be to neglect the structure of the boundary layer itself, throughout which the tangential stress, like the vorticity, is not uniform.

7. Conclusions

Our concluding picture is as follows. The periodic motion of the fluid produces in the first place boundary layers at both bottom and free surface whose thickness is of the order of $(\nu T)^{\frac{1}{2}}$, where ν denotes kinematic viscosity and T the period of the waves. In practical cases these oscillatory boundary layers have a thickness of only a few millimetres. But within the surface layer there is produced a second-order mean vorticity which, from the moment of starting the waves, begins to diffuse downwards into the fluid. After a time t the region affected by the vorticity is of order $(\nu t)^{\frac{1}{2}}$, provided t is not too great. This latter region may be thought of as a kind of outer boundary layer which finally may fill the whole fluid. Some vorticity may, however, be transported by convection as well as by viscous diffusion. Finally, the motion is no longer irrotational, but contains everywhere a second-order vorticity determined by the oscillatory layers at the boundaries.

I am indebted to the Director of the Hydraulics Research Station for permission to make use of the 185 ft. wind-wave tank there, and to Mr R. C. H. Russell and Mr F. A. Kilner for their interest and co-operation. The experiments described above were carried out with the assistance of Mr A. J. Bunting.

REFERENCES

Allen, J. & Gibson, D. H. 1959 Experiments on the displacement of water by waves of various heights and frequencies. *Min. Proc. Instn Civ. Engrs*, **13**, 363–86.

Bagnold, R. A. 1947 Sand movement by waves: some small-scale experiments with sand of very low density. *J. Inst. Civ. Engrs*, **27**, 447–69.

Harrison, W. J. 1908 The influence of viscosity and capillarity on waves of finite amplitude. *Proc. Lond. Math. Soc.* (2), **7**, 107–21.

Lamb, H. 1932 *Hydrodynamics*, 6th ed. Cambridge University Press.

Longuet-Higgins, M. S. 1953*a* On the decrease of velocity with depth in an irrotational water wave. *Proc. Camb. Phil. Soc.* **49**, 552–60.

Longuet-Higgins, M. S. 1953*b* Mass transport in water waves. *Phil. Trans.* A, **245**, 535–81.

RUSSELL, R. C. H. & OSORIO, J. D. C. 1958 An experimental investigation of drift profiles in a closed channel. *Proc. 6th Conf. on Coastal Engng, Miami*, 1957, pp. 171–93. Council on Wave Res., University of California, Berkeley.

STOKES, G. G. 1847 On the theory of oscillatory waves. *Trans. Camb. Phil. Soc.* **8**, 441–55; reprinted in *Math. Phys. Pap.* **1**, 314–26.

VINCENT, G. & RUELLAN, F. 1957 Contribution à l'étude des mouvements solides provoqués par la houle sur un fond horizontal. *Houille blanche*, B, **12**, 605–722.

VINCENT, G. 1958 Contribution to the study of sediment transport on a horizontal bed due to wave action. *Proc. 6th Conf. Coastal Engng, Miami*, 1957, pp. 326–55. Council on Wave Res., University of California, Berkeley.

The slow motion of a magnetized sphere in a conducting medium

By JAMES R. BARTHEL AND PAUL S. LYKOUDIS
School of Aeronautical Engineering, Purdue University, West Lafayette, Indiana

(Received 6 October 1959)

This paper considers the slow motion of a sphere, permanently and uniformly magnetized in one direction, in a viscous electrically conducting medium. The line of the magnetic poles is assumed to be parallel to the direction of the motion of the sphere. The velocity and pressure fields are calculated by two iterations. The distortion of the magnetic field is also calculated. An expression is obtained for total drag due to the viscous, pressure and magnetic forces.

Introduction

The motion of a sphere in a viscous, incompressible fluid at very low Reynolds numbers was analysed by Stokes. The Stokes formula for drag is close to experimental values up to about $R = 2$. Chester (1957) extended the above problem to the case of an electrically conducting fluid with a uniform magnetic field parallel everywhere to the free stream, the induced magnetic field being neglected.

If the fluid is an electrical conductor and the sphere is permanently magnetized, the Stokes flow field will be distorted by the action of the ponderomotive force $\mathbf{J} \times \mathbf{B}$. This force will reduce the gradients of velocity in the direction normal to the surface, and thereby reduce the viscous shearing forces. The reduction in shear drag will, however, be more than overcome by the drag due to the ponderomotive force.

The problem will be solved here, with the inertia forces neglected, for the particular case in which the sphere is uniformly magnetized, with the magnetic axis parallel to the ambient flow. The induced magnetic field will not be neglected. The case of the magnetic axis being perpendicular to the main flow will also be discussed.

The velocity, pressure, and magnetic field will be found by iteration in the following way. First, the ponderomotive force will be calculated from the known Stokes velocity field $\mathbf{V}_0$, and the known permanent magnetic field $\mathbf{H}_0$, and substituted into the equations of motion, which will yield a first approximation to the velocity, $\mathbf{V}_1$, and the pressure, P_1. Likewise, the current density will be calculated everywhere from the known $\mathbf{V}_0$, $\mathbf{H}_0$, and σ, and substituted into Maxwell's equations, which will yield a first approximation to the magnetic field, $\mathbf{H}_1$. Then the ponderomotive force will be calculated from $\mathbf{H}_1$ and $\mathbf{V}_1$ and used to find a second approximation $\mathbf{V}_2$, P_2. This method gives the solution at all points in the flow region, assuming that there is no separation of flow. The results of the present work may be applicable in the case of small meteorite particles made up of ferromagnetic materials and carrying a permanent magnetic field.

The equations of motion

The motion is determined by solving the following system of equations:

$$0 = -\nabla' P + \mu \nabla^2 \mathbf{V} + \mathbf{J} \times \mathbf{B} \quad \text{(conservation of momentum)}, \tag{1}$$

$$\nabla' . \mathbf{V} = 0 \quad \text{(conservation of mass)}, \tag{2}$$

$$\nabla' \times \mathbf{H} = \mathbf{J} \quad \text{(Ampere's Law)}, \tag{3}$$

$$\mathbf{J} = \sigma(\mathbf{E} + \mathbf{V} \times \mathbf{B}) \quad \text{(Ohm's law)}, \tag{4}$$

$$\nabla' . \mathbf{B} = 0 \quad \text{(statement that magnetic poles exist only in pairs)}. \tag{5}$$

In writing (1) to (5) the following assumptions were made: (*a*) the inertia forces are much smaller than the viscous forces; (*b*) all quantities are independent of time; (*c*) the electrical field and the electric charge density are zero everywhere, since the current lines are closed loops about the axis of symmetry; (*d*) the fluid is composed of particles whose collision frequency is much higher than the cyclotron frequency; this assumption insures that the scalar transport properties σ and μ are not changed by the magnetic field.

The following non-dimensional quantities are introduced:

$$\mathbf{v} \equiv \frac{\mathbf{V}}{V_\infty}, \quad \nabla \equiv a\nabla', \quad \mathbf{h} \equiv \frac{\mathbf{H}}{H_{mp}}, \quad p \equiv \frac{Pa}{V_\infty \mu}, \tag{6}$$

where a is the radius of the sphere and H_{mp} the field strength at the poles. In this notation, (1) to (5) become:

$$0 = -\nabla p + \nabla^2 \mathbf{v} + M(\mathbf{v} \times \mathbf{h}) \times \mathbf{h} \tag{7}$$

(here $M = \sigma B_{mp}^2 a^2/\mu$ is the square of the usual Hartmann number; this seems to be a more natural definition since it is a measure of the ratio of the magnetic forces to the viscous forces),

$$\nabla . \mathbf{v} = 0, \tag{8}$$

$$\nabla \times \mathbf{h} = R_m(\mathbf{v} \times \mathbf{h}) \tag{9}$$

(R_m is the magnetic Reynolds number $\sigma \mu_{m0} V_\infty a$, where μ_{m0} is the permeability of the conducting fluid),

$$\nabla . \mathbf{h} = 0. \tag{10}$$

For the first approximation, (7) becomes

$$0 = -\nabla p_1 + \nabla^2 \mathbf{v}_1 + M(\mathbf{v}_0 \times \mathbf{h}_0) \times \mathbf{h}_0. \tag{11}$$

Making the substitutions $\mathbf{v}_1 = \mathbf{v}_0 + M\mathbf{v}_1'$, $p_1 = p_0 + Mp_1'$, we obtain

$$0 = -\nabla p_1' + \nabla^2 \mathbf{v}_1' + (\mathbf{v}_0 \times \mathbf{h}_0) \times \mathbf{h}_0. \tag{12}$$

Equation (8) becomes

$$\nabla . \mathbf{v}_1' = 0. \tag{13}$$

Taking the curl of (9) and using (10), we find

$$\nabla^2 \mathbf{h}_1 = -R_m \nabla \times (\mathbf{v}_0 \times \mathbf{h}_0). \tag{14}$$

The substitution $\mathbf{h}_1 = \mathbf{h}_0 + R_m \mathbf{h}_1'$ gives

$$\nabla^2 \mathbf{h}_1' = -\nabla \times (\mathbf{v}_0 \times \mathbf{h}_0). \tag{15}$$

The right-hand side of (15) vanishes inside the sphere, since there is no current there. Equations (12), (13) and (15) will be solved later for $\mathbf{v}_1'$, p_1' and $\mathbf{h}_1'$.

The second approximation for velocity and pressure may be found by writing

$$0 = -\nabla p_2 + \nabla^2 \mathbf{v}_2 + M(\mathbf{v}_1 \times \mathbf{h}_1) \times \mathbf{h}_1. \tag{16}$$

Making the substitutions

$$p_2 = p_1 + M^2 p_2' + MR_m p_2'' \quad \text{and} \quad \mathbf{v}_2 = \mathbf{v}_1 + M^2 \mathbf{v}_2' + MR_m \mathbf{v}_2''$$

and using (12), we may write (16):

$$\begin{aligned} 0 = {} & M^2(-\nabla p_2' + \nabla^2 \mathbf{v}_2' + (\mathbf{v}_1' \times \mathbf{h}_0) \times \mathbf{h}_0) + MR_m(-\nabla p_2'' + \nabla^2 \mathbf{v}_2'' \\ & + (\mathbf{v}_0 \times \mathbf{h}_1') \times \mathbf{h}_0 + (\mathbf{v}_0 \times \mathbf{h}_0) \times \mathbf{h}_1') + MR_m^2(\mathbf{v}_0 + \mathbf{h}_1') \times \mathbf{h}_1' \\ & + M^2 R_m((\mathbf{v}_1' \times \mathbf{h}_1') \times \mathbf{h}_0 + (\mathbf{v}_1' \times \mathbf{h}_0) \times \mathbf{h}_1') + M^2 R_m^2(\mathbf{v}_1' \times \mathbf{h}_1') \times \mathbf{h}_1'. \end{aligned} \tag{17}$$

The last three terms will be neglected, since they are of one order higher than the first two, and would thus be accounted for in a third iteration. Since (17) holds for arbitrary values of M and R_m, each term must vanish. Equation (17), along with the conditions $\nabla \cdot \mathbf{v}_2' = 0$ and $\nabla \cdot \mathbf{v}_2'' = 0$, determines the second approximation.

The boundary conditions

The boundary conditions on the velocity field are the following: on the surface of the sphere, $\mathbf{v} = 0$ (no-slip condition), and at an infinite distance from the sphere, $\mathbf{v} \to \mathbf{v}_0$. Since $\mathbf{v}_0$ already meets these conditions, and since $\mathbf{v}$ must meet these conditions for arbitrary M and R_m, then we must set $\mathbf{v}_1' = \mathbf{v}_2' = \mathbf{v}_2'' = 0$ on the sphere and at infinity.

In determining the magnetic field distortion $\mathbf{h}_1'$, it will be assumed that the permeability μ_m of the sphere is a scalar. The boundary condition on $\mathbf{h}_1'$ at the surface of the sphere requires that the component of $\mu_m \mathbf{h}_1'$ normal to the surface and the component of $\mathbf{h}_1'$ tangential to the surface be continuous.

The iteration solution

The solutions for $\mathbf{h}$, $\mathbf{v}$, and p necessary to compute the drag of the sphere up to second order in M, neglecting the influence of R_m, have been carried out. The solution for $\mathbf{v}_1'$ and p_1' will be shown in detail. Since the second iteration consists of the same manipulations used in this solution, and is recorded in Barthel & Lykoudis (1959), it will not be carried out in detail here.

Into (12) we substitute the Stokes solution $\mathbf{v}_0$, and the undistorted field $\mathbf{h}_0$ of the permanently magnetized sphere, which is given by Harnwell (1949, p. 412):

$$\mathbf{h}_0 = -\nabla\left(\frac{1}{2}\frac{x}{r^3}\right) \quad \text{or} \quad \mathbf{H}_0 = -\nabla'\left(\frac{m_V a^3}{3\mu_{m0}}\frac{x}{r^3}\right), \tag{18}$$

where m_V is the magnetic moment density. After the calculation of the ponderomotive force, the components of (12) become:

$$\left.\begin{aligned} 0 &= -\frac{\partial p_1'}{\partial x} + \nabla^2 u_1' + \frac{9}{4}\frac{x^2}{r^{10}}(1-x^2)\left(\frac{1}{r}-1\right), \\ 0 &= -\frac{\partial p_1'}{\partial y} + \nabla^2 v_1' + \left(\frac{3}{4}\frac{x}{r^8} - \frac{9}{4}\frac{x^3}{r^{10}}\right)\left(\frac{1}{r}-1\right) y, \\ 0 &= -\frac{\partial p_1'}{\partial z} + \nabla^2 w_1' + \left(\frac{3}{4}\frac{x}{r^8} - \frac{9}{4}\frac{x^3}{r^{10}}\right)\left(\frac{1}{r}-1\right) z. \end{aligned}\right\} \tag{19}$$

Now, from (18), since $\nabla . \mathbf{v}_1' = 0$,

$$\nabla^2 p_1' = \nabla . [(\mathbf{v}_0 \times \mathbf{h}_0) \times \mathbf{h}_0] = -\frac{3}{4}\frac{x}{r^9} - \frac{9}{4}\frac{x^3}{r^{11}} + 3\frac{x^3}{r^{10}}. \tag{20}$$

The following identities will be needed in the course of the solution of (19) and (20):

$$\nabla^2\left(\frac{x^m}{r^n}\right) = m(m-1)\frac{x^{m-2}}{r^n} + n(n-1-2m)\frac{x^m}{r^{n+2}}, \tag{21a}$$

$$\nabla^2\left(\frac{x^m y}{r^n}\right) = m(m-1)\frac{x^{m-2}}{r^n}y + n(n-3-2m)\frac{x^m y}{r^{n+2}}, \tag{21b}$$

$$\nabla^2[(\ln r)\,\phi_K] = \frac{\phi_K}{r^2}(1+2K), \tag{21c}$$

where ϕ_K is a spherical harmonic which is homogeneous of degree K.

Equation (20) is Poisson's equation and has the following particular solution:

$$p_1' = -\frac{1}{8}\frac{x^3}{r^9} + \frac{3}{8}\frac{x^3}{r^8} - \frac{1}{8}\frac{x}{r^6}. \tag{22}$$

To obtain the general solution, we must add spherical harmonics with undetermined coefficients, as follows:

$$p_1' = -\frac{1}{8}\frac{x^3}{r^9} + \frac{3}{8}\frac{x^3}{r^8} - \frac{1}{8}\frac{x}{r^6} + F\frac{x}{r^3} + G\left(15\frac{x^3}{r^7} - 9\frac{x}{r^5}\right). \tag{23}$$

Since there are no specific conditions on p_1', except that p_1' must vanish at infinity, the constants F and G must remain arbitrary for the moment.

Next we substitute into (19) the derivatives of (23):

$$\nabla^2 u_1' = \frac{27}{8}\frac{x^4}{r^{11}} - \frac{21}{8}\frac{x^2}{r^9} + \frac{33}{8}\frac{x^2}{r^8} - \frac{21}{4}\frac{x^4}{r^{10}} - \frac{1}{8r^6} + F\left(\frac{1}{r^3} - \frac{3x^2}{r^5}\right) + G\left(-105\frac{x^4}{r^9} + 90\frac{x^2}{r^7} - \frac{9}{r^5}\right), \tag{24a}$$

$$\nabla^2 v_1' = \frac{27}{8}\frac{x^3 y}{r^{11}} - \frac{3}{4}\frac{xy}{r^9} + \frac{3}{2}\frac{xy}{r^8} - \frac{21}{4}\frac{x^3 y}{r^{10}} - 3F\frac{xy}{r^5} - 105G\frac{x^3 y}{r^9} + 45G\frac{xy}{r^7}, \tag{24b}$$

with a similar expression for $\nabla^2 w_1'$, y being replaced by z.

The general solution for the system of (24) is

$$u_1' = \frac{21}{32}\frac{x^4}{r^8} - \frac{5}{8}\frac{x^2}{r^6} + \frac{3}{32r^4} + \tfrac{3}{8}\ln r\left(-\frac{x^4}{r^9} + \frac{6}{7}\frac{x^2}{r^7} - \frac{3}{35r^5}\right) + \frac{15}{784}\frac{x^2}{r^7} - \frac{321}{19{,}600\,r^5}$$
$$+ \tfrac{15}{2}G\frac{x^4}{r^7} - \frac{3}{2}\frac{G}{r^3} + \frac{F}{2}\frac{x^2}{r^3} + A\left(\frac{x^4}{r^9} - \frac{6}{7}\frac{x^2}{r^7} + \frac{3}{35r^5}\right) + B\left(\frac{x^2}{r^5} - \frac{1}{3r^3}\right) + \frac{C}{r}, \tag{25a}$$

$$v_1' = \frac{21}{32}\frac{x^3 y}{r^8} - \frac{13}{32}\frac{xy}{r^6} + \tfrac{3}{8}\ln r\left(-\frac{x^3 y}{r^9} + \frac{3}{7}\frac{xy}{r^7}\right) + \frac{39}{784}\frac{xy}{r^7} + \frac{F}{2}\frac{xy}{r^3} + \tfrac{15}{2}G\frac{x^3 y}{r^7}$$
$$+ D\left(\frac{x^3 y}{r^9} - \frac{3}{7}\frac{xy}{r^7}\right) + E\frac{xy}{r^5}, \tag{25b}$$

and similarly for w_1'.

The boundary condition $u_1' = v_1' = w_1' = 0$ at $r = 1$ gives

$$\tfrac{21}{32} + \tfrac{15}{2}G + A = 0, \tag{26a}$$

$$-\frac{5}{8} + \frac{15}{784} + \frac{F}{2} - \frac{6A}{7} + B = 0, \tag{26b}$$

$$\frac{3}{32} - \frac{321}{19{,}600} - \tfrac{3}{2}G + \frac{3A}{35} - \frac{B}{3} + C = 0, \tag{26c}$$

$$\tfrac{21}{32} + \tfrac{15}{2}G + D = 0, \tag{26d}$$

$$-\frac{13}{32} + \frac{39}{784} + \frac{F}{2} - \frac{3D}{7} + E = 0. \tag{26e}$$

Using (25) in the continuity equation, we find:

$$(5E - 5B - \tfrac{15}{2}G)\frac{x^3}{r^7} - (3E - 3B - \tfrac{9}{2}G)\frac{x}{r^5} + \left(\frac{F}{2} - C\right)\frac{x}{r^3} = 0.$$

The coefficients must vanish, since the left side is zero everywhere. Thus:

$$E - B - \frac{3G}{2} = 0 \quad C = \frac{F}{2}. \tag{26f}$$

The solution of the system (26) is

$$A = D = -0{\cdot}516741, \quad B = 0{\cdot}167946, \quad C = -0{\cdot}005000,$$

$$E = 0{\cdot}140044, \quad F = -0{\cdot}010000, \quad G = -0{\cdot}018601. \tag{27}$$

Equations (27), when substituted into (23) and (25), complete the solution for p_1' and $\mathbf{v}_1'$.

The results of the second iteration will not be written here. The velocity $\mathbf{v}_2'$ and pressure p_2' have been determined whereas the quantities $\mathbf{v}_2''$ and p_2'' were not computed, since it was found by inspection that because of the antisymmetry of $\mathbf{v}_2''$ with respect to x and the symmetry of p_2'' with respect to x, neither contri butes to the drag.

The magnetic field distortion $\mathbf{h}_1'$ satisfying (15) was found to be

$$h_{1x}' = -\frac{3}{2}\frac{x^3}{r^6} + \frac{3}{4}\frac{x}{r^4} + \frac{3}{4}\frac{x^3}{r^5} + \frac{A'x}{r^3} + B'\left(\frac{x^3}{r^7} - \frac{3}{5}\frac{x}{r^5}\right), \tag{28a}$$

$$h_{1y}' = -\frac{3}{2}\frac{x^2y}{r^6} + \frac{3}{8}\frac{y}{r^4} + \frac{3}{4}\frac{x^2y}{r^5} + \frac{C'y}{r^3} + D'\left(\frac{x^2y}{r^7} - \frac{1}{5}\frac{y}{r^5}\right) \tag{28b}$$

outside the sphere. Inside the sphere, the solution is

$$h_{1x}' = E'x; \quad h_{1y}' = F'y. \tag{28c}$$

From the boundary conditions, it was found that

$$A' = C' = -\tfrac{1}{4}; \quad B' = D' = \frac{3}{4}\left(1 + \frac{\mu_m - 1}{4\mu_m + 6}\right); \quad E' = -2F' = \frac{1}{4(3 + 2\mu_m)}. \tag{29}$$

If $\mu_m \gg 1$,

$$B' \cong \tfrac{15}{16}; \quad E' \cong 0. \tag{30}$$

We should point out that the iteration method used in solving this problem does not succeed in the problem considered by Chester (1957); it was found by the present method that for Chester's problem the first-order perturbation in velocity increases without limit at large values of r, and therefore the condition $\mathbf{v}_1 = 0$ at infinity cannot be satisfied. On the other hand, the singular expansion method employed by Chester can, in principle, be applied to the problem studied in this paper. However, the equation (7) does not attain a form so simple as that of (12) of Chester's paper, even if $\mathbf{h} = \mathbf{h}_0$. Therefore the singular expansion method seems to be unwieldy in our problem. It was felt that the two approaches have comparable accuracy, since both eventually involve expansion in powers of M. The iteration approach was selected because each step of the iteration has a plausible physical interpretation and because the mathematical solution required at each step is quite straight-forward.

Calculation of the drag

The drag will be the sum of the contributions of the ponderomotive forces, the pressure forces, and the viscous shear. The contributions of the pressure terms p_0, p_1' and p_2' to the drag coefficient are respectively:

$$C_D(p_0) = \frac{D(p_0)}{\frac{1}{2}\rho V_\infty^2 \pi a^2} = -\frac{2}{\pi R}\iint_{r=1} p_0 \mathbf{i}.\mathbf{n}\, dS = \frac{4}{R}; \quad C_D(p_1') = -0{\cdot}040000\frac{M}{R};$$

$$C_D(p_2') = 0{\cdot}000300\frac{M^2}{R}. \tag{31}$$

The contribution of p_2'' is zero. The viscous shearing drag contributions due to the velocity terms $\mathbf{v}_0$, $\mathbf{v}_1'$ and $\mathbf{v}_2'$ are respectively:

$$C_D(\mathbf{v}_0) = \frac{2}{\pi R}\iint_{r=1}\left[2\times\frac{\partial u_0}{\partial x} + y\left(\frac{\partial u_0}{\partial y}+\frac{\partial v_0}{\partial x}\right) + z\left(\frac{\partial u_0}{\partial z}+\frac{\partial w_0}{\partial x}\right)\right] dS = \frac{8}{R};$$

$$C_D(\mathbf{v}_1') = -0{\cdot}080000\frac{M}{R}; \quad C_D(\mathbf{v}_2') = 0{\cdot}000616\frac{M^2}{R}. \tag{32}$$

The contribution of $\mathbf{v}_2''$ is zero. The contributions of the ponderomotive force terms up to the order M^2 are

$$C_D(m_0) = -\frac{2M}{\pi R}\mathbf{i}.\iiint_{r=1}^{\infty}(\mathbf{v}_0\times\mathbf{h}_0)\times\mathbf{h}_0\, d\tau = \frac{M}{5R}, \tag{33}$$

$$C_D(m_1') = -\frac{2M^2}{\pi R}\mathbf{i}.\iiint_{r=1}^{\infty}(\mathbf{v}_1'\times\mathbf{h}_0)\times\mathbf{h}_0\, d\tau = -0{\cdot}0013453\frac{M^2}{R}, \tag{34}$$

$$C_D(m_1'') = -\frac{2MR_m}{\pi R}\mathbf{i}.\iiint_{r=1}^{\infty}[(\mathbf{v}_0\times\mathbf{h}_1')\times\mathbf{h}_0 + (\mathbf{v}_0\times\mathbf{h}_0)\times\mathbf{h}_1']\, d\tau = 0. \tag{35}$$

The sum of (31) through (35) is:

$$C_D = \frac{12}{R}[1 + 0{\cdot}0066667M - 0{\cdot}00003578M^2]. \tag{36}$$

There is no term in (36) with the coefficient MR_m since, as previously mentioned, $\mathbf{v}_2''$ and p_2'' do not contribute to the shear drag and the pressure drag, and because the ponderomotive force in (35) is antisymmetric in x.

The magnetic drag in (33) was computed for the case in which the magnetic axis is perpendicular to the free stream velocity, for the purpose of comparison. The result is

$$C_D(m_0)\,(\text{perpendicular}) = \tfrac{11}{8} C_D(m_0)\,(\text{parallel}). \tag{37}$$

Discussion of the results

The first and second approximation to the total drag of the slowly moving sphere is given by (36) and plotted in figure 1. It is apparent from the manner in which the iteration was carried out that calculation of the higher approximations to the drag (containing both R and R_m) will prove them to be alternating around

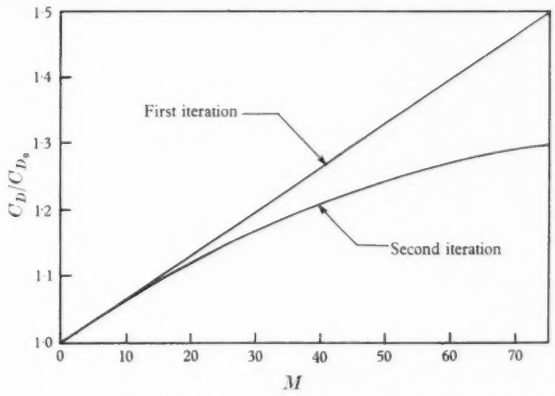

FIGURE 1. Ratio of total drag to Stokes drag as a function of Hartmann number, M, as defined in equation (7).

the true value; the last one must lie between the first and second approximations. That this is the case is obvious from the fact that the first approximation has been based on a ponderomotive force corresponding to the velocity field of the Stokes solution; as a result the calculated drag must be higher than the true one, whereas the velocity corresponding to this approximation must be lower than the actual one. On the other hand, the second approximation, based on this last velocity, will yield a drag lower than the exact one since now the ponderomotive force is being underestimated. From these remarks one may estimate the Hartmann number for which the difference in the total drag between the upper and lower limit will be $\epsilon\,\%$ of the drag due to the first correction term from the relation

$$M = 1{\cdot}87\epsilon.$$

For $\epsilon = 5\,\%$, $10\,\%$ and $20\,\%$, M takes the corresponding values of 9·35, 18·7 and 37·4.

The influence of moderate Hartmann numbers on the total drag is rather small. Physically, this is due to the very thick boundary layer, with the velocity being very small in the neighbourhood of the solid boundary where the magnetic field intensity is high. As one would expect, the drag when the magnetic axis is perpendicular to the main flow was found in the first approximation to be higher because in this case the velocity in the neighbourhood of the two poles intersects

the magnetic lines perpendicularly and at the same time it is higher in magnitude. In Chester's work the total drag was found to be considerably higher since the magnetic field remains constant in the region where the velocities are large.

If one thinks of a series of experiments similar to the ones verifying Stoke's analysis, but with permanently magnetized spheres, it is obvious that the effect of high Hartmann numbers will be to increase the maximum allowable radius for which a sphere will reach a terminal velocity corresponding to a Reynolds number of order one, since the terminal velocity will be reduced by the action of

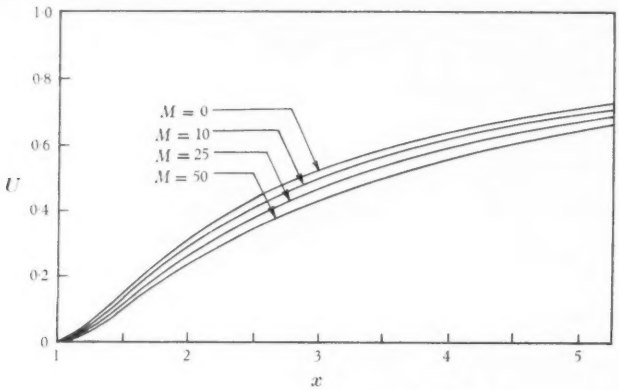

FIGURE 2. Variation of velocity along the axis of symmetry for $M = 0$, 10, 25 and 50.

the magnetic field. On the other hand, experimental verification of the present results seems to be rather difficult, because for a strong permanent magnetic field relatively large spheres are necessary, which is contrary to the requirement of small Reynolds numbers and therefore small dimensions.

Figure 2 shows the effect of the magnetic field on the velocity. The magnetic field has a quite similar effect on the variation of velocity along an axis normal to the flow axis. The velocity gradients, and hence the viscous drag, are reduced by the magnetic field. This is accompanied by a reduction in pressure drag. It is interesting to note that within the numerical accuracy of this work, it was found that the drag due to the pressure forces equals half the drag due to the shear forces, as in the classical Stokes case.

This Research was supported by the McDonnell Aircraft Corporation and by the Purdue Research Foundation.

REFERENCES

BARTHEL, J. R. & LYKOUDIS, P. S. 1959 The slow motion of a permanently magnetized sphere in an electrically conducting medium, *Rep. No. A-59-11, School of Aeronautical Engineering, Purdue University.*

CHESTER, W. 1957 The effect of a magnetic field on Stokes flow in a conducting fluid. *J. Fluid Mech.* **3**, 302.

HARNWELL, G. P. 1949 *Principles of Electricity and Electro-magnetism*, 2nd ed. New York: McGraw-Hill.

REVIEWS

Fluid Mechanics. By L. D. Landau and E. M. Lifshitz. (Translated from the Russian by J. B. Sykes and W. H. Reid.) London: Pergamon Press, 1959. 536 pp. £5 5*s*.

It is always fascinating to learn how others see us and to hear their views of situations in which we are deeply involved; and no less fascinating in the scientific world than in human affairs. Pleasures of this kind on a small scale come often enough, when the writer of some paper refers to our published work and goes on to comment and to extend. It is a strong-minded man who can resist turning to that aspect of the paper first and seeing the paper largely in terms of its treatment, favourable or otherwise, of his own work. On a grand scale, opportunities of hearing a new view of our own subject by some outsider or detached observer are less common, which is a pity, because, quite apart from the sheer enjoyment it provides, there is no better way of stimulating fresh ideas and developments.

The book under notice is just such a view of fluid mechanics. It is a comprehensive account of the subject, covering everything from boundary layers to combustion, by two distinguished authors who are outsiders in two separate senses. In the first place, they are Russians. I realize that science, and fluid mechanics as much as any other branch, is international and belongs to no one nation. However, there is no doubt that science has developed inside U.S.S.R. and outside U.S.S.R. independently to a large extent. There have been important points of contact and interconnexion of the two streams, and it is unlikely that they will ever diverge, but a glance at the lists of references in a number of papers in either stream will show that points of contact are uncommon. The translation from the Russian of a comprehensive book on fluid mechanics—that is, on a subject which Western scientists feel *they* have brought to a high pitch of development—is therefore a notable event. While reading the book I have been noting continually that here Russian fluid dynamicists can teach us a trick or two, while there we seem to have done better than they have. Many of the points of comparison, such as that arising from the authors' neat derivation of the relation between the lift on a wing and the circulation round it, are mainly of pedagogical interest, although others, such as their description of the velocity distribution near the point of separation of a laminar boundary layer, concern developments near the frontier of research; and all of them make reading the book a pleasure.

The second respect in which the authors may be regarded as detached observers is that they are theoretical physicists; Landau, it is true, has made several original contributions to fluid mechanics, but it is by no means his primary field of interest. *Fluid Mechanics* is one of a set of nine volumes by the same authors, the whole set making up a *Course of Theoretical Physics* of remarkable completeness on both 'modern' and 'classical' physics. It is a staggering thought that two authors with primary interests elsewhere have

mastered the wide range of fluid mechanics presented to us. But it is the point of view which gives the book its distinctive flavour. The authors emphasize theory and analysis, naturally enough, and make little attempt to reproduce experimental data; the book is by theorists and for theorists. (It is perhaps the most serious criticism of the book that this tendency is carried too far, and that the authors are content too often with the airy remark that observation 'confirms' their conclusions.) Also, as stated in the preface, they 'have tried to develop as fully as possible all matters of physical interest, and to do so in such a way as to give the clearest possible picture of the phenomena and their interrelation. Accordingly, we discuss neither approximate methods of calculation in fluid mechanics, nor empirical theories devoid of physical significance'. This is a refreshing change from the usual style of book, and it is a tonic to see the subject laid out in beautifully pure form and shorn of all the useful excrescences which, essential though they may be for practical ends, do conceal the fundamentals. By and large, the authors seem to me to have succeeded in their attempt to provide lucid analysis and physical understanding over the whole range of fluid mechanics, perhaps with different degrees of success in different parts of the subject, but with success none the less. Perhaps it reflects on the professionals of the subject that two 'outsiders' should have performed this service for us. Or are professionals handicapped by their knowledge of the vast *detail* of the subject? At all events, putting professional vanity aside, it seems to me that this book by Landau and Lifshitz ranks in importance as a comprehensive survey with Prandtl's work *The Essentials of Fluid Mechanics*; which is high praise.

In a book of this size and scope there are many points on which one might comment. I shall select here only a few which happen to be of particular interest to me and which may serve to convey a more detailed impression of the book.

The first four chapters, each about 50 pages long, cover the more conventional aspects of flow of incompressible fluid, the titles being 'Ideal fluids', 'Viscous fluids', 'Turbulence', and 'Boundary layers'. The chapter on viscous flow is good, which surprised me since this subject does not always appeal to physicists. Beginners would not find it easy going, since the notion of a stress tensor, for instance, is taken for granted and the derivation of the relation between stress and rate of strain is not really adequate (chiefly through omission of analysis of the relative motion in the neighbourhood of a point). Once these preliminaries are over, the authors treat a wide range of problems, the selection of which sometimes seems strange (for example, in the inclusion of the viscosity of suspensions but not of lubrication theory) although always stimulating. I was especially impressed with the way in which the neat vector proof of Stokes's law for the drag on a sphere is exploited in a wide variety of conditions; the same kind of mathematical argument is employed for a liquid sphere of arbitrary density and viscosity, for two (slowly) rotating concentric spheres, and for a sphere executing either translatory or rotary oscillations. Here and elsewhere I formed the impression, from the density of references to Russian papers (mostly given in the cryptic style 'Smithoff 1950', with no hint about the journal concerned), that problems involving small-scale viscous flow,

perhaps with an interface between two fluids or with temperature variations, of the kind encountered in chemical engineering, have been treated extensively in U.S.S.R. On the other hand, the otherwise excellent account of oscillatory viscous flow lacks any reference at all to the interesting phenomenon of secondary streaming.

The account of hydrodynamic stability is a little superficial, and seemed to me to be dominated unduly by Landau's own very original paper on the onset of turbulence. The authors have some interesting things to say about the relation between instability and transition to turbulence, but the why and how of instability for parallel flow is mostly lacking. Unless this happens to be a personal blind-spot of the authors, Russian work on instability is not well advanced. The discussion of turbulence is written with insight, as one would expect from fellow countrymen of Kolmogoroff and Obukoff, although to Western eyes it seems a rather partial and incomplete picture. All that is given on the decay of isotropic turbulence, for instance, is Kolmogoroff's deduction in 1941 from a similarity assumption and from Loitsianski's 'invariant' (now known not to be invariant, although the book may have been written in Russian before this finding) that the energy decays as $t^{-10/7}$; this was not one of Kolmogoroff's inspired results, and in any event it runs counter to a good deal of experimental work published since 1941. The discussion of turbulent jets, wakes and boundary layers is clear and concise, and relies for the most part on similarity arguments for the deduction of the dependence of width and mean velocity on distance downstream.

There follow three shorter chapters on 'Thermal conduction in fluids', 'Diffusion', and 'Surface phenomena', in which, as one might expect from such authors, thermodynamical considerations are exploited fully. The chapter on thermal conduction (which goes further than the title suggests and considers heat transfer and free convection) is particularly good in this respect. Most of the remaining chapters are concerned with the flow of a compressible fluid, beginning with a long chapter on 'Sound' which is a clearer and more searching account of that subject, within a single chapter, than any I have read. The evident ease with which the authors use the general principles and ideas of theoretical physics here shows to advantage. There is an excellent analysis of the emission of sound by oscillating bodies, although no mention of the generation of sound by fluctuations in the fluid velocity alone; nor is the scattering of sound by random non-uniformity of the medium included, which is more surprising in view of the known interest of Soviet scientists in this problem.

The chapters on 'Shock waves', 'One-dimensional gas flow', 'The intersection of surfaces of discontinuity', 'Two-dimensional gas flow' and 'Flow past finite bodies' are not ones which I feel able to assess critically, but my impression is that they are written even more expertly than the earlier chapters, despite the authors' reliance mostly on Russian work. The remaining chapters are 'Fluid dynamics of combustion', short but penetrating and written with an evident understanding of the physical and chemical aspects, and then three topics not usually included in a treatise on fluid mechanics, 'Relativistic fluid dynamics', 'Dynamics of super-fluids' (with no mention of the idea of quantized

circulation in helium II, which I had thought was part of the *lingua franca* of low-temperature physicists), and 'Fluctuations in fluid dynamics'.

There are of course a number of omissions, which to me at least seem odd. Surface waves provide the simplest and most tangible example of dispersive wave motion, as well as being the basis of a number of interesting phenomena in oceanography, but are given only eight pages in which the dispersive effect is not mentioned. Rotating fluids, cavitation, and, most surprising of all, magneto-hydrodynamics, are also overlooked (or is the latter topic to be treated in another volume?). But these and other omissions are pardonable, and come to mind only because the book has come so close to being a complete survey. There are blind-spots in the topics which are included, and several results which in Western circles would be regarded as well known and important are not given; evidently these two authors are no better informed about European and American work than we are about Soviet work. The blind-spots matter little, since we can fill in that part ourselves, and are at least equalized in number by the results and points of view which to us are new. Clearly, an essential preliminary to consideration of some problem or to preparation of a lecture in the future will be to see what Landau and Lifshitz have to say about the matter. It will be many years before I exhaust the supply of information in the numerous 'problems', complete with solutions (and having much more the character of a subsidiary investigation than of an exercise), given at the ends of sections. The whole work is very impressive, and will certainly have a good influence on future writing on fluid mechanics. The authority of these two authors may also lead theoretical physicists to do as they have done, and master the subject for the sake of its intrinsic interest.

G. K. BATCHELOR

Hypersonic Flow Theory. By WALLACE D. HAYES and RONALD F. PROBSTEIN. New York: Academic Press, 1959. 464 pp. $11.50.

Of the 280-odd references cited in this book, only fifty appeared before 1950 (although one of the most important is dated 1729). This is no indication of faulty scholarship, but confirmation that the pace of aerodynamic research, which was almost leisurely in the good old incompressible days, became brisk in the transonic and supersonic age, and downright frantic in the hypersonic decade. Thus a subject which was unnamed in 1945 is now properly termed classical. In the current scramble for outer space one may wonder whether, together with its companion, transonic flow, it is also becoming obsolete; but one missile engineer has solemnly assured the reviewer that it will always be necessary to fly through the hypersonic range.

Other books on hypersonic flow are appearing in both English and Russian. It is pleasant to record that the first of them is a distinguished work, and in many ways an exemplary one. It is devoted to the fundamentals of the theory, rather than applications, as treated from the point of view of continuum fluid mechanics. High-temperature gas dynamics is largely excluded, as is magneto-hydrodynamics. Inviscid flows are considered in the first two-thirds of the

book, and viscous effects (interpreted broadly to include diffusion and chemical reactions) in the remainder.

Every page bears evidence of careful writing and revision, in contrast to too many recent works in fluid mechanics which have been assembled with scissors and paste. The effort to co-ordinate and classify is seen, for example, in the first chapter on general considerations, where five different assumptions underlying inviscid hypersonic theory are labelled and discussed. The style is generally clear and literate, studded only occasionally with over-enthusiasms ('no tremendous distinction', 'the skin-friction is also of extreme importance').

An important feature is the conscientious coverage of Russian literature, which is seen to good advantage in the introductory pages to the second chapter, on small-disturbance theory. That theory is deduced (and generalized) following Hayes's original analogy with unsteady flow in one less space dimension, which to the reviewer still seems less satisfactory than the straightforward perturbation analysis. Among the examples is a useful resumé of Sedov's analytical solution for the point explosion. The treatment of other self-similar solutions is deficient by contrast.

The authors' individualism is most marked in the chapter on Newtonian theory. It opens with an appreciation showing that Newton's ideas, though based on what now seems a crude model, when translated into modern terminology foreshadow such concepts as Mach modelling and the hypersonic independence principle. A spirited defence is made of the study of Newtonian theory despite its inaccuracy and its curious anomalies. It is well known that the mass filling a volume is concentrated into a sheet covering the body surface. Here a second condensation into a line is pointed out, and finally, in unsteady motion, a threefold condensation on to a Newtonian shock point. Although these phenomena are admittedly unrealistic, it is suggested that their vestiges may persist in actual flows. Original results abound in the discussion of optimum shapes and of three-dimensional phenomena. The reader may wonder whether this difficult subject has been clarified by the introduction of three different conceptual models.

The notorious blunt-body problem is attacked in three successive chapters. First, the straightforward approximation of constant density is applied to the cone, circle, and sphere, and related to other methods. There follows a rather difficult and in some respects disappointing discussion of the theory of thin shock layers. Finally, a variety of other methods, mainly numerical, is discussed. In connexion with Belotserkovskii's scheme it may be remarked that his mysterious line of singular points is definitely not the sonic line, but lies downstream of it.

The indispensable numerical method of characteristics is outlined with admirable conciseness and clarity for flows that are either frozen or in thermodynamic equilibrium. A succinct explanation is found for the fact that taking pressure and stream angle as dependent variables yields by far the simplest formulation. The shock-expansion approximation, though almost equally useful, rests on shaky foundations, and some effort is devoted to surveying and extending the repeated attempts to account for its astonishing accuracy at high

speeds. Still lower in the hierarchy are the frankly empirical tangent-wedge and tangent-cone methods; here a correction is proposed in the case of large density ratios across the shock wave.

Viscous flows are introduced with a chapter on boundary layers (mainly laminar) assumed again to be either frozen or in thermodynamic equilibrium. Self-similar solutions play a predominant role and, because diffusion is important in a dissociating gas, the familiar simplifying assumptions of unit Prandtl number or viscosity proportional to temperature are now often supplemented by the supposition that the Lewis-Semenov number is one.

The authors several times employ the useful device of introducing a new phenomenon with a simplified model which displays the essential features. Thus the pressure interaction associated with the streamline deflexion due to the boundary layer is clearly illustrated for both extremes of weak and strong interaction by using qualitative estimates of boundary-layer thickness together with the tangent-wedge approximation. They then proceed to refine the analysis using accurate boundary-layer theory. Surprisingly, however, they retain the tangent-wedge approximation rather than adopt the logically unassailable self-similar small-disturbance solutions; this seems to violate their avowed aim of avoiding empirical approaches. A second type of viscous interaction is considered more briefly, in which the external vorticity engendered by the bow wave interacts with the boundary layer. It is too much to expect that a pioneering work like this one should be altogether free of conceptual errors, and here it appears that a recent dispute regarding the proper outer boundary condition to be imposed has been resolved incorrectly. As a consequence, the extra skin friction induced by external vorticity is probably seriously underestimated.

The final chapter treats free-molecule and rarefied-gas flows. A survey of general features opens with the warning that the concept of Knudsen number must be applied in context, and closes with a perhaps controversial classification of the spectrum between inviscid and free-molecule flows into no fewer than seven categories. An attempt is made to penetrate the first four or five of these using continuum theory, together with an imposing assortment of approximations, for the vicinity of the stagnation streamline on a blunt plane or axisymmetric body. Finally, free-molecule flow is surveyed, with emphasis on its similitude properties.

The book is magnificently indexed. In addition to a comprehensive subject index there is a detailed list of symbols with reference to their first appearance, and a similar list for authors. Finally there are the 280 references mentioned at the outset. Although the authors naturally disclaim any attempt at completeness, they have provided a splendid basic bibliography of the literature of hypersonic flow theory up almost to the month of publication, including all available Russian work.

This is in some parts a difficult book to read, it certainly contains errors yet undiscovered, and time will show that its emphasis is sometimes misplaced. But it is original, scholarly, and authoritative, and is certain to remain a standard reference in the literature of fluid mechanics.

MILTON VAN DYKE

JOURNAL OF FLUID MECHANICS

Volume 8, Part 2 June 1960

CONTENTS

Dynamics of a dissociating gas. Part 2. Quasi-equilibrium transfer theory
by M. J. LIGHTHILL *page* 161

On the tendency towards hexagonal cells in steady convection
by ENOK PALM 183

An improved perturbation theory for shock waves propagating through non-uniform regions
by M. P. FRIEDMAN 193

The forces on wing-fuselage combinations in supersonic flow
by JOSEPH H. CLARKE 210

Laminar convection in uniformly heated vertical pipes
by B. R. MORTON 227

On the collapse of an empty cavity in water
by C. HUNTER 241

Multiple shock compression using a piston of finite weight
by D. F. T. WINTER 264

On the effect of the molecular diffusivity in turbulent diffusion
by P. G. SAFFMAN 273

The compressible viscous heat-conducting vortex
by LESLIE M. MACK 284

Mass transport in the boundary layer at a free oscillating surface
by M. S. LONGUET-HIGGINS 293

The slow motion of a magnetized sphere in a conducting medium
by JAMES R. BARTHEL and PAUL S. LYKOUDIS 307

REVIEWS

Fluid Mechanics 315

Hypersonic Flow Theory 318

Printed in Great Britain at the University Press, Cambridge
(Brooke Crutchley, University Printer)